UNIVERSITÄT LEIPZIG

REPORT

Institute für Physik
The Physics Institutes

2002

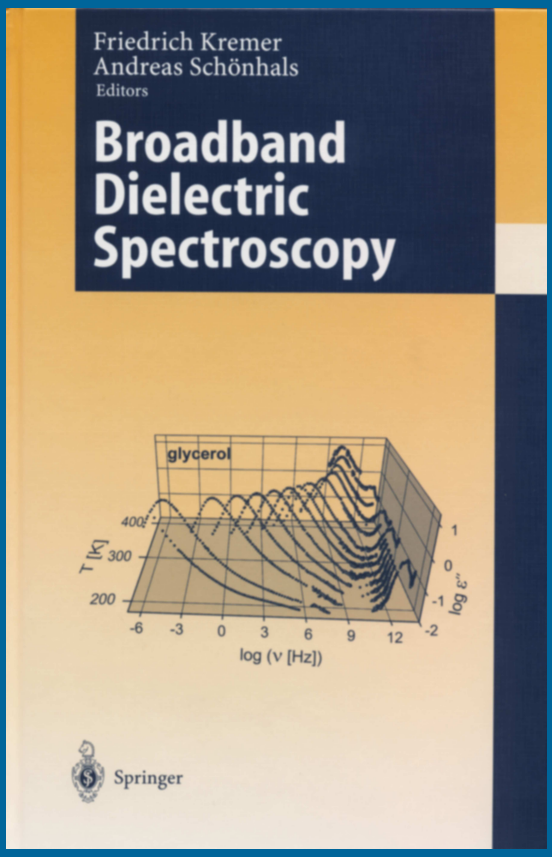

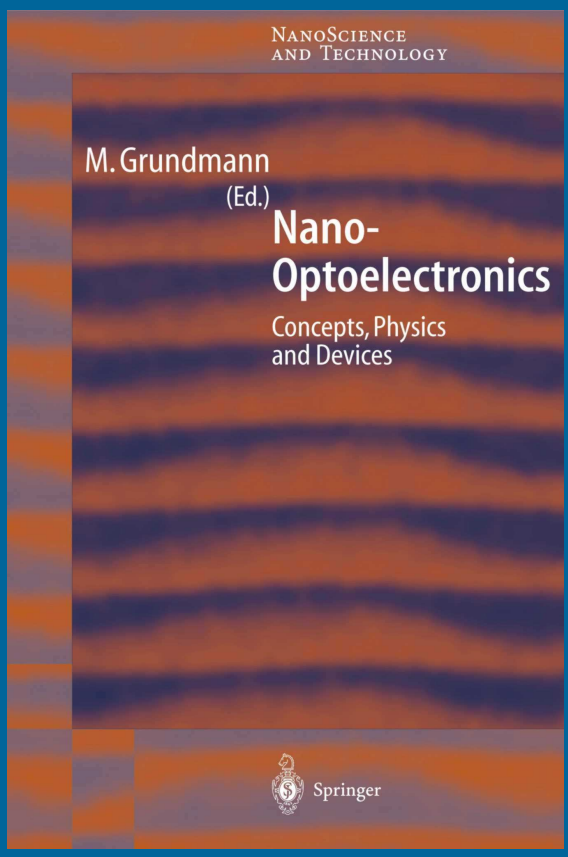

The Physics Institutes of Universität Leipzig, Report 2002
M. Grundmann, ed.
ISBN 3-934178-25-1

Printed in Germany by
MERKUR Druck und Kopierzentrum GmbH, Leipzig

on-line available at
http://www.uni-leipzig.de/~exph2/report_2002.pdf

Front cover

Books published in 2002

Back cover

Nerve cell with a growing axon on the right side guided by a weak optical tweezer. The green areas represent microtubules and the red areas stem from actin filaments

Institut für Experimentelle Physik I
Institut für Experimentelle Physik II
Institut für Theoretische Physik
Fakultät für
Physik und Geowissenschaften
Universität Leipzig

Institute for Experimental Physics II
Institute for Experimental Physics II
Institute for Theoretical Physics
Faculty of Physics and Geosciences
Universität Leipzig

Report 2002

Addresses

Institute for Experimental Physics I
Linnéstraße 5
D-04103 Leipzig, Germany
Phone: +49 341 9732 551
Fax: +49 341 9732 599
WWW: http://www.uni-leipzig.de/~gasse/nysid_a/inst/exp_1.htm

Institute for Experimental Physics II
Linnéstraße 5
D-04103 Leipzig, Germany
Phone: +49 341 9732 680
Fax: +49 341 9732 699
WWW: http://www.uni-leipzig.de/~exph2

Institute for Theoretical Physics
Vor dem Hospitaltore 1
D-04103 Leipzig, Germany
Phone: +49 341 9732 420
Fax: +49 341 9732 548
WWW: http://www.physik.uni-leipzig.de
Mailing address: Augustusplatz 10/11, 04109 Leipzig, Germany

CONTENTS

1 PREFACE

The Physics Institutes of Universität Leipzig present their joint report 2002. In the following, brief articles about the scientific activities and results are compiled. Key achievements in the Institutes for Experimental Physics were obtained in the fields of cell analysis with optical stretchers, laser-stimulated growth of nerve cells, pulsed field gradient NMR, confinement-induced relaxation processes in polymers, ion-beam nano-probes, acoustic microscopy, far-infrared magneto-ellipsometry, and preparation of high-quality epitaxial ZnO layers and nanowires. Highlights in the research of the Institute for Theoretical Physics were the study of non-commutative geometry (mathematical and physical aspects), critical behaviour of non-equilibrium phase transitions, Monte Carlo studies of a large variety of systems and the renormalization group flow of low dimensional systems. We invite you to look for further details in the report.

Funding for the BMBF "Wachstumskern" (growth nucleus) INNOCIS started in 2002 and many activities have evolved, among them the set-up of in-situ analytics for solar cell production and the analysis of thin film solar cells on flexible polymer foil from the Solarion GmbH pilot line.

We congratulate Mrs Heidemarie Schmidt for winning in the BMBF competition "Nanotechnology" for young researchers. A rather generous grant allows her to establish the "Nachwuchsgruppe" (research team) Nano-Spinelectronics in the Institute for Experimental Physics II; it will take up work in 2003 and is funded for 5 years.

Dr. Jochen Guck from the Soft Matter Physics Group was awarded the "Young Scientist Award in Biomedical Photonics" from Hamamatsu and the German Cancer Research Center (Deutsches Krebsforschungszentrum, DKFZ, Heidelberg) for his work on cell analysis with optical tweezers.

The Institute for Theoretical Physics hosted the main annual meeting of the German Physical Society with about 1600 participants. Gewandhaus and Opera were remarkable locations for the plenary sessions. Our guests enjoyed the conference and the city of Leipzig. At least the organizers did not record any serious problems!

We like to thank all people and agencies, listed in detail in the report, for their personal and financial support. We enjoy a very positive working atmosphere with a steadily increasing number of students, highly motivated and skilled PhD candidates and appealing working conditions.
We hope you enjoy reading our report which can also be browsed on-line (pdf-file) at `http://www.uni-leipzig.de/~exph2/report_2002.pdf` .

Leipzig, March 2003

Friedrich Kremer
Marius Grundmann
Klaus Sibold
Directors

2 Structure and Staff of the Institutes

2.1 Institute for Experimental Physics I

2.1.1 Office of the Director

Prof. Dr. Friedrich Kremer (director)
Prof. Dr. Jörg Kärger (vice director)

2.1.2 Groups of the Institute

2.1.2.1 Soft Matter Physics
Physik der weichen Materie

Prof. Dr. Josef A. Käs

Secretary
Claudia Honisch

Technical Staff
Dipl. Phys. Bernd Kohlstrunk
PTA Undine Dietrich
PTA Wolff Schneider
CTA Elke Westphal

Academic Staff
Prof. Dr. Herbert Schmiedel
Dr. Jochen Guck
Dr. Carsten Selle

Ph.D. candidates
Revathi Ananthakrishnan
Brian Gentry
David Smith
Allen Ehrlicher
Timo Betz
Daniel Koch
Bjoern Stuhrmann
Michael Goegler
Vanessa Bell
Falk Wottawah
Stefan Schinkinger
Bryan Lincoln
Doug Martin
Martin Forstner
Kristian Franze

Jens Gerdelmann
Soyeun Park

Students
Karla Müller
Claudia Brunner
Maren Mielke
Mireille Martin
Florian Huber
Peter Rödiger
Anatol Fritsch
Susanne Ebert
Frank Sauer

2.1.2.2 Physics of Interfaces
Grenzflächenphysik

Prof. Dr. Jörg Kärger

Secretary
Mrs. Ursula Krause

Technical staff
Dipl.-Ing. Bernd Knorr
Dipl.-Phys. Cordula Bärbel Krause
Lutz Moschkowitz
Ing. Dagmar Prager

Academic staff
Prof. Dr. Peter Bräuer
Priv.-Doz. Dr. Horst Ernst
Prof. Dr. Dieter Freude
Dr. Petrik Galvosas
Dr. Wilfried Heink
Prof. (i.R.) Dr. Dr. h.c. Harry Pfeifer
Dr. Frank Stallmach
Priv.-Doz. Dr. Brigitte Staudte
Dr. Sergey Vasenkov

Ph.D. candidates
Dipl.-Phys. Christian Chmelik
Dipl.-Phys. Oliver Geier
Dipl.-Chem. Stefan Gröger
Dipl.-Phys. Johanna Kanellopoulos
Dipl.-Chem. Enrico Lehmann

Dipl.-Phys. Thomas Loeser
Dipl.-Phys. Daniel Prochnow

Students
Cand.-Phys. Andreas Brzank
Cand.-Phys. Denis Schneider

2.1.2.3 Physics of Anisotropic Fluids
Physik anisotroper Fluide

Prof. Dr. Friedrich Kremer

Technical staff
Karin Girke
Ines Grünwald
Dipl.-Ing. Jörg Reinmuth
Dipl.-Phys. Wiktor Skokow

Academic staff
Prof. Dr. Siegbert Grande
PD Dr. Ralf Stannarius
Dr. Christine M. Papadakis
Dr. Banani Adhikari Das
Dr. Jian-Jun Li

Ph.D. candidates
Dipl.-Phys., Dipl.-Chem. Tune B. Bonné
Dipl.-Chem. Peter Busch
Dipl.-Phys. Kyuseok Cho
Dipl.-Phys. Lutz Hartmann
Dipl.-Phys. Thomas John
Dipl.-Phys. Ralf Köhler
Dipl.-Phys. Walter Lehmann
Dipl.-Phys. Jan Prigann
Dipl.-Phys. Heidrun Schüring
Dipl.-Phys. Anatoli Serghei
Dipl.-Biochem. Marc Struhalla
Dipl.-Phys. Michael Tammer

2.1.2.4 Polymer Physics
Polymerphysik

Prof. Dr. Dieter Geschke

Technical staff
Christine Adolph
Dipl.-Ing. Hans-Jürgen Rauchfuß
Dipl.-Phys. Uwe Weber

Academic staff
PD Dr. Martin Helmstedt
Dr. Jianjun Li

Students
Frank Feller, M. Sc.

2.2 Institute for Experimental Physics II

2.2.1 Office of the Director

Prof. Dr. Marius Grundmann (director)
Prof. Dr. Tilman Butz (vice director)

2.2.2 Groups of the Institute

2.2.2.1 Solid-state Optics and Acoustics
Festkörperoptik und -akustik

Prof. Dr. Wolfgang Grill

Secretary
Wilma Pfeiffer

Staff
Phys.-Lab. Adelheid Geyer
PTA Hans-Joachim vom Hofe
Dipl.-Phys. Friedrich Jilek
Dr. Zbigniew Kojro
Dr. Volker Riede
Dr. rer. nat. habil. Mathias Schubert
Dipl.-Ing. (FH) Ulrike Teschner
Privatdozent Dr. rer. nat. habil. Reinhold Wannemacher

PhD candidates
Nurdin Ashkenov, M. Sc.
Carsten Bundesmann (Staatsexamen Physik)
Dipl.-Phys. Erik v. d. Burg
Dipl.-Phys. Nils Harder
Dipl.-Phys. Tino Hofmann
Dipl.-Phys. Jens Jahny
Dipl.-Phys. Alexander Kasic
Dipl.-Phys. Oliver Lenkeit
Wilfred Ngwa, M. Sc.
Dipl.-Phys. Martin Schubert
Evgeny Twerdowski, M. Sc.

Students
Beri Mbenkum
Thomas Rudolph

2.2.2.2 Semiconductor Physics
Halbleiterphysik

Prof. Dr. Marius Grundmann

Secretary
Mrs. Wilhelmine Pfeiffer

Technical staff
Dipl.-Phys. Gabriele Benndorf
Ing. Gisela Biehne
Dipl.Ing. Holger Hochmuth
Dipl.-Phys. Jörg Lenzner
Ing. Dieter Natusch
PTA Gabriele Ramm
PTA Roswitha Riedel

Academic staff
Dr. Evgeni M. Kaidashev (on leave from Rostov-on-Don State University, Russia)
Dr. Michael Lorenz
Priv.-Doz. Dr. Rainer Pickenhain
apl. Prof. Dr. Bernd Rheinländer
Dr. Heidemarie Schmidt

Ph.D. candidates
Dipl.-Phys. Daniel Fritsch
Dipl.-Phys. Karsten Goede
Dipl.-Phys. Erick Guzmán Ramirez
Susanne Hardt (Staatsexamen Physik)
Dipl.-Phys. Rüdiger Schmidt-Grund
Dipl.-Phys. Alexander Weber
Dipl.-Phys. Holger von Wenckstern

Students
Jens Bauer
Wolfram Czakai
Thomas Nobis
Andreas Rahm

2.2.2.3 Nuclear Solid-state Physics
Nukleare Festkörperphysik

Prof. Dr. Tilman Butz

Technical staff
Dipl.-Ing. Bernd Krause
PTA Raimund Wipper
Dipl.-Ing. Lothar Wulke

Academic staff
Dr. Dietmar Lehmann
Dr. Tilo Reinert
Dr. Jiři Škopek (Marie Curie fellow)
Priv. Doz. Dr. Wolfgang Tröger
Dr. Jürgen Vogt

Ph.D. candidates
Dipl.-Phys. Frank Heinrich
Dipl.-Phys. Daniel Spemann

Students
Christoph Meinecke
Frank Menzel
Michael Schwertner

2.2.2.4 Physics of Dielectric Solids
Physik dielektrischer Festkörper

Prof. Dr. Dieter Michel

Secretary
Mrs. Ursula Seibt

Technical staff
Dr. Winfried Böhlmann
Dipl.-Ing. Joachim Hoentsch
Dipl.-Phys. Gert Klotzsche

Academic staff
apl. Prof. Dr. Rolf Böttcher (Hochschuldozent)
Prof. Dr. Georg Völkel
Dr. habil. Horst Braeter
PD Dr. Andreas Pöppl
Dr. André Pampel
Dr. Venkatesan Umamaheswari

Physical-technical assistent
Mrs. Ursula Heinich

Ph. D. candidates
Dr. Marlen Gutjahr (degree received in 2002)
Dr. Samir Mulla Osman (degree received in 2002)
Dr. Jörg Roland (degree received in 2002)
Emre Erdem
Özlen Erdem
Abdoullaye Taye

Students
Eike Bierwirth
Andreas Bunge

External members
Dima Yaskov
Pavel Sedykh
Maria Popova
PhD Students from St. Petersburg State University

2.2.2.5 Superconductivity and Magnetism
Supraleitung und Magnetismus

Prof. Dr. Pablo D. Esquinazi

Technical staff
Klaus Grünwald
Annette Setzer
Monika Steinhardt

Academic staff
Dr. Kyoo-hyun Han
Dr. Roland Höhne
Dr. H.-C. Semmelhack
Dr. Michael Ziese

Ph.D. candidates
Alberto Bollero Real
Heiko Kempa
Roberto Ocaña

Students
Ulrike Köhler
Uwe Schaufuß
Konstantin Ulrich

2.3 Institute for Theoretical Physics

2.3.1 Office of the Director

Prof. Dr. Klaus Sibold (director)
Prof. Dr. Manfred Salmhofer (vice director)

For the members and structure of the ITP please see page 249.

3 NUCLEAR SOLID-STATE PHYSICS — SCIENTIFIC ACTIVITIES

3.1 The high-energy ion nanoprobe LIPSION

T. Butz, D. Lehmann, F. Menzel, T. Reinert, M. Schwertner, D. Spemann, J. Vogt

The high-energy ion nanoprobe LIPSION at the University of Leipzig has been operational since October, 1998 (Fig.1). Its magnetic quadrupole lens system, arranged as a separated Russian quadruplet, was developed by the Microanalytical Research Centre (MARC), Melbourne and has a symmetrical demagnification factor of about 130. The single-ended 3 MV SINGLETRON™ accelerator (High Voltage Engineering Europa B.V.) supplies H^+ and He^+ ion beams with a beam brightness of approx. 20 $A \cdot rad^{-2} m^{-2} eV^{-1}$. Due to this high brightness, the excellent optical properties of the focussing system of the nanoprobe and the suppression of mechanical vibrations by founding the bed-plates of accelerator and probe in greater depths separately from the surroundings, lateral resolutions below 100 nm for the low current mode (STIM) and 300 nm at a current of 10 pA (PIXE) were achieved routinely. A beam diameter of 41 nm was achieved.

Fig. 1: LIPSION laboratory.

The UHV experimental chamber is equipped with electron, X-ray, and particle detectors to detect simultaneously the emitted secondary electrons (Ion Induced Secondary Electron Emission, SE), the characteristic X-rays (Particle Induced X-Ray Emission, PIXE), as well as the backscattered ions (Rutherford Backscattering Spectrometry, RBS) and - in case of thin

samples - the transmitted ions (Scanning Transmission Ion Microscopy, STIM, and Scanning Transmission Ion Micro-Tomography, STIM-T). A newly installed optical microscope allows sample positioning and inspection during measurement. The magnetic scanning system moves the focussed beam across the sample within a scan field of adjustable extent.
The data collection system MPSYS (MARC Melbourne) collects and stores the spectra of the several techniques at any beam position (Total Quantitative Analysis, TQA). In addition, optional windows can be set in the spectra for real-time elemental mapping. The pictures are viewed and printed as two-dimensional colour-coded intensity distributions.

New installations in 2002:

replacement of light guides for ion source control
installation of an active compensation system of stray magnetic fields using Helmholtz-coils (see fig. 1)
installation of an irradiation platform designed for single ion bombardment of living cells

Current work in nuclear nanoprobe performance is focussed on:

replacement of the old data acquisition system by the new MicroDAS (MARC Melbourne)
development of a new target chamber with x-y-z translation stage and new goniometer inside the chamber

Accelerator Statistics 2002:

operating hours: 1520 h
maintenance and conditioning: 110 h

3.2 Active Compensation of Stray Magnetic Fields at LIPSION

D. Spemann, T. Reinert, J. Vogt, J. Wassermann, T. Butz

Non-static stray magnetic fields caused, e. g., by trams, power supplies, and transformer stations can lead to a significant deterioration of the lateral resolution of ion micro- and nanoprobes even at low magnitudes of ~1 µT. So far, the lateral resolution in the low current mode of the high-energy ion nanoprobe LIPSION is primarily limited by beam spot fluctuations caused by slowly varying stray magnetic fields and, recently, by additional 50 Hz fields. Therefore, the active stray magnetic field compensation system AMK_5 developed by J. Wassermann, TU Wien, has been installed in the LIPSION laboratory. This system utilizes six coils in a Helmholtz-arrangement and advanced technology for magnetic field sensing and signal processing for its operation and allows to reduce the stray field fluctuations to excellent ±10 nT in all three directions for frequencies from true DC up to the kHz range. A compensation factor > 100 was obtained for the vertical direction. The compensation system was also used to determine the sensitivity of LIPSION to stray magnetic fields. It was found that the sensitivity is largest for stray fields along the beam direction leading to a beam spot movement of 1.1 m/T in both the horizontal and vertical direction. Thus, the residual stray field fluctuations of ±10 nT result in beam spot movements of ±13 nm assuming a homogeneous stray field and no contribution from stray fields outside the shielded volume.
Figure1 shows a STIM scan over a GaAs edge (scan size: 2.4 µm × 2.4 µm) with the beam scanned in the horizontal direction. First, the compensation was activated (upper part of the STIM map) which results in a distortion-free image of the edge. Then the compensation was switched off (lower part of the map) leading to strong distortions in the image. This demonstrates that the lateral resolution of LIPSION is significantly improved by the active compensation system.

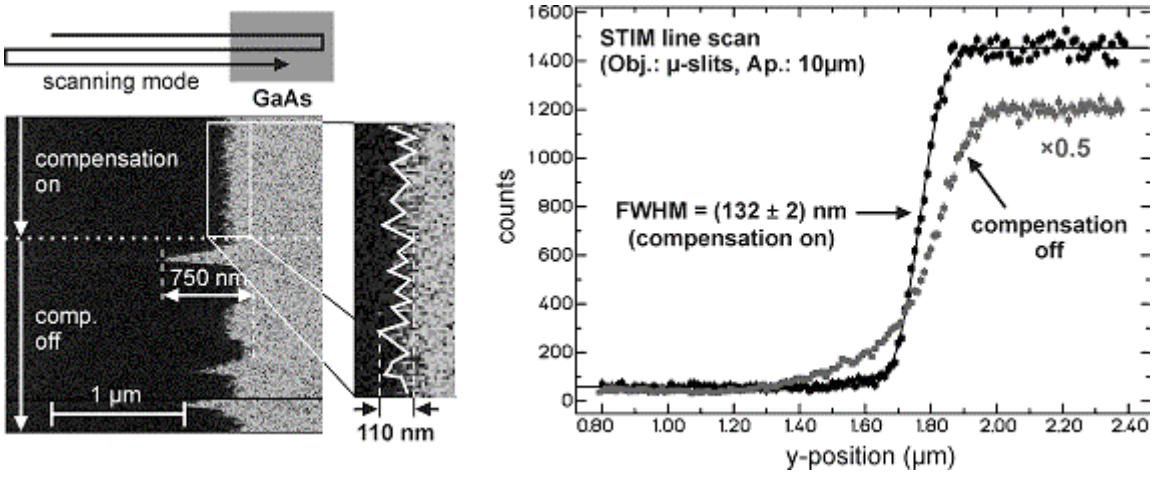

Fig. 1: STIM scan over a GaAs edge (scan size: 2.4 µm × 2.4 µm) with the beam scanned in horizontal direction. *Left:* STIM map taken with (upper part) and without (lower part) active compensation. The enlarged part shows residual beam spot fluctuations of approximately ±50 nm. *Right:* Horizontal beam profiles extracted from the upper and lower part of the map.

However, there are still beam spot fluctuations in both the vertical and horizontal direction dominated by ~50 Hz components which limit the resolution in the low current mode to approximately 130 nm. The source of these fluctuations seems to be mechanical vibrations of the target stage.

3.3 High Resolution STIM Micro-Tomography

T. Reinert, M. Schwertner, A. Sakellariou, J. Vogt, T. Butz

High resolution Scanning Transmission Ion Microscopy (STIM) is a powerful tool to visualize internal structures of small objects with a resolution down to 100 nm. The main advantage of ion microscopy is the capability of the high energy ions to penetrate relatively thick samples (~ 10 µm) without significant beam spreading. Therefore, this method is ideally suited to investigate the micron-scale 3D structures of biological systems including spores and cartilage structures.
A 3D-STIM-tomography experiment consists of recording a number of 2D-STIM images of the sample, called projections, under different incident angles from 0°...180° degrees (the 3rd dimension). For the experiments 360 projections of the samples were taken, each having a pixel resolution of 250×250 pixel. The data sets were reconstructed using the Backprojection of Filtered Projections (BFP) technique. The STIM tomography method was applied to investigate the inner structure of a cygospore. This spore has an optically non-transparent protecting shell which complicates the microscopic analysis of the nucleus' structure. The structure is of interest for the microbiological investigation of the sexual reproduction of the cygospores. The ion beam penetrates the spore thus probing the inner structure. A STIM tomography revealed a single, relatively large nucleus without any additional substructures larger than 1 µm.

(a) 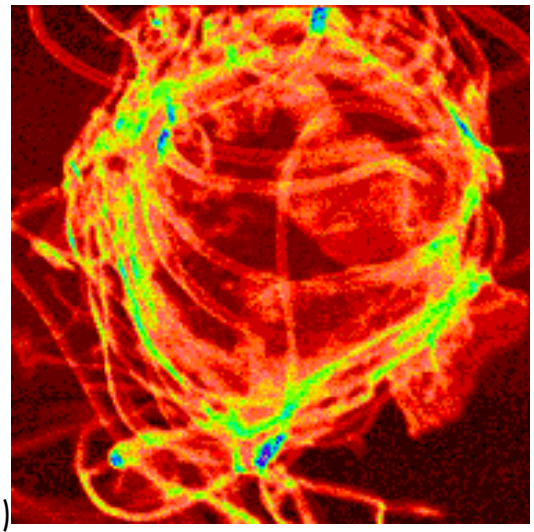 (b) 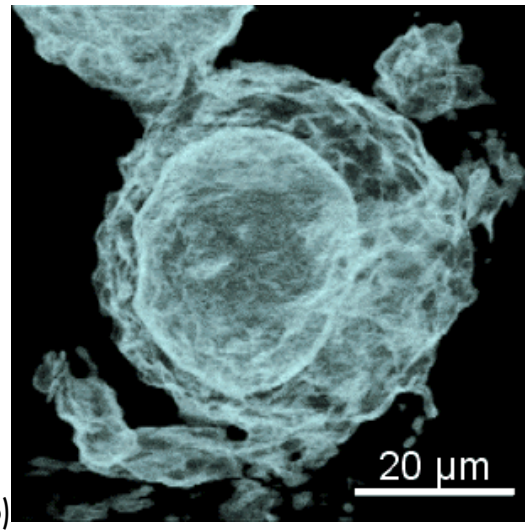

Fig. 1: (a) Ion induced secondary electron image of a cygospore which shows the outer morphological structure, long tubes for sexual reproduction. (b) Rendered density distribution image from a STIM tomography showing the nucleus of the spore.

3.4 Skin as a barrier to ultra-fine particles

F. Menzel, T. Reinert, U. Anderegg, M. Sticherling, J. Vogt, T. Butz

Micronised TiO_2 particles with a diameter of about 15 nm are used in sunscreens as physical UV filters. Due to the small particle size the suspicion exists that TiO_2 particles can pass through the uppermost horny skin layer (*stratum corneum*) through intercellular channels and penetrate into deeper vital skin layers. Accumulations of TiO_2 particles in the skin can decrease the threshold for allergies of the immune system or cause allergic reactions directly.
Spatially resolved ion beam analysis (PIXE, RBS, STIM and Secondary Electron Imaging) was carried out on freeze dried cross sections of biopsies of pig skin, on which four different formulations containing TiO_2 particles were applied. The investigations were carried out with a 2.25 MeV proton beam, which was focused to 1 µm diameter. The analysis concentrated on the penetration depth and on pathways of the TiO_2 particles into the skin.
In these measurements a penetration of TiO_2 particles through the *stratum corneum* into the underlying *stratum granulosum* via intercellular space was found (see Fig. 1). Hair follicles do not seem to be important penetration pathways because no TiO_2 was detected inside the follicles. The TiO_2 particle concentration in the *stratum spinosum* was below the minimum detection limit of about 1 particle/µm^2.
These findings show the importance of coating the TiO_2 particles in order to prevent damage of RNA and DNA of skin cells by photocatalytic reactions of the penetrated particles caused by absorption of UV light.

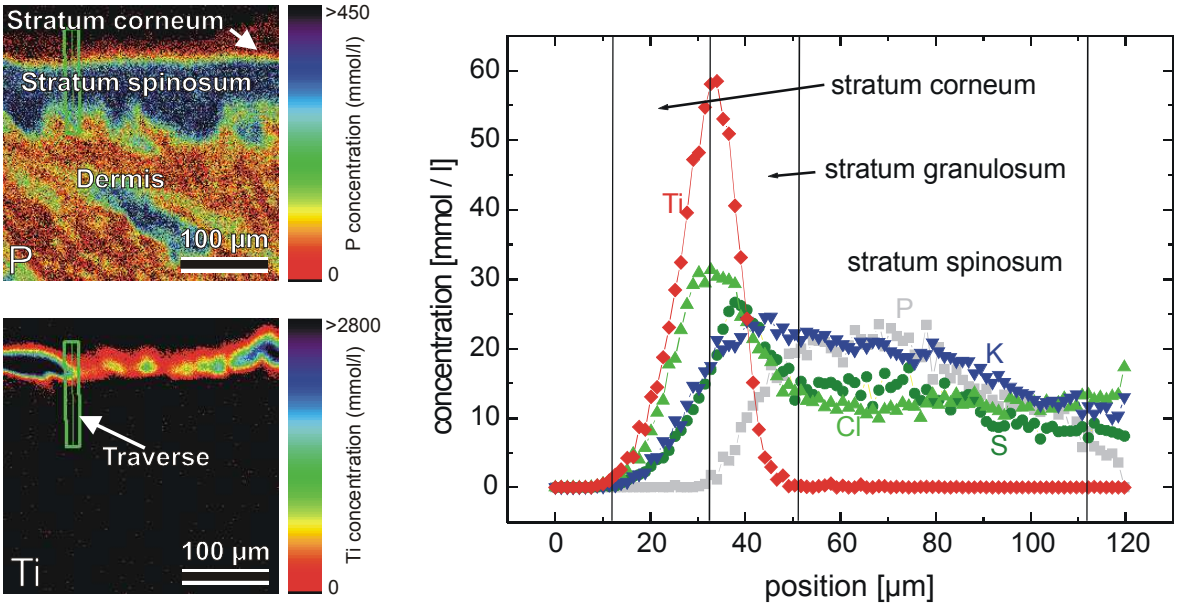

Fig. 1: Left: PIXE-maps showing the distribution of phosphorus and titanium in a cross-section of sunscreen treated pig skin. Titanium is located at the skin surface and in the area of the *stratum corneum*. Right: Elemental distribution along the traverse marked in the Ti-map. The skin strata can be distinguished and a penetration of TiO_2 through the *stratum corneum* into the *stratum granulosum* is recognizable.

3.5 Quantitative Microanalysis of Perineuronal Nets in Brain Tissue

T. Reinert, M. Morawski, Th. Arendt, T. Butz

The relevance of the perineuronal nets (specialised extracellular matrix surrounding a part of the neurons in brain tissue) as a possible protection of neurons against oxidative stress induced by metal ions (e.g. Al, Fe, Cu, and Zn) is an actively discussed hypothesis. It is assumed that the perineuronal nets are able to bind metal ions and thus reduce the oxidative stress to neurons. Therefore, we used nuclear microscopy (μPIXE) in order to investigate the concentration and distribution of iron in rat brain loaded with colloidal iron with special emphasis to the perineuronal nets in the extracellular matrix. The elemental microanalysis was performed on 6 μm thin resin embedded sections. The perineuronal nets accumulated more Fe than other extracelullar matrix components leading to well defined, neuron-related structures in the Fe-maps (Fig. 1a). In order to quantify the affinity, the iron-accumulations in the perineuronal nets were analysed for different Fe-loadings and normalized by the Fe-concentration of the extracellular matrix (Fig. 1b). Our data support the hypothesis of a neuroprotective effect of the perineural nets.

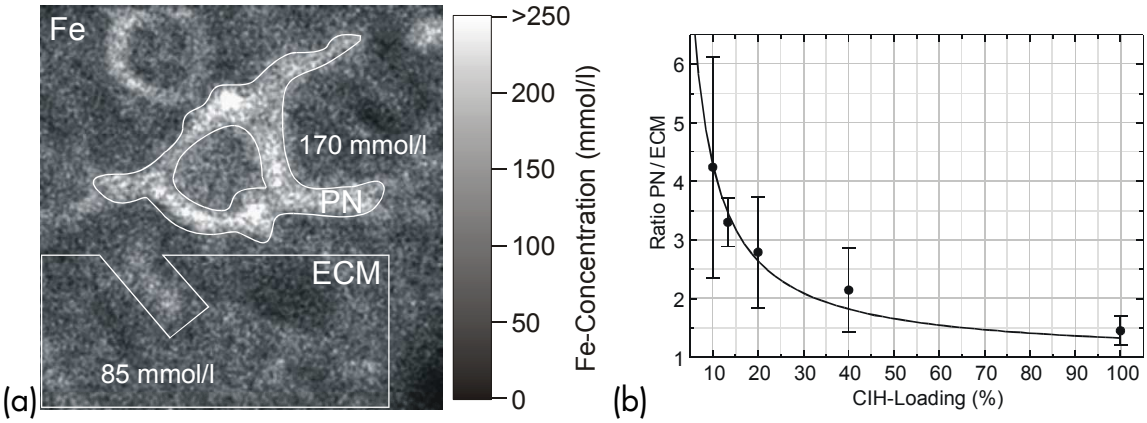

Fig. 1: (a) Distribution map of iron (50 μm × 50 μm) with encircled regions of perineuronal net (PN) and extracellular matrix (ECM) from which the concentrations were extracted. (b) The relation between the initial colloidal iron hydroxide (CIH) loading and the ratio of concentrations perineuronal net / extracellular matrix. The ratio can be described by a hyperbolic function with an offset of 1 from which an affinity of K_D = 33% (at PN/ECM = 2) was derived.

3.6 Single Ion Bombardment of Living Cells

A. Fiedler, T. Reinert, J. Škopek, J. Tanner, J. Vogt, T. Butz

Our key objective is the investigation of the cellular response to targeted irradiation with light ions, especially the radiation induced bystander effect. Therefore, we developed an irradiation platform for living cells. The platform enables the irradiation of living cells in a Petri-dish (due to the horizontal beam in a vertical position) and the detection and energy loss measurement of the projectile ions. Technically, our primary concern is to lower the hit precision to below 1 µm. Therefore, we use thin Si_3N_4 windows as beam exit window and Petri-dish bottom. A hit precision test in the form of a scanning transmission ion microscopic (STIM) image of a fixed cell showed excellent results (Fig. 1a).
Scientifically, our studies started with adhesion, survival and sedentariness tests with endothelial cells subjected to the following procedure as a control: medium removal, vertical positioning and a sham irradiation for 15 min, horizontal repositioning and restoring the usual medium level. About 95 % of the cells survived this procedure.
The first irradiation of living cells was carried out with 2.25 MeV protons homogeneously distributed over the cells. From the energy loss measurement we estimated that each cell has received a dose of about 0.5 Gy. We checked for survival after 15 minutes and 17.5 hours after irradiation. Almost all cells survived the irradiation (Fig. 1b). Further experiments with different doses and targeting areas with subsequent investigation of different endpoints (survival, apoptosis, micronuclei formation, cell signalling, reactive oxygen species detection) will follow.

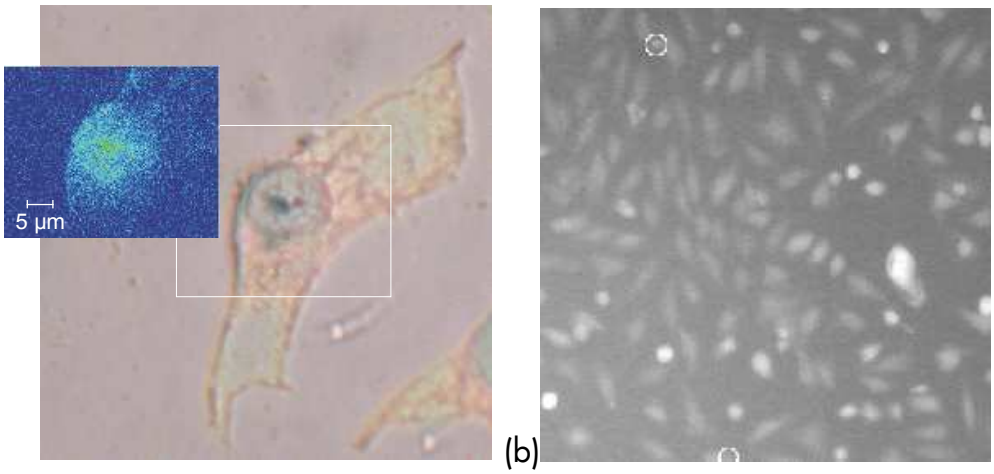

(a) (b)

Fig. 1: (a) Overlay of a STIM image on the optical image of a fixed endothelial cell showing the high resolution (= high precision targeting) under irradiation conditions. (b) Optical image (540 µm × 540 µm) of living endothelial cells 17.5 hours after irradiation (~0.5 Gy per cell). Fluorescein diacetate and propidium iodide staining revealed that almost all cells survived except two cells (encircled).

3.7 Evidence for intrinsic weak ferromagnetism in a C_{60} polymer by PIXE and MFM

D. Spemann, K.-H. Han, R. Höhne, T. Makarova, P. Esquinazi, T. Butz

In this study a C_{60} polymer was characterized for the first time with respect to impurity content and ferromagnetic properties by laterally resolved Particle Induced X-ray Emission (PIXE) and Magnetic Force Microscopy (MFM) in order to prove the existence of intrinsic ferromagnetism in this material.
In the sample studied the main ferromagnetic impurity found was iron with an average concentration of (175±16) µg/g within the sample volume probed by the ion beam. However, the Fe distribution is very inhomogeneous and characterized by micrometer-large impurity grains of almost pure iron surrounded by an almost pure carbon matrix. Therefore, large regions of the sample appear pure within the information depth of PIXE which is ~36 µm for Fe in carbon bulk (corresponding to 90% of the total yield).
Figure 1 shows the elemental maps of Cr, Mn, and Fe in a contaminated region of the sample together with an optical micrograph of the analysed area. The contaminations consist of irregularly shaped grains with sizes of several microns containing Fe, Cr, Mn, and Ni (not shown in Fig. 1) which are contained in the bulk of the sample. In fact, only the grain indicated by the arrow in Fig. 1 was optically visible. This grain was probably contained within the bulk and laid open by the sample polishing procedure.
With MFM, the ferromagnetic properties have been investigated both in pure and contaminated regions of the sample as determined by µPIXE. We found that ~30% of the area of pure regions (concentration of magnetic impurities <1 µg/g) is characterized by ferromagnetic domains, which are partly correlated with grains and grain boundaries. These magnetic domains are of intrinsic origin and not related to impurities. In contaminated regions of the sample the ferromagnetic properties are dominated by the impurities as expected from the high impurity concentrations. Detailed information about the MFM measurements and discussion can be found in [1].

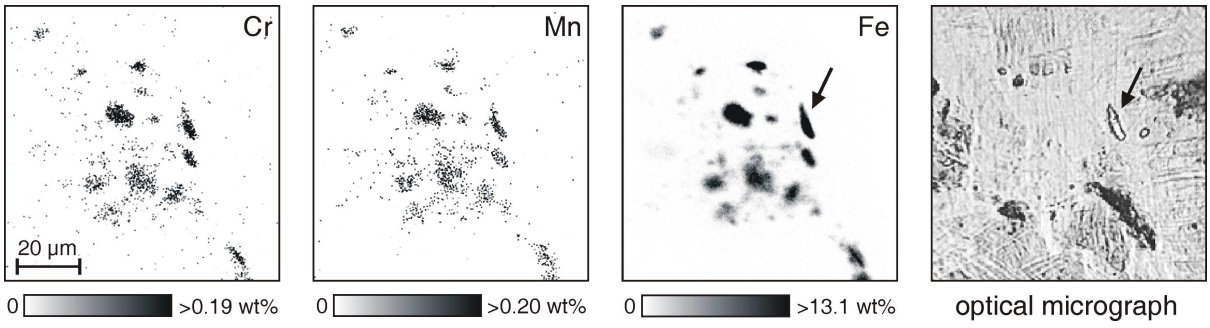

Fig. 1: Distribution of Cr, Mn, and Fe in a contaminated region of the sample together with an optical micrograph from the same scan area. The impurities are located in irregularly shaped grains. Only the grain indicated by the black arrow is optically visible. All other grains are located below the sample surface.

The combination of PIXE and MFM allowed us to separate between the intrinsic and extrinsic magnetic regions and to directly prove that intrinsic ferromagnetism exists in a C_{60} polymer.

[1] K.-H. Han, D. Spemann, R. Höhne, A. Setzer, T. Makarova, P. Esquinazi, T. Butz. *Carbon* 41(4), 785 (2003).

3.8 Ion beam analysis of epitaxial (Li, Mg, Cd)$_x$Zn$_{1-x}$O, ZnO, and ZnO:(Al, Ga) thin films grown on c-plane sapphire by pulsed laser deposition

D. Spemann, E. M. Kaidashev, M. Lorenz, J. Vogt, T. Butz

Transparent conducting oxides such as zinc oxide (ZnO) are technologically highly relevant, e.g. in flat-panel displays and in thin film photovoltaics. By means of doping and/or alloying with other elements the electronic properties, e.g. electronic band gap, resistivity etc., can be varied over a wide range.
ZnO thin films, nominally undoped, as well as doped with Al and Ga and alloyed with Li, Mg, and Cd, investigated in this study have been epitaxially grown on c-plane sapphire by pulsed laser deposition (PLD). In order to characterize the PLD process and to optimize the deposition parameters the films were analysed by RBS, PIXE, and Particle Induced Gamma-ray Emission (PIGE) using He^+ and H^+ ion beams. It was found that the element transfer from the PLD target to the film differs significantly for the individual doping and alloying elements, with concentration ratios between film and target ranging from ~5% for Cd to ~200% for Li and Mg. In spite of this, the films exhibited a metal to oxygen ratio of 1:1 in general.

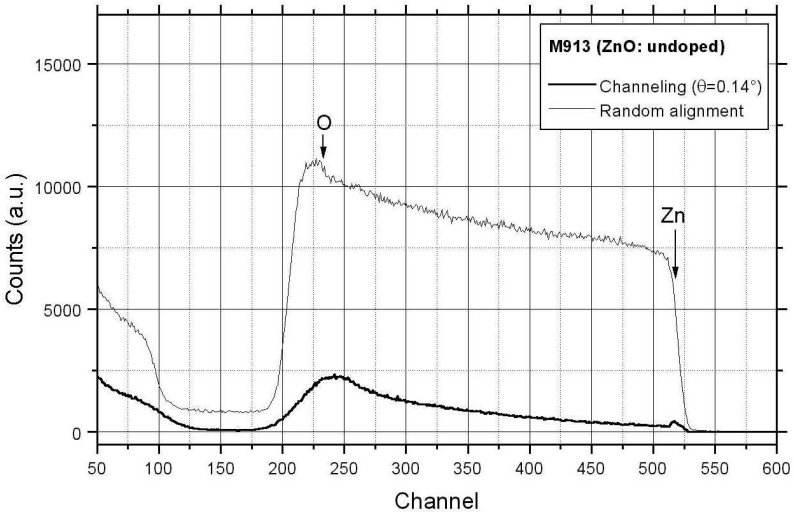

Fig. 1: RBS spectra from an undoped ZnO film under channeling (2 MeV He^+ beam along (0001) axis) and random alignment. The strongly reduced backscattering yield under channeling conditions demonstrates the excellent crystal quality of the film.

Furthermore, the crystal quality of the films was investigated using ion channeling. Especially, the undoped ZnO films which were deposited by a novel 3-step PLD process are characterized by an excellent crystal quality yielding a normalized minimum RBS yield of χ_{min}=3.3% under channeling conditions (see fig. 1).

3.9 The use of proton nanobeams for micromachining

J. Vogt, S. Roorda, T. Butz

Many innovative efforts are currently under way to develop technologies for the production of microstructures, e.g. photonic crystals, micro fluidic devices or micro sensors. One of these promising technologies is proton micromachining.
In a cooperation with the University of Montreal (S. Roorda) the sub-micron lateral resolution of LIPSION and the well defined range of a MeV proton beam are utilized to make maskless lithographic structures with a high aspect ratio in suitable polymers (e.g. PMMA, SU-8).
In first experiments simple structures were produced, consisting of arrays of pillars with different dimensions of their horizontal cross sections, ranging from 200 nm x 200 nm up to 5 µm x 5 µm. Polished Si samples were spin coated with SU-8 (negative) photo resist. The thickness of the resist layer after drying was app. 4 µm. For the bombardment of the resist a proton beam with 2 MeV energy, 100 nm diameter and an intensity of 5000 particles per second was applied. The beam was quickly moved electromagnetically over the area of each pillar to achieve a homogenous particle distribution. This is one of the prerequisites to obtain sharp edged structures; another one is the application of a suitable ion dose. For the purpose of dose optimisation we varied the applied dose from 0.5 nC/mm^2 up to 300 nC/mm^2. Well defined structures were obtained using an ion dose between 2 nC/mm^2 and 50 nC/mm^2 (Fig.1).

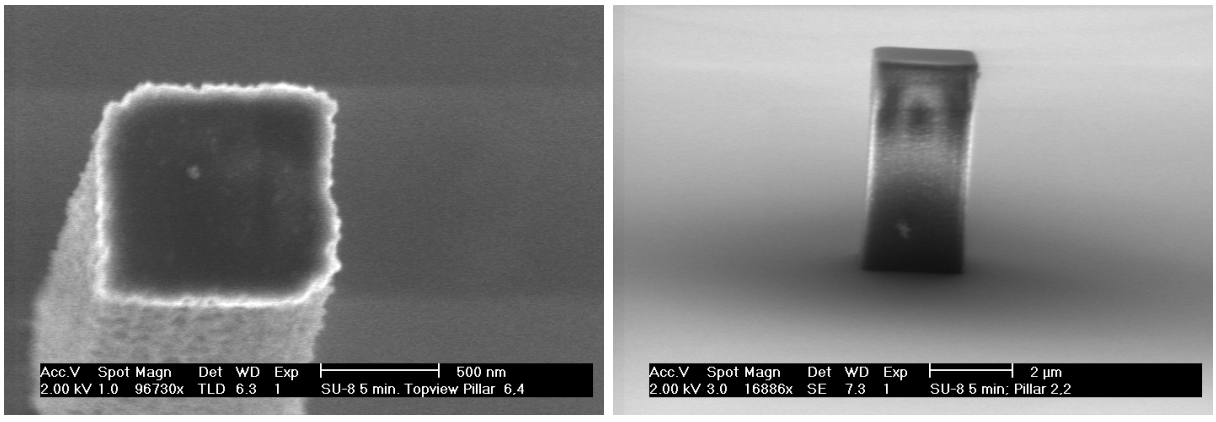

Fig. 1: Scanning electron microscopy pictures of SU-8 photo resist pillars produced by 2 MeV proton bombardment

3.10 TDPAC-Laboratory

W. Tröger, F. Heinrich, T. Butz

Nuclear probes are used to study the interaction of metals with biological macromolecules like, e.g., DNA and proteins. Many life processes are based on such interactions. The structure and dynamics of metal sites in biomolecules are important in determining the functional efficiency of these macromolecules. In order to study those metal sites close to physiological conditions a highly sensitive spectroscopic method is required, like Time Differential Perturbed Angular Correlation (TDPAC). Here, a radioactive atom is placed at the site of interest and by correlating the emitted γ-quanta in space and on a nanosecond time scale local structural information is provided. These investigations allow a deeper insight into the detoxification processes, switches, adaptivity and rigidity of metal sites in electron transfer proteins, and also the development of new radiopharmaceuticals in cancer therapy.

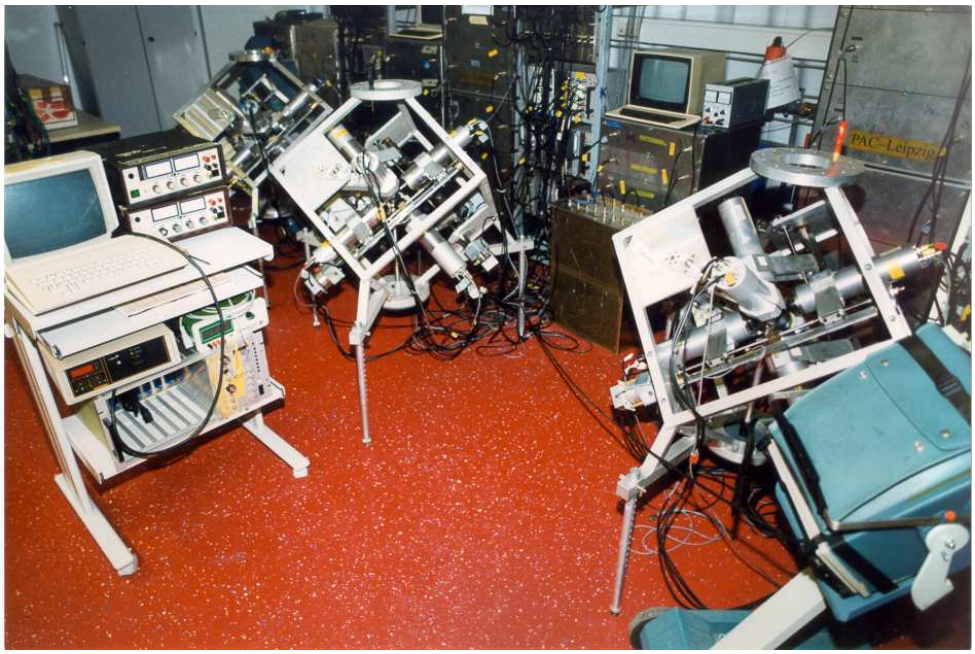

Fig. 1: TDPAC laboratory with three modern TDPAC-Cameras ("silver cubes").

Furthermore, TDPAC is also used in material science to obtain a better understanding of high T_c superconductors and materials with colossal magnetoresistance.
In 2002, two modern 6-detector-TDPAC spectrometer were installed permanently at the Solid State Physics Lab of the ISOLDE on-line isotope separator at CERN. This outstation of the Leipzig TDPAC Laboratory is dedicated for TDPAC experiments with rather short-lived TDPAC isotopes, like ^{111m}Cd or ^{199m}Hg, with half-lifes less than an hour.

3.11 Coordination Studies of the Metal Center of Hemocyanin via ^{199m}Hg Nuclear Quadrupole Interaction

W. Tröger, H. Decker, ISOLDE Collaboration

Hemocyanins are blue copper proteins serving as an oxygen carrier in the blood of arthropods. The reversible binding of oxygen is performed by a binuclear copper center generally referred as a "type 3" copper center. The classic type 3 copper center is found in Ascorbate Oxidase in which each Cu is coordinated by three histidines in a trigonal prismatic geometry; in Hc the same ligands are arranged in a trigonal antiprismatic coordination sphere. Triggered by our previous investigations of the metal coordination in the "type 3" copper center in the blue copper proteins Ascorbate Oxidase and Laccase by the nuclear quadrupole interaction (NQI) of the probe ^{199m}Hg monitored by Time Differential Perturbed Angular Correlation (TDPAC) we extended these investigations to Hemocyanins (Hc). Hc are hexamers, each subunit contains a binuclear copper site and has a molecular weight of *75* kDa. For our studies Hc from the tarantula *Eurypelma californicum* which consists of 4 hexamers, i.e. a "4×6" hemocyanin, is used which contains 48 copper atoms in 24 binuclear centers.

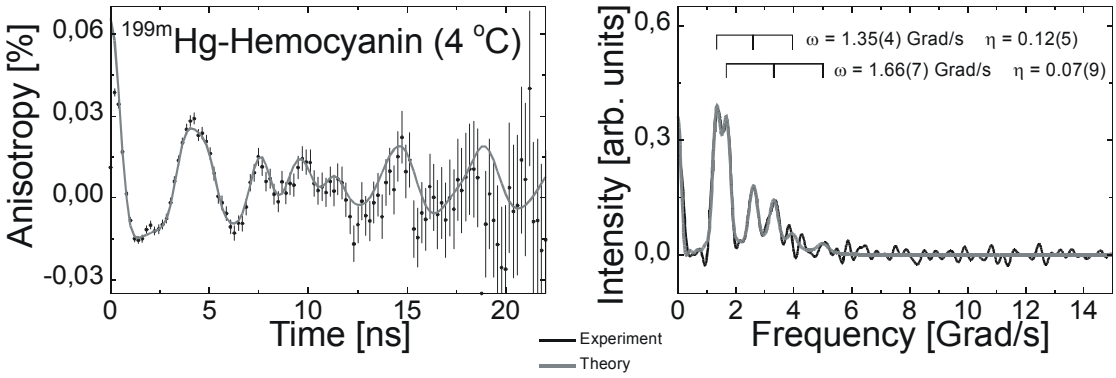

Fig. 1: The ^{199m}Hg time spectra (left) and its Fourier transform (right) of Hemocyanin in a highly viscous sucrose solution at 4°C. The NQI parameters precession frequency ω and asymmetry parameter η of each site are given in the Fourier spectra.

Copper free Hc was incubated with a $^{199m}Hg/HgCl_2$ solution under different stoichiometric conditions. We detected in every experiment two different ^{199m}Hg-NQI's. A typical spectrum is shown in figure 1. The populations of each NQI were identical in all experiments within the error margins, the Lorentzian line broadening was about 4 %.
The detected NQIs are completely different from those we found in Ascorbate Oxidase (ω = 0.98(1) Grad/s, η = 0.72(4)) or Laccase (ω = 0.89(1) Grad/s, η = 0.58(4)). The higher frequencies in Hc together with the significantly lower asymmetry parameter indicate a twofold coordination geometry in contrast to the suggested trigonal coordination.

3.12 ^{204m}Pb - A "new" TDPAC isotope for the "Home Laboratory"

W. Tröger, F. Heinrich, H. Haas

In an early effort in the seventies of the last century the nuclear quadrupole interaction of the isomeric TDPAC isotope ^{204m}Pb, which has a half-life of $t_{1/2}$=67 minutes only, was investigated in a variety of metals and compounds. However, in some cases only a rough estimate of the NQIs in these compounds was possible due to the pure statistical qualitiy of the data and serious limitations of the data analysis. In 2001 we could produce this isotope for the first time at the on-line isotope separator ISOLDE at CERN and determined the NQI of ^{204m}Pb in cadmium metal which was a factor of 2 different from a previous TDPAC experiment. In 2002 we extended our investigations to Pb(II) complexes which may also serve as model compounds for the structural investiations of biological macroproteins, the final goal of theses investigations.

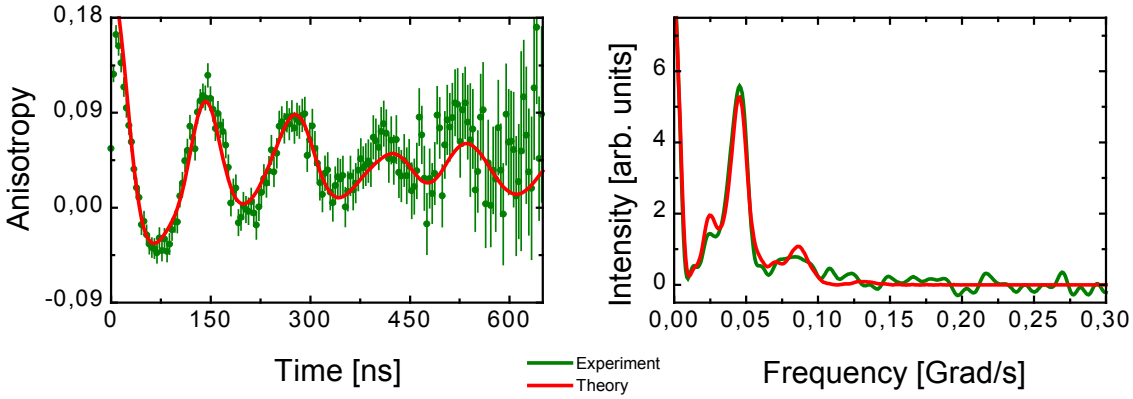

Fig. 1: The ^{204m}Pb time spectrum (left) and its Fourier transform (right) of a $PbCl_2$ precipitate, recorded in Leipzig.

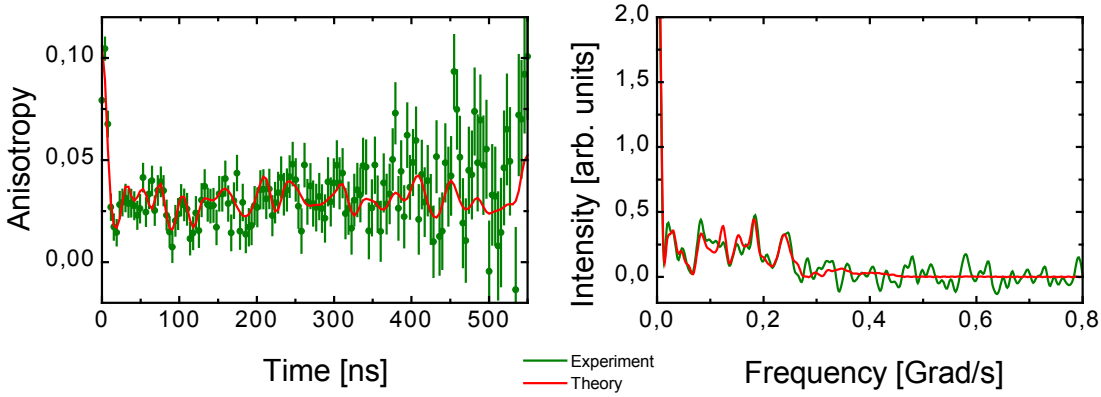

Fig. 2: The ^{204m}Pb time spectrum (left) and its Fourier transform (right) of ^{204m}Pb(II)-DNA in a frozen solution at -196 °C.

Besides the experiment at the ISOLDE facility we performed also ^{204m}Pb experiments in our "home laboratory" at the University of Leipzig with the help of a ^{204}Bi ($t_{1/2}$=11.4 h)/^{204m}Pb generator. The production of the ^{204}Bi activity was carried out at the Ionenstrahlalbor ISL of the Hahn-Meitner-Institut in Berlin. In Fig. 1 the $^{204m}PbCl_2$-TDPAC spectra are shown as

recorded in Leipzig. Figure 2 displays the first ^{204m}Pb spectra of a Pb(II) binding catalytic DNA molecule which might serve as metal sensor.
For TDPAC studies on heavy metals there are now all three possible isomeric PAC isotopes available: ^{111m}Cd, ^{199m}Hg, and ^{204m}Pb.

3.13 An Update on the Mercury(II) Binding to Metallothioneins

W. Tröger, F. Heinrich, À. Leiva-Presa, M. Capdevila, P. Gonzàlez-Duarte

Metallothioneins (MT) are ubiquitous, cysteine-rich proteins of low molecular weight which bind d^{10} metal ions such as Zn(II), Cd(II), Cu(I) and Hg(II) in metal-thiolate clusters. They play an important role in the metabolism and in the modulation of the essential trace element zinc and copper and in the binding of toxic heavy metals. The latter suggests also the involvement in cellular detoxification mechanisms. Several 3D structures have been solved for mammalian $Me(II)_7$-MT, containing Zn(II) and/or Cd(II) ions. These metal ions are tetrahedrally coordinated by both bridging and terminal thiolates in cluster structures. We studied the Hg(II) binding in these molecules by optical absorption spectroscopy and by time differential perturbed angular correlation (TDPAC) spectroscopy. The former gives information on the stoichiometry and degree of folding of the Hg(II)-MT species present in solution, and the latter has recently been used successfully to elucidate the primary coordination sphere of Hg(II) ions in soluble $Hg(SCys)_n$ species at physiological concentrations. The overall results provide information on the variables affecting the Hg/protein stoichiometries and structures of the species formed as well as on the evolution of the coordination geometry about Hg(II) at increasing Hg/MT molar ratios. The titration of high purity recombinant MT, and corresponding αMT and βMT fragments, with either $HgCl_2$ or $Hg(ClO_4)_2$, at pH 7 or 3, revealed mainly two- and fourfold Hg(II) coordinations depending on Hg(II) concentration and pH. At pH 3 twofold coordinations dominate whereas at pH 7 also higher coordination numbers occur (see Fig. 1).

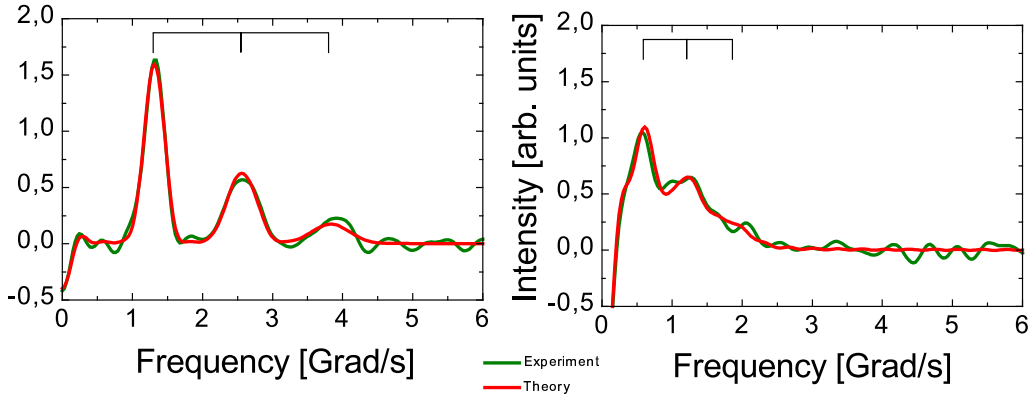

Fig. 1: The Fourier transformed TDPAC-spectra of MT at pH 3 (left) and pH 7 (right). The shift from higher to lower frequencies indicates the change of the twofold Hg(II) coordination to higher coordination numbers.

3.14 TDPAC-Solid State Physics: High T_c Superconductors and Colossal Magnetoresistive Oxides

J.G. Correia, J.P. Araujo, V.S. Ameral, F. Heinrich, T. Butz, W. Tröger

In the frame work of international cooperations we perform local studies on relevant structural problems of High T_c Superconductors (HTSC) and Colossal Magnetoresistive Oxides (CMO) by doping these with suitable radioactive isotopes for Perturbed Angular Correlations (TDPAC) and Emission Channeling (EC).
In the case of HTSC the characterization of the order/disorder in Hg planes of the HTSC family $Hg_1Ba_2R_{n-1}Cu_nO_{2n+2+\delta}$ due to the oxygen defect plays an major role.
In the case of the CMO the measurement of the nuclear quadrupole interaction (NQI) in insulators and conducting samples provides information on the coupling between the local structure and chemical doping (by oxygen and metal vacancies), magnetic and electric properties. The hyperfine magnetic field is also useful to probe magnetic ordering of Mn ions in the CMO familiy of manganites. The main issue adressed was the characterisation of local deformations in manganites, due to polaronic mechanisms, using appropriate radioactive ions, to study the effects of charge ordering and phase separation on a local scale. The variation of the NQI parameters near the charge-ordering transition in $Pr_{0.65}Ca_{0.35}MnO_3$ is shown in figure 1.

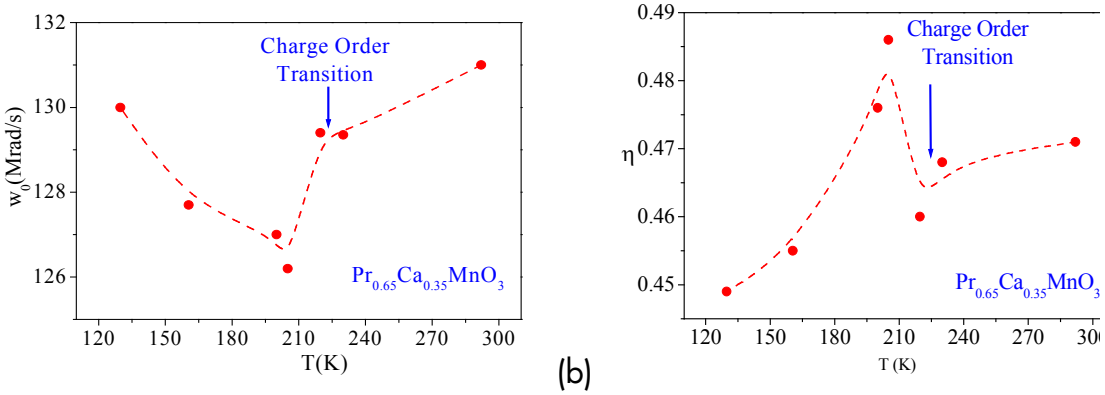

Fig. 1: The change of the nuclear quadrupole parameters precession frequency ω (a) and asymmetry parameter η (b) near the charge-ordering transition in $Pr_{0.65}Ca_{0.35}MnO_3$.

3.15 Metal Stoichiometries in Metalloproteins

A. Vogel, O.Schilling, W. Meyer-Klaucke, D. Spemann, W. Tröger

ElaC proteins are highly conserved metallohydrolases, ubiquitously present in all three domains of life. There is genetic evidence that mutations in human ElaC are associated with certain types of cancer. As a first characterization of an ElaC gene product we purified the protein and showed that this is a novel, zinc dependent phosphodiesterase with a binuclear zinc active site structurally related to the metallo-β-lactamase family. The catalytic mechanism and the substrate specificity are currently being investigated with the combined means of enzymology, molecular biology and spectroscopy. In order to identify the Zn-coordinating amino acids, the putative amino acids of the metal binding site are replaced by other aminoacids via site directed mutagenesis. The metal stoichiometry of these mutants was analyzed by Proton Induced X-Ray Emission (PIXE). Since the amino acid sequence of the protein is known, the number of sulphur containing amino acids is also known. The PIXE spectrum, as shown in figure 1, allows to determine the elemental content of a protein sample. The intensities of the sulphur and metal peaks are used to calculate the relative stoichiometry of these elements and since the absolute amount of sulphur in the protein is known, also the protein to metal stoichiometry is known. The protein mutant whose PIXE spectrum is displayed in Fig. 1 binds several other metals besides Zn indicating a complete change of the metal binding site.

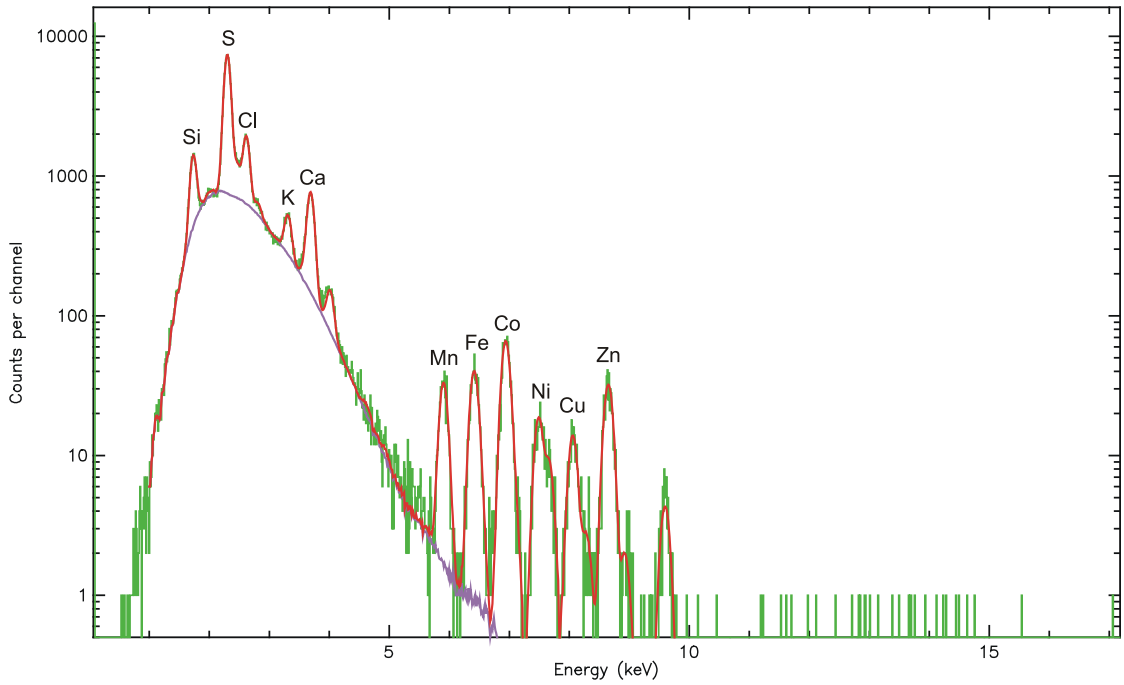

Fig. 1: The PIXE spectrum of a mutant of the novel zinc dependent phosphodiesterase.

3.16 Metal Induced Formation of Ligand-Receptor Pairs

M. Lekka, M.Marszalek, J.Lekki, F. Heinrich, W. Tröger

We investigated the molecular interaction between ligand-receptor pairs that are formed with the participation of metal ions (especially ions of Ca, Mg, Cu, Zn), which is particularly important in nuclear medicine for diagnostics and therapy. In order to determine the structural and chemical surrounding of metal ions in these complexes the method of Time Differential Perturbed Angular Correlation (TDPAC) was employed to monitor the static and dynamic nuclear quadrupole interaction (NQI) of the TDPAC probe ^{111}In/^{111}Cd in ligand receptor complexes with ethylenediaminetetraacetic acid (EDTA), diethylenetriaminepentaacetate (DTPA), and bovine serum albumin (BSA). The TDPAC probe ^{111}In/^{111}Cd exhibits an electron capture decay from ^{111}In to ^{111}Cd prior to the γ-γ-cascade used for the TDPAC measurement. The same γ-γ-cascade can be used also with the isomeric TDPAC probe ^{111m}Cd.
The data confirm the presence of a conformational transition from pH 7 to a faster rotating form at pH 3.5. The Cd-DTPA complex in a neutral aqueous solution is characterised by a reorientational correlation time of $7.7 \cdot 10^{-11}$ s, the NQI is given by the nuclear precession frequency ω = 188(8) Mrad/s and the asymmetry parameter η=0.74(5). A direct comparison of the results obtained at 293 K with neutral solutions of parent complexes of ^{111m}Cd-DTPA and ^{111}In-DTPA confirms a disintegration of complexes after ^{111}In electron capture due to the Auger process.

3.17 Funding

Verbundprojekt: Wachstumskern INNOCIS "Kostengünstige, flexible CIS-Photovoltaik"; Teilprojekt: „Elektronische und optische Eigenschaften, in-situ-Ramanstreuung, in-situ-Ellipsometrie und Ionenstrahlanalytik von flexiblen Cu-(In,Ga)-(Se,S)-Dünnfilm-Solarzellen"
Prof. M. Grundmann
BMBF, 03 WKI 09

Koordinationsstudien mit TDPAC an makrozyklischen Ag-Kronen und –Käfigen: Molekulare Integrität von ^{111}Ag-Radiopharmaka
Coordination studies with TDPAC on macrocyclic Ag-crowns and –cages: Molecular integrity of ^{111}Ag-radiopharmaca
Priv.-Doz. Dr. W. Tröger
Deutsche Forschungsgemeinschaft, Tr327/5-2

Radioactive Metal Probes as Diagnostic Tools in Biomolecules
Priv.-Doz. Dr. W. Tröger
Deutsche Forschungsgemeinschaft, Tr327/8-1

The Influence of Heavy Metals on Living Cells
Priv.-Doz. Dr. W. Tröger
Bundesministerium für Bildung und Forschung, Internationales Büro, Wissenschaftlich-technologische Zusammenarbeit mit Polen, POL-021-99

Single Ion Bombardment of Living Cells
Prof. T. Butz
Marie Curie-Development Host Fellowship, HPMD-CT-2000-00028

3.18 Organizational Duties

T. Butz
Member of the committees "Forschung mit nuklearen Sonden und Ionenstrahlen" (BMBF), and „International Symposium on Nuclear Quadrupole Interactions"
Member of the International Advisory Board of the „Hyperfine Interactions" conference
Vorsitzender des wissenschaftlichen Beirates des Instituts für Oberflächenmodifizierung e.V., Leipzig
Vertrauensdozent der Studienstiftung des deutschen Volkes
Reviewer: DFG, Studienstiftung des deutschen Volkes, The University of Melbourne
Referee: European Phys. Journal, J. of Physics C, J. of Physics D, Phys. Rev. B

T. Reinert
Referee: Nucl. Instr. Meth. Phys. Res. B

D. Spemann
Referee: Vacuum

W. Tröger
Referee: Hyperfine Interactions, J. of Physics (Condensed Matter), Mikrochim. Acta, Z. Naturforsch. A

3.19 External Cooperations

CENBG, Bordeaux, Prof. Ph. Moretto
CERN, Genf, ISOLDE Collaboration
Chalmers Technical Highschool, Göteborg
CSIRO, Exploration and Mining, Sydney, Dr. C. Ryan
EMBL Outstation Hamburg, Dr. W. Meyer-Klaucke, Dr. A. Vogel, O. Schilling
Fa. Hille & Müller, Dr. W. Olberding
FRM, Garching, Prof. E. Wagner, Dr. U. Wagner
FSU Jena, Dr. Ch. Schimek
FU Berlin, Prof. U. Abram
Gray Laboratory, London, Prof. B. Michael
GSI Darmstadt, Dr. D. Dobrev, Dr. B. Fischer
HMI, Berlin, Dr. D. Alber, Dr. H. Haas
IIF Leipzig, K. Franke
INFN-LNL, Legnaro-Padova, Prof. P. Mittner
Institute of Applied Physics, Sumy, Ukraine, Dr. S. Lebed
Institute of Nuclear Physics, Krakow
Institute of Nuclear Technology, Lisbon, Prof. J.C. Soares
IOM Leipzig, Dr. K. Zimmer, Dr. J. Gerlach
KVL, Kopenhagen, Prof. R. Bauer, Dr. E. Danielsen, Dr. L. Hemmingsen
Massenseparator-Kollaboration Bonn-Göttingen
MLU Halle-Wittenberg, Dr. J. Tanner
MPI für Biochemie, Martinsried, Prof. R. Huber, Dr. A. Messerschmidt
MPI für Mikrostrukturphysik, Halle/S., Dipl.-Phys. J. Heitmann
MPI für Polymerforschung, Mainz, Prof. W. Knoll
Panjab University, P. Sidhu
Paul-Flechsig-Institut, Prof. T. Arendt, M. Morawski
Prähistorische Staatssammlung München, Dr. R. Gebhard
PSI Villigen, Schweiz, Prof. P.A. Schubiger
Shanghai Institute of Nuclear Research, Shanghai, Prof. J. Zhu
Solarion GmbH
The University of Melbourne, Microanalytical Research Centre
TU Wien, Prof. K. Schwarz, Prof. P. Blaha
Universidade de Aveiro, Portugal, Prof. V.S. Amaral
Université de Montréal, Prof. S. Roorda
Universität Leipzig, Prof. R. Hoffmann, A. Fiedler
Universität Mainz, Dr. H. Decker
Universität Zürich, Prof. M. Vašák, Dr. P. Faller, Prof. R. Alberto
Universitätskliniken Leipzig, PD Dr. G. Hildebrandt, Prof. M. Sticherling

Universitat Autònoma de Barcelona, Dr. À. Leiva-Presa, Dr. M. Capdevila, Prof. P. Gonzàlez-Duarte
University of Illinois, Prof. Y. Lu, J. Liu
Dr. E. Zschau, Self-employed expert in materials research

3.20 Publications

3.20.1 Journals

Non-destructive 3D-characterization of $Zn_{2-2x}Cu_xIn_xS_2$ thin films with ion beam analysis.
D. Spemann, J. Vogt, T. Butz, D. Oppermann, K. Bente
Anal. Bioanal. Chem. 374, 626 (2002).

Suitable test structures for submicron ion beam analysis.
D. Spemann, T. Reinert, J. Vogt, D. Dobrev, T. Butz
Nucl. Instr. Meth. Phys. Res. B 190, 312 (2002).

Ion beam analysis of $Zn_{2-2x}Cu_xIn_xS_2$ films.
D. Spemann, J. Vogt, T. Butz, D. Oppermann, M. Lorenz, G. Wagner, K. Bente
Nucl. Instr. Meth. Phys. Res. B 190, 667 (2002).

STIM tomography at the Leipzig nanoprobe LIPSION.
T. Reinert, A. Sakellariou, M. Schwertner, J. Vogt, T. Butz
Nucl. Instr. Meth. Phys. Res. B 190, 266 (2002).

The architecture of cartilage: elemental maps and scanning transmission ion microscopy/tomography.
T. Reinert, U. Reibetanz, A. Sakellariou, M. Schwertner, J. Vogt, T. Butz
Nucl. Instr. Meth. Phys. Res. B 188, 1 (2002).

On the Calculation of Electric Field Gradients in Layered Compounds.
T. Butz
Z. f. Naturforschung A 57(6-7), 518 (2002).

The Nuclear Quadrupole Interaction of $^{187}W(\beta^-)^{187}Re$ in W(VI)-EDTA Complexes.
G. Sun, W. Liu, T. Butz
Z. f. Naturforschung A 57(6-7), 620 (2002).

The Nuclear Quadrupole Interaction of ^{204m}Pb in Cadmium Monitored by γ-γ-Perturbed Angular Correlations.
W. Tröger, M. Dietrich, J.G. Correia, H. Haas and the ISOLDE collaboration
Z. f. Naturforschung A 57(6-7), 586 (2002).

Coordination Studies of the Metal Center of Hemocyanin by ^{199m}Hg Nuclear Quadrupole Interaction.
W. Tröger, B. Ctortecka, P. Faller, H. Decker and the ISOLDE collaboration

Z. f. Naturforschung A 57(6-7), 623 (2002).

Ferromagnetism in oriented graphite samples.
P. Esquinazi, A. Setzer, R. Höhne, C. Semmelhack, Y. Kopelevich, D. Spemann, T. Butz, B. Kohlstrunk, M. Lösche
Phys. Rev. B 66(2), 024429 (2002).

Infrared dielectric functions and phonon modes of wurtzite $Mg_xZn_{1-x}O$ (x<= 0.2).
C. Bundesmann, M. Schubert, D. Spemann, T. Butz, M. Lorenz, E.M. Kaidashev, M. Grundmann, N. Ashkenov, H. Neumann, G. Wagner
Appl. Phys. Lett. 81(13), 2376 (2002).

The Leipzig High-Energy Ion-Nanoprobe LIPSION: Design of single-ion bombardment of living cells.
J. Tanner, D. Spemann, T. Reinert, J. Vogt, T. Butz
Radiation Research 158(3), 372 (2002).

Optical properties of ternary MgZnO thin films.
R. Schmidt, C. Bundesmann, N. Ashkenov, B. Rheinländer, M. Schubert, M. Lorenz, E.M. Kaidashev, D. Spemann, T. Butz, J. Lenzner, M. Grundmann
Proc. 26th Int. Conf. on the Physics of Semiconductors (ICPS-26), (2002).

3.20.2 Annual Reports

T. Butz (Editor)
NFP - Scientific Activities.
In: M. Grundmann (Ed.), Report 2001
Institut für Experimentelle Physik, Universität Leipzig, ISBN 3-934178-17-0 (2002).

3.20.3 Invited Talks

Ionenmikroskopie und Mikrotomographie
T. Butz
Graduiertenkolleg: „Bildgebende Verfahren“, TU Karlsruhe, 22.-23.7.2002

Einzelionenbeschuß lebender Zellen am LIPSION
T. Butz
Radiation Research - Science for the future, International Workshop, Giessen, 3.-7.10.2002

Ionenmikroskopie und Mikrotomographie
T. Butz
Rotary Club Leipzig, 31.10.2002

Ionenmikroskopie und Mikrotomographie

T. Butz
Institut für Strahlenphysik, Universität Stuttgart, 31.10.2002

Nuclear Probes in Life Sciences: TDPAC Studies of Metal Sites in Macromolecules
W. Tröger
Universitat Autònoma de Barcelona, 19.11.2002

3.20.4 Conference Contributions

Untersuchung der Korrosion von HILUMIN-Batterieelektroden mittels zeitdifferentieller γ-γ-Winkelkorrelationsspektroskopie (T)
F. Heinrich, W. Tröger
Frühjahrstagung der DPG, Regensburg, 12.03.2002

Zerstörungsfreie ionenstrahlanalytische 3D-Charakterisierung von $Zn_{2-2x}Cu_xIn_xS_2$-Dünnschichten (P)
D. Spemann, J. Vogt, T. Butz, D. Oppermann, K. Bente
Frühjahrstagung der DPG, Regensburg, 11.-15.03.2002

Mikroskopie und Tomographie mit Protonen (P)
T. Butz, T. Reinert, M. Schwertner, D. Spemann, J. Vogt
Frühjahrstagung der DPG, Regensburg, 11.-15.03.2002

Electronic and structural properties of n-type Zn(Ga, Al, Mg, Cd) oxide thin films (P)
M. Lorenz, E.M. Kaidashev, J. Lenzner, H. v. Wenckstern, D. Spemann, G. Wagner, C. Bundesmann, V. Riede, M. Grundmann
Frühjahrstagung der DPG, Regensburg, 11.-15.03.2002

Phonon modes and free-carrier-properties of ZnO, Zn(Mg, Cd)O and ZnO:Ga thin films (P)
C. Bundesmann, N. Ashkenov, A. Kasic, B. Mbenkum, M. Schubert, M. Lorenz, E.M. Kaidashev, D. Spemann, G. Wagner, M. Grundmann
Frühjahrstagung der DPG, Regensburg, 11.-15.03.2002

Ionenmikroskopie und Tomographie (T)
T. Butz
Ionenstrahltreffen, Göttingen, 29.-30.4.2002

Optical properties of ternary $Mg_xZn_{1-x}O$ thin films (P)
R. Schmidt, C. Bundesmann, N. Ashkenov, B. Rheinländer, M. Schubert, M. Lorenz, E.M. Kaidashev, D. Spemann, G. Wagner, A. Rahm, M. Grundmann
26th Int. Conf. on the Physics of Semiconductors (ICPS), Edinburgh, UK, 29.07.-02.08.2002

Active Compensation of Magnetic Stray Fields at LIPSION (P)
D. Spemann, T. Reinert, J. Vogt, J. Wassermann, T. Butz.

8th Int. Conf. on Nuclear Microprobe Technology and Applications (ICNMTA2002), Takasaki, Japan, 08.-13.09.2002

Evidence for Intrinsic Weak Ferromagnetism in a C60 Polymer by PIXE and MFM (P)
D. Spemann, K.-H. Han, R. Höhne, T. Makarova, P. Esquinazi, T. Butz
8th Int. Conf. on Nuclear Microprobe Technology and Applications (ICNMTA2002), Takasaki, Japan, 08.-13.09.2002

Quantitative Elemental Analysis of Biological Samples With Inhomogeneous Density Distribution (P)
T. Reinert, D. Spemann, T. Butz
8th Int. Conf. on Nuclear Microprobe Technology and Applications (ICNMTA2002), Takasaki, Japan, 08.-13.09.2002

Quantitative Microanalysis of Perineuronal Nets in Brain Tissue (T)
T. Reinert, D. Spemann, T. Butz
8th Int. Conf. on Nuclear Microprobe Technology and Applications (ICNMTA2002), Takasaki, Japan, 08.-13.09.2002

The Beta-1-Integrin and Interleukin-1-alpha Expression on the Bystander Effect Model via Medium Transport (P)
J. Österreicher, J. Jahns, G. Hildebrandt, J. Tanner, J. Vogt, J. Pejchal, T. Butz
ESTRO, Prague, 17.-21.9.2002

Ionenstrahlanalytische Untersuchung der perkutanen Aufnahme hochfeiner Titandioxid-partikel (T)
F. Menzel
WE-Heraeus-Ferienkurs 2002, Dresden, 23.9.2002

Einzelionenbeschuß lebender Zellen: die Bestrahlungsplattform an der Leipziger Nanosonde LIPSION und erste Ergebnisse zur Trefferverifizierung (T)
T. Butz
6. Jahrestagung der Gesellschaft für Biologische Strahlenforschung, Göttingen, 25.-27.9.2002

Ionenstrahlanalytische Untersuchung der perkutanen Aufnahme von ultrafeinen Titan-dioxidpartikeln (T)
F. Menzel, T. Reinert, J. Vogt, T. Butz
Arbeitstreffen Forschung mit nuklearen Sonden und Ionenstrahlen, Bonn, 1.10.2002

Raster-Protonenmikroskopie und -tomographie (T)
T. Butz, T. Reinert, D. Spemann, J. Vogt
Materialica, München, 30.9.–2.10.2003

^{204m}Pb - Eine TDPAC-Sonde für das Heimlabor (T)
W. Tröger, F. Heinrich, H. Haas
Arbeitstreffen Forschung mit nuklearen Sonden und Ionenstrahlen, Bonn, 1.10.2002

Dielectric properties of Fe-doped $BaTiO_3$ thin films on polycrystalline substrate for temperature from –35°C to +85°C (P)
M. Lorenz, H. Hochmuth, M. Schallner, R. Heidinger, D. Spemann, M. Grundmann
9th International Workshop on Oxide Electronics, St. Pete Beach, FL, USA, 20.-23.10.2002

Optical and electrical properties of epitaxial $(Mg, Cd)_xZn_{1-x}O$, ZnO, and ZnO:(Ga, Al) thin films on c-plane sapphire grown by PLD (P)
M. Lorenz, E.M. Kaidashev, H. von Wenckstern, V. Riede, G. Benndorf, H. Hochmuth, C. Bundesmann, D. Spemann, J. Lenzner, G. Wagner, M. Grundmann
9th International Workshop on Oxide Electronics, St. Pete Beach, FL, USA, 20.-23.10.2002

The bystander effect of ionizing radiation (P)
J. Österreicher, J. Tanner, J. Vogt, T. Butz
NATO HFMP Task group 006, Hradec Kralove, Czech Republic, 21.-24.10.2002

Early and late changes in irradiated lungs and treatment possibilities (P)
J. Österreicher, M. Kralik, J. Peichel, J. Skopek, L. Navratil, A. Macela
NATO HFMP Task group 006, Hradec Kralove, Czech Republic, 21.-24.10.2002

Structural, optical, and electrical properties of epitaxial ZnO, $(Mg, Cd)_xZn_{1-x}O$, and ZnO:(Ga, Al) thin films on sapphire grown by PLD (T)
M. Lorenz, E.M. Kaidashev, H. von Wenckstern, V. Riede, C. Bundesmann, D. Spemann, G. Benndorf, R. Schmidt, H. Hochmuth, A. Rahm, H.-C. Semmelhack, M. Schubert, M. Grundmann
2002 MRS workshop series: Second Int. Workshop on Zinc Oxide, Dayton, OH, U.S.A., 25.10.2002

Ionenmikrotomographie
T. Butz
Ionenstrahlmeeting, Stuttgart, 24.-26.11.2002

Scanning Proton Microscopy and Micro-Tomography (T)
T. Butz
Granzer-Workshop 2002, GSI Darmstadt, 2.-3.12.2002

Phonons, excitons, band-to-band transitions, and optical constants on MgZnO (T)
R. Schmidt, C. Bundesmann, N. Ashkenov, B. Rheinländer, M. Schubert, M. Lorenz, E.M. Kaidashev, D. Spemann, T. Butz, G. Wagner, C.M. Herzinger, J.A. Woollam, M. Grundmann
MRS Fall Meeting, Boston, MA, U.S.A., Dezember 2002

3.21 Graduations

3.21.1 Diploma Theses

F. Menzel
Ionenstrahlanalytische Untersuchung der perkutanen Aufnahme von ultrafeinen Partikeln
Diplomarbeit, Universität Leipzig (2002)

4 PHYSICS OF ANISOTROPIC FLUIDS — SCIENTIFIC ACTIVITIES

4.1 Broadband Dielectric Spectroscopy (F. Kremer, A. Schönhals, eds.)

4.2 Glass transition and molecular dynamics in thin polymer films

F. Kremer, L. Hartmann

Thin polymer films are an ideal system to study the influence of finite size effects on the polymer dynamics [1-3]. We focus on measurements of dipole fluctuations by dielectric spectroscopy to reveal deviations from the bulk behaviour when reducing the film thickness. In case of poly(dimethyl siloxane) (PDMS) we have studied the influence of different preparation techniques (grafted and spin cast films) on the molecular dynamics of this particular polymer besides that of mere variation of the film thickness [3].
In thin films of grafted PDMS of thickness d above and below the radius of gyration R_g we find bulk-like behavior for d=41nm>R_g whereas for d<R_g the dynamic glass transition (α-relaxation) is faster by up to two orders of magnitude than in the bulk. This behavior is explained by a increased free volume due to the grafting procedure. The α-relaxation in spin cast films compares well with that of the bulk with respect to the thermal activation down to a film thickness d of 14 nm. However, in these films a new relaxation shows up which is again faster than any relaxation in the bulk. It is presently assumed that this process has to be assigned to the relaxation of dipoles being situated close to the film surface. In all films the α_c-relaxation related to fluctuations in the amorphous fraction of PDMS above crystallization has been observed showing no particular dependence of the geometric confinement.

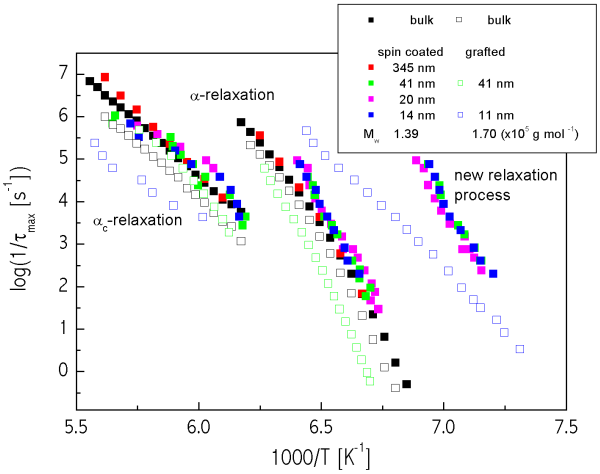

Activation plot for PDMS of two adjacent molecular weights in the bulk (black symbols), as grafted layers (open colored symbols) and as spin cast films (full colored symbols).

References:

[1] L. Hartmann, W. Gorbatschow, J. Hauwede, F. Kremer, Eur. Phys. J. E 8, 145 (2002).
[2] L. Hartmann, K. Fukao, F. Kremer, Molecular Dynamics in Thin Polymer Films "Broadband Dielectric Spectroscopy" p. 433, (Springer Verlag, Berlin, 2002), F. Kremer, A. Schönhals (Eds.)
[3] L. Hartmann, F. Kremer, P. Pouret, L. Léger, Molecular Dynamics in grafted layers of poly(dimethylsiloxane) (PDMS) , J. Chem. Phys., in press (2002).

Collaborators: Dr. W. Gorbatschow (Kiev), Dr. Y. Grohens (Lorient), Dr. H.-G. Braun (Dresden), Prof. L. Léger (Paris)

4.3 A novel confinement-induced relaxation process in thin films of cis-polyisoprene

F. Kremer, A. Serghei

Broadband Dielectric Spectroscopy is employed to investigate the molecular dynamics of thin layers of cis-1,4-polyisoprene (PI) down to thicknesses smaller than the end-to-end distance of the PI chains. Two relaxation processes are observed in the bulk, which take place on two different length scales: the segmental mode (corresponding to the dynamic glass transition) and the normal mode, which originates from the relaxation of the end-to-end vector of the chain. With decreasing thickness a novel confinement-induced mode is observed between the segmental and the normal relaxation process. It becomes faster with increasing confinement and does not show a molecular weight dependence. It is assigned to fluctuations of terminal subchains which are formed due to the immobilization of chain segments at an interface. In contrast, the segmental and the normal mode are not affected in their relaxation rate down to thicknesses of 2 R_{EE}, but the dielectric strength of the normal mode shows a steep decline with decreasing thickness.

Simulations of the chains as ideal random walks reveal the existence of a confinement-induced and thickness dependent distribution for the terminal subchains, which arises from chains immobilized at one interface and reflected at the other one. It is shifted to shorter values with increasing confinement and does not show a molecular weight dependence, in full agreement with the experiment.

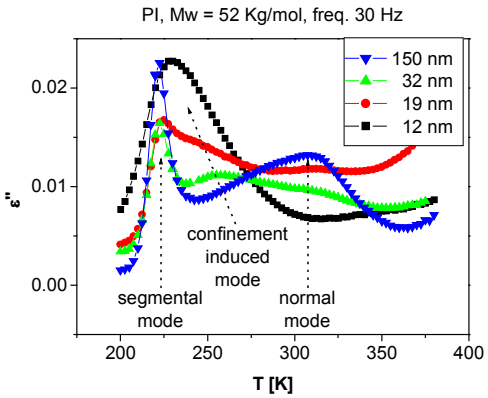

Fig. 1

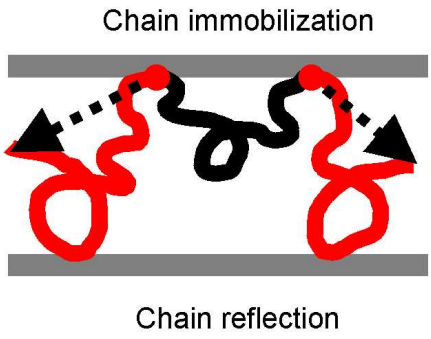

Fig. 2

Fig. 1 Dielectric loss versus temperature for different thicknesses.
Fig. 2 Terminal subchains formed by immobilization of chain segments at an interface.

References:
[1] A. Serghei, F. Kremer, submitted to PRL
[2] A. Serghei, F. Kremer, W. Kob, submitted to EJPE

Collaborators:
W. Kob (Montpellier, France)

4.4 Optical tweezers as a tool to unfold RNA-aptamers

F. Kremer, M. Salomo, M. Struhalla, J. Reinmuth, V. Skokow

Optical tweezers are commonly used to manipulate microscopic particles, with applications in cell manipulation, colloid research, manipulation of micromachines and studies of the properties of light beams. With their extraordinary resolution in space (~2 nm) and force they became a irreplaceable tool for such purposes (~0.1 pN).
In our projects we want to use them to study folding and unfolding mechanisms of nucleic acids.
Our first project deals with the unfolding of RNA-aptamers. We want to immobilize a single aptamer molecule between two polystyrene particles. One of them is fixed with a femtotip. The other one is held in the beam of an optical tweezer. To realize the necessary distance between the two colloids the aptamer-RNA was elongated by 500 bases on both ends. The immobilization between the two particles is then realized by DNA/RNA-hybrids (Figure 1). With the use of this experimental set-up it is possible to apply forces in the range of piconewtons on the folded RNA-sequence. The aim of these experiments is to investigate the behaviour of two aptamers that have specific binding partners, an aptamer that binds to the antibiotic moenomycin A and a second one that has thrombin as binding partner. We want to investigate the differences in their folding behaviour in absence and presence of their binding partners.

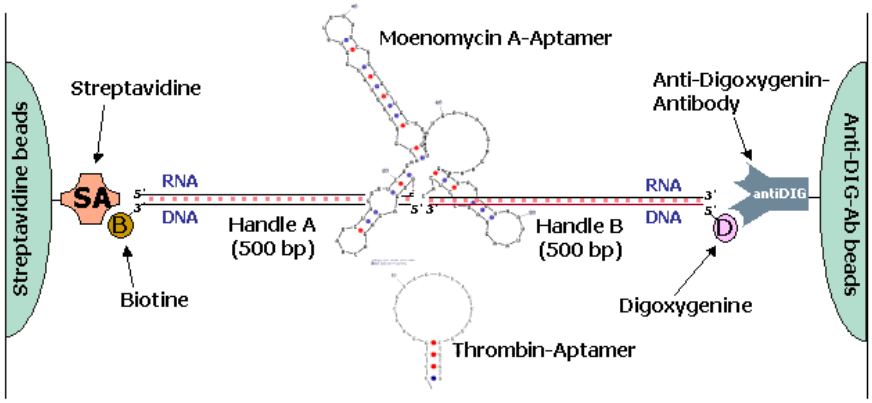

Figure1: Schematic representation of the molecular arrangement between the two beads.

We achieved first successes in our research, because we were able to immobilize these constructs between two particles and additionally it was possible to hold these constructs stable in the optical tweezer.

References:
[1] J. Liphardt et al., Science 292, 733-737 (2001)

Collaborators :
Prof. Dr. U. Hahn (University of Hamburg)

4.5 Investigating DNA-binding proteins with optical tweezers

F. Kremer, M. Salomo, M. Struhalla, J. Reinmuth, V. Skokow,

Sac7d belongs to a class of small chromosomal proteins identified in the hyperthermophilic archaeon Sulfolobus acidocaldarius. It is extremely stable to heat, acid and chemical agents and binds strongly to the minor groove of DNA, causing a sharpe kinking of the DNA helix leading to a shortening of the DNA (Figure 2). Our project has the aim to investigate the influence of this DNA-binding Protein on a DNA-double helix immobilized between two particles. We want to use the optical tweezer to measure the dimension of this shortening. Theoretically the protein binds to the DNA every 3 bp leading to a theoretical compaction ratio of ~1.2. At the moment we are about to produce and purify the protein. Further on we made some experiments to immobilize a DNA-double helix between two polystyrene particles and we were able to establish a system as shown in Figure 1. There can see two particles, one is fixed by a glass micropipette, the other is held by the optical tweezers. Via Streptavidin/Biotin- and Digoxigenin/Anti-Digoxigenin interactions we were able to immobilize a single DNA-molecule between these particles.

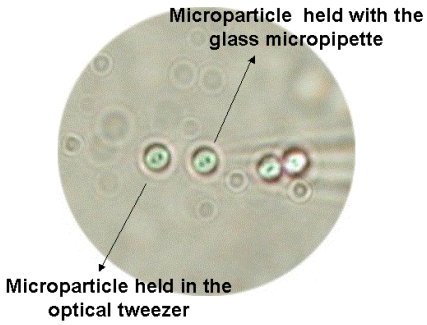

Fig. 1

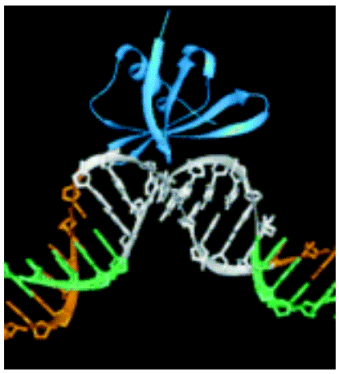

Fig. 2

Fig. 1:Two beads (∅ 2.2 µm) of which one is hold by a nanotip while the other fluctuates in the photonic potential. Fig. 2 Model of the binding mechanism of the Sac7d protein (blue) to a DNA helix.

References:

[1] H. Robinson et al.; Nature 392, 202-205 (1998)
[2] J.G. McAfee et al. ; Bioch. 34, 10063- 10077 (1995)
[3] D. Kulms et al.; Biol. Chem. 378, 545-551(1997)

Collaborators: Prof. Dr. U. Hahn (University of Hamburg)

4.6 Michelson-interferometry of smectic elastomers

F. Kremer, M. Tammer

Ferroelectric liquid crystals embedded into a polymer network can show high electrostriction in the C* phase due to a mesogenic tilt forced by external electric fields [1]. By a photochemically induced crosslinking reaction of additional sidechains, the hereby formed ferroelectric liquid crystal elastomers (FLCE) are prevented from flow and thin (~µm) free standing films with viscoelestic properties can be prepared. The smectic layer normal in such films is parallel to the surface normal and the change in thickness of the individual layers can result in a high expansion of the film thickness.
An ultra stable Michelson interferometer is used to detect any change in optical path length for the Laser beam transmitted through the sample during the application of an AC field up to 2.5 MV/m. The interferometer is equipped with a reflection microscope in order to control the spot of the sample where the Laser beam hits the film. Together with the small Laser diameter of around 0.2 mm, this assures a measurement in a homogeneous region of the free standing film. The smallest phase shift detectable by this setup equals a thickness change of less than 0.1 nm depending of the frequency of the AC field. One example of the resolution is given in the graph for a 1 kHz AC field.

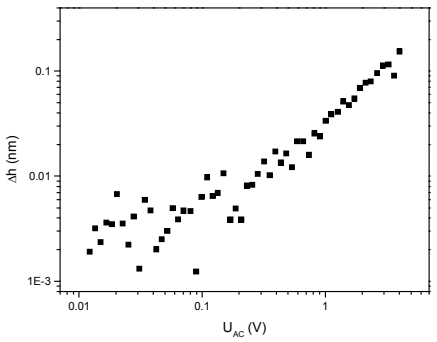

The goal of the project is to optimize the interferometer setup for measurements of thickness changes of less than 1 nm at low frequencies below 100 Hz and to specify the magnitude of the electrostrictive effect in FLCEs and its dependence on temperature, number of crosslinked sidechains and the type of crosslinking (interlayer and intralayer).
Various FLCEs with different mesogens and different numbers of crosslinking groups are synthesized by the group of Prof. Zentel [2].

References:
[1] W. Lehmanm, H. Skupin, C. Tolksdorf, E. Gebhard, R. Zentel, P. Krüger, M. Lösche, F. Kremer, Nature 410, 447 (2001).
[2] E. Gebhard, R. Zentel, Macromol. Chem. Phy. 201, 902 (2000)

Collaborators:
Prof. Dr. R. Zentel (Mainz)

4.7 An AFM and GISAXS study of the lamellar orientation in thin diblock copolymer films

Christine M. Papadakis, Peter Busch

Block copolymer thin films offer an opportunity for patterning of surfaces on the sub-micrometer scale. We find that molar mass is a parameter allowing control of nano-patterning in thin films of symmetric, lamellae-forming polystyrene-polybutadiene (PS-PB) diblock copolymers [1]. By means of tapping mode AFM, information about the surface topography can be obtained (Fig. 1a). The structure within the film can be elucidated in grazing-incidence small-angle X-ray scattering (GISAXS, Fig. 1b). This technique allows the detection of both the lateral and vertical structural correlations within the films. The use of a high-resolution CCD camera leads to a large amount of detail in the two-dimensional GISAXS maps. A quantitative understanding of the scattering intensity can be gained using the distorted-wave Born approximation, which includes scattering as well as reflection from the film/substrate interface.
For low molar masses, the lamellae are parallel to the surface, as confirmed by the terraces at the surface topography observed by AFM and the modulated intensity in the scattering plane. For high molar masses, however, the lamellae are perpendicular to the surface, as evidenced by a lamellar surface texture (Fig. 1a) and out-of-plane Bragg rods (Fig. 1b). The combination of these methods is thus a powerful tool to gain detailed information about the film structure. We suspect that this behavior is due to the weak enthalpic interactions of both blocks with air and the film substrate together with the molar-mass dependent entropic interactions of the stretched copolymers and the film interfaces.

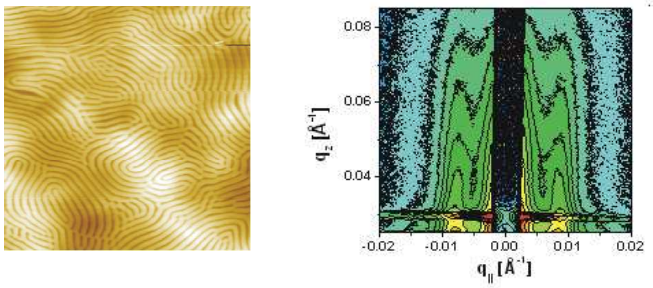

Fig. 1: (left) Surface topography (3×3 µm scan size) and (right) 2D GISAXS map of a thin film of PS-PB having a molar mass of 183 kg/mol, a lamellar thickness of 839 Å and a film thickness of 2350 Å.

Collaborators:
PD Dr. Bernd Rheinländer (University of Leipzig), Prof. Dr. Dorthe Posselt (Roskilde University, Denmark), Dr. Detlef Smilgies (Cornell University, Ithaca, NY, USA), Prof. Dr. Igor I. Potemkin (Moscow State University), Dr Markus Rauscher (MPI für Metallforschung, Stuttgart).

References:
[1] D.-M. Smilgies, P. Busch, D. Posselt and C.M. Papadakis, Synchr. Rad. News, 15, 35 (2002).

4.8 A GISAXS study of thin films of binary block copolymer blends

C.M. Papadakis, P. Busch

Binary blends of symmetric diblock copolymers only differing in molar mass form in the bulk either a lamellar one-phase state or a macrophase-separated state consisting of lamellar domains having different lamellar thicknesses [1]. The aim of the present study was to gain information on the influence of the thin film geometry on the phase behavior and structure of such blends [2]. Blends of polystyrene-polybutadiene diblock copolymers forming in the bulk lamellar domains with lamellar thicknesses 200 and 400 Å were studied. Atomic force microscopy revealed only weakly textured film surfaces. We therefore used grazing-incidence small-angle X-ray scattering (GISAXS) in order to elucidate the structures *within* the films (Fig. 1).
The GISAXS maps (Fig. 2) show Bragg rods outside the scattering plane (i.e. at finite q_y) for a sample from the bulk one-phase state, indicating that the lamellae are perpendicular to the film surface. In the macrophase-separated state, Bragg rods are observed as well. In addition, more and more intense intensity modulations are observed along the q_z-axis (film normal) as the volume fraction of short copolymers is increased, pointing to a lamellar structure parallel to the film surface. The thin film geometry thus has a significant influence on the lamellar structure of the blends.

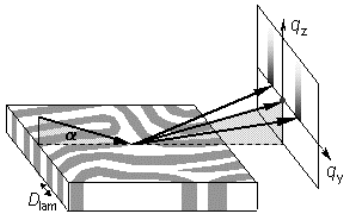

Fig. 1 (left): Setup of the GISAXS experiment
Fig. 2 (below): GISAXS maps from the thin films studied. Logarithmic intensity scale.

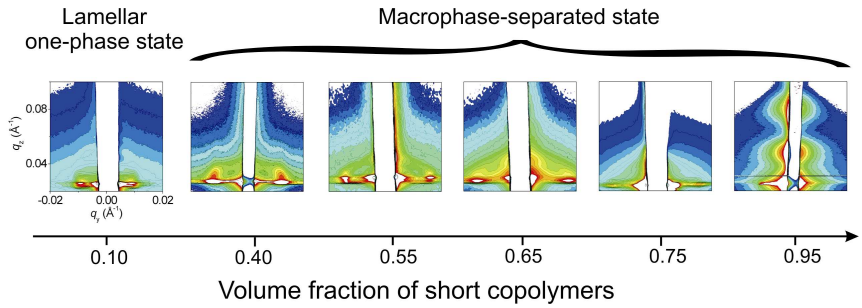

References:

[1] C.M. Papadakis, K. Mortensen, D. Posselt, Eur. Phys. J. B 4, 325 (1998).
[2] P. Busch, F. Kremer, C.M. Papadakis, D. Posselt, D.-M. Smilgies, submitted to the Proceedings of the Sino-German Meeting on Macromolecules, Beijing, April 2002.

Collaborators:

D. Posselt (Roskilde, Dänemark), D.-M. Smilgies (Ithaca, NY, USA)

4.9 Fluorescence correlation spectroscopy investigations of diffusion of water-soluble polymers

C. M. Papadakis, T. B. Bonné

Fluorescence correlation spectroscopy is a method to study the self-diffusion of fluorescence-labeled molecules. With this method, the detection volume is very small (approx. 1 μm^3), and the measurements are carried out on the basis of very few molecules.

We have studied aqueous solutions of water-soluble poly(oxazoline) based polymers. They have the advantage of being very versatile in architecture and degree of hydrophobicity, for instance. We have determined the virial coefficient of poly(methyloxazolin) homopolymers of different molar mass, labeled with a fluorescent dye. In order to achieve high concentrations and to minimize the influence of the fluorescence label on aggregation, we increase concentration by adding the identical non-labeled polymers.

We have also studied the micellization of poly(methyloxazoline)-poly(nonyloxazoline) (PMeOx–PNoOx) diblock copolymers in aqueous solution. Fig. 1 shows the concentration dependence of a PMeOx40-PNoOx7 diblock copolymer (the numbers indicate the degrees of polymerization) where the fluorescence label is attached to the hydrophobic block The non-labeled polymers show a single diffusion process, whereas in solutions containing both labeled and non-labeled polymers, two diffusion processes are observed. The latter can be attributed to the diffusion of unimers (fast process) and micelles (slow process).

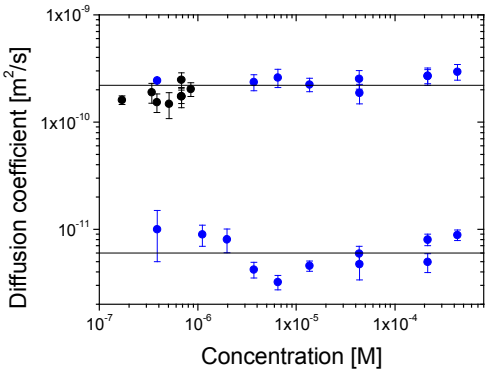

Fig. 1: Diffusivities of PMeOx40-$PNoOx_7$. Black circles: Solutions of labeled polymers only, blue circles: solutions of labeled and non-labeled polymers. The lines indicate the average values of the two diffusion coefficients.

Collaborators:
Prof. Dr. Ulrich Hahn (University of Hamburg), Dr. Thomas Greiner-Stöffele (Fakultät für Biowissenschaften, Pharmazie und Psychologie, Uni Leipzig), Dr. Rainer Jordan, Dipl.-Chem. Karin Luedtke (TU München).

4.10 Collective dynamics and self-diffusion in a body-centered cubic diblock copolymer melt

C.M. Papadakis

Strongly asymmetric diblock copolymers in the melt form a body-centered cubic (bcc) phase with spherical micelles formed by the shorter blocks at the lattice points. We have studied a low molar mass poly(ethylene propylene)-poly(dimethyl siloxane) (PEP-PDMS) diblock copolymer melt having a volume fraction of PEP of 0.16 in a large temperature range. By means of small-angle neutron scattering (SANS), we could identify the bcc structure (Fig. 1a) below the order-to-disorder transition temperature (240°C). The dynamics were studied using dynamic light scattering (DLS) and pulsed field gradient (PFG) NMR [1].

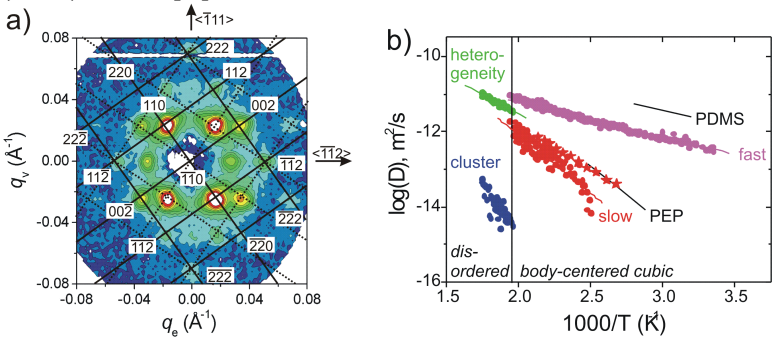

Fig. 1: (a) Indexed 2D SANS image on a macroscopically aligned sample in the bcc state. (b) Arrhenius representation of the diffusivities obtained using DLS (circles) and PFG NMR (stars) together with the diffusivities from the corresponding homopolymers.

In the disordered state at high temperatures, we observe in DLS the well-known heterogeneity mode which is due to the diffusion of single copolymers through the melt and the usually observed slow cluster mode (Fig. 1b). In the bcc phase, two diffusive processes are found: The fast process has an activation energy very similar to the one of pure PDMS and is not observed in PFG NMR, i.e. it is not due to long-range diffusion. We ascribe it to overdamped fluctuations of the positions of the micellar cores (PEP), relaxing by deformation of the brushes formed by the corona blocks (PDMS). A similar dynamic process has been observed in colloidal systems [2]. The slower process in the bcc state coincides with the one observed in PFG NMR, and it is due to the activated long-range self-diffusion of single copolymers from micelle to micelle or to the diffusion of entire micelles. The dynamics in the bcc phase thus display both colloidal and polymeric features.

References:

[1] C.M. Papadakis, F. Rittig, K. Almdal, K. Mortensen, P. Štěpánek, Eur. Phys. J. E., submitted

[2] M. Hoppenbrouwers, W. van de Water, Phys. Rev. Lett. 80, 3871 (1998)

Collaborators: J. Kärger (University of Leipzig), F. Rittig (BASF), K. Almdal, K. Mortensen (Roskilde, Denmark), P. Štěpánek (Prague, Czech Republic)

4.11 Noise driven dynamic patterns and On-Off intermittency

R. Stannarius, T. John

We study fundamental principles of spontaneous dissipative pattern formation under stochastic excitation. In nematics exposed to electromagnetic fields, electrohydrodynamic convection (EHC) patterns represent flow equilibrium structures. Polarizing microscopy and laser diffraction methods are exploited here to characterize these patterns [1-4].
In stochastically driven EHC, *on-off intermittency* has been discovered experimentally [1,2]. The nematic EHC cell serves here as a simple and easily controllable model system where fundamental scaling laws for this phenomenon can be tested [2-4]. The nematic is exposed to a stochastic driving voltage (dichotomous Markov process), and trajectories of the pattern amplitudes are determined from records of the diffraction peak intensities.

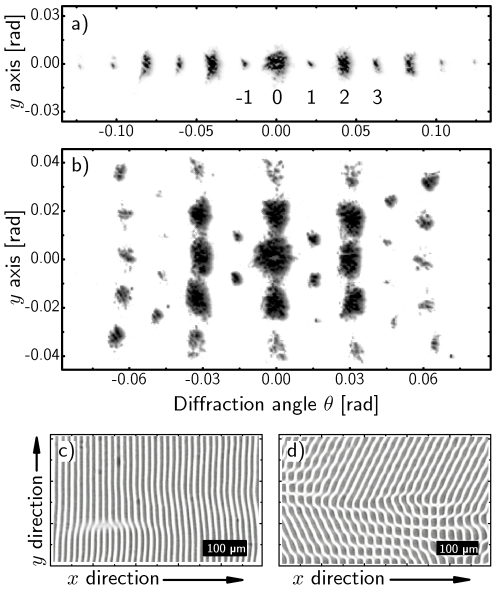

The pictures show diffraction images of electroconvection rolls in a planar cell of 25.8 µm thickness driven by deterministic AC voltages of 30 Hz (a) and 10 Hz (b). The corresponding shadow graph images of the rolls are shown in the bottom images (c) and (d) for the same frequencies of 30 Hz and 10 Hz, respectively.
In order to establish quantitative relations between the diffraction profiles and the pattern amplitudes, an analytical and numerical treatment of light propagation in 2D inhomogeneous director field has been elaborated [5]. The calculated diffraction efficiencies for different diffraction order peaks are in good agreement with the experiment. These calculations do not only allow to determine the director deflection amplitudes of EHC quantitatively, but they are relevant for other experiments where 2D inhomogeneous anisotropic optical media are involved.

References:

[1] H. Amm, U. Behn, T. John, R. Stannarius, Mol. Cryst. Liq. Cryst. 304 525 (1997).
[2] T. John, R. Stannarius, and U. Behn. Phys. Rev. Lett. 83 749, (1999).
[3] U. Behn, T. John, R. Stannarius, AIP Conf. Proc, 622 381 (2002).
[4] T. John, U. Behn, R. Stannarius, Phys. Rev. E 65 046229 (2002).
[5] T. John, U. Behn, R. Stannarius, Europhys. J. B (subm. 2002).

Collaboration:
Prof. Dr. U. Behn (ITP Leipzig),
Dr. T. Scharf (Neuchatel)

4.12 Surface and interface tensions of smectic and isotropic phases

R. Stannarius, H. Schüring

Isotropic inclusions in freely suspended thin smectic films are investigated my means of polarizing microscopy. From the shapes and dynamics of isotropic droplets in the film one can derive information about surface and interface tensions of smectogens in different phases. A model that considers all relevant interface tensions and the difference of surface tensions in smectic and isotropic phase has been developed. The surface tension difference between both phases can be explained within a microscopic model, on the basis of the assumption of a surface phase transition from the isotropic phase to a smectic surface interphase. An extension of the model to inhomogeneously thick films explains the spontaneous arrangement of droplets at film thickness steps (see image), and the capillary force driven motion of droplets in the direction of the film thickness gradient.

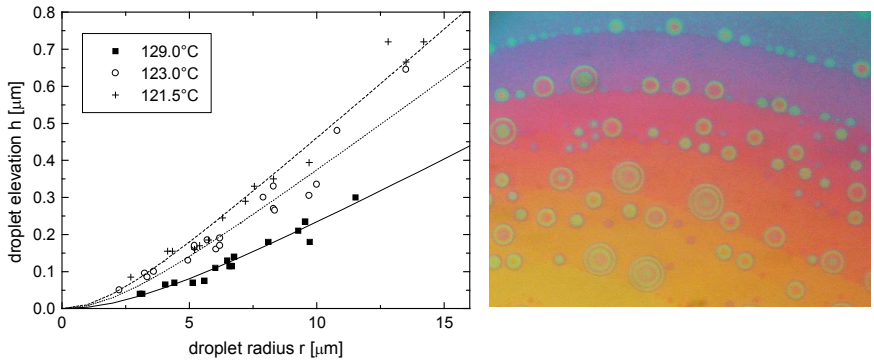

Fig. 1 Isotropic droplets in a thin (~250nm thick) freely suspended film of a smectic polymer near the clearing point (right) and droplet height vs. radius dependence (right).

References:
[1] H. Schüring, R. Stannarius, Langmuir. 18 9735 (2002),
[2] H. Schüring, R. Stannarius, Mol. Cryst. Liq. Cryst. (submitted 2002).

Collaboration:
Prof. Dr. W. Weißflog (Halle)

4.13 Liquid Crystals in Confining Geometries

R. Stannarius, F. Kremer

Due to their complexity and long range orientational order, the behaviour of liquid crystalline (LC) phases can be substantially influenced by geometrical restrictions even in cavities of macroscopic (micrometer) scale.
Confinement in nanometer cavities influences the very character of LC mesophases [1-3], phase transition temperatures are shifted and the orientational order changes depending upon the geometry of the porous matrix and interactions of the mesogens with the substrate. Our recent research activities are focussed on the study of collective dynamic properties of confined ferroelectric smectic phases [4-8]. The ferroelectric properties depend crucially on the cavity sizes and pore geometry. Adsorber materials investigated are sol-gel glasses, cellulose membranes and ordered Anopore filters.

From dielectric studies of Anopore adsorbed high spontaneous polarization material, the existence of a new flexoelectric mode has been proposed [8]. Of particular interest in our studies of confined LCs are systems with irregular geometrical structure like cellulose membranes, which can induce a state of randomly frozen disorder in the liquid crystal configuration [6,7].

References:
[1] Ch. Cramer, Th. Cramer, F. Kremer, R. Stannarius. J. Chem. Phys. 106, 3730 (1997).
Ch. Cramer et al. Mol. Cryst. Liq. Cryst. 303, 209, (1997).
[2] S. Rozanski et al. Mol. Cryst. Liq. Cryst. 303, 319 (1997).
[3] S. Rozanski, R. Stannarius, F. Kremer. Z. Phys. Chem., 211 147, (1999).
S. Rozanski et al. Proc. SPIE 3181, 119 (1997); 3318, 233 (1998).
[4] L. Naji, F. Kremer, R. Stannarius. Liq. Cryst. 25 363 (1998).
[5] S. Rozanski, L. Naji, F. Kremer, R. Stannarius. Mol. Cryst. Liq. Cryst. 329 1095, (1999).
[6] S. Rozanski, F. Kremer, and R. Stannarius Proc. IEEE 8 488 (2001).
[7] S. Rozanski, R. Stannarius, F. Kremer, S. Diele, Liq. Cryst. 28 1071 (2001).
[8] S. Rozanski, R. Stannarius, F. Kremer, SPIE Pl 4759 178 (2002).

Collaboration:
Dr. St. Rozanski (Pila)

4.14 Smectic liquid crystalline elastomers

R. Stannarius, R. Köhler

A fundamental property of smectic liquid crystalline phases is their ability to form ultrathin stable films with controlled thickness from two to several thousand molecular layers. Liquid crystalline elastomer (LCE) balloons can be prepared by UV irradiation of bubbles of crosslinkable smectic polymers. Elastic forces balance the pressure difference, the pressure/radius yields elastic moduli of the anisotropic rubber [1-3]. A model considering both rubber elastic (entropic) contributions and smectic layer compression on the stress-strain characteristics of smectic LCE balloons has been developed. We observe an anomalous '*soft elastic*' behaviour in the tilted smectic C* phase of some elastomers[4].
Thin planar elastomer films for dilatometric experiments can be prepared by crosslinking planar free standing polymer films in a planar frame. By means of a novel technique, we are able to partially crosslink films, so that nanometer thick polymer strips of a few micrometers length can be obtained (see image). The picture shows part of a 250 nm thick film with a lateral extensions of 3 mm x 1 mm that has been mechanically stretched unidirectionally in the film plane by ~66%.

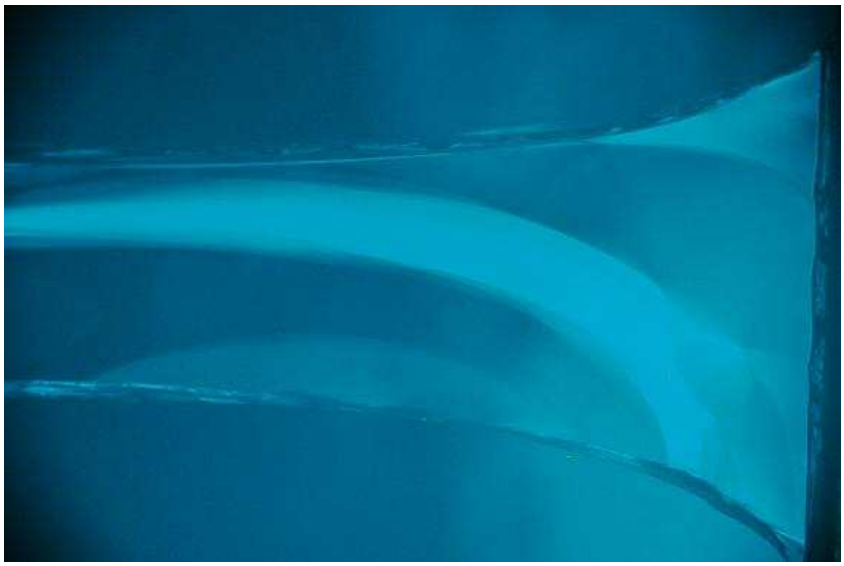

References:
[1] H.Schüring, R. Stannarius, C. Tolksdorf, R. Zentel. Mol. Cryst. Liq. Cryst., 364 305 (2001); Macromolecules 34 3962 (2001).
[2] R. Stannarius, R. Köhler, U. Dietrich, J.-J. Li, M. Lösche, C. Tolksdorf, R. Zentel, Phys. Rev. E 65 041707 (2002).
[3] C. Tolksdorf, R. Zentel, R. Köhler, U. Dietrich, M. Lösche, and R. Stannarius. Mat. Res. Soc. Symp. Proc., 709 23 (2002).
[4] R. Köhler et al., Proc. SPIE 4759 483 (2002)

Collaboration: Prof. Dr. R. Zentel (Mainz) , Prof. Dr. M. Lösche (IEP I Leipzig)

4.15 Thermoreversible liquid crystalline hydrogen bonded gels

J.-J. Li, R. Stannarius,

Liquid crystalline (LC) gels have been investigated extensively during the last decade, and several applications in display and storage devices have been proposed. The formation of a gel network influences, e.g. orientational order and switching characteristics of ferroelectric smectic phases. One of the technical aspects is the stabilization of thin cells with ferroelectric material with a gel network to achieve linear electro-optic response of the cells ('*v-shaped switching*') for grey scale capabilities of displays [1].
.
We study the electro-optic characteristics of these hydrogen bonded LC gels in free standing film geometry by means of polarizing microscopy. The gel network is phase-separated from the LC and grows anisotropically. It exhibits a domain structure which is directly connected with the mesogenic orientation during network formation. The gel films can be switched by means of in-plane electric fields of a few kV/m. Whereas the reorientation of the orientational axis is only slightly hindered by the formation of the gel, mass flow related effects as e. g. electroconvection are massively suppressed.

Recent activities include the search for appropriate gel former materials in different smectic and nematic phases, and the characterization of novel mixtures by means of NMR and polarizing microscopy.

References:
[1] J.-J. Li, X. Zhu, L. Xuan, X. Huang, Ferroelectrics (subm. 2001).
[2] C. Tolksdorf, R. Zentel, Adv. Materials 13 1307 (2001),
[3] J.-J. Li, R.Stannarius, Ch. Tolksdorf, R. Zentel, PhysChemChemPhys (in press 2002).

Collaboration:
Prof. Dr. R. Zentel (Mainz),
Prof. D. Geschke

4.16 Banana and hockey stick shaped mesogens

J.-J. Li, R. Stannarius,

Liquid crystal mesogens with unusual sterical properties have been found to exhibit exotic mesophases with extraordinary symmetry properties. Banana-shaped non-chiral mesogens can form chiral smectic antiferroelectric or ferroelectric phases. We study the structure and dynamics of freely suspended films of these materials and determine their electro-optical characteristics[1,2]. Special focus is laid upon novel types of 'hockey stick' shaped material, which exhibits a ferroelectric phase although the molecular shape deviates only marginally from commonly known calamitic mesogens [3].

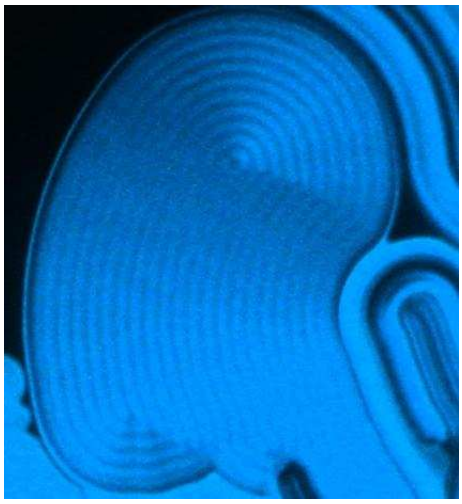

Another interesting aspect is the first observation of freely suspended films in the B7 phase. Such films develop a spontaneous splay deformation which results in a typical stripe texture. Investigations of stripe distances and structure and the optical features of such films are being performed to understand the molecular structure of the B7 mesophase.

The image shows a typical texture of a B7 film taken at 110°C, the stripe distance in the central domain is approximately 2.5µm. The image is taken in monochromatic light in a reflection microscope,

References:

[1] R. Stannarius, C. Langer, and W. Weißflog. Ferroelectrics, 277 177, (2002).
[2] R. Stannarius, C. Langer, and W. Weißflog. Phys. Rev. E, 66 031709, (2002).
[3] R. Stannarius, J. Li, and W. Weißflog. Phys. Rev. Lett., (in press 2002).

Collaboration:
Prof. Dr. W. Weissflog (Halle)

4.17 NMR investigations of banana-shaped molecules

S. Grande, A. Eremin, W. Weißflog

NMR measurements are used to determine orientational order, conformation and constitution of banana shaped molecules in typical the liquid crystalline phases (B_2, B_5, B_7 and others). Different substituents at carbon 10 (Cl, CN, D), C11 (F, D) and C12 (CH3) change the phase sequences. The substitution of H by F at C2 offers new NMR information and gives a richer polymorphism [1, 2]. The polymorphism $S_{C,}$ B_X for the mono-substituted CN and disubstituted Cl is especially interesting [2].

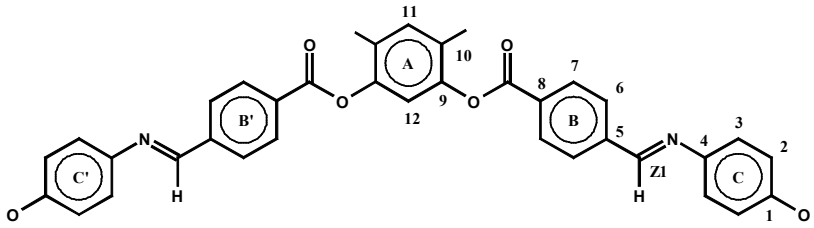

Fig. 1 Structure of banana-shaped molecules

An homogeneous orientation of the molecular long axes in the strong measuring magnetic field (11.7T) is important for well resolved spectra. This is usually obtained for B_2 and B_5 phases but not for the B_7 phase, a few B_2 phases behave like B_7.The anisotropic ^{13}C shifts and proton splittings of the atoms in the central ring are used to calculate the orientational order parameters S and D [1, 2, 3, 4, 5]. S is in the order of 0.8 in the B_2 and B_5 and does not change markedly with the temperature. From the 2H-quadrupol splitting a D=0,05 in the B2 phase is calculated, the anisotropy in the order fluctuations is of the same order as for calamitic systems. The comparison with reference compounds of known geometry allows a quantitative calculation of the geometry of the legs with respect to the long axis (tilt angle). The tilt depends on substitution [3], it increases with lower temperatures in 10-CN and 10-Cl compound [1, 2, 4].

References:

[1] I.Wirth, S. Diele, A. Eremin, G. Pelzl, S. Grande, L. Kovalenko, N. Pancenko, W. Weissflog, New Variants of polymorphism in banan-shaped mesogens with cyano-substituted central core, J. Mat. Chem., im Druck

[2] A. Eremin, S. Diele, G. Pelzl, H. Nadasi, W: Weissflog, 30. Freiburger Arbeitstagung Flüssigkristalle, 2002

[3]. B. Das, S. Grande, S. Diele, A. Eremin, G. Pelzl, H. Nadasi, W. Weißflog, 30. Freiburger Arbeitstagung Flüssigkristalle, 2002

[4] H. Nadasi, W. Weissflog, A. Eremin, G. Pelzl, S. Diele, B. Das, S. Grande, J. Mater. Chem. accepted

[5]] H. Nadasi, U. Dunemann, W. Weissflog, A. Eremin, S. Grande, G. Pelzl, S. Diele, 30. Freiburger Arbeitstagung Flüssigkristalle, 2002

Collaborators: Prof. Pelzl, Prof. Weißflog, Institut für Physikalische Chemie des Fachbereiches Chemie, Universität Halle

4.18 Conformation of hockey-stick molecules

S. Grande, A. Das, G. Pelzl

The special phase sequences of bended banana-shaped molecules and the polar properties of this phases activates the synthesis of new compounds with bended geometries. The m-substitution of an alkoxy-chain in a three ring compound ($C_nH_{2n+1}O$-C_6H_4-COO-C_6H_4-CHN-C_6H_4m-O C_nH_{21} with n=10/A, n=11/B, n=12/C) bends the molecule quite different from the classical banana shape.

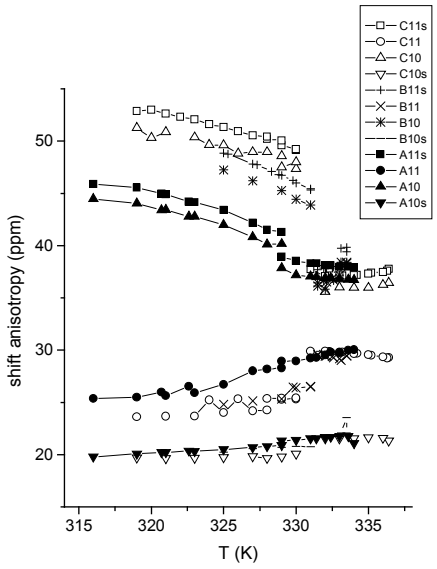

X-ray and NMR investigations are used to characterize the phases. The polymorphism begins at high temperatures with a smA phase followed by smC phase and a second smC phase. The second phase transition is not visible in the x-ray data but changes the NMR spectra drastically. We use ^{13}C and ^{1}H NMR for the characterization of orientational order and molecular conformation the in the different phases [1,2]. The S_{eff} increases for the three compounds in the high phases but decrease in the low phase. We interpret this as a consequence of a tilt of the whole molecule with respect to the field. Assuming a continuos increase of S we obtain tilt angles between 15 ° and 30°. Since the director is already tilted in the high temperture SmC phase, we interpret the NMR results by a symmetry breaking du to the formation of an anticlinic tilt structure. The transition is triggered by a change in the conformation of the right aromatic ring. The temperature dependence of the shift anisotropy in the molecuar frame (Fig) can only explained by a change in the geometry of right ring. The plane of this ring together with the chain rotates from a more perpendicular to a more planar conformation. The molecular shape is then more bended and the molecular packing prefers a zick-zack arrangement of the central segments.

References:
[1] S. Diele, , S. Grande, J. Kain, G. Pelzl, W. Weissflog,
Mol. Cryst. Liq. Cryst. 362, 111 (2001)
[2] B. Das, S. Grande, W. Weissflog, A. Eremin, W. Schröder, G. Pelzl, S. Diele, H. Kresse,
Liquid Crystals, in press (2002)

Collaborators:
Prof. Pelzl, Prof. Weißflog, Institut für Physikalische Chemie des Fachbereiches Chemie, Universität Halle

4.19 Funding

Prof. Dr. F. Kremer
Dynamik und Mobilität in (ultra)-dünnen Polymerfilmen
SFB 294, TP G6 (2000–2002)

Dr. R. Stannarius, Prof. Dr. F. Kremer
Flüssigkristalline Phasen in einschränkenden Geometrien
SFB 294, TP G9 (2000–2002)

Prof. Dr. F. Kremer
Optische Pinzette als mikroskopische Sensoren und Aktuatoren zum Studium der Wechselwirkung zwischen einzelnen Biomolekülen
SMWK-Projekt 7531.50-02-0361-01/11 (2001-2003)

Dr. C. M. Papadakis, Prof. Dr. J. Kärger
Molekularer Transport und Struktur in mehrphasigen Polymersystemen
SFB 294, TP G4 (2000–2002)

Dr. C. M. Papadakis
Strukturbildung in dünnen Filmen aus symmetrischen Diblockcopolymeren
DFG-Projekt, PA 771/1-1 (2001-2003)

Dr. C. M. Papadakis, Dr. I.I. Potemkin (Moscow State University)
Structure formation in thin diblock copolymer films
NATO Collaborative Linkage Grant (2001-2003)

Prof. Dr. U. Behn, Dr. R. Stannarius
Stabilität und statistische Charakterisierung von EHC in Nematen unter stochastischer Anregung
DFG-Projekt, Be 1417/4 (1999-2003)

Dr. R. Stannarius
Struktur und Dynamik dünner Flüssigkristallfilme
SFB 294, TP F4 (2000-2002)

Dr. R. Stannarius
Rayleigh-Benard-Konvektion in freitragenden smektischen Filmen
DFG-Projekt, Sta 425/8 (1998-2002)

Dr. R. Stannarius
Flüssige Filamente
DFG-Projekt, Sta 425/14 (2002-2004)

Dr. R. Stannarius
Mechanische Eigenschaften smektischer Elastomere
DFG-Projekt, Sta 425/15 (2002-2005)

4.20 External cooperations

Industry
Novocontrol
Hundsangen, Deutschland

Comtech GmbH
München, Deutschland

ISTAG AG
Research&Development Center
Egliswil, Schweiz

4.21 Publications

Brodowsky, H. M., E. M. Terentjew, F. Kremer, and R. Zentel
"Induced roughness in thin films of smectic C* elastomers"
Europhysics Letters Vol. **57**, 1, 53-59 (2002)

Shilov, S. V., M. Müller, D. Kruerke, G. Heppke, H. Skupin and F. Kremer
"Molecular arrangements and reorientation behavior in ferroelectric columnar liquid crystals as studied by time-resolved FT-IR spectroscopy"
Phys.Rev. E **65**, 021707 (2002)

Kremer, F.
"Dielectric spectroscopy – yesterday, today and tomorrow"
J. of Non Crystalline Solids **305**, p.1-9 (2002)

Prigann, J., Ch. Tolksdorf, H. Skupin, R. Zentel and F. Kremer
"FT-IR spectroscopic studies on reorientation of ferroelectric liquid crystals in a thermoreversible gel network"
Macromolecules **35,** pp. 4150-4154 (2002)

Huwe, F. Kremer
"Molecular dynamics in confining geometries"
in Liquid Dynamics, Experiments, Simulation and Theory, Editor John T. Fourkas,
ACS Symposium Series **820**, 268-283 (2002)

Rozanski, S. A., R. Stannarius and F. Kremer
"Indication for a flexoelectric mode in nanoconfined ferroelectric liquid crystal"
Proceedings of SPIE Vol. **4759**, 178-183 (2002)

Hartmann, L., W. Gorbatschow, J. Hauwede and F. Kremer
"Molecular dynamics in thin films of isotactic PMMA"

Eur.Phys. J. E **8**, 145-154 (2002)

Massalska-Arodz, M., V.Yu. Gorbachev, J. Krawczyk, L. Hartmann and F. Kremer
"Molecular dynamics of the liquid crystal 6O2OCB in nanopores"
J. Phys.: Condens Matter, **14**, 1-9 (2002)

Sinha Roy, S., W. Lehmann, E. Gebhardt, Ch. Tolksdorf, R. Zentel and F. Kremer
"Inverse piezoelectric and electrostrictive response in freely suspended FLC elastomer film as detected by interferometric measurements"
Mol. Cryst. Liq.Cryst. Vol. **375**, 253-268 (2002)

Lehmann, E., Ch. Chmelik. H. Scheidt, S. Vasenkov, B. Staudte, J. Kärger, F. Kremer, G. Zadrozna and J. Kornatowski
"Regular intergrowth in the AFI type crystals: Influence on the intracrystalline adsorbate distribution as observed by interference and FTIR-microscopy"
J. Am. Chem. Soc. **124**, 8690-8692 (2002)

Li, J.-J., H. Schüring, and R. Stannarius
"Gas permeation through ultrathin liquid layers."
Langmuir **18**, 112 (2002)

Stannarius, R., R. Köhler, U. Dietrich, M. Lösche, C. Tolksdorf, and R. Zentel.
"Structure and elastic properties of smectic liquid crystalline elastomer films."
Phys. Rev. E **65**, 041707 (2002)

John, T., U. Behn, and R. Stannarius
"Fundamental scaling laws of on-off intermittency in a stochastically driven dissipative pattern forming system."
Phys. Rev. E **65**, 046229 (2002)

Gröger, S., F. Rittig, F. Stallmach, K. Almdal, P. Št□pánek, C. M. Papadakis
"A pulsed field gradient nuclear magnetic resonance study of a ternary homopolymer/diblock copolymer blend in the bicontinuous microemulsion phase"
J. Chem. Phys. **117**, 396 (2002).

Papadakis, C.M., P. Busch, R. Weidisch, D. Posselt
"Phase behavior of binary blends of chemically different, symmetric diblock copolymers"
Macromolecules, **35**, 9263 (2002).

Smilgies, D.-M., P. Busch, D. Posselt, C.M. Papadakis
"Characterization of polymer thin films with small-angle X-ray scattering under grazing incidence (GISAXS)"
Synchrotron Radiation News **15**, no. 5, p. 35 (2002)
(eingeladener Beitrag)

Köhler, R., U. Dietrich, J.-J. Li, M. Lösche, R. Stannarius, C. Tolksdorf, and R. Zentel.
"Layer structure of free-standing smectic lc elastomer films."

Proc. SPIE **4759**, 483 (2002)

Tolksdorf, B., R. Zentel, R. Köhler, U. Dietrich, M. Lösche, and R. Stannarius
"Free standing smectic LC elastomer films."
Mat. Res. Soc. Symp. Proc. **709**, 23-28 (2002)

Stannarius, R., C. Langer, and W. Weissflog
"Domain walls and electro-optic switching in an antiferroelectric B_2 liquid crystalline freely suspended film."
Ferroelectrics **277**, 177 (2002)

Grigutsch, M. and R. Stannarius
"Stripe patterns in the magnetic reorientation of a glass-forming nematic liquid crystal."
Europhys. J. E **8**, 365 (2002)

Stannarius, R., C.Langer, and W. Weissflog
"Electro-optic study of antiferroelectric freely suspended films of bent-core mesogens in the B_2 phase."
Phys. Rev. **E** 66, 031709 (2002)

Schüring, H. and R. Stannarius
"Isotropic droplets in thin free standing smectic films."
Langmuir **18**, 9737 (2002)

Stannarius, R., J. Li and W. Weissflog
"A ferroelectric smectic phase formed by achiral straight core mesogens"
Phys. Rev. Lett. **90**, 025502 (2003)

R. Zorn, L. Hartmann, B. Frick, D. Richter, F. Kremer
"Inelastic neutron scattering experiments on the dynamics of a glassforming material in mesoscopic confinements"
J. Non-Cryst. Solids, **307**, 547 (2002)

- in press -

Spange, S. A. Gräser, A. Huwe, F. Kremer and P. Behrens
"Kationische Wirt-Gast-Polymerization von N-Vinylcarbazol und Vinylethern in MCM-41, MCM-48 und nanoporösen Gläsern"
Angewandte Chemie (in press) 2002

Barmatov, E. B., A. P.Filippov, M. V.Barmatova, F. Kremer, V. P. Shibaev "
"Elastic constants K_1 and K_3 of hydrogen-bonded blends of the functionalized LC polymer with a low molecular weight non-mesogenic dopant"
Liquid Crystals in press (2002)

Wirth I., S. Diele, A. Eremin, G. Pelzl, S. Grande, L. Kovalenko, N. Pancenko, W. Weissflog,

"New Variants of polymorphism in banan-shaped mesogens with cyano-substituted central core"
J. Mat. Chem., in press (2002)

Y. Feldman, J. Berberian, F. Kremer (Eds.)
Proceedings of the 1st International Conference on "Dielectric Spectroscopy on Physical, Chemical, Biological Applications"
"Journal of Non-Crystalline Solids" (Special Issue) Vol. 305, Nos.1-3 (2002)
Elsevier Science

- accepted -

Barmatov, E. B., M. V.Barmatova, F. Kremer, V. P. Shibaev
"Phase behavior of functionalized liquid crystalline copolymers containing maleic acid fragments"
Macromol. Rapid. Commun., accepted for publication (2002)

Barmatov, E., S.Grande, A. Filippov, M. Barmatova, F. Kremer, V.Shibaev
"Order parameter for hydrogen-bonded blends of the functionalized liquid crystalline polymer with a low molecular weight dopant"
Macromol. Rapid. Commun., accepted for publication (2002)

Pilippov, A. P. L. N.Andreeva, E. B.Barmatov, M. V.Barmatova, F.Kremer, V. P.Shibaev,
"Effect of intra- and intermolecular hydrogen bonds on the order parameter and elasticity constants of side-chain functionalized LC polymers"
Macromol. Chem. Phys.,accepted for publication (2002)

Li, J., R. Stannarius, C. Tolksdorf, R. Zentel
"Hydrogen Bonded Ferroelectric Liquid Crystal Gels in Freely Suspended Film Geometry"
Phys. Chem. Chem. Phys., accepted for publication (2002)

Kremer, F., A. Huwe, A. Gräser, St. Spange and P. Behrens
"Molecular dynamics in confinig space"
book chapter to "*Nanoporous Crystals*", Wiley VCH, accepted for publication (2002)

Hartmann, L., F. Kremer, P. Pouret and L. Léger
"Molecular Dynamics in grafted layers of poly(dimethylsiloxane) (PDMS)"
J. of Chem.Phys., accepted for publication (2002)

Schüring, H., R. Stannarius
"Isotropic droplets in smectic films"
Mol. Cryst. Liq. Cryst., accepted for publication (2002)

Nadasi, H., W. Weissflog, A. Eremin, G. Pelzl, S. Diele, B. Das, S. Grande,
J. Mater. Chem., accepted for publication (2002)

- submitted -

Papadakis, C.M., F. Rittig, K. Almdal, K. Mortensen, P. Štěpánek

"Collective dynamics and self-diffusion in a diblock copolymer melt in the body-centered cubic phase"
subm. to Eur. Phys. J. E. (2002)

John, T., U. Behn, R. Stannarius
"Laser diffraction by periodic dynamic patterns in anisotropic fluids"
subm. to Europhys. J. B (2002)

Hartmann, L., Th. Kratzmüller, H.-G. Braun, F. Kremer
"Molecular dynamics of grafted PBLG in the swollen and in the dried state"
(Paper DRP 2000 Spala) *subm. to IEEE Transactions DEI* (2001)

Massalska-Arodz, M., W. Gorbatschow, W. Witko, L. Hartmann and F. Kremer
"Dielectric relaxation in 4-(2-hexyloxy-ethoxy) 4' -cyanobiphenyl (6O2OCB)"
subm. to Liquid Crystals (2001)

Das, B., S. Grande, W. Weissflog, A. Eremin, W. Schröder, G. Pelzl, S. Diele, H. Kresse,
"Structural and conformational investigations in SmA and different SmC phases of new hockey-stick-shaped compounds"
subm. to Liqid Crystals (2002)

Busch, P., F. Kremer, Ch. M. Papadakis, D. Posselt and D.-M. Smilgies
"The structure of thin films of binary diblock copolymer blends - A combined AFM and grazing-incidence small-angle X-ray scattering study"
submitted to: The proceedings of the Sino-German Young Scientists Forum on *Polymer Science*, Beijing, China, April 2002

Busch, P., D. Posselt, F. Kremer and Ch.M. Papadakis
"Molar mass dependence of the lamellar orientation in thin diblock copolymer films investigated by AFM", subm. to Surface and Interface Analysis 2002

4.22 Graduations

4.22.1 Ph.D.

Dipl.-Phys. Holger Skupin
29.01.2002
"Zeitaufgelöste Fourier-Transform-Infrarotspektroskopie an ferroelektrischen flüssigkristallinen Polymeren und Elastomeren"

4.23 Guests

Dr. Abbas Khaidarov
Academy of Science of Republic Uzbekistan
15.09.-15.12.02

Dr. Viktor Pergamenshchik
University of Kiev, Ukraine
01.10.-15.12.02

Prof. Dr. Dorthe Posselt
Roskilde University, Denmark
04.11.-10.11.02

Prof. Dr. Igor Potemkin,
Moscow University, Russia,
29.10.-10.11.02

Dr. Stanislaw Rozanski
University of Poznan, Poland
01.09.-30.09.02

5 PHYSICS OF DIELECTRIC SOLIDS — SCIENTIFIC ACTIVITIES

5.1 New NMR equipment

Dieter Michel, Gert Klotzsche

For our NMR based research several spectrometers with superconducting wide bore (89 mm) magnets are available covering a magnetic field range from 2.35 T to 17.62 T (corresponding to proton resonance frequencies between 100 and 750 MHz). The installation of the new high-field solid-state NMR spectrometer "AVANCE 750" in a wide-bore magnet provides excellent possibilities for fundamental and applied research. The beginning of the regular measuring regime, in which various groups in Leipzig, Jena, Regensburg and others are involved, has been connected with the organization of the symposium "New Developments in High-Field NMR" held from April 25 to 26, 2002 in Leipzig. Moreover, an AMPERE Summer School was held in Leipzig from July, 10 - 12, 2002 in Leipzig in close connection with the 31st Congress AMPERE on Magnetic Resonance and Related Phenomena organized from July 14 - 19, 2002 in Poznan/Poland. The Summer School provided some basic principles and applications of solid-state NMR spectroscopy, NMR microscopy and imaging techniques in solid-state physics, biology and material science. Large molecules, interfaces, nano-structured materials, as well as transport phenomena were considered and the participants took the opportunity of practical demonstrations at our modern NMR techniques. In the autumn 2002 our capabilities were still improved by a 400 MHz AVANCE NMR-spectrometer. Both spectrometers of the AVANCE-series of Bruker Biospin (Karlsruhe) are equipped with a comparable modern electronics enabling applications of advanced pulse techniques, like shaped pulses and back-to-back pulses important for solid-state NMR applications. All NMR spectrometers are suitable for experiments on solid-state matter as well as for investigations at systems with restricted mobility (e.g. interface systems, biological membranes). We now have possibilities to measure with very strong (more than 1000 W) radio-frequency fields at any desired form in two or more channels simultaneously. Magic Angle Spinning (MAS) up to 32 kHz is possible to simplify powder patterns, but we can also orient and rotate stepwise single crystals using goniometer probeheads. Typical solid state NMR-measurements using broad band excitation may be performed in a wide temperature region from 4.2 K to about 800 K.

For more details please contact Dipl.-Phys. Gert Klotzsche and Dr. André Pampel.
klotzsch@physik.uni-leipzig.de, anpa@physik.uni-leipzig.de

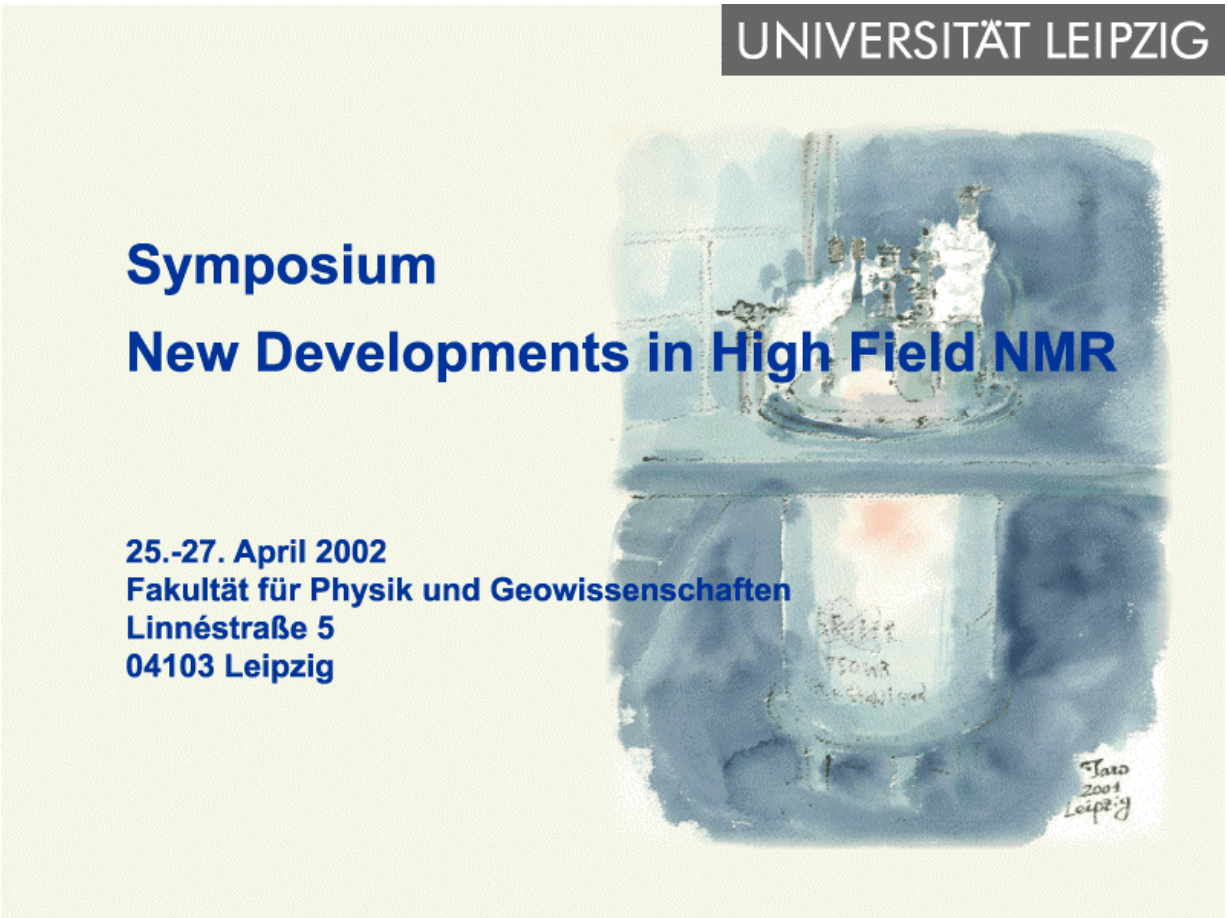

Fig. 1: Announcement of the symposium "New Developments in High-Field NMR" with a painting of the 17.6 T magnet by Taro Ito.

5.2 Active surface sites in heterogeneous catalysts

Andreas Pöppl, Marlen Gutjahr

A major research topic of our group is the study of active surface sites in heterogeneous catalysts by electron paramagnetic resonance (EPR) spectroscopy. To apply ESR methods to such systems the catalytically active sites have to be either paramagnetic species by themselves (eg. paramagnetic transition metal ions) or paramagnetic probe molecules have to be adsorbed on the studied diamagnetic surface sites (eg. acid centers and transition metal ion species).
The last approach has been used to characterize Lewis acid sites and Cu(I) cations in various zeolite materials. Nitric oxide (NO) and Di-tert-butyl nitroxide (DTBN) probe molecules were employed in these studies. The geometrical and electronic structures of the resulting adsorption complexes with Lewis acid aluminum defect centers and metal cations could be determined by a combined application of several EPR techniques at low temperatures. Besides continuous wave multifrequency EPR spectroscopy, pulsed electron nuclear double resonance (ENDOR) at X and W band as well as hyperfine sublevel correlation (HYSCORE) spectroscopy have been used to measure the weak superhyperfine (shf) interactions between the unpaired electron spin at the probe molecule and the nuclear spins at the metal ion adsorption sites. These shf interactions are the key information in the structural analysis of such paramagnetic surface sites. ESR methods give also access to the acid properties of the Lewis sites. Their electron pair acceptor strength could quantitatively be characterized from the spin density distribution in the adsorption complexes and the dynamics and stability of the formed complexes at elevated temperatures /1,2/.
An attractive example for the application of modern ESR methods for the study of catalytically active transition metal ion species is the elucidation of the incorporation site of vanadyl ions in $H_4PVMo_{11}O_{40}$ heteropolyacid catalysts. In these materials the heteropolyanions have the well-known structure of the Keggin molecule. Interactions of the unpaired electrons of the paramagnetic vanadyl ions (VO^{2+}) with all relevant nuclei (^{1}H, ^{31}P and ^{51}V) could be resolved. The complete analysis of the hyperfine coupling tensor for the phosphorous nucleus in the fourth coordination sphere of the V(IV) ion by HYSCORE and ENDOR spectroscopy at W- and X-band allowed for the first time a detailed structural analysis of the paramagnetic ions in in hydrated and dehydrated heteropolyacid catalysts. The vanadyl species are found to be coordinated to four or three bridging oxygen atoms from one $PVMo_{11}O_{40}^{-4}$ heteropolyanion in a trigonal-pyramidal or slightly distorted square-pyramidal coordination geometry, respectively /3/.
Currently, this research subject is extended to the study of V(IV) ions in alkali metal ion modified heteropolyacid catalysts. Recent progress has been achieved by the development of an home-built Q band pulsed ENDOR spectrometer that allowed the measurement of weak ^{133}Cs shf couplings between the unpaired electron at the V(IV) ion and the cesium nuclei in the void space between the Keggin molecules.

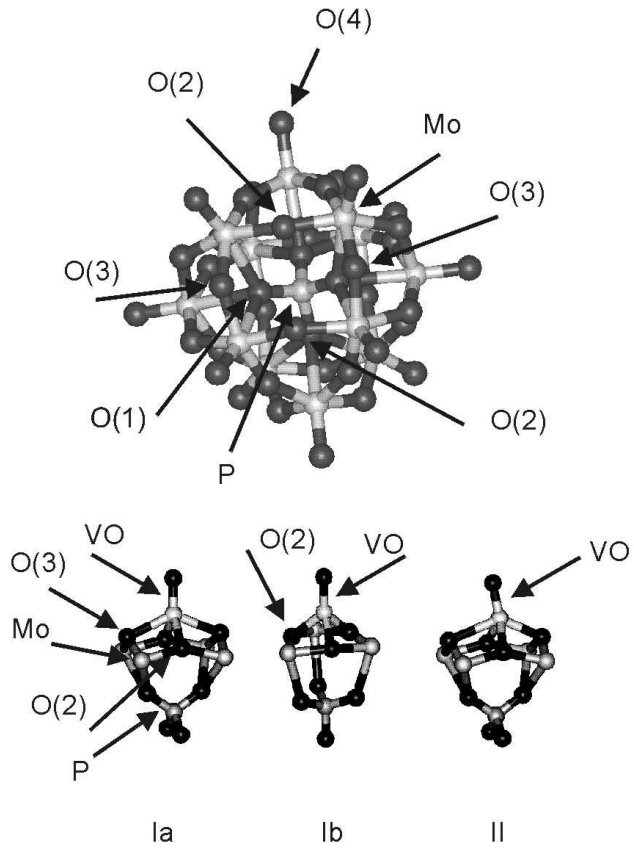

Structure of the $PVMo_{11}O_{40}^{-4}$ heteropolyanion (top) and schematic drawings of the proposed vanadyl complexes in dehydrated catalyst (bottom).

/1/ M. Gutjahr, R. Böttcher, A. Pöppl
Characterization of the Di-tert-butyl Nitroxide: Li^+ Adsorption Complex in LiY Zeolites by One- and Two-Dimensional Electron Spin-Echo Envelope Modulation Spectroscopy, J. Phys. Chem. B 106 (2002) 1345 – 1349
/2/ T. Rudolf, W. Böhlmann, A. Pöppl, Adsorption and Desorption Behavior of NO on H-ZSM-5, Na-ZSM-5, and Na-A as Studied by EPR, J. Magn.Res. 155 (2002) 45-56
/3/ A. Pöppl, P. Manikandan, K. Köhler, P. Maas, P. Strauch, R. Böttcher, D. Goldfarb: Elucidation of Structure and Location of V(IV) Ions in Heteropolyacid Catalysts $H_4PVMo_{11}O_{40}$ as studied by Hyperfine Sublevel Correlation Spectroscopy and Pulsed Electron Nuclear Double Resonance at W- and X-Band Frequencies; J. Am. Chem. Soc., 123 (2001) 4577-4584.

5.3 Local ordering occuring in ferroelectrics, dipolar glasses and modulated phases

Georg Völkel

EPR can be a powerful tool for the study of the peculiar local ordering occuring in ferroelectrics, dipolar glasses and modulated phases. Often, NMR and EPR complement each other because of their different time windows of investigation. Such an interesting case we meet with Dimethylammonium Aluminum Sulfate Hexahydrate (DMAAS) and Dimethylammonium Gallium Sulfate Hexahydrate (DMAGaS) where EPR investigations are the appropriate tool to enlighten the until now unknown nature of the low.temperature phaseof DMAGaS.
DMAGaS and DMAAS are isomorphous and ferroelastic at room temperature. Both they show an order-disorder type transition into a ferroelectric phase but only DMAGaS exhibits a further first-order transition into a low temperature non-ferroelectric phase. We performed electron paramagnetic resonance (EPR) measurements of chromium doped DMAAS and DMAGaS giving a new insight into the peculiar reorientation order of the polar DMA units on a microscopic level not known before. We found that the low-temperature phase of DMAGaS below T_{C2} = 115 K is a modulated phase with commensurate regions and discommensurations before it becomes antiferroelectric at T* = 60 K. This unusual phase sequence can be well explained by means of a Landau approach using a large number of sublattice polarizations and more generally by the microscopic extended DIFFOUR (discrete frustrated ϕ^4) model of a linear chain of electric dipoles (van Raij, van Bemmel, Janssen, 2000). Dielectric measurements of a $DMAGa_{0.9}Al_{0.1}S$ mixed crystal show shifts of the transition temperatures according to these model predictions. DMAGaS and DMAAS seem to represent a similar interesting model system with a very complex phase sequence of commensurate and incommensurate phases as the famous betaine calcium chloride dihydrate (BCCD).

G. Völkel, R. Böttcher, Z. Czapla, D. Michel, EPR Studies of Chromium Doped Dimethylammonium Gallium and Aluminium Sulfate Hexahydrate (DMAGAS and DMAAS),
Ferroelectrics 268 (2002) 181-186

G. Völkel, N. Alsabbagh, J. Banys, H. Bauch, R. Böttcher, M. Gutjahr. D. Michel,
A. Pöppl, Local Ordering Processes in Ferroelectric, Glass-like and Modulated Phases: An EPR Study, Adv. in Solid State Physics 42 (2002) 241-251

5.4 NMR spectroscopy of liquid-crystal phases

André Pampel

Part of the research program of our group is also the investigation of so called "soft-matter" or "semi-solid matter", especially of systems in liquid-crystalline phases as drug delivery systems and models for biological membranes. We are applying a multidisciplinary approach using mainly NMR spectroscopy to reveal structural and dynamical aspects of such systems.
NMR spectroscopy has definite advantages over diffraction techniques in the structure elucidation of liquid-crystalline structures, which exhibit very low short-range order. These advantages, however, are frequently offset by resonance broadening mechanisms, which are caused by the anisotropic NMR parameters. Therefore, for this research we are using methods, which have been developed for the High-resolution NMR spectroscopy of solids. Main parts of our activities include the development and the optimization of methods of High-resolution MAS techniques for the investigation of liquid-crystalline phases.
As a novel technique for investigation of such system we have introduced the combination of pulsed Field Gradient NMR and HR MAS NMR spectroscopy. It was used investigating cubic liquid-crystalline phases (cubic phases) in development as drug delivery systems. Such porous system can be used as a host system for several drugs of different polarity. The PFG MAS method was used to study the diffusion of the components of the system. The determination of biophysical parameters of such system on sub-nanometer scale helps to improve the possibilities for fabrication of new drug delivery systems and it has direct impact into the drug development and medical research, which is being done at the MDC in Berlin.
Recently, we have focused on further development of the PFG MAS method for investigations of diffusion in phospholipid membranes. Current research projects include investigations of models of biological membranes with the main focus is on the determination of structure and dynamical behavior of molecules within membranes, e.g. peptides and proteins. In figure a sketch of a membrane composed of lipids and water that hosts a membrane peptide is shown.

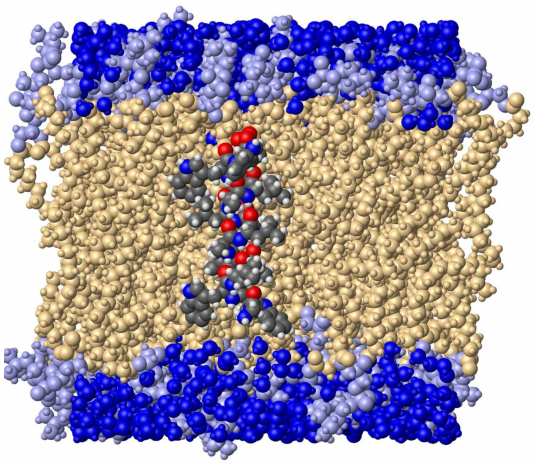

5.5 Nanocrystalline perovskite-structure ferroelectrics

Rolf Böttcher, Emre Erdem

The examination of nanocrystalline ferroelectrics with perovskite structure and the determination of their physical and chemical properties are one of the challenges of the solid state physics and material science due to their potential application in device technology (thin film capacitors, micro-mechanical devices, non-volatile random access memories, chemical and pyroelectric sensors). The aim of our research group is to investigate the structural properties of nanocrystalline perovskites $BaTiO_3$ and $PbTiO_3$ by means of Electron Paramagnetic Resonance (EPR) spectroscopy in different frequency bands (X, Q and W). By using combined polymerisation and pyrolysis route we synthesise samples in a wide range of particle size (~1 μm - 20 nm) /1, 2/. This wide size range of the samples enables us

i) to get more information about the local configurational instability of paramagnetic ion in Ba(Pb)TiO_3 by measuring the spectral parameters and their distribution functions,

ii) to probe the ferroelectric properties by measuring their temperature dependence,

iii) to understand the physical background of the size effects.

In our group EPR measurements are carried out on ultrafine $PbTiO_3$ nanopowders doped with Cr^{3+} ions. In addition to the Cr^{3+} centre D_1 in $PbTiO_3$, previously measured in single crystals and ceramics /3, 4/, additional centres (D_2, D_3 and D_4) were identified (see Figure 1). Their spin-Hamiltonian parameters were determined by the simulation of the EPR spectra measured in the different frequency bands (Table 1).

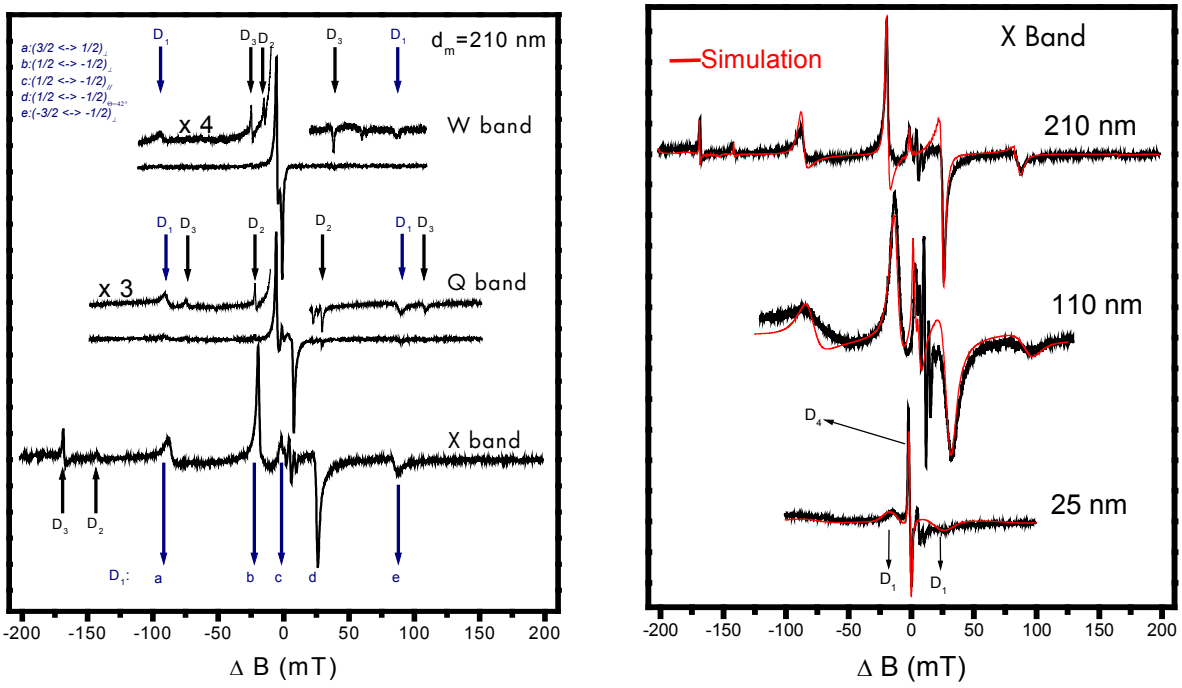

Figure 1. Left: Frequency dependence of the EPR spectrum for the 210 nm nanocrystalline $PbTiO_3$ powder. Right: Size effect in the room temperature EPR spectrum of $PbTiO_3$: Cr^{3+} measured in X band.

d_m=210 nm

Centre	Spin	$g_{//}$	$g_{\perp}$	D [cm^{-1}]	δD [G]	ΔB [G]
D_1	S=3/2	1.9726	1.9787	0.0820	40	9
D_2	S=3/2	1.9715	1.9719	0.1603	<10	6
D_3	S=3/2	1.9662	1.9696	0.3095	<10	6

d_m=110 nm

D_1	S=3/2	1.9726	1.9787	0.0830	120	9

d_m=25 nm

D_1	S=3/2	1.9726	1.9787	0.0790	180	18
D_4	S=3/2	1.9711	1.9734	<5	<10	18

Table 1. Size dependence of g-values, fine structure parameter D, its distribution width δD and the linewidth ΔB.

The Newmann superposition model (SPM) enables us to form microscopic models for the paramagnetic centres. These calculations have been done as a function of the displacement of the Cr^{3+} ions from the centre of the oxygen octahedron along the $\pm c$ direction. Thus one can determine the locations of the paramagnetic ions and the oxygen vacancies inside the host lattice cell.

/1/ H.-J. Gläsel, E. Hartmann, R. Böttcher, C. Klimm, B. Milsch, D. Michel, H.-C. Semmelhack, J. Hormes "Preparation of barium titanate ultrafine powders from a monomeric metallo-organic precursor by combined solid-state polymerisation and pyrolysis route" J. Mater. Sci. 34 (1999) 1.

/2/ E. Erdem, R. Böttcher, H.-C. Semmelhack, H.-J. Gläsel, E. Hartmann, D. Hirsch "Preparation of lead titanate ultrafine powders from combined polymerisation and pyrolysis route" J. Mater. Sci. (in press).

/3/ R. Heidler, W. Windsch, R. Böttcher, C. Klimm "EPR investigations on Cr^{3+} modified $PbTiO_3$ ceramics" Chem. Phys. Lett. 175 (1990) 55.

/4/ V.V. Laguta, T.V. Antimirova, M.D. Glinchuk, I.P. Bykov, J. Rosa, M. Zaritskii, "Local configurational instability of Cr^{3+} in $PbTiO_3$" J. Phys.: Condens. Matter. 9 (1997) 10041.

5.6 Synthesis of Matrix Materials for Studies of Molecules in confined Geometry

Winfried Böhlmann, Dieter Michel

The fields of applications for porous materials have been extended greatly over the last years with the possibility of generating new supramolecular structures by in situ or post synthesis incorporation of guest molecules into pores of zeolites and/or molecular sieves. New materials based on well known zeolite structures, the molecular sieve MCM-41and other porous compounds attracted high attention and their synthesis and characterization is a new challenge in the material science. Zeolites and molecular sieves allow the inclusion of a variety of guest molecules to study the interactions between the host material and the molecules adsorbed in a confined geometry. The defined pore systems can act as an ordering framework for incorporated species which leads to materials with new properties. Another important point is the possibility to modify the properties of either the guest molecules or the host framework independently. Following the route of incorporating guest species in the channel or pore system of zeolites and mesoporous molecular sieves, it was of interest for our work to synthesize materials which can potentially applied as matrixes.
Therefore we focussed our study on two different kinds of materials, the synthesis of zeolite ZSM-5 (or silicalite-1) with a pore diameter of about 5.1 Å and the molecular sieve MCM-41 possess pore diameters between 30...50 Å. The latter was formed by isomorphous substitution of heteroatoms, particularly aluminum, indium and tungsten, into the silica network [1,2]. All materials were characterized using ^{27}Al, ^{29}Si, ^{115}In, and ^{1}H MAS NMR spectroscopy, powder X-ray diffraction, nitrogen adsorption-desorption, and temperature programmed desorption (TPD).
The substances were used to include organic molecules like ethylene glycol and n-dodecane to study the phase transitions by means of MAS NMR spectroscopy and in comparison to dielectric measurements.
Using in particular the high resolution (HR) MAS NMR spectroscopy at high d.c. magnetic fields the dynamics of olefinic hydrocarbons in NaX zeolites couod be studied in detail. For the first time conformational changes of adsorbed molecules in the adsorbed state could be investigated. By combining NOESY-NMR with of heteronuclear high resolution NMR spectroscopy a model for the reorientation dynamics of the mocules adsorbed in faujasite type zeolites could be developed and compared with results of PFG NMR diffusion studies by Kärger et al.

[1] W. Böhlmann, O.Klepel, D. Michel, and H. Papp
Synthesis and Characterization of In-MCM-41 Mesoporous Molecular Sieves with Different Si/In Ratios. Stud. Surf. Sci. and Cat. 142b (2002) 1155
[2] W. Böhlmann, O.Klepel, H. Dathe, D. Michel, and H. Papp
Direct Synthesis of In-MCM-41 Mesoporous Molecular Sieves with Different Si/In Ratios, submitted to J. Phys. Chem. B

5.7 Study of the dynamic of incommensurately modulated crystals by means of nuclear magnetic resonance spectroscopy

D. Michel and A. Taye
(in close cooperation with Professor Jörn Petersson, University of the Saarland, Saarbrücken)

Nuclear magnetic resonance (NMR) using nuclei with quadrupole moments has been proved to be an accurate and sensitive tool for investigating IC phases. The static part of the electric field gradient (EFG) is a local physical property whose components are distributed in a characteristic manner because of the structurally incommensurate modulation. Accordingly, a spectrum of NMR frequencies occurs which shows edge singularities as a typical feature. This renders possible to relate the EFG unambiguously to the static order parameter (OP) enabling the determination of the critical exponents β and $\overline{\beta}$. The fluctuating part of the EFG being dominated by the local dynamics (background contribution) as well as the OP fluctuations (critical contribution), is related to the probabilities of transitions between the nuclear spin levels. The spin lattice relaxation rate $1/T_1$ of the nuclear magnetization at a certain Larmor frequency is given as a linear combination of these probabilities. This allows special insights into the collective dynamics in the normal phase close to the IC transition: the critical exponent $\zeta^{fml} = 2\gamma - 3\nu$ may be measured if the critical fluctuations are faster than the Larmor frequency. In the IC phase the phason and amplitudon dynamics is accessible. For all critical exponents measured so far an excellent agreement is found with the predictions of the renormalization group (RNG) theory, i.e. the 3d-XY model characterised by a two-dimensional order parameter with three-dimensional interactions. These predictions were confirmed by investigating various crystal with IC modulated phases. Recently detailed investigations are carried out on bis(4-chlorophenyl)sulphone [BCPS] showing a very broad IC region below about 150 K presumably down to 0 K. In previous work it was concluded for this molecular crystal that the predictions of the RNG are not applicable. For this reason, the temperature dependence of the line shape and the spin-lattice relaxation at the ^{35}Cl NMR central transitions lines ($-1/2 \leftrightarrow +1/2$) have been measured with great accuracy. The recorded spectra show an increasing characteristic broadening of the NMR line precisely indicating the phase transition in a structurally incommensurate phase at the temperature T_i = 149.7 K. Moreover, the dynamics of the incommensurate (IC) modulation is investigated in the normal high temperature phase close to the temperature T_i by means of nuclear spin-lattice relaxation measurements. The temperature dependence of the critical contribution to the ^{35}CL NMR spin-lattice relaxation rate above T_i can be again described by the critical exponent $\zeta \approx 0.67$ which is fully consistent with the predictions of the universality class of the three-dimensional (3d) XY model and which nicely confirms our general conclusion about IC phases in contrast to other work [A. Taye, D. Michel, and J. Petersson, Phys. Rev. B 66, 174102 (2002)].

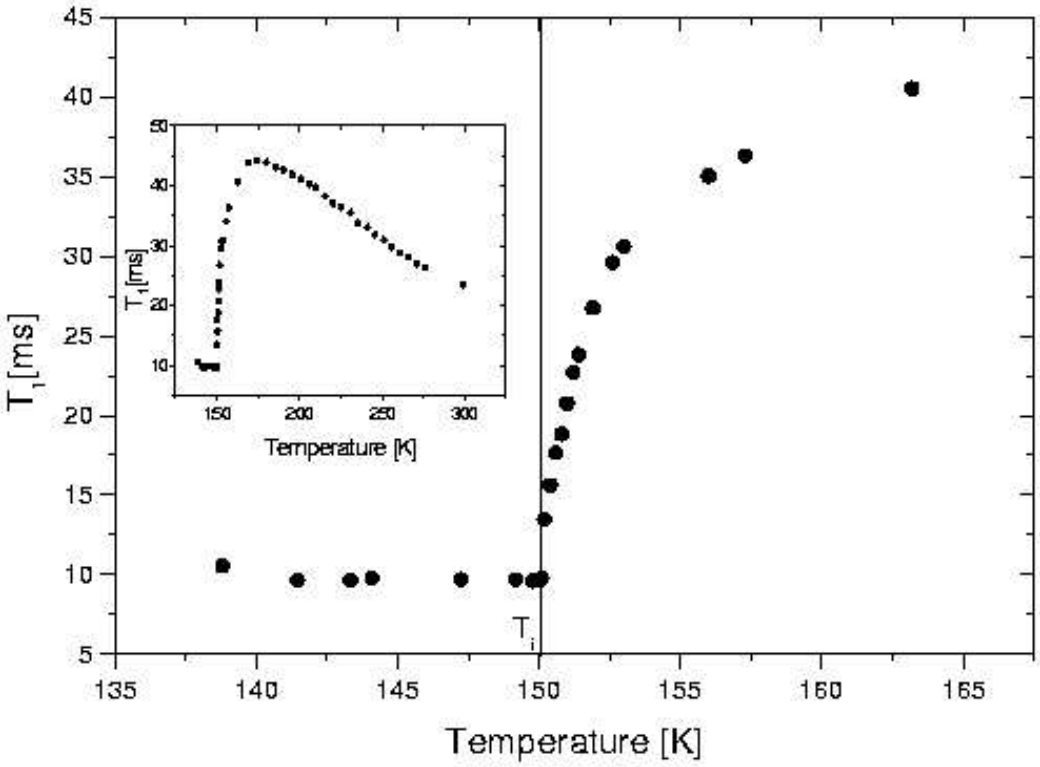

Fig. 1. Temperature dependence of the ^{35}Cl NMR spin-lattice relaxation time T_1 in a single crystal of BCPS measured in the normal phase above T_i and at the higher frequency edge singularity in the incommensurate phase below T_i. The measurements were run at the central line in a static magnetic field of B_o = 11.7 Tesla using a Bruker MSL 500 NMR spectrometer. The insert shows the temperature dependence of the ^{35}Cl NMR spin-lattice relaxation time T_1 in the whole measuring range. A critical slowing down of the T_1 values starts below temperatures of ca. 180 K. Note that the lowest T_1 values appear at T_i where the phase transition temperature was controlled by the NMR line shape. Below T_i the relaxation times are nearly constant in the temperature interval $T_i \geq T \geq T_i$-10 K. The limits of experimental error in the T_1 measurements are estimated to be ± 5%, the temperature can be controlled with an accuracy of ± 0.1 K.

5.8 ^{35}Cl and ^{14}N NMR studies of phase transitions in tetramethyl-ammonium cadmium chloride (TMCC)

Dieter Michel, Samir Mulla-Osman, Georg Völkel
in close co-operation with Prof. Z. Czapla, Wroclaw (Crystal Synthesis) and Prof. G. Madariaga, Bilbao (XRD)

Crystals of the isostructural family $(CH_3)_4NMX_3$, with the bivalent metals M = Mn, Ni, Cd, Cu, or V and the halogen atoms X = Cl, Br or I, have attracted much attention because of their one-dimensional type structure. They are built up from infinite chains of MX_6 octahedra. The space between the chains is occupied by the $[(CH_3)_4N]^+$ (tetramethylammonium, TMA) cations. In particular, crystals of $(CH_3)_4NMnCl_3$ (TMMC) has been intensively investigated because of its quasi-ideal one-dimensional magnetic properties. $(CH_3)_4NCdCl_3$ (TMCC) is a diamagnetic analogue for TMMC for which also a quasi-one-dimensional behaviour was found. TMMC and TMCC undergo a number of structural phase transitions which are suggested to be governed essentially by the dynamics of the TMA groups. ^{14}N NMR and ^{35}Cl NMR investigations are performed on TMCC in the temperature range from 297 to 80 K. Besides the structural changes at the phase transitions the NMR measurements clearly show a ferroelastic twin domain structure in phase II (see the Figure). The saturated rotational angle between the epitaxially grown domains of $\Theta_{exp.} = 4°$ is in a very good agreement with the theoretical value of $\Theta_s = 3.5°$ calculated from the ferroelastic strain tensor. This work has shown that NMR spectroscopy is able to derive subtle structural details which are also essential for the interpretation of XRD measurements [1]. The sequence of the structural phase transitions in this crystal family was previously described in the framework of the Landau theory [2]. To proof these predictions, ^{14}N NMR and ^{1}H NMR spin-lattice relaxation time measurements were run. They finally lead to the conclusion that the phenomenological treatment in [2] is not sufficient to describe the order-disorder behaviour of the TMA groups. A more detailed theoretical interpretation should be possible on the base of a pseudo spin model already introduced in [2]. This work is still in progress.

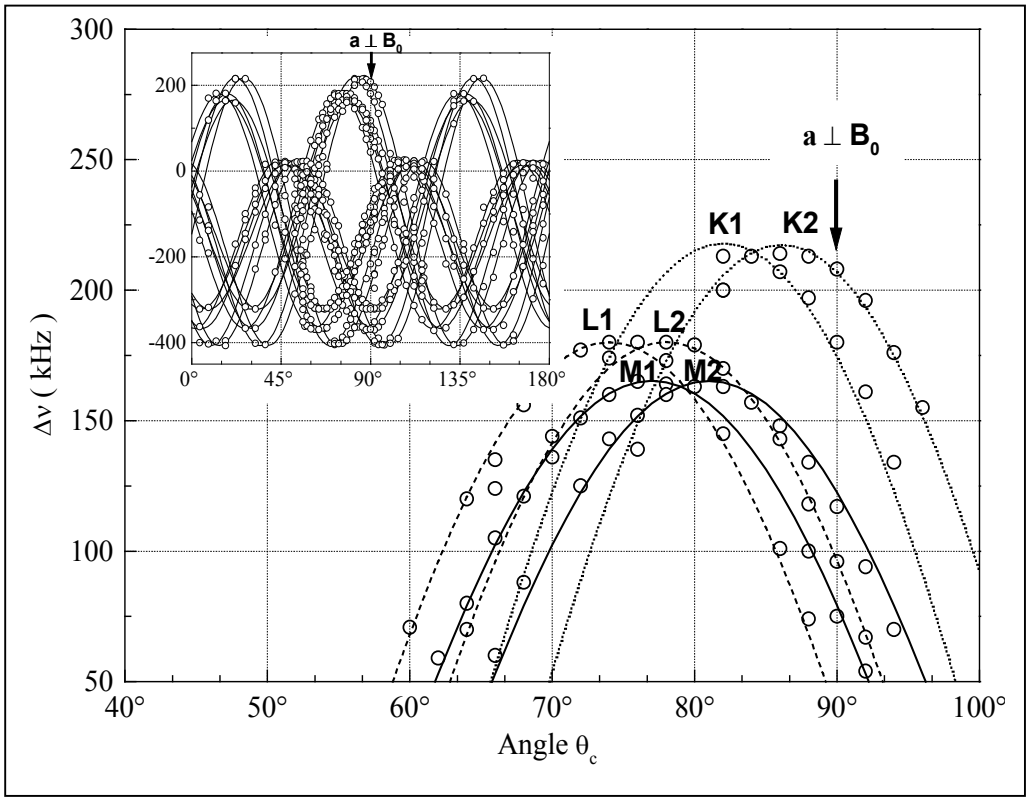

^{35}Cl NMR rotational patterns (central transition) around the crystallographic c axis of a TMCC single crystal at 115 K in phase II. The insert shows the full 180° pattern. The cutting with rotation angles between 40° and 100° presented in the main part of the figure shows the splitting of each of the line groups K, L, M into pairs K_1, K_2; L_1, L_2; M_1, M_2 with an angular difference of 4° between them due to the formation of epitaxial domains. Circles: experimental values, lines: results of fitting

[1] I. Peral, G. Madariaga, A. Perez-Etxebarria and T. Breczewski, Acta Cryst. B 56 215 (2000); S. Mulla-Osman, D. Michel, G. Völkel, I. Peral and G. Madariaga, ^{35}Cl-NMR studies of the domain structure of tetramethyl-ammonium cadmium chloride (TMCC) at lower temperatures, J. Phys.: Condens. Matter 13 (2001) 1119-1131
[2] M. N. Braud M N, M. Couzi and N. B. Chanh, J. Phys.: Condens. Matter 2, 8243 (1990)

5.9 Advanced Signal Processing for Magnetic Resonance

Dieter Michel and André Pampel

Quantitation of time domain data is a very useful tool for the estimation of spectral parameters in magnetic resonance spectroscopy (MRS) and for applications in magnetic resonance imaging (MRI).

This work was part of a European Project (with participants from the Belgium, France, Germany, Greece, the Netherlands and Spain) in which a program system for Medical Magnetic Resonance Imaging and Spectroscopy is developed with a special "Magnetic Resonance User Interface (MRUI)". The co-ordinator of this EU project was Prof. Dirk Van Ormondt, Technische Universiteit Delft (NL).

Software development is one of the goals of the EU Project, "Advanced Signal Processing for Medical Magnetic Resonance Imaging and Spectroscopy", formerly in the Human Capital and Mobility Networks programme (HCM , CHRX-CT94-0432, 1994-1997) and later in the programme Training and Mobility of Researchers (TMR, FMRX-CT97-0160, 1997-2001).

The Advanced Time Domain Signal Processing Package includes
-Black box quantitation based on Singular Value Decomposition (SVD)
-Non Linear Least Squares quantitation (NLLS)
-Preprocessing algorithms
-Error estimation: Cramér-Rao lower bounds

Details are available in:
http://azur.univ-lyon1.fr/TMR/tmr.html
(see also <Dr. Danielle Graveron>)
http://www.mrui.uab.es/mrui/mruiHomePage.html
(see also <Dr. Miguel Cabanas>)

The programme system is freely accessible and is already used world wide.

5.10 NMR and acoustic studies of the melting-freezing phase transition of gallium in vycor glass

Dieter Michel
in close co-operation with B. F. Borisov[1], E. V. Charnaya[1], D. Yaskov[1], C. Tien[2], C. S. Wur[2], and Yu. A. Kumzerov[3]

[1] Institute of Physics, St.Petersburg State University, St.Petersburg, 198904, Russia
[2] Department of Physics, National Cheng Kung University, Tainan, 701 Taiwan
[3] A.F.Ioffe Physico-Technical Institute RAS, St.Petersburg, 194021, Russia

The main topics of this work include

- the study of phase transitions in confined geometry, in particular melting and freezing of metallic gallium nanoparticles within porous matrices;
- the influence of size effects on the mobility in confined liquids, e.g. the mobility of melted metallic gallium in pores;
- the effect of confinement on electronic properties of metals which may be sensitively studied by means of alterations of the Knight shift for gallium within pores.

Samples of porous glasses (with pore diameter of 3.5 to 200 nm) and synthetic opals (regular spheres of silica) were used as matrices.

The melting-freezing phase transition of gallium confined within Vycor glass was studied by NMR and acoustic techniques. A pronounced depression of the freezing and melting phase transition temperatures and a hysteresis in the melting-freezing processes were found and discussed. NMR studies on liquid confined gallium revealed a noticeable decrease in the Knight shift and a drastic acceleration in gallium spin-lattice relaxation. These changes depend on the size and the geometry of the pores. The relaxation measurements were used to estimate the thermal correlation times of the Ga atoms in the confined geometry and to relate them with atomic diffusion.

5.11 Funding

Strukturaufklärung der Tieftemperaturphase des Dimethylammoniumgalliumsulfat (DMAGaS) und der Untersuchung des Ordnungs-Unordnungs-Verhalten der Dimethylammoniumgruppen mit Hilfe der EPR-Spektroskopie
Investigation of the low-temperature phase in demethylammoium gallium sulfate (DMAGaS) and the order disorder behaviour of the dimethylammonium groups (DMA) by means of EPR
R. Böttcher, D. Michel Bo 1080/7

Strukturaufklärung nanokristalliner Ferroelektika mit Perwoskitstruktur durch Hochfeld-EPR-Spektroskopie
Investigation of nanocrystalline ferroelectrics with pervoskite structure by means of high-field-EPR spectroscopy
(im Rahmen des Schwerpunktprogrammes 1051)
R. Böttcher Bo 1080/6-3

Hochfeld-ESR Spektroskopie von monomerem und dimerem Stickstoffoxid-Komplexen in Zeolithen
High field EPR spectroscopy of monomer and dimer nitric oxide complexes in zeolites
(im Rahmen des Schwerpunktprogrammes 1051)
A. Pöppl, M. Hartmann PO 426/2-3

Synthese und Strukturaufklärung von Vanadium-Phosphat-Systemen mittels ENDOR-und ESEEM-Spektroskopie
Synthesis and determination of the structure of vanadium-phosphate systems by means of ENDOR and ESEEM spectroscopy
A. Pöppl, K. Köhler PO 426/3-1

ESR, ENDOR, und ESEEM Spectroskopie zum Studiium der Struktur und Dynamik paramagnetischer Moleküle in microporösen Festkörpern
ESR, ENDOR, and, ESEEM spectroscopy of the structure and dynamics of para-magnetic molecules adsorbed on acid sites in microporous solids
Pöppl, SFB 294, Teilprojekt F7

Untersuchung der Dynamik inkommensurabel modulierter Kristalle mit Methoden der kernmagnetischen Resonanz
Study of the dynamic of incommensurately modulated crystals by means of nucleamagnetic resonance spectroscopy
D. Michel Mi 390/9-3 (together with Professor J. Petersson, Saarbrücken)

Signalbearbeitung für Medizinische Magnetresonanz-Tomographie und –Spektroskopie
Advanced Signal Processing for Medical Magnetic Resonance Imaging and Spectroscopy
D. Michel (mit A. Pampel)
(im Rahmen des EU-Programms TMR: Contract No. ERBFMRXCT970160)

Etablierung und Anwendungen der Doppelrotations- und Multiquanten-Meßtechnik für

Hochfeld-NMR-Untersuchungen an Quadrupolkernen in Festkörpern
Double Rotation and Multiple Quantum NMR Spectroscopy in High Magnetic Fields for the Study of Quadrupole Nuclei in Solids
D. Freude (mit D. Michel), DFG, Fr 902/9-2

Höchstauflösungs-Kernresonanzspektrometer mit einer Protonenspinresonanzfrequenz von 750 MHz
High-Resolution NMR Spectrometer with a Proton Resonance Frequency of 750 MHz
D. Michel, DFG, Mi 390/5-3

Dynamik, Ordnungsverhalten und Reaktivität von Molekülen in mikro- und mesoporösen Materialien
Dynamics, order behaviour and reactivity of molecules in microporous and mesoporous materials
D. Michel, SFB 294, Teilprojekt G8

5.12 External Cooperations

Institut für Oberflächenmodifizierung - IOM Leipzig (Dr. E. Hartmann)
Universität Kaiserslautern, Fachbereich Chemie, Technische Chemie (Dr. M. Hartmann)
Technische Universität München, Anorganisch-chemisches Institut (Prof. K. Köhler)
The Weizmann Institute of Science, Department of Physical Chemistry, Rehovot, Israel (Prof. D. Goldfarb)
Vilnius University, Radiophysics Department (Dr. J. Banys)
Wroclaw University, Institute of Experimental Physics (Prof. Z. Czapla)
University of Opole, Institute of Mathematics (Prof. V. A. Stephanovich)
Max-Delbrück-Center for Molecular Medicine (Dr. R. Reszka)
Universität des Saarlandes, Saarbrücken (Prof. J. Petersson et al.)
St. Petersburg State University (Prof. E. V. Charnaya, Prof. B. N. Novikov, Prof. V. I. Chizhik)
Ioffe Institute St. Petersburg (Prof. J. A. Kumzerov)
Kirensky Institute of Physics of the Sibirian Branch of the Russian Academy of Sciences, Krasnoyarsk (Prof. I. P. Aleksandrova, Dr. J. Ivanov)
A. Mickiewicz University of Poznan (Prof. S. Jurga)
Universität Leipzig, Fakultät für Biowissenschaften, Pharmazie und Psychologie (Prof. A. Beck-Sickinger)
Martin-Luther-Universität Halle-Wittenberg
Department of Physics (Dr. H. T. Langhammer, Prof. Dr. H. Schneider, Prof. Dr. H. Beige)
Martin-Luther-Universität Halle-Wittenberg
School of Pharmacy, Institute for Pharmaceutics (Prof. R. H. H. Neubert, Prof. Dr. S. Wartewig)

5.13 Publications

5.13.1 Conference Contributions

Characterization of active sites in catalysts by means of EPR spectroscopy (T)

A. Pöppl
Symposium des SFB 294 „ Molecules in Interaction with Interfaces“, Leipzig, 2002

Electron Spin Echoes and Electron Spin Relaxation (T)
A. Pöppl
24th Discussion Meeting of the Magnetic Resonance Spectroscopy Division of the GDCH, Tutorial: Pulsed EPR and ENDOR spectroscopy, Bremen, 2002

Pulsed EPR and ENDOR spectroscopy (T)
A. Pöppl
24th Discussion Meeting of the Magnetic Resonance Spectroscopy Division of the GDCH, Tutorial: Pulsed EPR and ENDOR spectroscopy, Bremen, 2002

14. Deutsche Zeolithtagung, Frankfurt/M., 06.03.-08.03.2002
In-MCM-41 Mesoporous Molecular Sieve: A Further Member of the M41S Family
W. Böhlmann, O. Klepel, H. Papp, and D. Michel
(Poster)

DPG-Jahrestagung in Regensburg 10. - 15. März 2002, Arbeitskreis Festkörperphysik:

- Vortrag: NMR- and NQR-Study of Domain Structure in TMCC Crystals
D. Michel, S. Mulla-Osman, G. Völkel, Z. Czapla*
University of Wroclaw, Institute for Experimental Physics
- Hauptvortrag J. Petersson und D. Michel): NMR in Incommensurately Modulated Crystals
Hauptvortrag von G. Völkel, Lokale Ordnungsvorgänge in ferroelektrischen, glasartigen und modulierten Phasen: EPR-Untersuchungen

Juras Banys, Arminas Kajokas, Saulius Lapinskas, Jan Macutkevic, Georg Völkel, Carola Klimm und Andreas Klöpperpieper: New approach to the dielectric spectroscopy (Invited Lecture)

Juras Banys, Arminas Kajokas, Saulius Lapinskas, Jan Macutkevic, Georg Voelkel und Carola Klimm: Dielectric spectroscopy of ferroelectric betaine phosphite with admixture of the antiferroelectric betaine phosphate

31th Colloque AMPERE on Magnetic Resonance and Related Phenomena, Poznan, Polen, 14-19 July 2002, NMR study of the critiocal dynamics at structural phase transitions, D. Michel , F. Decker, P. Mischo, J. Petersson, A. Taye
(Plenary Lecture)

31th Colloque AMPERE on Magnetic Resonance and Related Phenomena, Poznan, Polen, 14-19 July 2002,
High Field NMR Spectroscopy of Molecules Sorbed in Porous Systems
D. Michel, J. Roland, Ö. Erdem
(Poster)

31th Colloque AMPERE on Magnetic Resonance and Related Phenomena, Poznan, Polen, 14-19 July 2002,
Spin relaxation enhancement in liquid gallium confined within porous glasses and artificial opals
E. V. Charnaya, T. Loeser, D. Michel, C. Tien, D. Yaskov, Yu. A. Kumzerow
(Poster)

X AMPERE Summer School, Zakopane, Poland, 2-7 June 2002,
^{1}H NMR spectroscopy of molecules adsorbed in porous media and on interfaces at ultra high magnetic field
D. Michel
(Invited Lecture)

Experimental Nuclear Magnetic Resonance Conference (EENC), 9-14 June 2002, Prag, Czech Republic,
Structure and Dynamics of Molecules Adsorbed in Porous Materials
Ö. Erdem, J. Roland and D. Michel
(Contributed Lecture)

Experimental Nuclear Magnetic Resonance Conference (EENC), 9-14 June 2002, Prag, Czech Republic,
NMR Studies of Atomic Mobility in Confined Liquid Gallium
E. V. Charnaya,T. Loeser, D. Michel, C. Tien[2]
(Poster)

Experimental Nuclear Magnetic Resonance Conference (EENC), 9-14 June 2002, Prag, Czech Republic,
Longitudinal ^{13}C relaxation in CH_2 groups in the presence of internal motion
G. S. Kupryanova, D. Michel
(Poster)

2nd FEZA Conference, Giardini Naxos-Taormina, Italy, 01.09.-05.09.2002
Synthesis and Characterization of In-MCM-41 Mesoporous Molecular Sieves with Different Si/In Ratios
W. Böhlmann, O. Klepel, D. Michel, and H. Papp
(Poster)

2nd International Conference on Broadband Spectroscopy and its Applications, Leipzig, Germany, 02.09.-06.09.2002
Broadband Dielectric Spectroscopy of SBA-15 and MCM-41 mesoporous molecular sieve materials.
A. Pöppl, G. Völkel, W. Böhlmann, M. Hartmann, and J. Banys
(Poster)

NMR studies of structure and dynamics of adsorbed molecules
D. Michel
Symposium des SFB 294 „ Molecules in Interaction with Interfaces“, Leipzig, 9 to 11

October 2002

XV th Czech-Polish Seminar "Structural and Ferroelectric Phase Transitions", Nectiny Castle (Czech Republic), May 20 – 24, 2002
G. Völkel, R. Böttcher, Z, Czapla, and D. Michel, Modulated Phases in
Chromium Doped Dimethylammonium Gallium Sulfate Hexahydrate (DMASGaS) Studied by EPR (Contributed Lecture)

J. Banys, A. Kajokas, S. Lapinskas, J. Macutkevic, G. Völkel, C. Klimm, and A. Klöpperpieper, Distribution of the Relaxation Times in the Mixed BP/BPI Crystals (Invited Lecture)

Euro Summer School, Advanced Course on Modern EPR Spectroscopy, 1-7 December 2002, Antwerp, Belgium
"Size effect in Cr^{3+}-doped $PbTiO_3$ nanopowders studied by EPR and XRD"
E. Erdem, R. Böttcher, H.-C. Semmelhack, E. Hartmann, H.-J. Gläsel
(Poster)

5.14 Journals

M. Gutjahr, R. Böttcher, A. Pöppl
Characterization of the Di-tert-butyl Nitroxide: Li^+ Adsorption Complex in LiY Zeolites by One- and Two-Dimensional Electron Spin-Echo Envelope Modulation Spectroscopy
J. Phys. Chem. B 106 (2002) 1345 – 1349

T. Rudolf, W. Böhlmann, A. Pöppl
Adsorption and Desorption Behavior of NO on H-ZSM-5, Na-ZSM-5, and Na-A as Studied by EPR
J. Magn.Res. 155 (2002) 45-56

Martin Hartmann, A. Vinu, S.P. Elangovan, V. Murugesan, Winfried Böhlmann
Direct synthesis and catalytic evaluation of AlSBA-1
Chem. Commun. (2002) 1238-1239

André Pampel, Dieter Michel, Regina Reszka
Pulsed field gradient MAS-NMR studies of the mobility of carboplatin in cubic liquid-crystalline phases
Chem. Phys. Letters 327 (2002) 131-136

E.V. Charnaya, T. Loeser, D. Michel, C. Tien, D. Yaskov, Yu. A. Kumzerov
Spin-Lattice Relaxation Enhancement in Liquid Gallium Confined within Nanoporous Matrices
Phys. Rev. Lett. 88 (2002) 097602-1-097602-4

M. Gutjahr, R. Böttcher, A. Pöppl
Analysis of Correlation Patterns in Hyperfine Sublevel

Correlation Spectroscopy of S = ½, I = 3/2 Systems
Appl. Magn. Reson. 22 (2002) 401-414

G. Völkel, R. Böttcher, Z. Czapla, D. Michel
EPR Studies of Chromium Doped Dimethylammonium
Gallium and Aluminum Sulfate Hexahydrate (DMAGAS
and DMAAS)
Ferroelectrics 268 (2002) 181-186

G. Völkel, N. Alsabbagh, J. Banys, H. Bauch, R. Böttcher, M. Gutjahr. D. Michel, A. Pöppl
Local Ordering Processes in Ferroelctric, Glass-like and Modulated phases: An EPR Study
Adv. in Solid State Physics 42 (2002) 241-251

D. Michel, J. Totz, Yu. N. Ivanov, A.A. Sukhovsky,
I.P. Aleksandrova, J. Petersson
The Mechanism of Proton Conductivity in Quasi-One Dimensional
Hydrogehn-Bonded Crystals
Ferroelectrics 267 (2002) 303-310

H. Trommer, R. Böttcher, A. Pöppl, J. Hoentsch, S. Wartewig,
R.H.H. Neubert
Role of Ascorbic Acid in Stratum Corneum Lipid Models Exposed
to UV Irradiation
Pharmaceutical Research 19 (2002) 982-991

C. Bussai, S. Vasenkov, H. Liu, W. Böhlmann, S. Fritzsche, S. Hannongbua,
R. Haberland, J. Kärger
On the diffusion of water in silicalite-1: MD simulations using ab initio
fitted potential and PFG NMR measurements
Applied Catalysis A: General 232 (2002) 59-66

D. Michel, J. Roland
High Field NMR Spectroscopy of Molecules Adsorbed in Porous Media and
on Interfaces at Ultra High Magnetic Field
Proceeding of the 30th Congress AMPERE on Magnetic Resonance and Related Phenomena Lisbon, Portugal, 23 – 28 July 2000, Eds.: A. F. Martins, A. G. Feio,
J. G. Moura, ISBN 972-98802-0-4, p. 184-187

G. Völkel, N. Alsabbagh, R. Böttcher, D. Michel, Z. Czapla, J. Furtak
EPR and NMR Studies of the Ferroelectric Ordering of Dimethyl Ammonium Ions in
Dimethylammonium Aluminum Sulfate Hexahydrate (DMAAS)
Proceeding 30th Congress AMPERE on Magnetic Resonance and Related Phenomena,
Lisbon, Portugal, 23 –28 July 2000, Eds.: A. F. Martins, A. G. Feio, J. G. Moura,
pp. 303 – 306, ISBN 972-98802-0-4, 2002

R. Böttcher, C. Klimm, H.-C. Semmelhack, G. Völkel, H.-J. Gläsel, E. Hartmann

Finite Size Effect in Mn^{2+} Doped Ferroelectric $BaTiO_3$ Nanopowders Studied by EPR in X, Q and W Band
Proceeding 30th Congress AMPERE on Magnetic Resonance and Related Phenomena, Lisbon, Portugal, 23 –28 July 2000, Eds.: A. F. Martins, A. G. Feio, J. G. Moura, pp. 299 – 302, ISBN 972-98802-0-4, 2002

W. Böhlmann, O. Klepel, D. Michel, H. Papp
Synthesis and Characterization of In-MCM-41 Mesoporous Molecular Sieves with Different Si/In Ratios
Studies in Surface Science and Catalysis 142B (2002) 1355-1362

A. Taye, D. Michel, J. Petersson
^{35}Cl nuclear magnetic resonance study of critical fluctuations in bis(4-chlorophenyl)sulphone $[(ClC_6H_4)_2SO_2]$
Phys. Rev. B 66 (2002) 174102-1-7

H. Trommer, R. Böttcher, R. H. H. Neubert
Ascorbinsäure – ein Vitamin wie Dr. Jekyll & Mr. Hyde
Pharm. Ztg. 147 (2002) 22-31

A. Taye, D. Michel
^{35}Cl Nuclear Magnetic Resonance Study in Bis(4-Chlorophenyl)Sulphone $[(ClC_6H_4)_2SO_2]$
phys.stat.sol. (b) 233 No. 3 (2002) 519 - 529

Banys J, Lapinskas S, Kajokas A, Matulis A, Klimm C, Volkel G, Klopperpieper A
Dynamic dielectric susceptibility of the betaine phosphate (0.15) betaine phosphite (0.85) dipolar glass
Phys. Rev. B 66 (14) (2002) art. no. 144113

Banys J, Brilingas A, Grigas J, Kajokas A, Klimm C, Matulis A, Volkel G, Lapinskas S,Klopperpieper A
Radio and microwave spectroscopy of the betaine phosphate/betaine phosphite mixed crystals
Ferroelectrics 267 (2002) 285-292

Banys J, Kamba S, Klopperpieper A, Volkel G
Infrared spectrum of deuterated betaine phosphite
phys.stat.sol. (b) 231 (2) (2002) 581-588

Winfried Böhlmann and Norbert Volkmann
Solid Residues of Lignite Hydrogenation: News from Petrography and NMR spectroscopy
Proceedings – Annual International Pittsburgh Coal Conference 2001, 18th, 2695, C.A. (2002) 137, 49499f

A. Pöppl, M. Hartmann
High-field EPR spectroscopy of Cu(I)-NO complexes in zeolite CuZSM-5; Impact of Zeolites and other Porous Materials on the New technologies at the Beginning of the

New Millennium, Eds.: A. Aiello, G., Giordano, F. Testa,
Studies in Surface Science and Catalysis, Vol. 142, Elsevier, Amsterdam (2002) p. 375

Bettino, V. Gutewort, A. Pöppl, M. C. Dinger, O. Zschörnig, K. Arnold,
C. Toniolo, A. B. Beck-Sickinger
Electron Paramagnetic Resonance Backbone Dynamics Studies on Spin-Labelled Neuropeptide Y Analogues
J. Peptide Sci. 8 (2002) 671 - 682

U. Kempe, M. Plötze, A. Brachmann, R. Böttcher
Stabilisation of divalent rare earth elements in natural fluorite
Mineralogy and Petrology 76 (2002) 213-234

J. Roland, D. Michel, A. Pampel
Investigation of conformational changes of organic molecules sorbed in zeolites by HR MAS NMR spectroscopy
J. Fraissard and O. Lapina (eds.), Magnetic Resonance in Colloid and Interface Science (2002) 83 – 95, Kluwer Academic Publishers. Printed in the Netherlands

5.15 Graduations

5.15.1 Ph.D.

M. Gutjahr
ESR- und ESEEM-Untersuchungen von Nitroxidradikal-Adsorptions-komplexen in Y-Zeolithen
Juli 2002

S. Mulla-Osman
NMR- und NQR-Untersuchungen zur Domänenstruktur und zum Mechanismus der Phasenübergänge in Tetramethylammonium-cadmiumchlorid (TMCC)-Einkristallen
Juni 2002

J. Roland
HR-MAS-NMR-Untersuchungen zur Strukturänderung und Dynamik von adsorbiertenMolekülen in Zeolithen
Februar 2002

6 PHYSICS OF INTERFACES — SCIENTIFIC ACTIVITIES

The highlights in research and education of our group are intimately related to the recent, substantial progress in our PFG NMR instrumentation. These achievements are documented in Petrik Galvosa's extraordinary thesis and a patent grant. Within the EC-sponsored project TROCAT, under our coordination, nine groups from five countries are jointly exploring the interrelation between molecular diffusion and conversion in heterogeneous catalysis. The so far attained results of both fundamental and industrial relevance were unconceivable without this strong experimental basis within the Magnetic Resonance Centre of our University. With the special focus on diffusion in zeolites, we initiated the establishment of an international (British/French/German) research team, jointly sponsored by EPSRC, CNRS and DFG. Together with colleagues form the Universities of Hannover and Siegen, we have suggested the nomination of Professor Douglas M. Ruthven, University of Maine, for the Humboldt-Research-Award 2002. Prof. Ruthven is one of the pioneers in the field of zeolitic diffusion and its technological exploitation. We are happy, that Doug Ruthven, having received this award in fall 2002, will significantly contribute to the further success of this team.

Development of Instrumentation and Methodology

6.1 PFG NMR Diffusion Measurement with Ultra-High Field Gradients

P. Galvosas, F. Stallmach, G. Seiffert, J. Kärger

Pulsed field gradient (PFG) NMR permits a most direct access to the non-destructive and non-invasive investigation of transport properties of fluids in complex materials.
To overcome the severe experimental limitations if such studies are performed with systems with short nuclear magnetic relaxation times such as molecules adsorbed in meso- and microporous host materials, a 400 MHz (^{1}H) NMR spectrometer FEGRIS 400 NT was developed which combines the high NMR sensitivity of a high-field NMR spectrometer with our technology to generate stable bipolar pulsed field gradients of very high intensities. By using two TECHRON 8604 amplifiers in a push-pull configuration we are able to switch current pulses of up to ±100 A with a maximum supply voltage of ±300 V. This concept of the power supply yields pulsed gradient intensities in an actively screened Anti-Helmholz coil of up to ±35 T/m over the active sample volume of 7.5 mm diameter and 10 mm length. The measured averaged gradient rise and fall time is 300 T/m per millisecond. 35 T/m are achieved after 150 µs!
By using shaped pulsed field gradients with controlled deviation from rectangular shape [1], a high electronical and mechanical stability of the system is guaranteed. This is the precondition for the implementation of an automatic routine for the adjustment of the pairs of pulsed field gradients, which is based on the determination of the spin echo position in the time domain. The high stability and this automated pulsed field gradient adjustment

routine enable very long signal averaging times which now also permit ^{13}C PFG NMR measurements on zeolitic adsorbate/adsorbent systems.
Additionally, the gradient power supply as well as the spectrometer control enable the use of PFG NMR pulse sequences with bipolar field gradients as suggested by Cotts et al. [2]. They are inevitable if diffusion measurements in systems with strong internal field inhomogeneities are to be performed.

Details of the probe (sample holder, gradient coil, probe without the case) (left) and parts of the spectrometer electronics (rf and gradient power amplifier, spectrometer console, temperature control) (right).

[1] Galvosas, P.; Stallmach, F.; Seiffert, G., 2002, Verfahren zur Steuerung von Verstärkern
Deutsches Patent- und Markenamt Aktenzeichen 102 16 493.2
[2] Cotts, R. M. et al., J. Magn. Reson. 83 252 – 266 (1989).

6.2 PFG NMR Measurement of Multicomponent Diffusion

P. Galvosas, S. Gröger, F. Stallmach, J. Kärger

In NMR studies of adsorbed species in zeolites one usually observes broad NMR lines corresponding to small transverse relaxation times (T_2 and T_2^*) as well as low translational mobilities [1]. Under such conditions, measurements of self-diffusion by PFG NMR requires the application of short and high intensity pulsed field gradients. However, the use of high gradient intensities necessitates procedures to match the field gradient intensities [2,3] which in turn often prevent the acquisition of high-resolution NMR spectra. We developed a method for matching ultra-high-intensity pulsed field gradients retaining, at the same time, spectral resolution. The procedure consists of three steps:
Measurement of a possible mismatch of the field gradient pulses by detecting the spin echo in the presence of a read gradient,
correcting for this mismatch by changing the read gradient during the preparation period, and
acquisition of chemical-shift-resolved spectra without the read gradient during the detection period.
The outlined procedure is applied to monitor intracrystalline self-diffusion of an n-butane/benzene mixture in zeolite NaX by the 13-interval PFG NMR pulse sequence [4].

Distinct lines for benzene and n-butane in the ^{1}H NMR spectra, which are not distorted by a mismatch of pulsed field gradients as recently reported by Price et al. [2], are observed for pulsed field gradient intensities of up to 20 T/m. The matching procedure in conjunction with ultra-high pulsed field gradient intensities allows FT PFG NMR measurements of self-diffusion coefficients as low as 10^{-12} m^2/s as observed, e.g., for benzene in the present system (Fig. 1).

References:
[1] J. Kärger, H. Pfeifer, *Zeolites* ***7*** (1987), 90.
[2] W.S. Price et al., *J. Magn. Reson.* **139** (1999), 205.
[3] P. Galvosas et al., *J. Magn. Reson.* **151** (2001), 260.
[4] R.M. Cotts et al., *J. Magn. Reson.* **83** (1989), 252.

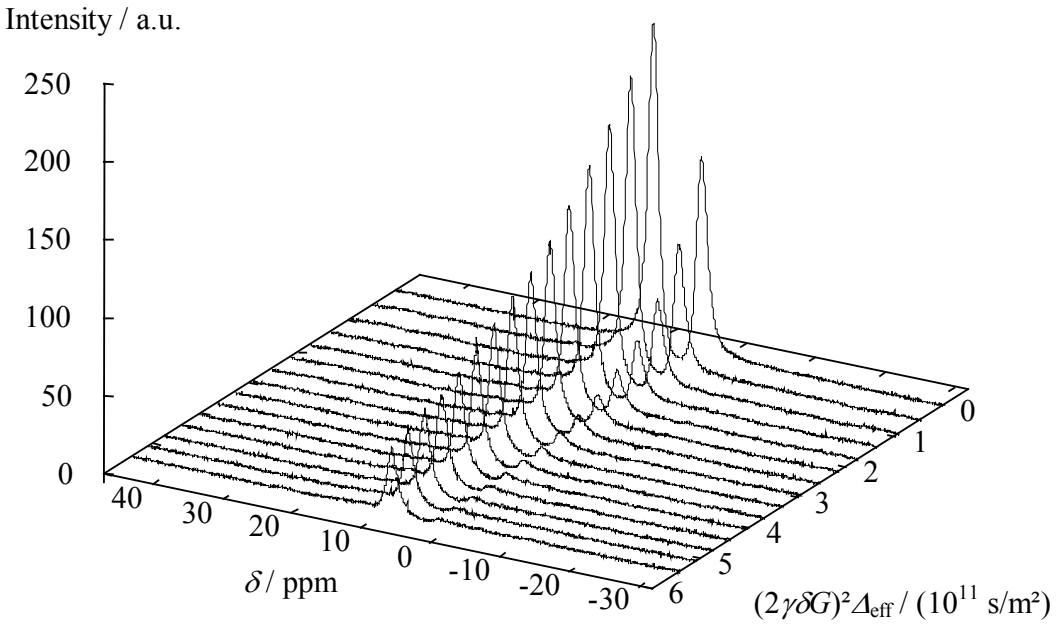

Fig. 1: Chemical-shift-resolved signal attenuation as a function of the applied pulsed magnetic field gradient intensity measured with the 13-interval pulse sequence. The self-diffusion coefficients calculated from the slope of the fitted data are $(1.03\pm0.04)\times10^{-11}$ m^2/s for n-butane and $(2.94\pm0.05)\times10^{-12}$ m^2/s for benzene at an observation time Δ = 25 ms.

6.3 Laser -Supported High-Temperature MAS NMR for *in situ* Studies of Reaction Steps in Heterogeneous Catalysis

H. Ernst, D. Freude, J. Kanellopoulos, D. Prager, D. Schneider

Surface sites capable of donating protons or accepting electrons from adsorbed molecules are essential for heterogeneous catalysis. Magic-angle-spinning nuclear magnetic resonance spectroscopy (MAS NMR) has been successfully applied to the study of the interaction between acid sites in zeolites and base molecules and to the catalytic conversion of organic molecules. The *in situ* technique became the most important tool for such studies. A new technique making use of a laser beam makes it possible to switch from room temperature, at which the reaction is too slow to be measured, to temperatures up to 800 K, at which the reaction takes place within a few seconds.

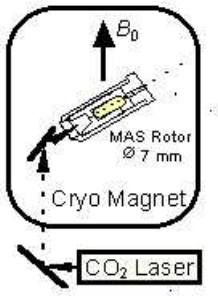

Experimental setup for *in situ* MAS NMR

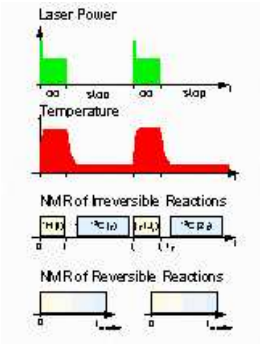

Experimental techniques

Temperature-jump relaxation MAS NMR experiments are for the first time applied to study a heterogeneously catalyzed reaction. This offers the possibility to obtain the reaction rates and activation energies for both forward and backward reactions.

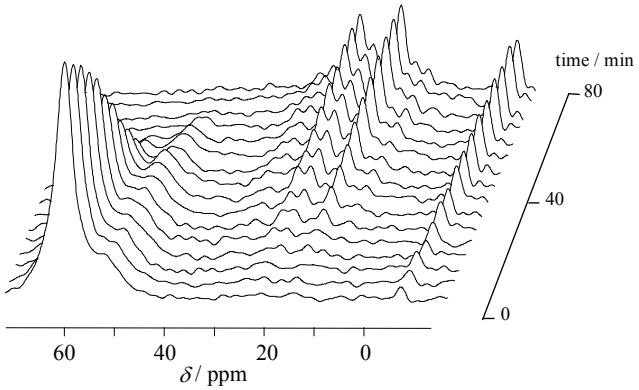

Proton-decoupled ^{13}C MAS NMR spectra of methanol-loaded zeolite H-ZSM-5 during a *stop-and-go* experiment with *go* periods of 5 minutes at 280 °C. Every spectrum was acquired during a *stop* period of 1 hour. The first spectrum at the bottom was recorded after the first *go* period.

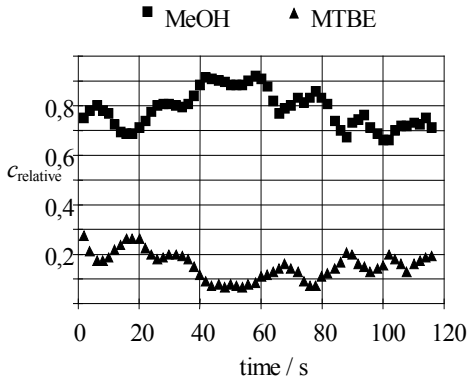

Time-dependent relative concentrations of MTBE and MeOH as deduced from the ^{13}C MAS NMR data of a boron pentasil zeolite loaded with a 1:1 mixture of isobuten and ^{13}C-enriched methanol. 400 FID sets were accumulated.

6.4 ^{17}O MQ MAS and DOR NMR Studies of Alumosilicates with Si/Al-ratio = 1 in very High Magnetic Fields

Th. Loeser, H. Ernst, D. Freude, J. Kärger, B. Knorr, D. Michel*, D. Prager, D. Prochnow *
Institute for Experimental Physics II, Physik Dielektrischer Festkörper

Alumosilicates of Si/Al-ratio 1 were analysed by means of ^{17}O MQMAS (multiple-quantum magic-angle spinning) and DOR (double rotation) NMR in the fields of 17.6 and 11.7 T. The samples under study covered a range in Si-O-Al bond angle of about 30°. The ^{17}O signals in MQMAS, DOR and MAS NMR could be assigned to the oxygen sites in the zeolites.

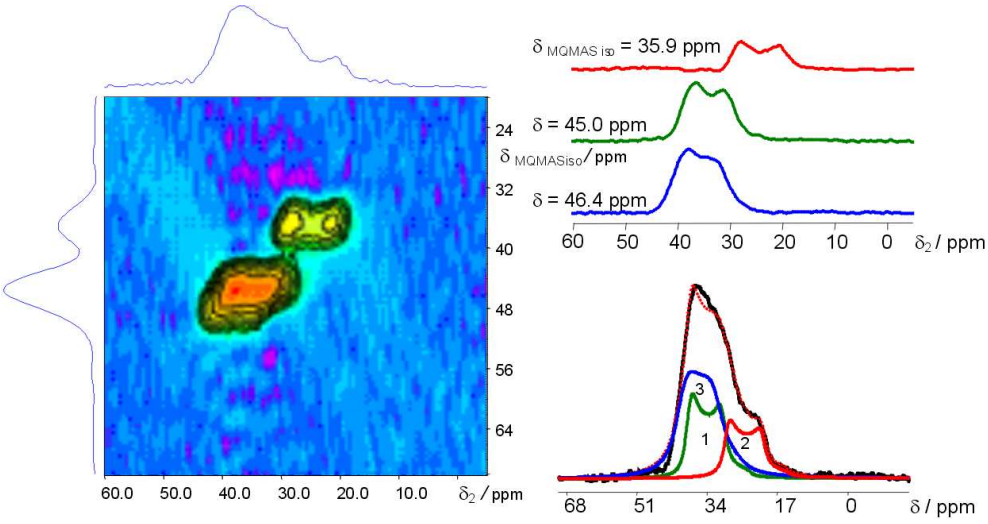

Fig.1: ^{17}O 3QMAS NMR spectrum of the hydrated zeolite Tl-A with anisotropic projection on the top and with isotropic projection on the left hand side. Anisotropic slices of the 2D spectrum for the three isotropic values are given on the right-hand side above. The spectrum below is a usual MAS spectrum with a fit, which uses the results of the 2D spectrum.

For the correlation of the s-character of the oxygen hybrid orbitals ρ and the isotropic ^{17}O chemical shift δ (^{17}O) we have found individual linear correlations for the various zeolites The slopes of these linear dependencies could be explained on the basis of structural parameters, e.g. the Si-O- and Al-O-distances The increase of the basicity of the oxygen framework of the zeolite is reflected by a low-field shift going from the lithium to the cesium form of the zeolites.

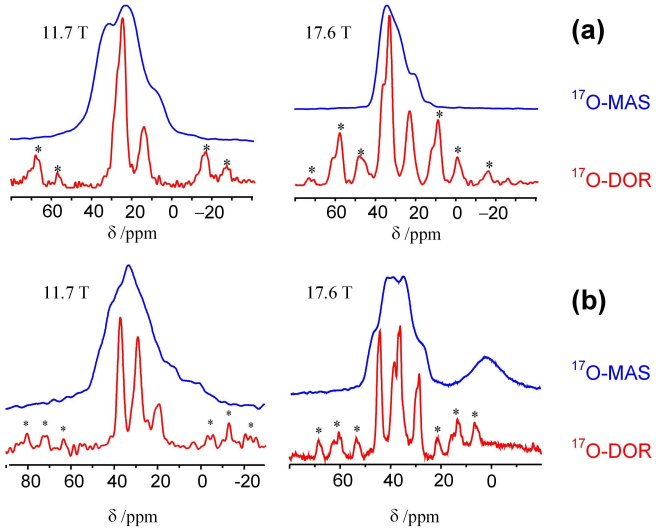

Fig. 2: ^{17}O DOR NMR- and MAS NMR-spectra of the hydrated zeolites Na-A (a) und Na,K-LSX. (b). To get the isotropic values of the chemical shift, measurements at two different magnetic fields are necessary.

6.5 Development and Application of Interference and FTIR-Microscopy for Investigating Regular Intergrowths in AFI-Type Crystals

E. Lehmann, C. Chmelik, S. Vasenkov, O. Geier, B. Staudte, F. Kremer*, J. Kärger
* Instiute for Experimental Physics I, Physik Anisotroper Fluide

Interference microscopy and FTIR microscopy were applied to study intracrystalline concentration profiles of methanol in CrAPO-5 zeolite crystals [1]. By using both techniques, the high spatial resolution of interference microscopy is complemented by the ability of FTIR spectroscopy to pinpoint adsorbates by their characteristic IR bands. For the first time two-dimensional concentration profiles of an unprecedented quality were observed (fig. a). The recorded profiles revealed a highly inhomogeneous intracrystalline distribution of the adsorbate molecules in the zeolite crystal under equilibrium with the adsorbate vapour. Fig. b demonstrates good agreement between the results obtained by both techniques. The observed inhomogeneities in the intracrystalline concentration were ascribed to the regular intergrowth effects in CrAPO-5 crystals. On the basis of the measured intracrystalline concentration profiles, a model for the internal structure of the crystals has been proposed (fig. c).

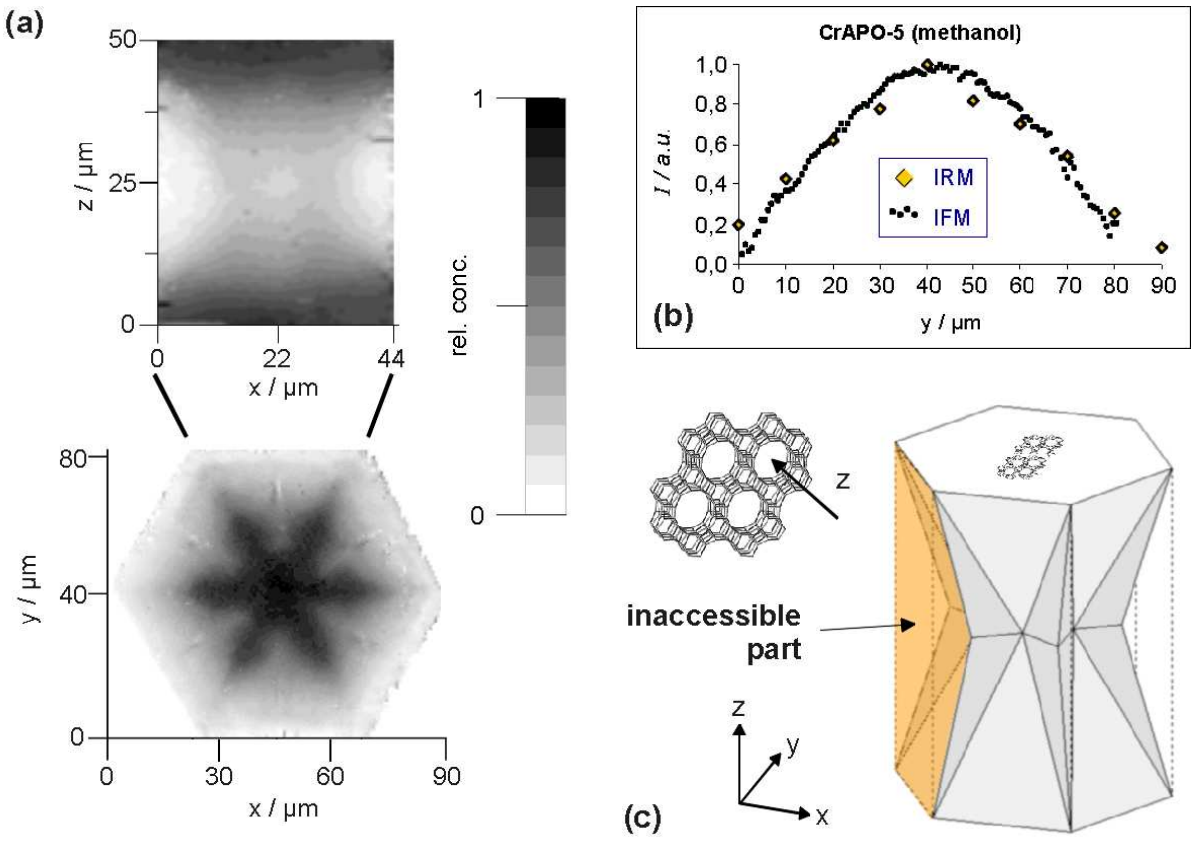

[1] E. Lehmann, C. Chmelik, H. Scheidt, S. Vasenkov, B. Staudte, J. Kärger, F. Kremer, G. Zadrozna and J. Kornatowski, *J. Am. Chem. Soc.* **124** (2002) 8690-8692.

Fundamental Research in Interface Science

6.6 Fractal Geometry of Surface Areas of Sand Grains Probed by Pulsed Field Gradient NMR

F. Stallmach, C. Vogt, F. Jacobs*, J. Kärger
* Institute of Geophysics and Geology

Pulsed Field Gradient NMR (PFG NMR) diffusion measurements are applied to probe the external surface of sand grains. This procedure is based on the fact that in the limit of short observation times the effective diffusivity (being proportional to the mean square displacement of the fluid molecules) decreases linearly with the square root of time, with a slope being proportional to the surface-to-(fluid)volume ratio ([1], cf. fig., left). For the grains of a glacial sand deposit (Rückmarsdorf, central Germany, about 10 km northwest of Leipzig, cf. fig., right) it turns out that the measured surface increases with a power of 2.2 with increasing mean grain diameter [2]. This fits nicely to the results of previous studies with the conventional adsorption technique [3], where for quartz sands fractal dimensions of the same order have been obtained. This procedure implies that the probed diffusion paths have to be smaller than the lower cutoff of the fractal structure

under study. If they are comparable, an alternative version of analysizing the PFG NMR data has to be used [4,5].

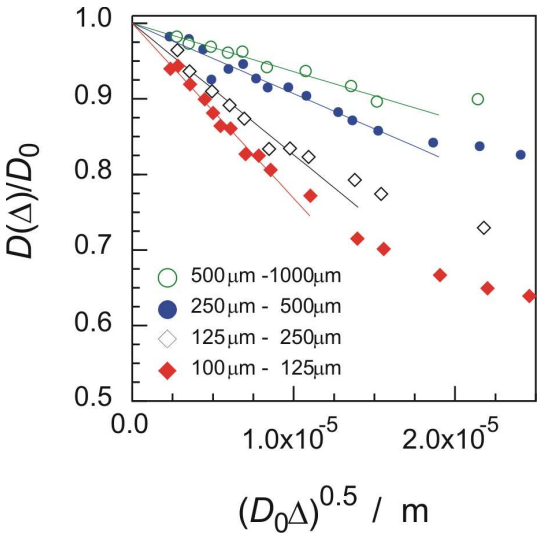

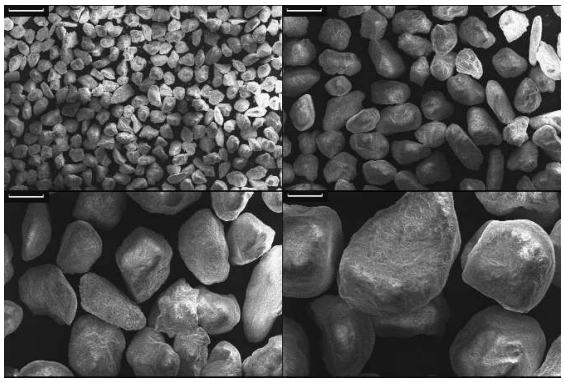

left: Relative effective self-diffusion coefficients $D(\Delta)/D_0$ as a function of $(D_0\Delta)^{0,5}$ for water in the four grain size fractions of the sand. The solid lines represent the results of the fits of the theoretical expression to the early time dependence of these data yielding the surface-to-volume ratio.
right: SEMs of the four grain size fractions of the sand. The bars represent a lenght of 300 µm

[1] P. P. Mitra, P. N. Sen and L. M. Schwartz, Phys. Rev. B 47 (1993) 8565
[2]F. Stallmach, C. Vogt, J. Kärger, K. Helbig, F. Jacobs, Phys. Rev. Lett. 88 (2002) 105505
[3] D. Avnir, D. Farin, P. Pfeifer, J. Coll. Interf. Sci. 103 (1985) 112
[4] D. Candela, Po-zen Wong, Phys. Rev. Lett. 90 (2003) 039601
[5] F. Stallmach, J. Kärger, Phys. Rev. Lett 90 (2003) 039602

6.7 Investigation of the Dependence of the Tortuosity Factor in the Diffusion Regime

O. Geier, S. Vasenkov, J. Kärger

The pulsed field gradient (PFG) NMR technique was applied to study the ethane diffusion in beds of NaX zeolites for displacements, which are orders of magnitude larger than the size of the individual crystals. This study was mainly focused on the question, whether the tortuosity factor in the bulk regime, in which the diffusion is controlled by molecule-molecule collisions, remains the same as in the Knudsen regime, in which molecule-solid collisions dominate.
In order to probe the self-diffusion in the bulk and in the Knudsen regime the measurements were performed in a wide temperature range (193 K – 413 K). The transition from the Knudsen to the bulk regime occurs with increasing temperature as a consequence of

the temperature dependence of the distribution of the molecules in the gaseous and adsorbed phases of the zeolite sample.
The obtained results present the first direct experimental evidence that the apparent tortuosity factor in zeolite beds may be significantly larger in the Knudsen regime than in the bulk regime [1]. The tortuosity factors were obtained by comparison of the measured diffusivities with those calculated using simple gas kinetic theory. The difference in the apparent tortuosity factors is not surprising in view of the different diffusion mechanisms in the Knudsen and in the bulk regimes. The reported results are in qualitative agreement with recent findings of dynamic MC simulations of gas diffusion in various porous systems [2,3].

References
[1] O. Geier, S. Vasenkov, and J. Kärger
Pulsed field gradient nuclear magnetic resonance NMR study of long–range diffusion in beds of NaX zeolite: Evidence for different apparent tortuosity factors in the Knudsen and bulk regimes, J. Chem. Phys. ,117, 1935 (2002).
[2] V. N. Burganos. Gas diffusion in random binary media, J. Chem. Phys., 109, 6772 (1998).
[3] K. Malek, M.-O. Coppens. Effects of Surface Roughness on Self- and Transport Diffusion in Porous Media in the Knudsen Regime, Phys. Rev. Lett., 87, 125505 (2001).

6.8 Study of Tracer Exchange in Single-File Systems

S. Vasenkov, J. Kärger

For the first time a complete description of the time dependence of tracer exchange in single-file systems is given [1]. It is based on the combined application of dynamic Monte Carlo simulations and analytical calculations. The tracer exchange is found to have three different time regimes (viz. the regime of single-particle diffusion, the time regime of single-file diffusion and the regime of center-of-gravity diffusion) related to transport modes of either normal diffusion or single-file diffusion (Fig.1).
The validation of the different regimes for tracer exchange kinetics in real nature is one of the current challenges of experimental research. To our knowledge, the only detailed experimental investigation of particle exchange in single-file systems has been carried out with laser-polarized ^{129}Xe NMR spectroscopy [2]. The observed exchange pattern complies with the time regime of single-file diffusion. Finding examples for the entity of patterns and their mutual transitions remains an attractive task of future experimental work.

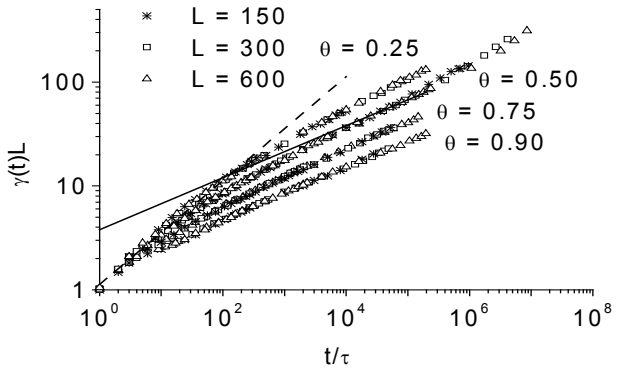

Fig.1 The normalized tracer exchange curves in single-file systems obtained by dynamic Monte-Carlo simulations for different channel length (L) and occupation probability (θ) (points). The dashed and solid lines show the best fit lines for θ=0.5 with the slops of ½ and ¼ expected for the mechanism of normal and of single-file diffusion, respectively, in the limit of short times.

[1] S. Vasenkov and J. Kärger, Phys. Rev. E 66, 052601 (2002)
[2] T. Meersmann, J.W. Logan, R. Simonutti, S. Caldarelli, A. Comotti, P. Sozzani, L.G. Kaiser, and A. Pines, J. Phys. Chem. 104, 11665 (2000)

6.9 Adsorption and Reaction in Single-File Networks

P. Bräuer, A. Brzank, J. Kärger

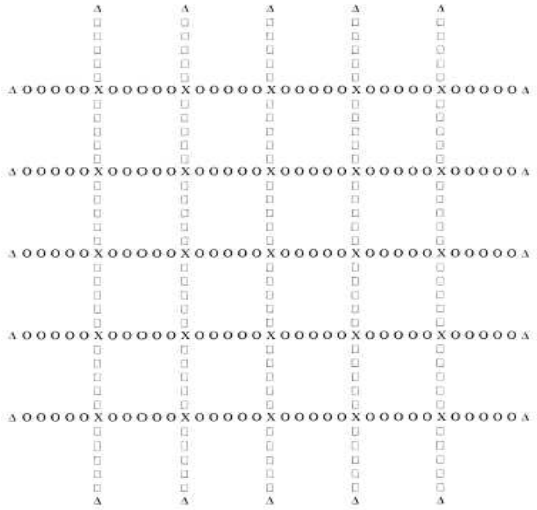

Fig. 1: Quadratic lattice of crossing single-file systems.

Mutually intersecting arrays of single-file systems can serve as a model system for the simulation of reactivity enhancement by confinement, the phenomenon of so-called 'molecular traffic control' (MTC)[1,2]. The expression MTC has been chosen to describe chemical reactions in nanoporous materials where reactant and product molecules prefer different pathways for their diffusion. The concept of MTC implies that the difference in the residence probabilities of reactant and product molecules in the two channel systems

causes a reduced transport inhibition, which in the case of transport-controlled reactions[3,4] leads to an enhanced output of product molecules.

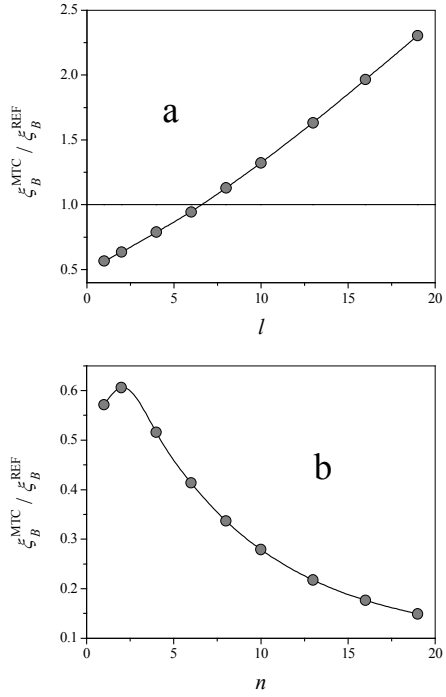

Fig. 2: Benefit $\xi_B^{\mathrm{MTC}}/\xi_B^{\mathrm{REF}}$ of the MTC system in comparison with the REF system for n = 3 channels as a function of the number l of sites in the channel segments between two neighboring intersections (Fig. a) and for l =1 in dependence on the number n of α- and β-channels (Fig. b).

The possibility of reactivity enhancement by molecular traffic control (MTC) is rationalized by dynamic Monte Carlo simulations in a network of single-file systems (Fig.1). The present study[5] clarifies under which conditions the superiority of the MTC system versus the REF system is maintained. It turns out that the MTC system becomes progressively beneficial over the REF system with increasing file lengths between the intersection points (Fig.2). Thus, the benefit of the MTC system is found to be purchased by (i) stronger transport inhibition and (ii) a reduced density of active sites (since in the model considered the sites in the channel segments – being accessible by only one type of molecules – had to be required to be inactive for molecular conversion).

(1) Derouane, E. G.; Gabelica, Z. *J. Catal.* **1980**, 65, 486
(2) Derouane, E. G. *Appl. Catal., A*, **1994**, 115,
(3) Kärger, J.; Ruthven, D. V. *Diffusion in Zeolites and Other Microporous Solids*; Wiley; New York, 1992.
(4) Chen, N. Y.; Degnan, T. F.; Smith, C. M. *Molecular Transport and Reaction in Zeolites*; VCH; New York, 1994.
(5) P. Bräuer, A. Brzank, J. Kärger: „Adsorption and Reaction in Single-File Networks ", J. Phys. Chem., B, 2003, in press

6.10 Correlated Diffusion Anisotropy in Nanoporous Crystals (Zeolites)

J. Kärger, S. Fritzsche*, F. Stallmach
* Institute for Theoretical Physics

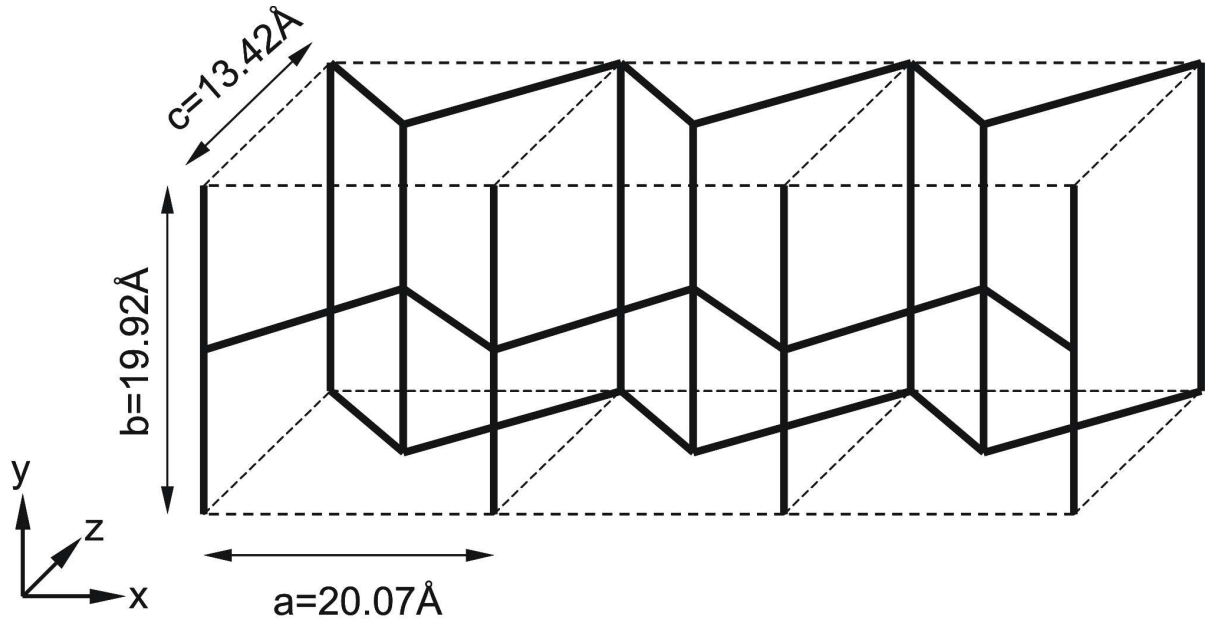

Fig. 1:Topology of the channels in silicalite-1.

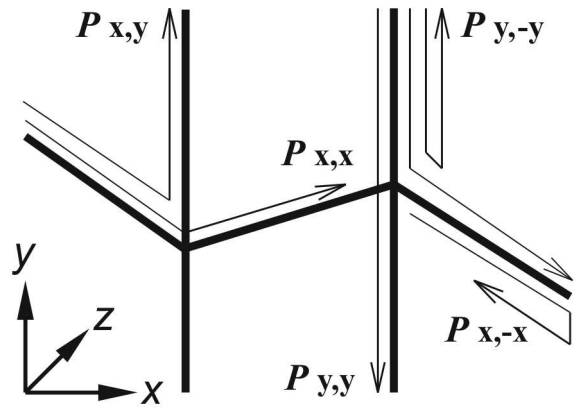

Fig. 2: Illustration of the transisition probabilities

As a consequence of the architecture of the host system (e.g. nanoporous crystalline materials like zeolites), the diffusion rates of guest molecules into different crystallographic directions may be found to be interrelated with each other [1] . As to our knowledge, this feature of structure-mobility correlation has so far been only discussed in the context of molecular guest-host systems like zeolitic adsorbate-adsorbent systems (see, e.g., [2]), though it might as well be applicable to diffusion in genuine solids. The quantitative expression of this interrelation is a function of the host geometry and of the correlation between subsequent diffusion steps (i.e. the particle "memory"). In the case of negligible memory effects, e.g., the principal values of the diffusion tensor for guest molecules in MFI-type zeolites, e.g. (cf. fig.1), are mutually interrelated by the expression

$c^2/D_z = a^2/D_x + b^2/D_y$, with *a*, *b* and *c* denoting the crystal unit cell dimensions. Memory effects in the sequence of displacements between subsequent channel intersections lead to deviations from this simple correlation rule. Following [3], this deficiency is remedied by introducing a parameter set of conditional probabilities of molecular displacements within the pore network as schematically displayed in fig. 2 [4]. They allow the establishment of closed forms for the correlation rule of diffusion anisotropy in MFI-type zeolites, which are able to take account of the memory effects during molecular propagation. They are found to be in excellent agreement with the results of MD simulations [4].

1. J. Kärger, J. Phys. Chem. 95 (1991) 5558
2. S. Jost, Thesis, Leipzig University, Institute for Theoretical Physics, in preparation
3. F. Jousse, S. M. Auerbach and D. P. Vercauteren , J. Chem. Phys. 112 (2000) 1531
4. S. Fritzsche, J. Kärger, J. Phys. Chem. 2003 (in press)

Applications

6.11 n-Butene Conversion on H-Ferrierite Studied by ^{1}H and ^{13}C MAS NMR

D. Freude, A. G. Stepanov*, H. Ernst
* Russian Academy of Science, Novosibirsk

^{1}H and ^{13}C MAS NMR (figures 1 and 2) spectroscopy of the temperature-dependent conversion of *n*-but-1-ene on H-ferrierite in a batch reactor offers information about the mechanism of isomerization and the formation of carbonaceous deposits, which is important also for processes in a flow reactor.
The following successive steps in the olefin conversion at increasing temperature of the reaction were distinguished: a double bond shift reaction affording *n*-but-2-enes; scrambling of the selective ^{13}C-label in *n*-but-2-enes, oligomerization (dimerization), conjunct polymerization, formation of condensed aromatics, formation of simple aromatics.
Selective ^{13}C-label scrambling in *n*-but-2-ene and oligomerization as well as the absence of *iso*-butene among the products of *n*-but-1-ene isomerization, provide evidence for a bimolecular pathway of *n*-but-1-ene isomerization on a fresh zeolite.

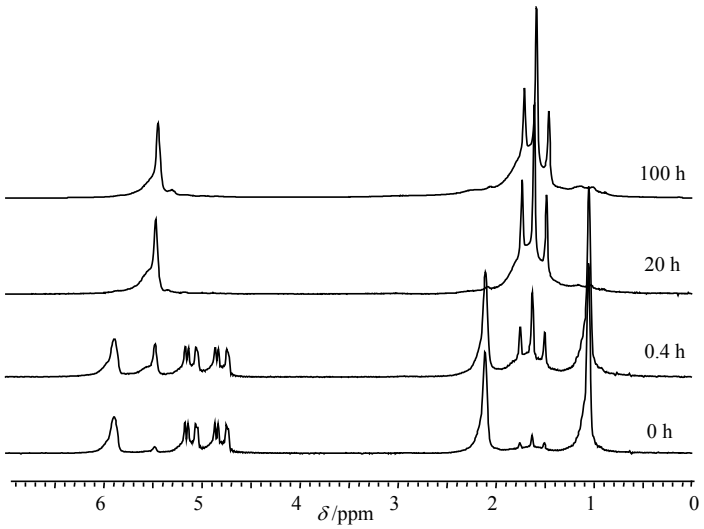

Fig.1: ^{1}H MAS NMR spectra of the zeolite H-FER loaded with [1-^{13}C]-*n*-but-1-ene1 at 300 K in dependence on the reaction time

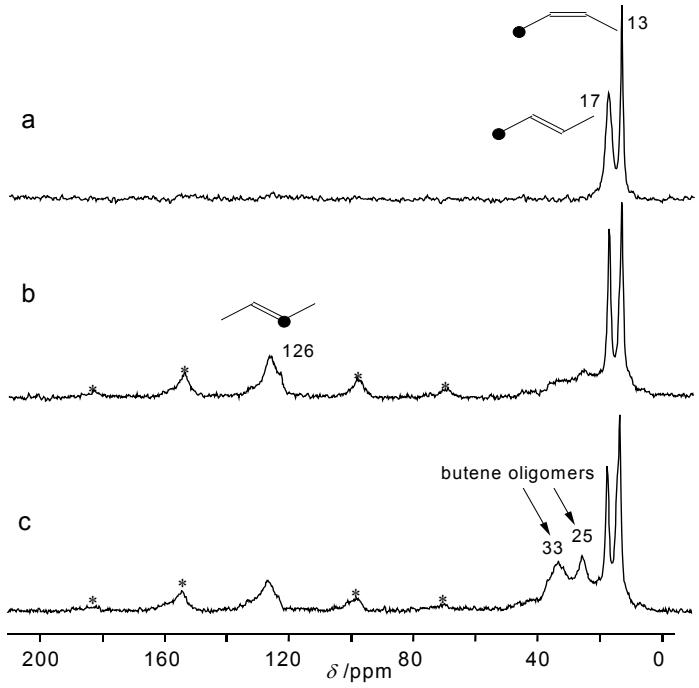

FIG.2**:** ^{13}C CP/MAS NMR spectra of the zeolite H-FER loaded with [1-^{13}C]-*n*-but-1-ene 1. (a) zeolite kept for 15 min at 300 K; (b) zeolite kept for one week at 300 K; (c) zeolite kept for 1 h at 373 K and then measured at 300 K.

6.12 In-situ ^{11}B MAS NMR Study of the Synthesis of a Boron Containing MFI-Type Zeolite

H. Liu , H. Ernst, D. Freude , F. Scheffler* , W. Schwieger*
* University of Erlangen-Nürnberg, Dept. of Technical Chemistry

The transformation of porous glass spheres into MFI-spheres was observed by *in situ* ^{11}B MAS NMR spectroscopy (cf. figure). The sealed quartz ampoules containing the reaction mixture were put into the spinner, then heated up in the rotating spinner to the reaction temperature and analyzed at this temperature in dependence on the reaction time. The yield of crystalline material could be determined by means of the intensity of a narrow signal at -3.7 ppm in the ^{11}B MAS NMR spectra. Information about changes in the basicity of the solution could be obtained *in situ* from the chemical shift of the "liquid" boron signal. It could be shown that crystallization of MFI zeolite takes place with a strongly increased crystallization time under the influence of the about 10^5-fold of the standard acceleration of gravity.

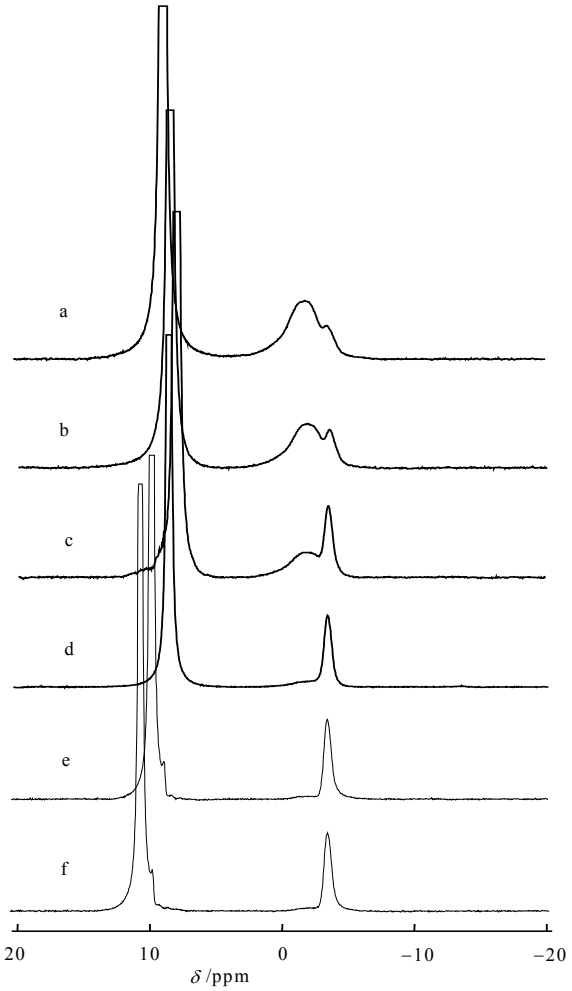

In situ ^{11} B MAS NMR spectra of synthesis measured at the reaction temperature of 448 K: (a) 96h-spectrum, (b) 168 h-spectrum, (c) 216 h-spectrum, (d) 316 h-spectrum, (e) 348 h-spectrum, (f) 376 h-spectrum. The "liquid" lines were cut off, in order to enhance the "solid" signals.

6.13 Surprising Drop of the Diffusivities of Benzene in a Mesoporous Material of Type MCM-41

C. Krause, J. Kärger, L. Moschkowitz, F. Stallmach

With the advent of ordered mesoporous materials like MCM-41, adsorption science and technology has been accomplished by a further most attractive subject. Interestingly enough, among the numerous studies devoted to this novel field of research, only very few deal with the investigation of the transport properties of these new materials. This is mainly due to the fact that - unlike their nanoporous crystalline counterparts, the zeolites - ordered mesoporous materials are generally not available as well-shaped particles.
We have applied Pulsed Field Gradient (PFG) NMR to study molecular diffusion of benzene in a commercial sample of MCM-41 (fig.1). Over a very small concentration range at medium pore filling factors the diffusivity is found to sharply drop by up to one order of magnitude, while it remains essentially constant over the total remaining range from vanishing concentrations up to over-saturation (fig.2). Similarly extreme deviations from monotonous concentration patterns have so far not been described in the literature. The observed effect may be rationalised as a consequence of the onset of capillary condensation in the transport pores in the hyper-structure of the MCM-41 particles under study.

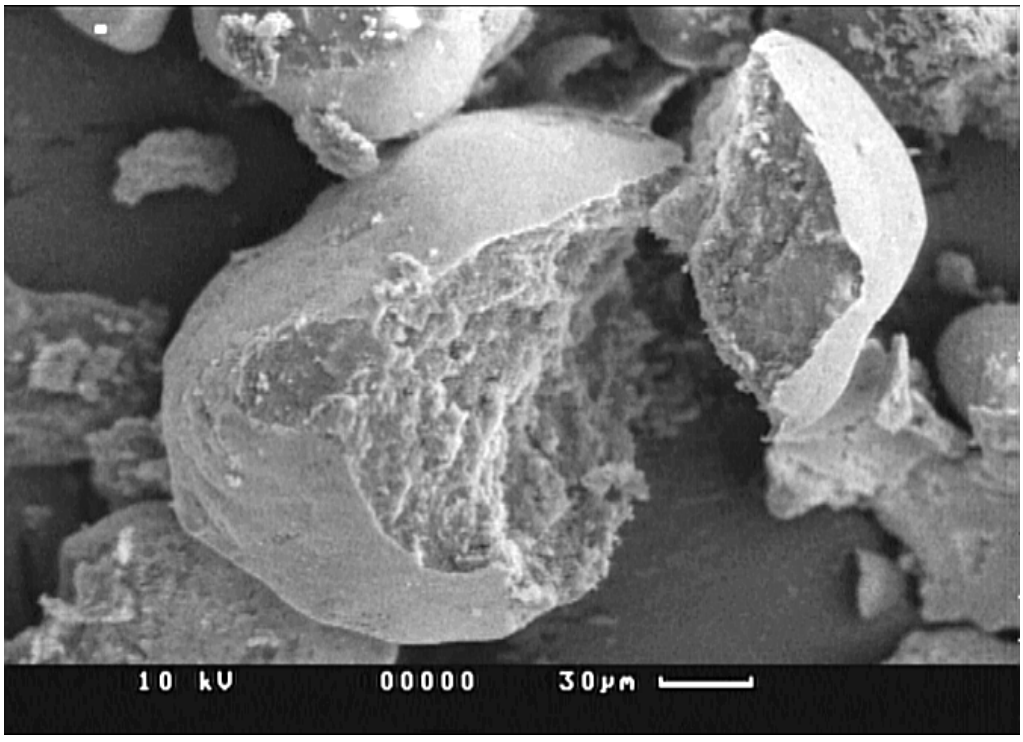

Fig. 1: Electron micrographs of the investigated MCM-41 material.

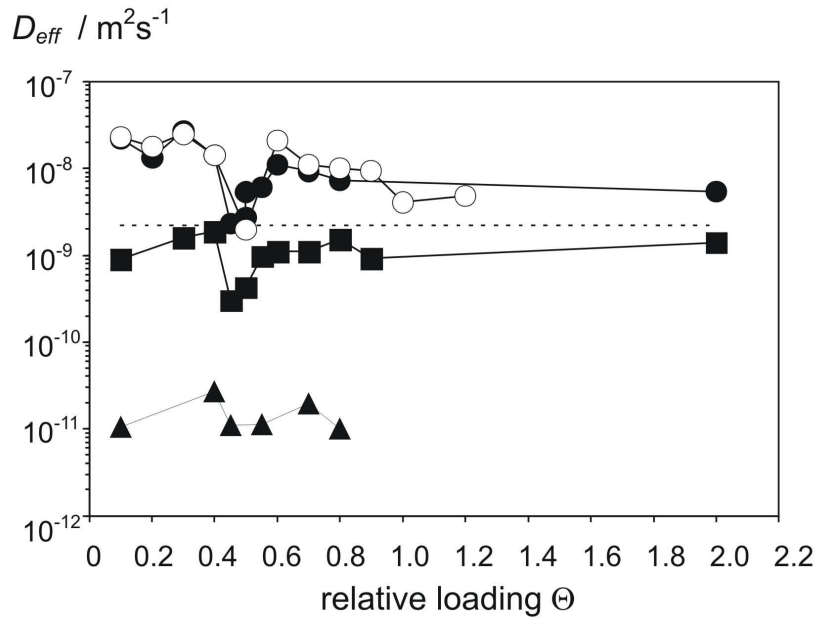

Fig. 2: Concentration dependence of benzene diffusivity in MCM-41. Effective diffusion coefficients versus relative loading (Θ=1.0 refers to complete occupation of the channel pores) at 298 K (open and filled circles, refer to two different sets of samples), 258 K (squares) and 208 K (triangles), dashed line: diffusivity of liquid benzene at 298 K.

[1] Oberhagemann, U., Jeschke, M., Papp, H., *Micropor. Mesopor. Mat.*, 33, 165 (1999)
[2] Stallmach, F., Kärger, J. Krause, C., Jeschke, M., Oberhagemann, U., *J. Am. Chem. Soc.*, 122, 9237-9242 (2000).
[3] Krause, C., Stallmach, F., Mönicke, D., Spange, S., Kärger, J., Adsorption, in press

6.14 Homopolymer Diffusion in a Bicontinuous Polymeric Microemulsion – A PFG NMR Study

Stefan Gröger, Frank Stallmach, Jörg Kärger, C. M. Papadakis*
*Instiute of Experimental Physics I, Physik Anisotroper Fluide

Ternary polymer blends form a variety of mesoscopically structured phases, such as the homogeneously disordered, the swollen lamellar and the macrophase-separated phase, and can serve as a model system for studying the influence of the structure on polymer diffusion.

The system under investigation consists of poly(dimethylsiloxane) (PDMS) and poly(ethylethylene) (PEE) homopolymers and a small amount of symmetric PEE-PDMS diblock copolymers. As a function of temperature, it forms a bicontinuous microemulsion and the homogeneously disordered phase. We have applied temperature-dependent pulsed field gradient NMR to investigate the diffusional behavior of this ternary polymer blend in the bicontinuous microemulsion phase [1].

Comparison with the self-diffusion coefficients of the parent homo- and diblock copolymers enabled us to identify two diffusional processes in the microemulsion phase (Fig. 1): A fast process, which is due to the diffusion of PDMS homopolymers, is slowed down compared to bulk PDMS self-diffusion. A slow process, which is assigned to the diffusion of PEE homopolymers, is slightly faster than the PEE self-diffusion in the bulk. These findings show that the diffusivities are both influenced by the tortuosity of the bicontinuous structure and by the exchange of the homopolymers between domains having significantly different viscosities.

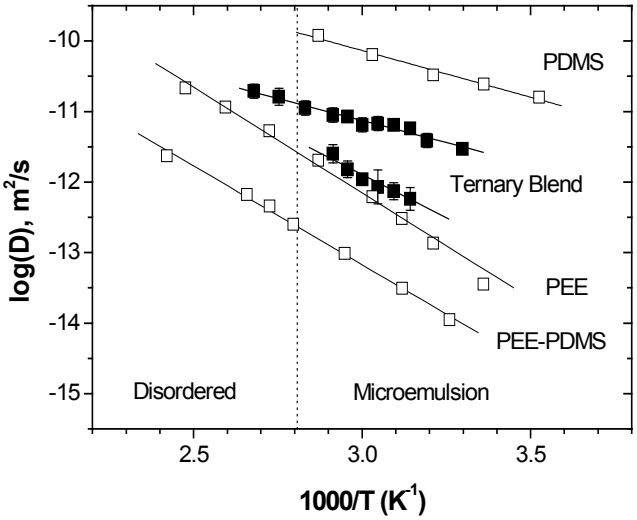

Fig.1: Arrhenius plot of the diffusivities observed by PFG NMR. Open squares: parent polymers. Filled squares: slow and fast process observed in the ternary blend. Dotted line: Phase transition temperature of the ternary blend.

6.15 Focal Issue and First Results of the EC Project "TROCAT"

O. Geier, S. Vasenkov, D. Freude, J. Kärger

In this project, our intention is to find the routes of the production of fluid catalytic cracking (FCC) catalysts, which lead to improved catalytic performance due to optimization of the transport of reactants and products in these materials.
The direct investigation of molecular transport in solid catalysts has become possible only recently with the progress in the pulsed field gradient technique of nuclear magnetic resonance (PFG NMR). Application of this technique allows, for the first time, the direct observation of molecular migration (diffusion) in microporous catalysts. In the TROCAT project this technique is used to overcome one of the main shortcomings in the optimization of FCC catalyst, i.e. the lack of an optimization with respect to the transport properties. Using PFG NMR, initially, the transport properties of the samples of the reference formulated catalyst and of the reference zeolite Y were investigated. Zeolite Y represents the most important, catalytically active part of the FCC formulated catalysts. The reference samples were chosen to closely resemble those of the catalysts currently used in the modern refineries. Further work resulted in the production of new samples of ultra-stabilized Y zeolite, which were prepared under various dealumination conditions.

The transport properties of these samples were studied using for the most part PFG NMR. Investigations of the transport properties of the samples were complemented by the characterization of their catalytic and structural properties, by special syntheses and by molecular modelling performed by our partners in the University of Athens, CEPSA (Madrid), Grace (Worms), the Heyrovsky Institute Prague, SINTEF (Oslo), the Stuttgart University and WITEGA (Berlin). The obtained results indicate that there are certain correlations between the catalytic performance and the transport properties. The existence of such correlations was found in some cases to be paralleled by a better catalytic performance of the new samples in comparison with the reference samples. Future project activities will be aimed at a more complete understanding of these correlations. Based on this understanding new routes to produce improved FCC catalysts will be developed. In this task, the simulations of molecular transport in FCC catalysts, which are an intrinsic part of the project, will play an important role.

6.16 Intracrystalline Monitoring of Molecular Uptake into the One-dimensional Channels of AFI Type Crystals Using Interference Microscopy

E. Lehmann, C. Chmelik, O. Geier, S. Vasenkov, J. Kärger

Intracrystalline concentration profiles of methanol during its adsorption into the one-dimensional channels of CrAPO-5 crystals were reported [1]. The exceptionally high spatial resolution of the recorded profiles was achieved by applying the interference microscopy technique recently introduced in our laboratory. In order to get quantitative information the measured concentration profiles were compared with those simulated by the dynamic Monte Carlo method. This approach allowed us to investigate separately the influences of (i) the intracrystalline diffusion, (ii) the transport barriers on the external crystal surface and (iii) the effects of the intergrowth structure on molecular uptake. The results indicate that although the rate of methanol uptake is mainly determined by the intracrystalline diffusivity of methanol, this rate is somewhat reduced due to the existence of transport barriers on the crystal surface. Thus, we have demonstrated that the method introduced by this work for uptake studies in one-dimensional adsorbate systems has clear advantages in comparison with conventional uptake methods.

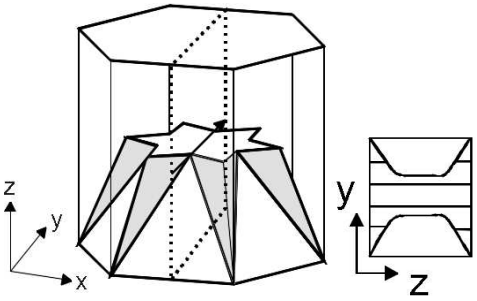

Assumptions (MC): 1. one-dimensional random walk in the lattice, 2. probability of diffusion step is independent of concentration.

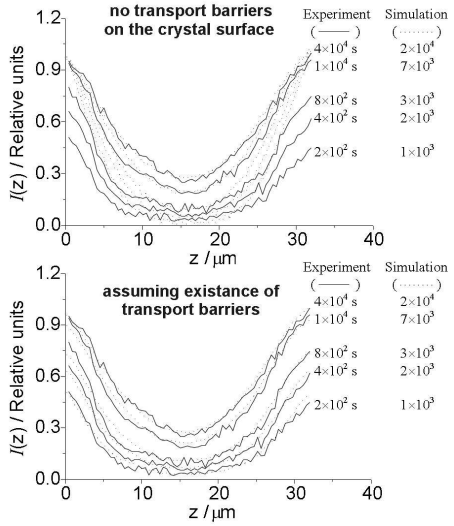

[1] E. Lehmann, S. Vasenkov, J. Kärger, G. Zadrozna and J. Kornatowski, *J. Chem. Phys*. Vol. **118** (2003), in press.

6.17 Funding

Prof. Dr. D. Freude, Dr. H. Ernst
^{17}O NMR spectroscopy of the interaction of molecules with the zeolite framework / SFB 294 - F5

Prof. Dr. D. Freude, Dr. H. Ernst
In situ MAS NMR studies of the n-butene isomerization over ferrierites / SFB 294 - G2

Prof. Dr. J. Kärger
Diffusion of mixtures in zeolites / SFB 294 - G3

Prof. Kärger, Dr. Ch. M. Papadakis
Molecular transport and structure in polymers / SFB 294 - G4

Prof. Dr. J. Kärger
Structure-stimulated reactions / SFB 294 - H3

Prof. Dr. D. Freude, Prof. Dr. J. Kärger, Prof. (i.R.) Dr. Dr. h.c. H. Pfeifer
In situ studies of catalytic reactions by MAS- and PFG-NMR / Graduiertenkolleg „Physikalische Chemie der Grenzflächen“ - A4

Prof. Dr. J. Kärger
PFG NMR of surfactants in interaction with porous solids / Graduiertenkolleg „Physikalische Chemie der Grenzflächen“ - C2

Prof. Dr. D. Freude, Dr. H. Ernst
Characterization of elementary steps of the crystallisation of zeolites in porous glasses by in situ MAS NMR / FR 902 / 6-2

Prof. Dr. D. Freude, Prof. Dr. D. Michel
DOR and multi-quantum MAS NMR for high field NMR studies of quadrupole nuclei on solids /
FR 902 / 9-1

Prof. Dr. J. Kärger
Permeation of monomers in nanoporous host/guest-systems / Schwerpunktprogramm „Nanoporöse Materialien“ Ka 953/13-1 und 13-2

Prof. Dr. J. Kärger
Development of new ceramics / EC-Project GRD1-1999-11207

Prof. Dr. J. Kärger
Molecular diffusion in nanoporous materials / DFG-CNRS-Project Ka953/14-1, Ka953/14-2

Prof. Dr. J. Kärger
New dealumination routes to produce transport-optimised catalysts for crude oil conversion / EC-Project GRD2-2000-30364

Prof. Dr. J. Kärger, Dr. F. Stallmach
Diffusion optimation of microporous membranes and particle batches / EC-Project HPMD-CT-2000-00029

Prof. Dr. J. Kärger, Dr. F. Stallmach
PFG NMR investigations on technical catalysts / BASF AG

Dr. F. Stallmach, Prof. Dr. J. Kärger
NMR and MRI studies of aquifer rock / UFZ Halle-Leipzig GmbH

6.18 Organizational Duties

D. Freude
Project Reviewer: Deutsche Forschungsgemeinschaft
Membership in Editorial Boards: Solid State NMR
Referee: Chem. Phys. Lett., J. Chem. Phys., J. Phys. Chem., J. Magn. Res., Solid State NMR

J. Kärger
Ombudsman of Leipzig University
Membership in the Programme Committee "Magnetic Resonance in Porous Media" (Ulm 2002, Paris 2004), "Fundamentals of Adsorption" (Serona, Arizona, USA, 2004), International Zeolite Conference (Capetown 2004) and in the permanent DECHEMA committees "Zeolites" and "Adsorption"
Membership in Editorial Boards: Adsorption, Microporous and Mesoporous Materials
Referee: Phys. Rev., Phys. Rev. Lett., Europhys. Lett., J. Chem. Phys., J. Phys. Chem., Langmuir, Micropor. Mesopor. Mat., PCCP, J. Magn. Res.
Project Reviewer: Deutsche Forschungsgemeinschaft, National Science Foundation (USA)

F. Stallmach
Referee: J. Magn. Res., Micropor. Mesopor. Mat., Phys. Rev. Lett.

B. Staudte
Referee: Micropor. Mesopor. Mat.

S. Vasenkov
Referee: J. Am. Chem. Soc., Micropor. Mesopor. Mat.

6.19 External cooperations

Academic

Acad Sci Czech Republ, Inst Macromol Chem, Czech Republic,
Prof. Konak, Prof. Stepanek
Acad Sci Czech Republ, Heyrovsky-Inst. Phys. Chem., Czech Republic,
Dr. Kocirik, Dr. Zikanova
Delft University, Inst.Chem. Tech., Delft, Niederlande
Prof. Kapteijn
Institut de Recherches sur la Catalyse, CNRS, Villeurbanne, France
Dr. Jobic
Institut Francais du Petrole, Malmaison, France
Dr. Methivier
KFA Jülich GmbH, Forschungszentrum, Inst Biotechnol, Jülich, Germany
Dr. Schoberth
Max Planck Institut für Kohlenforschung, Mülheim, Germany
Dr. Schmidt, Prof. Schüth
Max Planck Institut für Metallforschung, Stuttgart, Germany
Dr. Majer
Russian Acad Sci, Boreskov Inst Catalysis, Siberian Branch, Novosibirsk, Russia
Dr. Stepanov
TU München, Lehrstuhl Technische Chemie 2, Germany
Dr. Kornatowski, Prof. Lercher
Università di Sassari, Dipartimento Chimica, Sassari, Italy
Prof. Demontis, Prof. Suffritti
Universiät Eindhoven, Schuit Institute, Eindhoven, Niederlande
Prof. van Santen
Universität Erlangen Nürnberg, Dept Chem Engn, Erlangen, Germany
Prof. Emig, Prof. Schwieger
Universität Hannover, Dept Phys.Chem, Hannover, Germany
Prof. Caro, Prof. Heitjans
Universität Leipzig, Institut für Analytische Chemie, Leipzig, Germany
Prof. Berger
Universität Leipzig, Institut für Technische Chemie, Leipzig, Germany
Prof. Einicke, Prof. Papp
Universität Leipzig, Institut für Medizinische Physik und Biophysik, Leipzig, Germany
Prof. Arnold, Prof. Gründer
Universität Leipzig, Instiut für Pharmazeutische Technolgie, Leipzig, Germany
Prof. Süß
Universität Leipzig, Wilhelm Ostwald Institut für Physikalische & Theoretische Chemie, Leipzig, Germany
Dr. Hunger, Dr. Knoll
Universität Regensburg, Institut Biophysik & Physikalische Biochemie, Regensburg, Germany
Prof. Brunner
Universität Stuttgart, Institut für Technische Chemie, Stuttgart, Germany
Prof. Hunger, Prof. Weitkamp
University Athens, Dept Chem. Engn., Athens, Greece
Prof. Theodorou

University of Maine, Dept. Chem. Engin., USA
Prof. Ruthven

Industry
Air Prod & Chem Inc, Allentown
Dr. Coe, Dr. Zielinski
BASF, Ludwigshafen
Dr. Müller
Cepsa, Madrid
Dr. Perez
Grace, Worm
Dr. McElhiney
Resonance Instruments Ltd., Witney, UK
J. McKendry
SINTEF, Oslo
Prof. Stöcker
Tricat, Bitterfeld
Dr. Tufar
WITEGA, Berlin
Dr. Lutz

6.20 Patents

Galvosas, P.; Stallmach, F.; Seiffert, G., 2002, Verfahren zur Steuerung von Verstärkern Deutsches Patent- und Markenamt Aktenzeichen 102 16 493.2

6.21 Publications

6.21.1 Journals

Bräuer P., Brzank A., Kärger J.:
Adsorption by single-file networks under molecular traffic control.
Appl. Surf. Sci. 196 (2002) 273.

Bussai C, Vasenkov S, Liu H, Böhlmann W., Fritzsche S., Hannongbua S., Haberlandt R., Kärger J.:
On the diffusion of water in silicalite-1: MD simulations using ab initio fitted potential and PFG NMR measurements.
Appl. Catal A-Gen 232 (2002) 59.

Cabrita E. J., Berger S., Bräuer P., Kärger J.:
High-resolution DOSY NMR with spins in different chemical surroundings: Influence of particle exchange.

J. Magn. Reson. 157 (2002) 124.

Datka J., Gil B., Baran P., Staudte B.:
Combined IR and catalytic studies of the role of Lewis acid sites in creating acid sites of enhanced catalytic activity in steamed HZSM-5.
Stud. Surf. Sci. Catal. 135 (2002) 154.

Datka J., Gil B., Baran P., Staudte B.:
Distribution of the strength of acid sites in mildly steamed HZSM-5 studied by IR spectroscopy.
Reaction Kinetics Catal. Lett. 77 (2002) 209.

Freude D., Kärger J.: NMR Techniques, in: *Handbook of Porous Solids*, Edited F. Schüth, K.S.W. Sing, J. Weitkamp, Wiley-VCH, Vol. 1, 2002, p. 465-505

Fritzsche S., Kärger J.:
Correlation in anisotropic Diffusion of Guest Molecules in Silicatite-1.
Stud. Surf. Sci. Catal. 142 (2002) 1955.

Geier O., Vasenkov S., Kärger J.:
Pulsed field gradient nuclear magnetic resonance study of long-range diffusion in beds of NaX zeolite: Evidence for different apparent tortuosity factors in the Knudsen and bulk regimes.
J. Chem. Phys. 117 (2002) 1935.

Gröger S., Rittig F., Stallmach F., Almdal K., Stepanek P., Papadakis C.M.:
A pulsed field gradient nuclear magnetic resonance study of a ternary homopolymer/diblock copolymer blend in the bicontinuous microemulsion phase.
J. Chem. Phys. 117 (2002) 396.

Kärger J.:
The random walk of understanding diffusion.
Ind. Eng. Chem. Res. 41 (2002) 3335.

Kärger J.:
Comment on “Study of diffusion and counter-diffusion of para- and ortho-xylene in H-SSZ-24 and H-ZSM-11 zeolites" by R. Roque-Malherbe and V. Ivanov,
[Micropor. Mesopor., Mater. 47 (2001) 25-38]
Microporous Mesoporous Mater. 56 (2002) 321.

Kärger J., Stallmach F.: NMR Diffusion Studies of Molecules in Nanoporous Materials, in: J. Fraissard and O. Lapina (eds.) *Magnetic Resonance in Colloid and Interface Science*, 2002 Kluwer Acad. Publ., 57-70

Kärger J., Freude D.:
Mass transfer in micro- and mesoporous materials.
Chem. Eng. Technol. 25 (2002) 769.

Kärger J., Ruthven D.M.: Mass Transfer in Porous Solids, in: *Handbook of Porous Solids*, Edited F. Schüth, K.S.W. Sing, J. Weitkamp, Wiley-VCH, Vol. 4, 2002, p.2089-2173

Kalies G., Bräuer P., Schmidt A., Messow U.:
Calculation and Prediction of Adsorption Excesses on the Ternary Liquid Mixture/Air Interface from Surface Tension Measurements.
J. Colloid Interface Sci 247 (2002) 1.

Lehmann E., Chmelik C., Scheidt H., Vasenkov S., Staudte B., Kärger J., Kremer F., Zadrozna G., Kornatowski, J.:
Regular inter-growth in the AFI-type crystals: Influence on the intracrystalline adsorbate distribution as observed by interference and FTIR-microscopy.
J. Am. Chem. Soc. 124 (2002) 8690.

Liu H., Ernst H., Freude D., Scheffler F., Schwieger W.:
In situ ^{11}B MAS NMR study of the synthesis of a boron-containing MFI type zeolite.
Microporous Mesoporous Mater. 54 (3): (2002) 319.

Nestle N., Qadan A., Galvosas P., Süss W., Kärger J. :
PFG NMR and internal magnetic field gradients in plant-based materials.
Magnetic Resonance Imaging 20 (2002) 567.

Nestle N., Zimmermann C., Dakkouri M., Kärger J.:
Transient high concentrations of chain anions in hydrating cement - indications from proton spin relaxation measurements.
J. Phys. D Appl. Phys. 35 (2002)166.

Ngwa W., Geier O., Stallmach F., Naji L., Schiller J., Arnold K.:
Cation Diffusion in Cartilage Measured by Pulsed Field Gradient NMR.
Eur. Biophys. J. 31 (2002) 73.

Paoli H., Methivier A., Jobic H., Krause C., Pfeifer H., Stallmach F., Kärger J.:
Comparative QENS and PFG NMR diffusion studies of water in zeolite NaCaA.
Microporous Mesoporous Mater. 55 (2002) 147.

Scheffler F., Schwieger W., Freude D., Liu H., Heyer W., Janowski F:
Transformation of porous glass beads into MFI-type containing beads.
Microporous Mesoporous Mater. 55 (2002): 181

Stallmach F., Vogt C., Kärger J., Helbig K., Jacobs F.:
Fractal geometry of surface areas of sand grains probed by pulsed field gradient NMR.
Phys. Rev. Lett. 88 (10): art. no. 105505.

Stepanov A.G., Luzgin M.V., Arzumanov S.S., Ernst H., Freude D.:
n-Butene Conversion on H-Ferrierite Studied by ^{13}C MAS NMR.
J. Catal. 211 (2002)165.

Trampel R., Schiller J., Naji L., Stallmach F., Kärger J., Arnold K.:
Self-diffusion of polymers in cartilage as studied by pulsed field gradient NMR.
Biophys. Chem. 97 (2002) 251.

Vasenkov S., Geier O., Schemmert U., Kärger J., Rakoczy R.A., Weitkamp J.
Application of Interference Microscopy and Monte Carlo simulations for ComparativeStudies of Intracrystalline Diffusion in Zeolites.
in Fundamentals of Adsorption 7, Edit.: K. Kaneko, H. Kanoh, and Y. Hanzawa, Publ.: IK Internat. Ltd. Shinjuku, Chuo-ku, Japan.

Vasenkov S., Kärger J.:
Evidence for the existence of intracrystalline transport barriers in MFI-type zeolites: a model consistency check using MC simulations.
Microporous Mesoporous Mater. 55 (2002) 139.

Vasenkov S., Kärger J.:
Different time regimes of tracer exchange in single-file systems.
Phys. Rev. E 66 (2002) art. no. 052601

Vogt C., Galvosas P., Klitzsch N., Stallmach F.:
Self-diffusion studies of pore fluids in unconsolidated sediments by PFG NMR.
Journal of Applied Geophysics 50 (2002) 455.

6.21.2 in press

Bräuer P., Brzank A., Kärger J.:
Adsorption and reaction in single-file networks.
J. Phys. Chem. B

Fritzsche S., Kärger J.:
Tracing memory effects in correlated diffusion anisotropy in MFI-type zeolites by MD simulation.
J. Phys. Chem.

Geier O., Vasenkov S., Freude D., Kärger J.:
PFG NMR observation of an extremely strong dependence of the ammonia self-diffusivity on its loading in H-ZSM-5.
J. Catal.

Jobic H., Paoli H., Methivier A., Ehlers G., Kärger J., Krause C.:
Diffusion of n-hexane in 5A zeolite studied by the neutron spin echo and pulsed field gradient NMR technique.
Micropor. Mesopor. Mater.

Kärger J.:

Measurement of diffusion in zeolites – a never ending challenge?
Adsorption

Kärger J., Stallmach F., Vasenkov S.:
Structure-mobility relations of molecular diffusion in nanoporous materials.
Magnetic Resonance Imaging

Krause C., Stallmach F., Hönicke D., Spange S., Kärger J.:
A surprising drop of the diffusivity of benzene in a mesoporous material of type MCM-41.
Adsorption

Loeser T., Freude D., Mabande G. T. P., Schwieger W.:
^{17}O NMR studies of sodalites.
Chem. Phy. Lett.

Stallmach F., Kärger J.:
Using NMR to measure fractal dimensions – Reply.
Phys. Rev. Lett.

6.21.3 Invited Talks

J. Kärger:
Physikalisches Kolloquium der Universität Darmstadt, 1.2.2002:
Struktur-Beweglichkeits-Relationen bei der Diffusion in Poren-Netzwerken (T)

Institutskolloquium „Physikalische Chemie und Elektrochemie", Universität Hannover, 4.1.2002:
Diffusion in Zeolithen (T)

Instituts-Kolloquium am Hahn-Meitner-Institut Berlin, 24.6.2002
Anomalous diffusion in nanoporous materials (T)

6th Intern. Conf. Magnetic Resonance in Porous Media, Ulm, 8.–12.9.2002
Structure-mobility relations of molecular diffusion in nanoporous materials (T)

Konferenz der Niederländischen Akademie der Wissenschaften "On the Molecular Basis of Catalysis", Amsterdam, 18.-20. 11. 2002
Structure-mobility relations in zeolitic diffusion (T)

F. Stallmach:
6th Intern. Conf. Magnetic Resonance in Porous Media, Ulm, 8. – 12. 9. 2002
Pore Structure of Aquifer Sediments Studied by PFG NMR and MRI (T)

DPG Frühjahrstagung 20.03.2002, Leipzig
Untersuchungen zum Wassertransport und zur Porenstruktur in Sedimenten mittels Kernmagnetischer Resonanz (T)

6.21.4 Conference contributions

(T: talks, P: posters)

D. Freude:
2002 Fuel Cell Seminar , Amsterdam Niederlande, 24.-25-Sept. 2002
Characterization of proton conducting polyphosphate composites (T)

2002 Fuel Cell Seminar, Palm Springs, California 18. -20.Nov. 2002
Proton Conductivty of polyphosphate composites (P)

D. Prochnow, D. Freude, U. Stimming, A.-R- Grimmer:
43rd ENC, April 14-19, 2002, Asilomar
Solid-State Studies of Proton Conducting Polyphosphate Composites and ^{17}O Enriched Pyrophosphates (P)

T. Löser, D. Freude:
43rd ENC, April 14-19, 2002, Asilomar
^{17}O NMR Studies of Alumosilicates with Si/Al-Ratio=1 (P)

2nd International FEZA Conference (Federation of the European Zeolite Associations), Taomina, Italy, 1.-5. September 2002:
Studies in Surface Science and Catalysis 142, R. Aiello, G. Giordano, F. Testa (Eds), Elsevier 2002
S. Fritzsche, J. Kärger:
Correlations in Anisotropic Diffusion of Guest Molecules in Silicalite-1
Part B, 1955-1962 (P)

J. Datka, B. Gil, P. Baran, B. Staudte:
Combined IR and catalytic studies of the role of Lewis acid sites in creating acid sites of enhanced catalytic activity in steamed HZSM-5
Part A, 439-444 (P)

Symposium Collaborative Research Centre „Molecules in Interaction with Interfaces" (SFB 294), Leipzig, 09-11 October 2002:
J. Kärger:
Structure-related diffusion (T)

T. Loeser:
^{17}O NMR – A new tool for catalyst characterization (T)

14. Deutsche Zeolith-Tagung Frankfurt/M. 06.-08.03.2002
E. Lehmann, C. Chmelik, H. Scheidt, S. Vasenkov, B. Staudte, J. Kärger, F. Kremer, J. Kornatowski
Observation of Regular Intergrowth Effects and their Influence on the Intracrystalline Adsorbate Distribution in CrAPO-5 Crystals by Interference and FTIR Microscopy (T)

6.22 Graduations

6.22.1 PhD

Petrik Galvosas
PFG NMR-Diffusionsuntersuchungen mit ultra-hohen gepulsten magnetischen Feldgradienten an mikroporösen Materialien

Katrin S. Weih
Bewegungskorrektur der diffusionsgewichteten Magnetresonanzbildgebung (within the collaboration with the MPI of Cognitive Neuroscience, Leipzig)

6.22.2 Postdoctoral lecture qualification (Habilitation)

Nikolaus Nestle
Structure, transport phenomena and liquid balance in complex porous materials

6.23 Guests

Dr. Taro Ito/Sapporo, Juni 2002
Dr. Krysztof Banas/ University of Krakov, since July 2002
Dr. Federico Brandani/ University of Maine, since July 2002
Prof. Dr. Randall Q. Snurr/ University of Evanston, September 2002
Ruslan Arkhipov / Kazan, September-November 2002
Dr. Alexander G. Stepanov/ Novosibirsk, November-December 2002

7 POLYMER PHYSICS — SCIENTIFIC ACTIVITIES

7.1 Space charge distribution in conjugated polymers

D. Geschke, F. Feller, U. Weber

The decay of space charge in conjugated polymers due to detrapping from deep traps after the turn-off of an external bias has been investigated. A novel experiment was introduced which allows measuring of time resolved laser intensity modulation method (LIMM) spectra with a resolution of about 1 second. For this pyroelectric current transients have been recorded at different temperatures from 220 to 360 K. The data have been analysed assuming detrapping of charge carriers from single energy trap levels to a Gaussian distribution of transport levels to be the predominating process of the space charge decay. In poly[2-methoxy,5-(2'-ethyl-hexyloxy)-p-phenylene-vinylene] (MEH-PPV) hole trapping was found with a trap depth of E_t=0.6 eV and a trap density $N_t>2x10^{21}$ m^{-3}. In poly(2,5-pyridinediyl) (PPY) both, electron and hole trapping was observed and the analysis of the decays yield E_t=0.55 eV and $N_t>10^{21}$ m^{-3}. No deep trapping could be observed in poly (9,9-dioctylfluorene) (PFO) confirming the high chemical purity of this polymer.

References:
[1] Feller, F., Geschke, D., Monkman, A. P., Polymer 43 (2002) 4011-4016
[2] Feller, F., Rothe, C., Tammer, M., Geschke, D., Monkman, A. P., Journal of Applied Physics 91 (2002) 9225-9231
[3] Feller, F., Geschke, D., Monkman, A. P., J. Phys.: Condens. Matter 14 (2002) 8455-8462
[4] Feller, F., Geschke, D., Monkman, A. P., Polymer International 51 (2002) 1184-1189

In cooperation with:
- A. P. Monkman, "Organic Electroactive Materials" Group, Department of Physics, University of Durham, UK
- J. Honerkamp, "Statistical Data Analysis" Group, Freiburg Materials Research Center, Freiburg, Germany

Financial support: DFG Ge 718 / 7-1

7.2 Funding

Prof. Dr. D. Geschke
Raumladungsverteilung in konjugierten Polymeren
DFG-Projekt Ge 718 / 7-1 (2001-2003), ...TDM

7.3 Publications

Riede, A., Helmstedt, M., Sapurina, I., and Stejskal, J.
In Situ Polymerized Polyaniline Films 4. Film Formation in Dispersion Polymerization of Aniline
Journal of Colloid and Interface Science 248 (2002) 413-418

Feller, F., Geschke, D., Monkman, A. P.
Space charge and internal electric field distribution in poly(2,5-pyridinediyl)
Polymer 43 (2002) 4011-4016

Feller, F., Rothe, C., Tammer, M., Geschke, D., Monkman, A. P.
Temperature dependence of the space-charge distribution in injection limited conjugated polymer structures
Journal of Applied Physics 91 (2002) 9225-9231

Feller, F., Geschke, D., Monkman, A. P.
Spatial distribution and dynamics of space charges in poly(2, 5-pyridinediyl)
J. Phys.: Condens. Matter 14 (2002) 8455-8462

Holstein, P., Bender, M.
Application of Electric Fields in NMR
Macromol. Symp. 184 (2002) 137-152

Feller, F., Geschke, D., Monkman, A. P.
Distribution of space charges in luminescent conjugated polymers
Polymer International 51 (2002) 1184-1189

Bansil, R., Nie, H., Konak, C., Helmstedt, M., Lal, J.
Structure and Dynamics of Solutions of a Polystyrene-Polybutadiene Pentablock Copolymer in a Styrene-Selective Solvent
Journal of Polymer Science: Part B: Polymer Physics 40 (2002) 2807-2816

7.4 Graduations

7.4.1 Ph.D.

Dipl.-Phys. Andrea Riede
22.04.2002
"Optische und elektrische Eigenschaften von Polyanilindispersionen und Polyanilinfilmen"

7.5 Guests

Prof. Dr. C. Konak
(Visiting Professor of the AvH Foundation)
Czech Academy of Sciences, Institute of Macromolecular Chemistry, Prague

Samuel Dodoo (IAESTE student)
Kwame Nkrumah University of Science & Technology,
Department of Physics, Kumasi, Ghana

8 SEMICONDUCTOR PHYSICS — SCIENTIFIC ACTIVITIES

8.1 Materials base for II-VI semiconductor research: Pulsed laser deposited ZnO thin films

M. Lorenz, E. M. Kaidashev, H. Hochmuth, D. Natusch, G. Ramm, M. Grundmann

Nominally undoped and doped ZnO thin films for regional, national, and international activities in basic and applied research have been grown by pulsed laser deposition (PLD). The PLD was recently combined with process control by in-situ spectroscopic ellipsometry (Fig. 1). An innovative multistep PLD process was established for epitaxial, undoped ZnO thin films on c-plane sapphire substrates. These films show state of the art electron mobilities from 115 up to 155 cm^2/Vs at 300 K in a narrow carrier concentration range from 2 to 5×10^{16} cm^{-3} [1]. Clear correlation of mobility and grain size of the ZnO films was found (see AFM picture in Fig. 1). Structurally optimized PLD ZnO thin films show narrow high-resolution X-ray diffraction peak widths of the ZnO(0002) ω– and 2Θ–scans as low as 151 and 43 arcsec, respectively, and narrow photoluminescence line widths of donor bound excitons of 1.18 meV at 2 K.
Furthermore, n-type conducting Ga- and Al-doped ZnO films, MgO- and CdO- alloyed ZnO films with shifted optical absorption edges, and Ga+N-, Sb-,and Li_3N-doped ZnO films as attempts for p-type conducting material, and ZnO:Fe films for spintronics are grown in epitaxial quality using the highly flexible PLD method.

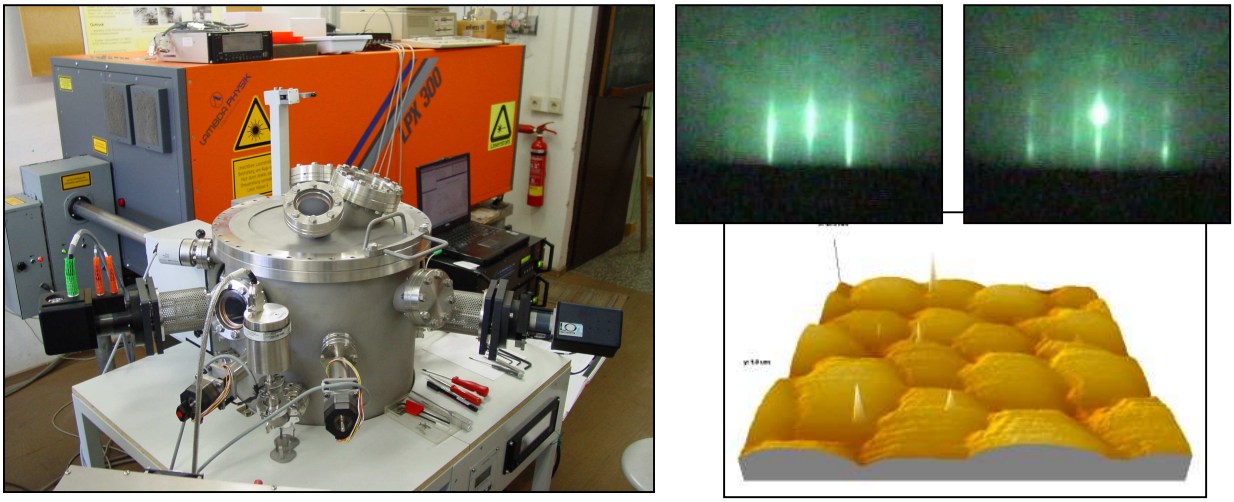

Fig. 1. New PLD chamber for ZnO thin films with in-situ spectroscopic ellipsometry (left), RHEED patterns of ZnO on c-plane sapphire (sample No. E 027) with three-dimensional surface reconstruction indicating high structural quality (top right), and AFM surface scan 1 x 1 μm^2 of ZnO on a-plane sapphire (M 1060) with hexagonal grains (bottom right, R_a = 2.1 nm).

[1] E. M. Kaidashev, M. Lorenz, M. Grundmann et al., Appl. Phys. Lett. (2003), in press

Supported by the BMBF-Wachstumskern INNOCIS 03WKI09.

8.2 X-ray Analysis of MgZnO Thin Films

A. Rahm, H.-C. Semmelhack, E.M. Kaidashev*, M. Lorenz, D. Spemann, and M. Grundmann

PLD grown 0.3-3 µm thick $Zn_{1-x}Mg_xO$ (x=0-0.55) films have been investigated using high resolution X-Ray diffraction (HR-XRD). A Phillips X´Pert HR-Diffractometer equipped with a Bartels monochromator and an analyzer crystal has been employed. The composition of the ternary compound has been determined by RBS. The influence of the sapphire substrate orientation, the Mg content and the oxygen partial pressure during growth has been investigated. Table 1 summarizes the epitaxial relationships and widths of the ZnO(0002) peak of ZnO on c-, a- and r-Al_2O_3, respectively extracted from reciprocal space maps, Φ- and ω–Φ-scans. Films grown on c- and a-sapphire exhibit a very good overall crystalline quality as indicated by FWHM values in 2Θ of 42″ and 44″, respectively. The c-lattice constant of ZnMgO depends on the Mg content (x) as well as on oxygen pressure during growth (Fig.1a). The a-lattice constant increases linearly with x. Occurrence of a cubic MgO phase is seen only for very high values of x>0.5 (Fig. 1b).

substrate	epitaxial relationship layer / substrate		FWHM ZnO(0002) 2Θ	FWHM ZnO(0002) Ω
c-sapphire	(0 0 0 1)||(0 0 0 1)	[1 0 -1 0]||[2 -1 -1 0]	0.012-0.027°	0.042-0.128°
a-sapphire	[0 0 0 1]||[1 1 -2 0]	<1 1 -2 0>||[0 0 0 1]	0.012-0.015°	0.061-0.079°
r-sapphire	(1 1 -2 0)||(0 1 -1 2)	[0 0 0 1]||[0 -1 1 1]		

Table 1. Epitaxial relationships for ZnO on sapphire with three different orientations and FWHMs of the ZnO(0002) peak.

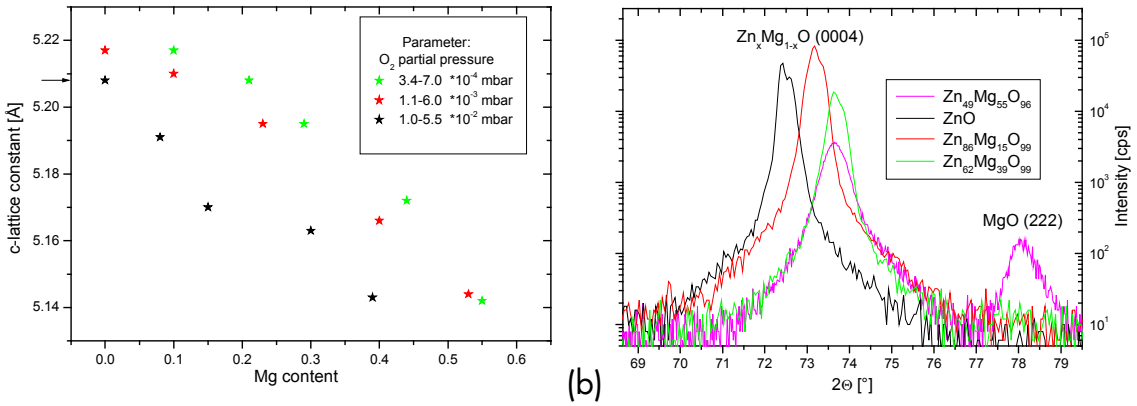

(a) (b)

Fig. 1. (a) Influence of O_2 partial pressure vs. Mg content dependence, (b) Phase separation at high Mg during growth on the c- lattice constant concentration.

8.3 Birefringence, band-to-band transitions and excitonic properties of ternary MgZnO thin films

R. Schmidt-Grund, B. Rheinländer, M. Schubert, M. Lorenz, M. Grundmann

Optical properties (band-to-band transition-energies, exciton binding energy and the refractive indices normal and perpendicular to the optical axis) of PLD grown ternary wurtzite type $Mg_xZn_{1-x}O$ ($0 \le x = 0.29$) films, which are useful for band gap engineering of ZnO-based heterostructures, were determined by spectroscopic ellipsometry in the UV-VIS-NIR energy range. Cation substitution of Zn by Mg leads to a significant blue-shift of the fundamental band gap energy with increasing Mg-content as expected. The dependence of the three band gap energies $E_0^{A,B,C}$, A, B and C corresponding to the spin orbit and crystal field splitting of the valence band, can be fitted by 2nd order polynomial (Fig 1, left). The exciton binding energy $E_{ex,B}$ (neglecting the A,B,C fine structure) reduces by ~ 10 meV for 17% Mg, and recovers to the value for ZnO (~ 60 meV) for x = 0.29, supposedly caused by competing effects of disorder and alloying (Fig. 1, right). The ordinary refractive index $n_\perp$ below the fundamental band gap energy decreases with x and can be linearly fitted with a three therm cauchy approximation (Fig. 2, left). The uniaxial birefringence $n_{||} - n_\perp$ ($n_{||}$ is the extraordinary index of refraction) reverses from positive (ZnO) to negative ($Mg_xZn_{1-x}O$) (Fig. 2, right).

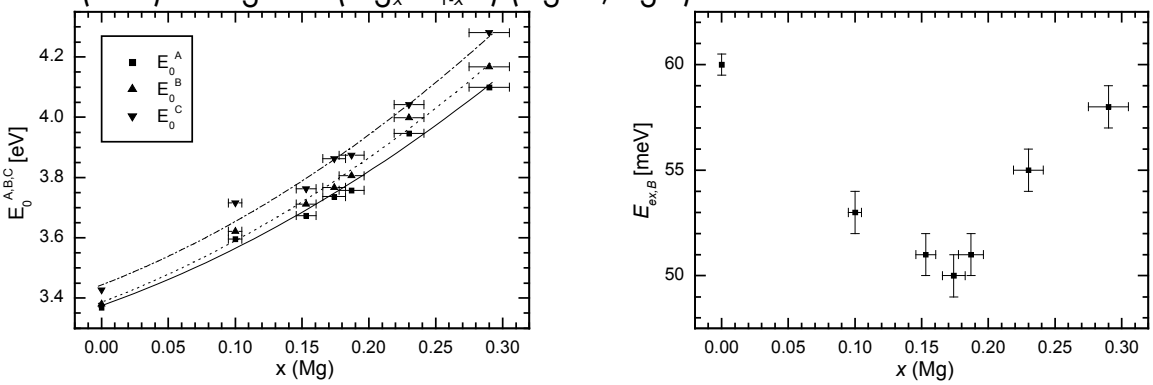

Fig. 1: left: Band gap energies of $Mg_xZn_{1-x}O$; right: exciton binding energy $E_{ex,B}$.

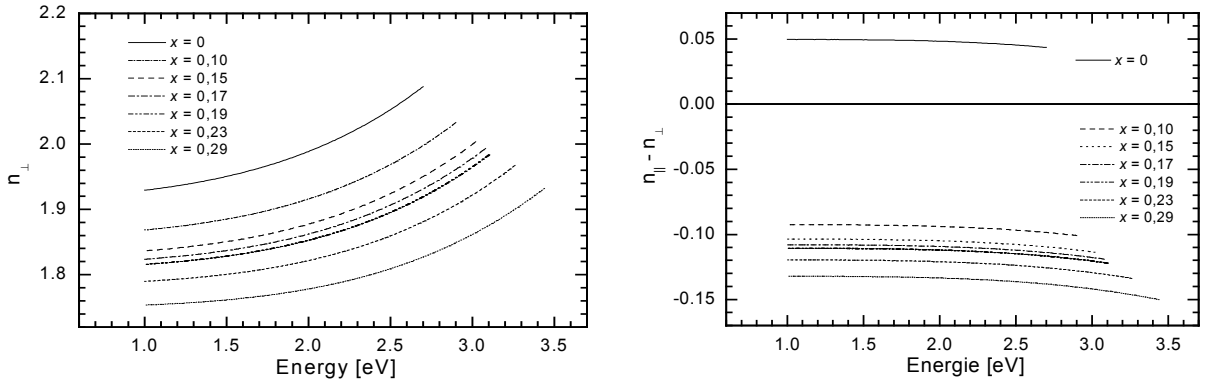

Fig. 2: left: ordinary refractive index $n_\perp$; right: birefringence $n_{||} - n_\perp$ of $Mg_xZn_{1-x}O$, corresponding to thre-therm cauchy approximations.

Reference: R. Schmidt, B. Rheinländer, M. Schubert, D. Spemann, T. Butz, J. Lenzner, E. M. Kaidashev, M. Lorenz, M. Grundmann, APL 82, 2260 (2003).

8.4 Light beam induced current (LBIC) mapping of ZnO Schottky diodes

Th. Nobis, J. Lenzner, R. Pickenhain, M. Grundmann

An optical microscope was set up facilitating a variety of spatially resolved measurements, particularly LBIC-mapping. The beam of a HeCd-laser with a wavelength of 325 nm is expanded and focussed to a spot of <1 µm in diameter on the sample. It acts as excitation source for the LBIC-mapping of ZnO-Schottky contacts. The generated photocurrent is detected by a low noise current amplifier. Scanning is done using positioning stages featuring travelling ranges up to 10 cm with a resolution of 100 nm. Hence the LBIC mappings can cover small as well as large sample areas.

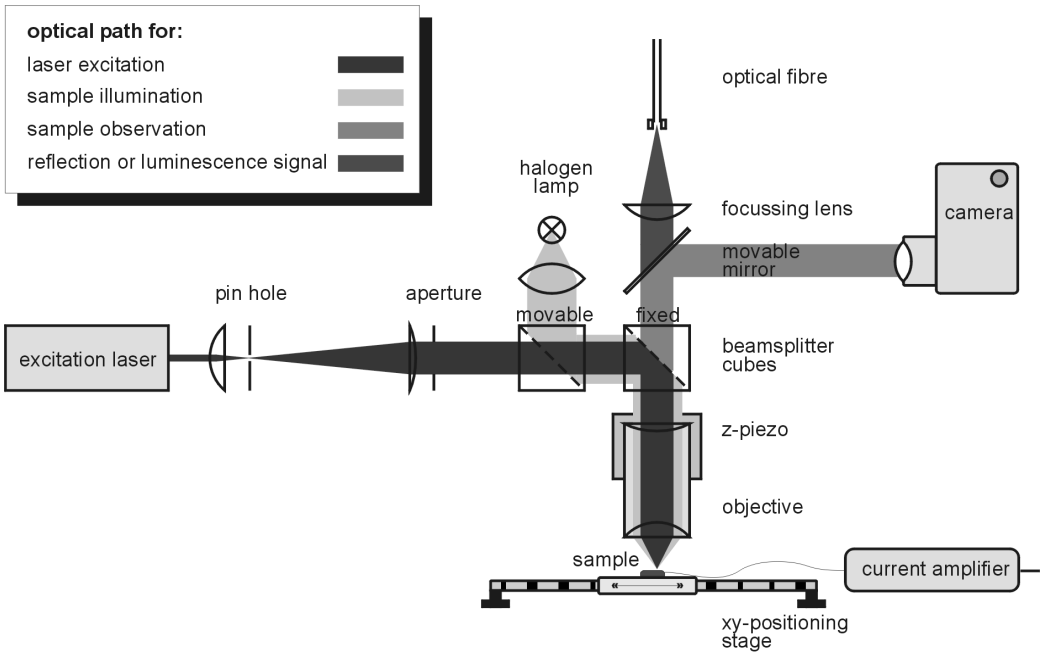

Fig. 1: Schematical set-up showing light paths for LBIC, confocal reflection or luminescence and sample inspection.

Figure 2 shows typical maps of a circular Palladium Schottky-contact on a ZnO single crystal measured with LBIC. The generated dc-photocurrent is plotted versus the x and y coordinates using a logarithmic current scale. The dark areas represent contact regions generating low photocurrent. The contact wire that simply absorbs all the excitation light is responsible for the dark-gray zone in the center of Fig. 2 (a). The other black regions at the outer part of both figures belong to the pure semiconductor surface not covered with the metal and therefore not producing photocurrent. The bright points of Fig. 2 (a), one of which is scanned in higher lateral resolution in Fig. 2 (b), generate locally a high photocurrent and are found identically in EBIC (electron beam induced current) maps possibly indicating micro-plasms.

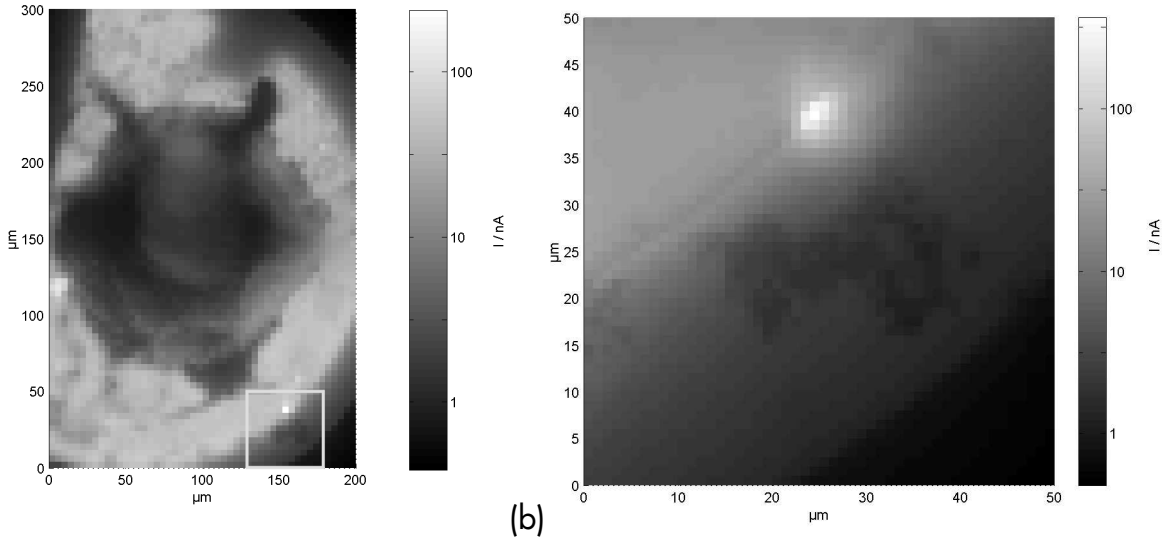

(a) (b)

Fig.2: (a) LBIC map of a circular Pd Schottky-contact, (b) is a higher resolution image of the area indicated in (a) by the square.

8.5 Photoluminescence of PLD ZnO thin films

W. Czakai, G. Benndorf, E.M. Kaidashev, M. Lorenz, M. Grundmann

Photoluminescence (PL) investigations have been performed on undoped ZnO thin films deposited by pulsed laser deposition (PLD) on c-plane (0001), a-plane (11-20), and r-plane (01-12) sapphire substrates. PL is excited by a He-Cd laser (325 nm) with a maximum power of 60 mW. Typical low temperature luminescence spectra are shown in Fig. 1, typically exhibiting several narrow lines. The dominant peak is due to a transition of an exciton bound to an impurity. The full width at half maximum (FWHM) of the ZnO layer on a-plane substrate is smallest (1.4 meV, minimal 1.18 meV, presently). In the higher energy range the recombination of the ground state and the excited state of the free exciton are visible. We observe phonon replica at lower energies.

By comparing the PL-intensity and FWHM of the bound exciton transition we conclude that the ZnO film on a-plane substrate has the best optical characteristics. This is in agreement with X-ray experiments, which confirmed that the structural properties of those films are the best.

The temperature dependence of the PL from 4 K to 300 K is shown in Fig. 2a. The bound exciton intensity at low temperature is the highest. With increasing temperature bound excitons dissociate and the transition from the free excitons dominate in the spectra above 90 K. The temperature dependence of the energy position of the free exciton X_A can be fitted well with the Bose-Einstein-expression [1]

$E(T)=E(0)-\alpha\Theta/[\exp(\Theta/T)-1]$ (Fig. 2b).

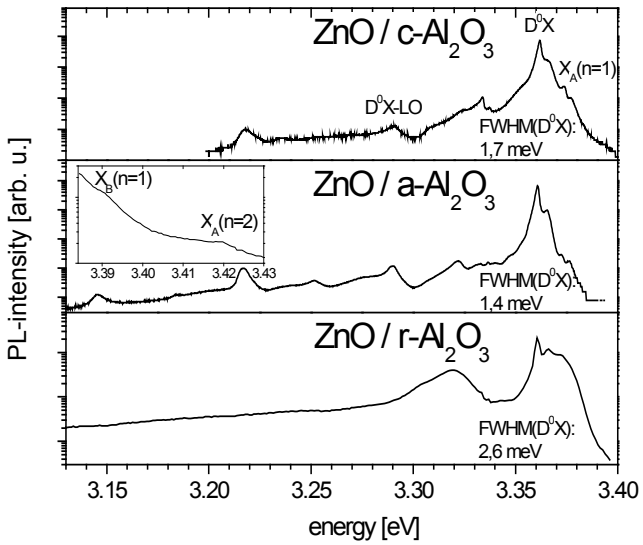

Fig. 1 : PL at 2 K of ZnO films on different oriented substrate.

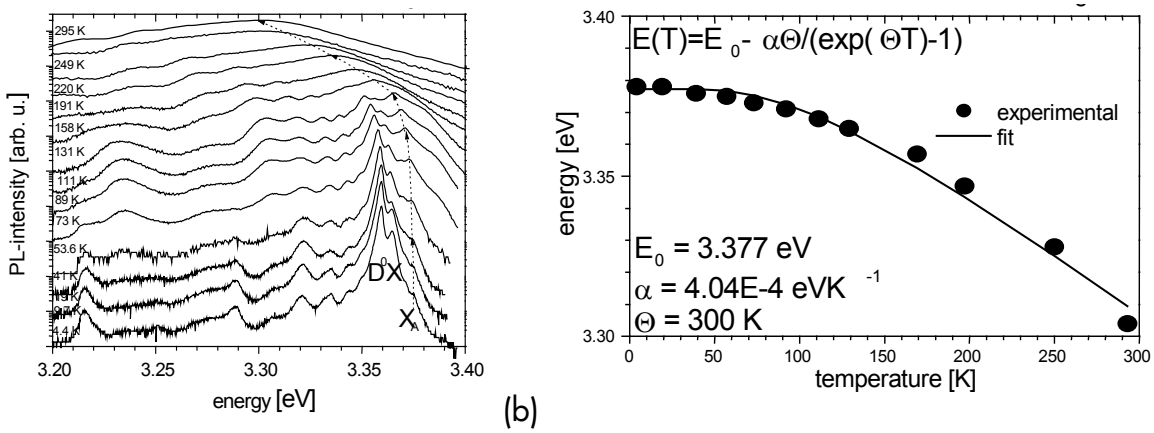

Fig. 2: (a) PL spectra of ZnO/a- Al_2O_3 from 4 K to 300 K, (b) energy of free exciton as a function of temperature.

[1] L. Vina et al., Phys. Rev. B 30, 1979 (1984)

8.6 Characterization of Schottky Contacts on n-type ZnO

H. v. Wenckstern, M. Lorenz, E. M. Kaidashev, G. Biehne, R. Pickenhain,
V. Gottschalch, and M. Grundmann

ZnO is a direct-band-gap semiconductor with a band gap of 3.37 eV at room temperature [1]. Therefore, ZnO is a suitable material for the realization of UV-photodetectors. For that, Schottky contacts (SC) of high quality have to be fabricated on ZnO-films. We examined the behavior of SC on n-type ZnO by investigating the influence of the surface preparation and the influence of the contact metal. We have used four different kinds of surface preparation. The methods were: (a) cleaning the surface with acetone, (b) cleaning first in acetone, than in toluene, and finally in dimethylsulfoxide (DMSO), (c) etching with hydrochloric acid, (d) deposition of a small layer in a N_2O Plasma-CVD chamber. We have also used four different contact metals: palladium, silver, gold, and nickel. The investigated samples were (0001)- or (000-1)- oriented single crystals and

(0001)- or (11-20)-oriented PLD-thin films grown within the semiconductor physics group, respectively. All contacts were realized ex-situ by the evaporation of the metal.
The single crystals and the PLD-thin films were nominally undoped but showed clearly n-type conduction as confirmed by Hall measurements. The origin of the n-type conduction is still in debate but either intrinsic defects as Zn-interstitials, O-vacancies, or hydrogen as shallow donor are the most probable candidates. Current-voltage (I-V) measurements were performed in a range from -1 V to 2 V. The barrier height Φ_B, the ideality factor n, and the series resistance were obtained by fitting the measured forward currents. From capacitance-voltage (C-V) measurements the barrier height Φ_B may also be determined. Further, the net dopant concentration can be obtained in dependence on the depletion width W. Figure 1 depicts the measured C-V curve, a $1/C^2$-V plot from which the barrier height can be obtained, and the depth profile of the net dopant concentration of a single crystal.

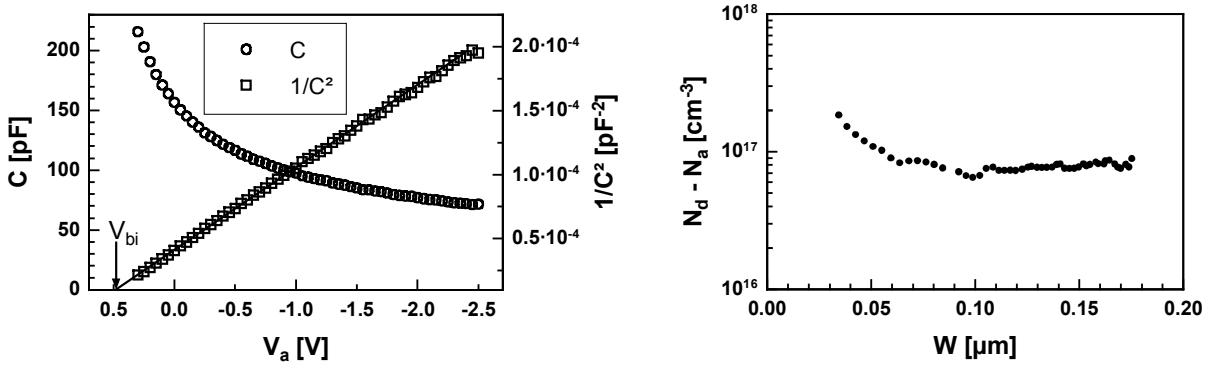

Fig. 1: C-V curve and $1/C^2$-V plot (left), depth profile of the net dopant concentration (right).

The common feature of the net dopant profiles of all investigated SC is an increase of the net dopant concentration towards the metal-semiconductor interface. A possible cause, which still has to be confirmed, is the drift of hydrogen ions within the electric field of the space charge region. The parameters, that were determined by the evaluation of the I-V and C-V measurements, are summarized in the tables 1 and 2.

Single crystal	(a)	(b)	(c)	(d)
Φ_B (meV)	740	700	500	X
n	2	1.75	1.4	X
PLD-thin film				
Φ_B (meV)	630	680	X	600
n	1.7	1.4	X	1.95

Table 1: Influence of the different preparation methods on the properties of SC with palladium as contact metal.

Single crystal	Silver	Palladium	Gold	Nickel
Φ_B (meV)	560	730	560	620
n	1.5	1.75	2	1.7
PLD-thin film				
Φ_B (meV)	590	680	X	X
n	1.4	1.4	X	X

Table 2: Influence of the contact metal on the properties of SC produced on samples cleaned with method (b).

In conclusion, the variation of the barrier heights is smaller than predicted by the Schottky-Mott model. A correlation between the electro-negativity of the used contact metal and the barrier height, as supposed by the Schottky-Mott model, was not found. Further, the influence of the cleaning method on the contact properties is rather strong. Therefore, we conclude, that surface states and chemical reactions between the metal and the semiconductor surface determine the properties of the metal-semiconductor interface. The orientation of the samples has no significant influence on the contact properties.

[1] R. Schmidt, B. Rheinländer, M. Schubert, D. Spemann, T. Butz, J. Lenzner, E. M. Kaidashev, M. Lorenz, M. Grundmann, APL 82, 2260 (2003).

8.7 Annealing of epitaxial n-type ZnO thin films

H. v. Wenckstern, M. Lorenz, E. M. Kaidashev, G. Biehne, C. Bekeny, and M. Grundmann

In general, nominally undoped ZnO samples always exhibit n-type conduction. This is due to the low formation energy of intrinsic donor-like defect states as Zn-interstitials or O-vacancies, respectively. Another source of this n-type conductivity could be the incorporation of hydrogen as a shallow donor on an interstitial site. In order to apply ZnO as material in the UV-optoelectronics, p-type ZnO films of good quality are needed. A promising dopant for achieving p-type conduction in ZnO is nitrogen. If nitrogen is incorporated at oxygen site, it acts as acceptor. It is of substantial importance, to incorporate atomic nitrogen, since N_2 complexes on O-site act as a double donor in ZnO and lead to n-type conduction. We have investigated the influence of post growth annealing steps on the electric properties of two PLD-thin films. Sample 1 was tempered at 850°C for 30 min in an oxygen atmosphere. Sample 2 was tempered at the same temperature and for the same time in air. Figure 1 depicts the temperature dependence of the free carrier concentration (FCC) and the Hall mobility of the as-grown and the annealed samples.

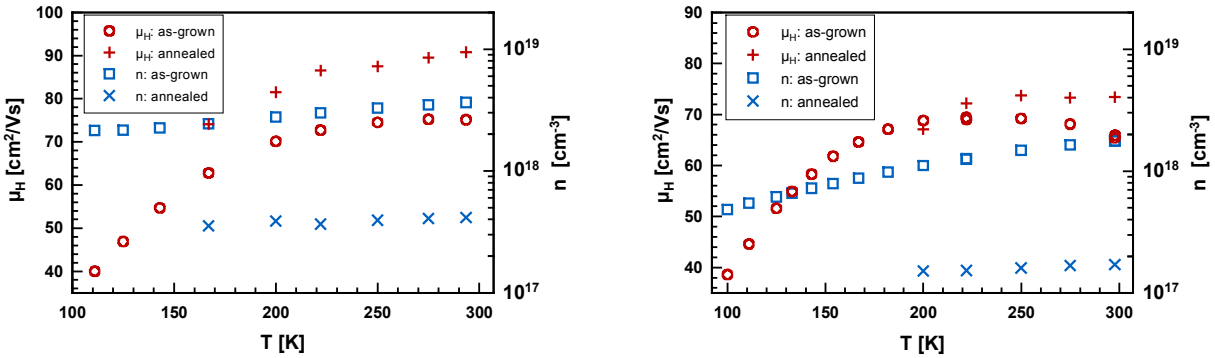

Fig. 1: Free carrier concentration and Hall mobility of as-grown and annealed PLD-thin films: annealing in O_2 (left) and in air (right).

The annealing in oxygen reduces the FCC at room temperature (RT) by a factor of 8.8. The FCC at RT of sample 2 decreases after the anneal by a factor of 10.5. The RT Hall mobility increased after the anneal in either atmosphere, but the decrease of the Hall mobility with decreasing temperature is much stronger for sample 2 than for sample 1. Further, the Hall mobility of sample 2 after the annealing falls below that of the as-grown sample. This can be explained by a higher scattering rate at ionized impurities. For that, the density of ionized impurities must have increased in sample 2 after the anneal in air. We conclude, that atomic nitrogen was incorporated at O-sites. With that, the larger decrease of the FCC at RT and the behavior of the Hall mobility can be explained. Further, sample 1 was electrically compensated after the anneal at about 150 K, while sample 2 was already compensated at about 200 K. That indicates, too, that the density of acceptors in sample 2 increased after the annealing.

8.8 Determination of impurity levels in n-type ZnO

H. v. Wenckstern, M. Lorenz, E. M. Kaidashev, G. Biehne, R. Pickenhain,
M. Grundmann

ZnO has attracted much interest in the last years. Possible applications as in UV-opto-electronics or as ferromagnetic semiconducting material are to come, if the intrinsic n-type conductivity is understood in detail and if the reproducible growth of high quality p-type ZnO is achieved. For that, the determination of the energetic position, the density, and the cross-section of impurity levels is a necessity.
We performed temperature dependent Hall measurements (TDH) and deep level transient spectroscopy (DLTS) to obtain these key parameters. The samples, we have used during this study, were either n-type ZnO single crystals or n-type epitaxial ZnO-thin films grown by pulsed laser deposition. The TDH were conducted in the temperature range from 20 K to 300 K. Since ZnO is a wide band semiconductor only electrons from shallow impurities will contribute to the electric conduction in the investigated temperature range and only parameters of these shallow impurities are accessible by TDH measurements. Therefore, DLTS was used to obtain information about deeper impurity levels, as well. The DLTS measurements were conducted between 4 K and 300 K. Figure 1 depicts the dependence of the free carrier concentration of a PLD-thin film on the temperature and the data of a DLTS measurement performed on a single crystal.

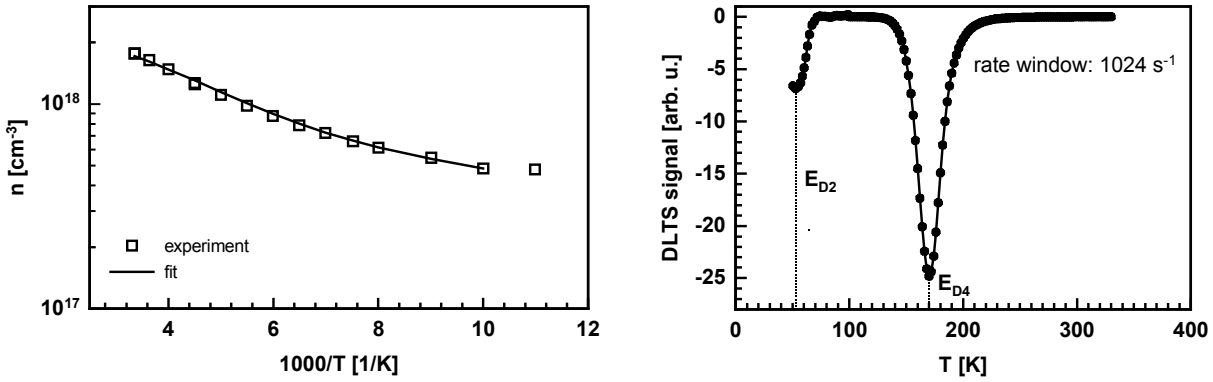

Fig. 1: Free carrier concentration and its fit of a PLD-thin film (left), DLTS measurement of a single crystal (right).

The impurity parameters determined by the TDH and the DLTS measurements are summarized in table 1. The superscripts of the labels of the impurity levels indicate the experimental method used to obtained these values.
In conclusion, we have found five different impurity levels in n-type ZnO. The impurity level labeled E_{D1} could be due to the incorporation of hydrogen as predicted by [1] and experimentally confirmed for the single crystals by [2]. The impurity level labeled E_{D2} is an effective mass impurity. The chemical nature of that level could be e.g. aluminum or gallium, respectively. The chemical identity of the other levels remains so far unsolved and is subject to further investigations.

Single crystal	$^{TDH}E_{D0}$	$^{TDH}E_{D1}$	$^{TDH}E_{D2}$	$^{DLTS}E_{D2}$	$^{DLTS}E_{D3}$	$^{DLTS}E_{D4}$
E_t (meV)	X	35	56	56	X	281
N_d (cm^{-3})	X	1.6×10^{17}	4.6×10^{16}	X	X	X
PLD-thin film						
E_t (meV)	< 1	39	X	X	84	X
N_d (cm^{-3})	1×10^{18}	8.2×10^{18}	X	X	X	X

Table 1: Parameters of impurity levels in n-type ZnO single crystals and n-type ZnO PLD-thin films.

[1] C. G. Van de Walle, PRL 85, 1012 (2000).
[2] D. M. Hofmann, A. Hofstaetter, F. Leiter, H. Zhou, F. Henecker, B. K. Meyer, PRL 88, 045504-1 (2002).

8.9 Application of the Empirical Pseudopotential Method to II-VI binary compound semiconductors and ternary alloys

Daniel Fritsch, Heidemarie Schmidt, M. Grundmann

Recently, wurtzitic ZnO has attracted much attention due to its wide-bandgap (3.437 eV at 2 K) and its large excitonic binding energy at room temperature (60 meV). Furthermore, by alloying ZnO with CdO and MgO its bandgap can be tuned over a large energy range. We investigate the bandstructure of the ternary material system Zn(Mg, Cd)O which became the focus for new optoelectronic devices in the green, blue and ultraviolet region by means of the EPP method. In order to accomplish the possible technological applications of Zn(Mg, Cd)O, we mainly study the fundamental material parameters, as for example bandgap energies, effective masses and Luttinger-like parameters in dependence on the Mg and Cd content. As a first step we have determined the EPP parameters of the ionic model potentials for Zn, Mg, Cd, and O on the basis of an empty core model by fitting experimental low-temperature transition energies of several binary compounds in zincblende structure (ZnS, ZnSe, CdS) and rocksalt structure (CdO, MgO). The transferability of the obtained model potential parameters for the II-VI compounds has been proven for example by reproducing the energy dispersion of wurtzite-type ZnO (Fig. 1, Tab.1) or rocksalt-type MgO (Fig. 2) using the fitted model potential parameters.

Preliminary results for the bandstructure of the wurtzitic ternary $Zn_{1-x}Mg_xO$ alloy were obtained by means of the virtual crystal approximation (VCA). The calculated fundamental transition energies in dependence on the Mg-content x well correspond to experimentally determined bandgap energies. Our further work aims at directly fitting model potential parameters to experimental low-temperature transition energies of wurtzitic compounds containing Zn, Mg, Cd, or O as constituents. Furthermore, we want to surpass the drawbacks of VCA by calculationg the energy bandstructure of ternary II-VI alloys in a supercell approach.

	Γ_{3v}	Γ_{3c}	M_{4v}	M_{1c}	$A_{1,3v}$	$A_{5,6v}$
This work	-4.842	6.875	-0.590	7.882	-2.918	-0.338
	-4.32	6.64	-0.58	7.16	-2.62	-0.38

Table 1: Energetical position of valence and conduction bands in wurtzitic ZnO with respect to the valence band maximum which has been set to zero on energy scale.

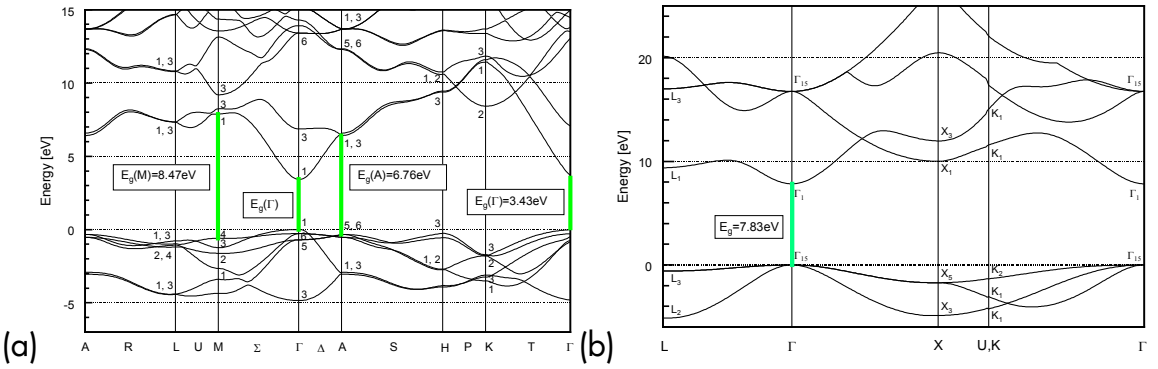

Fig. 1: (a) Energy dispersion of wurtzite-type ZnO (a) and rocksalt-type MgO (b) along special lines in the Brillouin zone.

8.10 a-Si/SiO_x Bragg-reflectors on micro-structured semiconductors

R. Schmidt-Grund, T. Nobis, V. Gottschalch, B. Rheinländer, M. Grundmann

Lateral Bragg-confinement for micro-resonator light emitters improves the ratio of the number of the axial resonant modes to the number of the spontaneously emiting lateral modes. Si/SiO_x Bragg-reflectors (BR) are attractive for such micro-structured resonators. The large step of the refractive indices leads to a high value of reflectivity already for a small number N of layer pairs, typically N = 4.5, in the VIS-NIR-region.
On the basis on detailed investigations on planar a-Si/SiO_x/SiN_x BRs [1], High reflectivity a-Si/SiO_x BRs were grown on GaAs- and InP-Substrates with various three-dimensional and corrugated structures like micro-staircases and spherical micro-ditches using plasma enhanced chemical vapor deposition. The optical properties of the BR have been studied by spectroscopic ellipsometry (SE) on planar samples and by a detection-focal micro-SE (μE) technique on curved samples. From the model analysis of the measured ellipsometric Ψ-, Δ- and depolarisation-spectra thickness inhomogenities and layer thicknesses of the Bragg stacks were determined. The reflectivity (R) was generated from the ellipsometry model analysis and compared with the reflectivity measured by confocal micro-reflection (μR). In Fig. 1, the μE-analysis of an a-Si/SiO_x BR on a sperical micro-ditch and the comparison of R generated from the μE model approach with R measured by μR is shown. The agreement of the experimental with the generated μE spectra and the lineshape of the R spectra show the good quality of the BR. The experimental and generated spectra of R, determined by SE and μR, of BR on the steps 1–3, where step 3 is the topmost, of the micro-staircase are shown in Fig. 2 (right). The redshift of the stop-band for the part of the staircase step that is closer to the gas-source indicates an increase of the layer thickness.

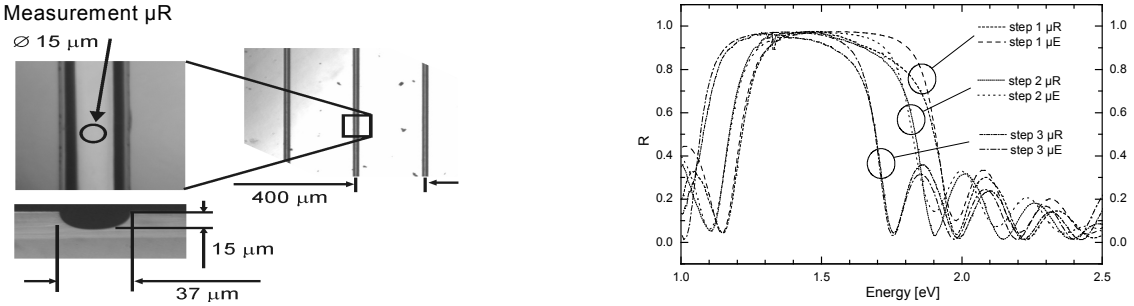

Fig. 1: left: photographic plan view (top) and cross-sectional (bottom) image of a spherical micro-ditch.; right: R generated from SE and meassured by μR for steps 1–3.

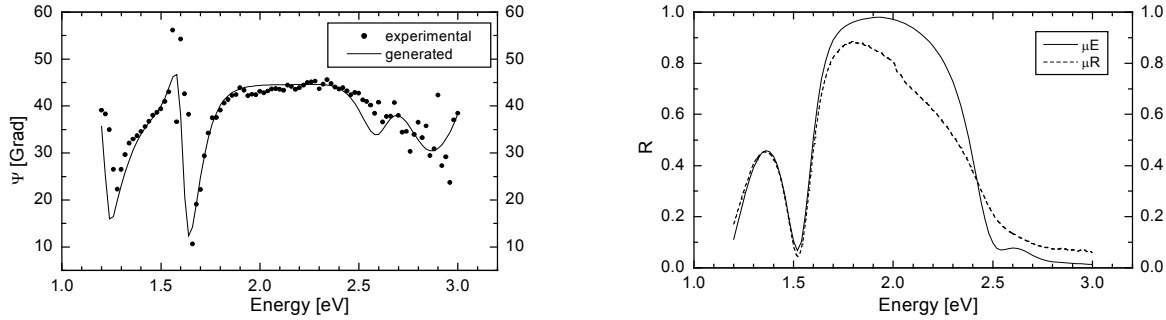

Fig. 3: Experimental and generated μE-spectra for the micro-ditch (left); reflectivity generated by μE-analysis and measured by μR (right).

[1] V. Gottschalch, R. Schmidt, B. Rheinländer, D. Pudis, S. Hardt, J. Kvietkova, G. Wagner, R. Franzheld, Thin Solid Films 416 (2002) 224-232

8.11 ZnO nanowires and microcrystallites grown by carbothermal evaporation

E. M. Kaidashev, M. Lorenz, J. Lenzner, M. Grundmann

ZnO microcrystallites and nanowires have been grown by carbothermal evaporation [1] on a-plane and r-plane sapphire substrates. This work is a first step on the way to more sophisticated ZnO-based nanoenesembles with modulated composition along the growth direction for applications in nanophotonics, nanoelectronics, and nanosensorics [2].

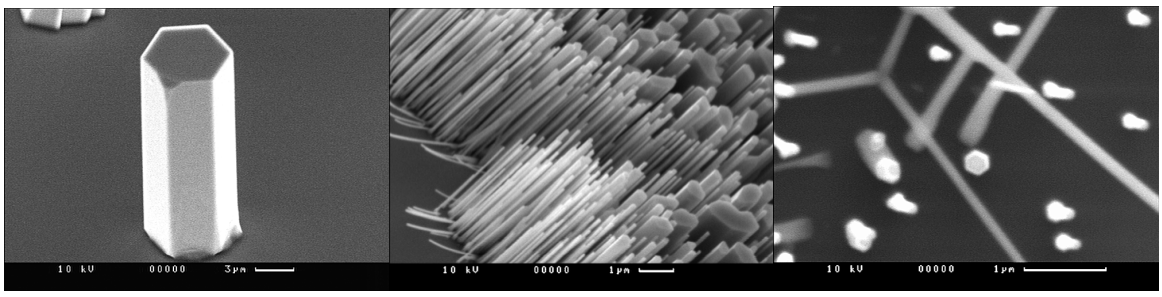

Fig. 1. ZnO microcrystals (left) and nanowires (right) grown on a-plane sapphire covered with Au-nanoclusters in air or Ar stream, respectively.

Evaporation of a carbon - zinc oxide target (1:1) at 900-1100°C and downstream transport and reaction of the evaporated species in air or Ar gas enables the growth of

ZnO nanocrystals of various size and arrangement as shown in figure 1. The cathodoluminescence spectra of single ZnO nanowires (figure 2) show features and peak widths comparable to commercial ZnO single crystals.

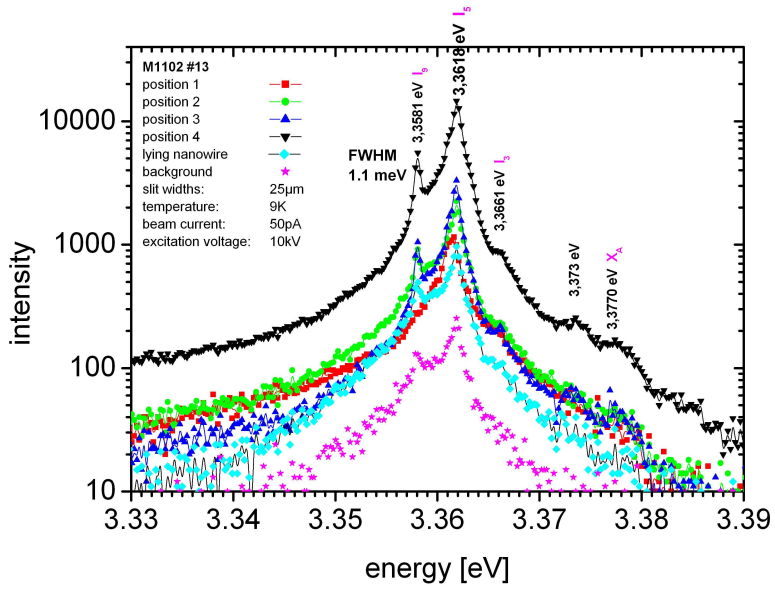

(a)

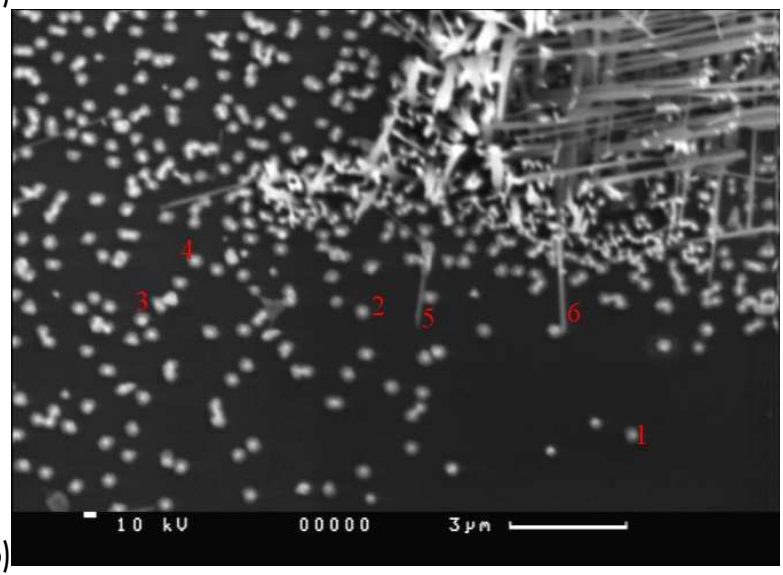

(b)

Fig. 2. Cathodoluminescence spectra (a) of single ZnO nanowires (b) at 9 K show narrow bound exciton peaks with FWHM of 1.1 meV similar to ZnO bulk single crystals (FWHM of bound exciton peak 0.7 meV).

[1] B. D. Yao et.al. Appl. Phys. Lett. 81 (2002) 757
[2] E. M. Kaidashev, M. Lorenz et.al. DPG-Frühjahrstagung 2003 Dresden, poster HL 49.56

8.12 SNMS depth profiling of solar cell structures on flexible polymer substrate

M. Lorenz, G. Ramm, H. Hochmuth, M. Grundmann

The Institute of Experimental Physics II is involved in a new BMBF "Wachstumskern" project ("INNOCIS") to support the series production of $CuInSe_2$ solar cells on flexible polymer substrates. The "Wachstumskern" is coordinated by Solarion Photovoltaik GmbH in Leipzig, a young innovative spin-off company. Within this project, the Semiconductor Physics Group makes available its know-how about ZnO for transparent front contacts and several sophisticated methods for detailed investigation and optimization of the solar cell structures, including photo- and cathodoluminescence, light beam induced current, Hall effect, and pulsed laser deposition with in-situ spectroscopic ellipsometry, and secondary neutrals mass spectrometry (SNMS).
In SNMS the time profile of selected atomic and molecular isotopic species is measured during Ar-sputtering of multilayer film structures. The advantage of SNMS is the very high depth resolution down to 2 nm and the easier quantification of elemental concentrations compared to secondary ion mass spectrometry (SIMS). The investigation of electrically isolating samples as ceramics, glass or polymers is possible by sputtering with high frequency AC voltage. Two examples of SNMS measurements are shown in Fig. 1. The left time profile shows a sputter-deposited multistructure of 19 single Ti and Cu films of total thickness of about 3 µm on glass substrate. The right time profile is obtained from a first solar cell test structure of $InSnO_3$ (ITO)/ZnO/Mo/Ti on flexible polyimid substrate. As demonstrated in Fig. 1, SNMS shows the appearance of all single films. In addition, information is given about interdiffusion and roughness effects at the interfaces.

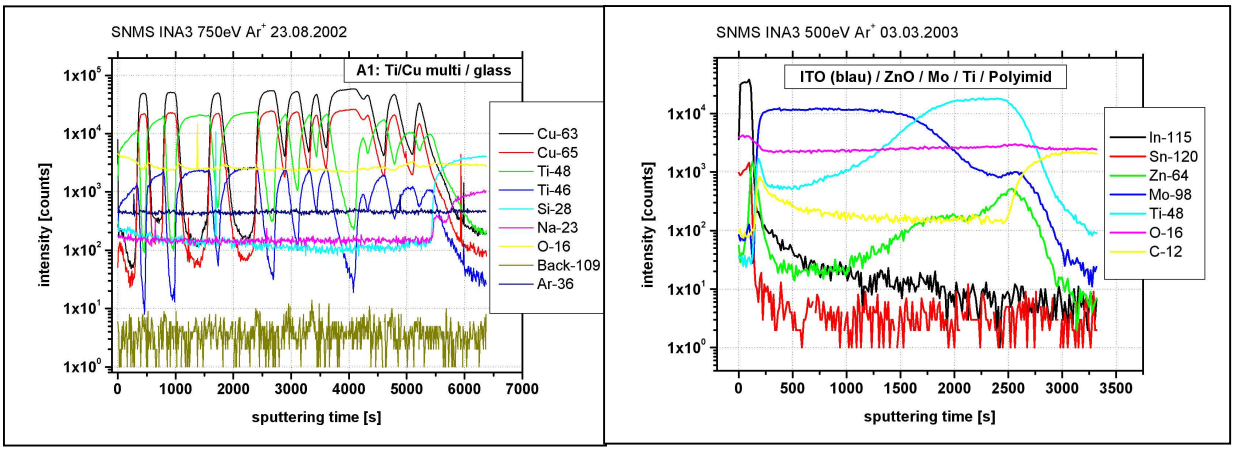

Fig. 1: SNMS concentration time profiles of 19 Ti and Cu films on glass substrate (left, total sputter depth is 3.15 µm). Right profile shows a solar cell structure ITO (InSnO) / ZnO / Mo / Ti / polyimid with total sputter depth of 1.3 µm. All single films are clearly resolved. The legends give the selected isotopes of each particular time profile.

Supported by the BMBF-Wachstumskern INNOCIS 03WKI09.

8.13 Carrier localization in two-dimensional GaN substitution layers embedded in GaAs

Heidemarie Schmidt, Georg Böhm*
*Institute for Surface Modification (IOM), Permoserstraße 15, 04303 Leipzig, Germany

A theoretical investigation of the electrical and optical properties of the GaN/GaAs system is motivated by the great number of attempts to fabricate damage free GaN/GaAs heterostructures for a robust GaAs surface passivation material or to produce GaN/GaAs diodes. In the present work we study the electronic bandstructure of the GaN/GaAs double heterojunction by means of the empirical pseudopotential (EPP) method in a periodic modelling approach and compare it with the corresponding bandstructure of the unordered GaAsN alloy [1]. The smallest N content in our model supercells amounts to 6.6 %.

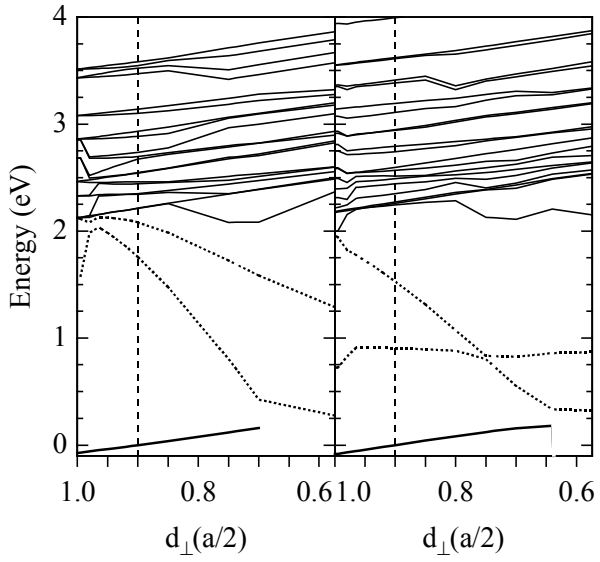

Fig. 1: Γ-point eigenstates of the $GaAs_{1,s}/GaAs_{14,us}$-structure (left panel) and the $GaN_{1,s}/GaAs_{14,us}$-structure (right panel) in eV in dependence on the vertical spacing parameter $d_\perp$ (without SO-coupling correction). $d_\perp$ varies from a/2, i.e., unstrained substitution layer, to 0.6 a/2.

We find a single electron eigenstate ca. 850 meV below the GaAs bandgap. This conduction band minimum (CBM) is localized on the GaN substitution layer and shows strong mixing effects with X- and L-states of the host material. Furthermore, we find that the second lowest conduction band (CB1) is also localized on the GaN layer. In order to investigate the physical origin of the bandstructure anomaly of the GaN/GaAs system, i.e., not only *one* but *two* states in the lower conduction band region of the GaAs host material are perturbed, we have analyzed how this anomaly depends on size (Fig. 1) and chemical effects. The electronic properties of CBM and CB1 of GaN/GaAs can be correlated with those of the lowest conduction band state E_0 and the N impurity state a_1(N) of GaAsN, respectively. Finally, we conclude that (001)-ordering of "anomalous'' alloys does not remove their bandstructure anomalies.

[1] H. Schmidt and G. Böhm, Physica E (2003), in press.

8.14 Intersublevel transitions in quantum dots

A. Weber, M. Grundmann

Studies of radiative intersublevel transitions in semiconductor quantum dots are of particular interest because they permit the investigation of the transition energies and of the relaxation paths of excited carriers. Furthermore they are intended to lead to the development of new mid infrared (MIR) light sources, which are important for applications in optical infrared spectroscopy and gas detection. This is because the phonon scattering between states in the quantum dots is expected to be reduced (compared to quantum wells) due to the phonon bottleneck effect.

The MIR emission of near infrared (NIR) quantum dot lasers has been examined. The presence of the NIR interband lasing during the observation of MIR intersublevel emission is expected to assure a continuous depopulation of the ground state and thus preventing the MIR emission from premature saturation due to state filling. The sample is equipped with a 1.26 µm thick large optical cavity and its active region consists of 6 layers of InGaAs quantum dots embedded in a GaAs matrix. It has been optically excited with a pulsed (10 ns) diode-pumped solid-state laser at 532 nm wavelength which was focused with a cylindrical lens. The resulting MIR emission was collected by a mirror optics and spectrally resolved with a Fourier Transform infrared spectrometer equipped with a He-cooled bolometer.

Fig. 1a shows the NIR output power of the laser (lasing at ~980 nm) in dependence of the excitation power. The MIR emission spectra for three different pump powers are shown in Fig. 1b. Two peaks can be clearly observed at 40 meV and 70 meV with widths of 10 meV and 20 meV, respectively. They are attributed to radiative intersublevel transitions in the quantum dots. However, with increasing pump power a saturation of the emission is observed.

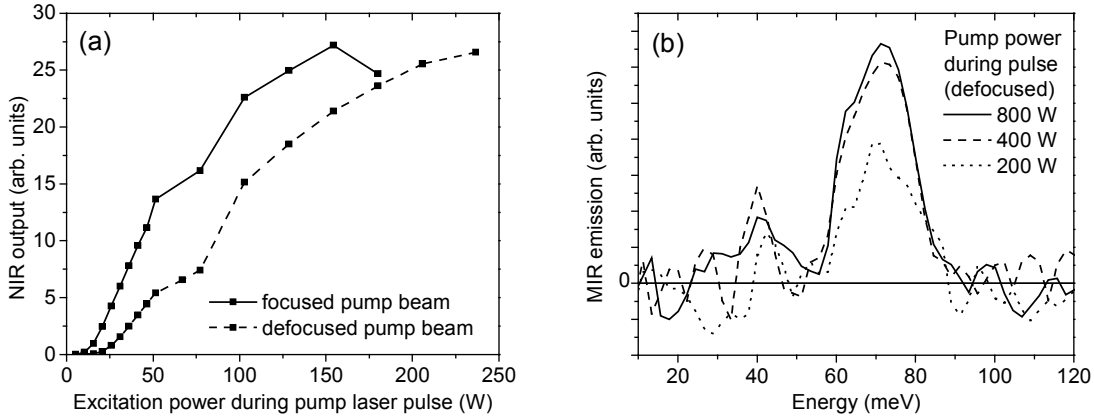

Fig. 1: (a) NIR output power (lasing at ~980 nm) vs. optical pump power; (b) spectra of MIR emission for different pump powers.

8.15 Photoluminescence investigations of GaN_yAs_{1-y} and $B_xGa_{1-x}As$ alloys

G. Benndorf, V. Gottschalch*, G. Leibiger*, M. Grundmann
*Department of Inorganic Chemistry, Semiconductor Chemistry Group, University Leipzig

Photoluminescence (PL) investigations were used to characterize MOVPE grown GaN_yAs_{1-y} and $B_xGa_{1-x}As$ alloys [1,2]. The PL measurements were carried out at temperatures ranging from 4 K to 290 K using the 514 nm line of an Ar^+-laser as excitation source. Fig. 1 shows the temperature dependence of the PL spectra of a $GaN_{0.023}As_{0.977}$/ GaAs SQW with a 8 nm thick well layer grown at 600°C using DMHy and AsH_3 after annealing at 650°C for 10 min. Fig. 2 shows corresponding spectra of a $B_xGa_{1-x}As$/ GaAs MQW structure consisting of 10 periods of 10 nm $B_{0.022}Ga_{0.978}As$ embedded in $Al_{0.05}Ga_{0.95}As$. The inset shows the PL-peak energies of the BGaAs sample in comparison with the $GaN_{0.023}As_{0.977}$ layer in dependence of the temperature. The overall difference between the PL-peak energies measured at 2K and at room temperature amounts to 52 meV in the case of GaNAs, which is much smaller than the corresponding value of GaAs (approximately 90 meV) and BGaAs (inset Fig. 2). The reduced temperature dependence in GaNAs can be explained by assuming that two different mechanisms are responsible for the PL. For low temperatures, PL emission is due to excitons bound to localized states caused by potential fluctuations of the conduction band, which explaines the reduced temperature dependence of the PL energies in the low-temperature region [3]. With increasing temperature, excitons will be dissociated into band states due to thermal activation, and band-to-band recombination becomes the dominant PL mechanism [3].

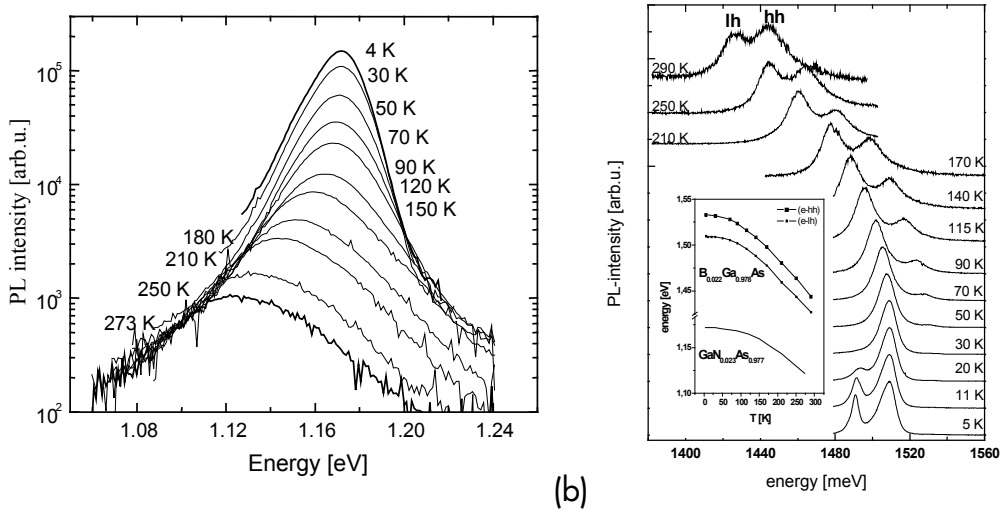

(a) (b)

Fig.1: (a) PL of a $GaN_{0.023}As_{0.977}$/GaAs SQW sample (d_{well} = 8 nm) recorded at different temperatures. (b) Temperature dependence of PL spectra of a $B_{0.022}Ga_{0.978}As$ layer. The inset shows the PL-peak energies of the BGaAs layer in comparison with the GaNAs layer

[1] V.Gottschalch, G.Leibiger, G.Benndorf, J. Cryst. Growth 248 (2003) 468.
[2] G.Leibiger, V.Gottschalch, G.Benndorf, M.Schubert, J.Sik, in Compound semiconductor heterojunctions: physics and applications by W.Cay and others, Transworld Research Network 2003 (in press).
[3] K. Onabe, D. Aoki, J. Wu, H. Yaguchi, and Y. Shiraki, phys. stat. sol. (a) 176 (1999) 231.

8.16 Boron and nitrogen incorporation in $In_xGa_{1-x}As$

V. Gottschalch*, G. Leibiger*, G. Benndorf
*Department of Inorganic Chemistry, Semiconductor-Chemistry Group, University Leipzig

We have grown $B_xGa_{1-x}As$ ($0 \le x \le 0.03$), GaN_yAs_{1-y} ($0 \le y \le 0.05$), and lattice matched $B_xGa_{1-x-y}In_yAs$ and $In_xGa_{1-x}N_yAs_{1-y}$ layers on (001) GaAs substrates using low-pressure MOVPE [1,2]. In order to examine the layer quality, nitrogen and boron concentration and optical properties, double-crystal X-ray diffraction, transmission electron microscopy, photoluminescence (PL) and spectroscopic ellipsometry investigations have been performed. Besides the strong redshift of the band-gap energies in the case of GaN_yAs_{1-y} (Fig.1), we obtain decreasing PL intensities and increasing FWHM values with increasing N incorporation. The $E_g(y)$ dependence can be modelled by a constant bowing parameter of 18 eV for N compositions up to approximately 2%: $E_g(y)=1.42+ 1.88y–18y(1-y)$ *[eV].* For the $B_xGa_{1-x}As$ layers, we obtain also a decrease of the PL intensity and an increase of the splitting of the PL peak with increasing boron incorporation.The PL peak energies of $B_xGa_{1-x}As$ samples with different B-content is shown in Fig. 1, too. The splitting of the PL peak can be explained by the effect of tensile strain due to the pseudomorphic growth. The strain removes the valence-band (VB) degeneracy at the Γ point between the heavy- (hh) and light-hole (lh) VB. From the PL investigations we derived the $E_g(x)$ dependence to $E_g(x) = 1.42 + 2.08\ x –1.7\ x\ (1-x)$ *[eV].*

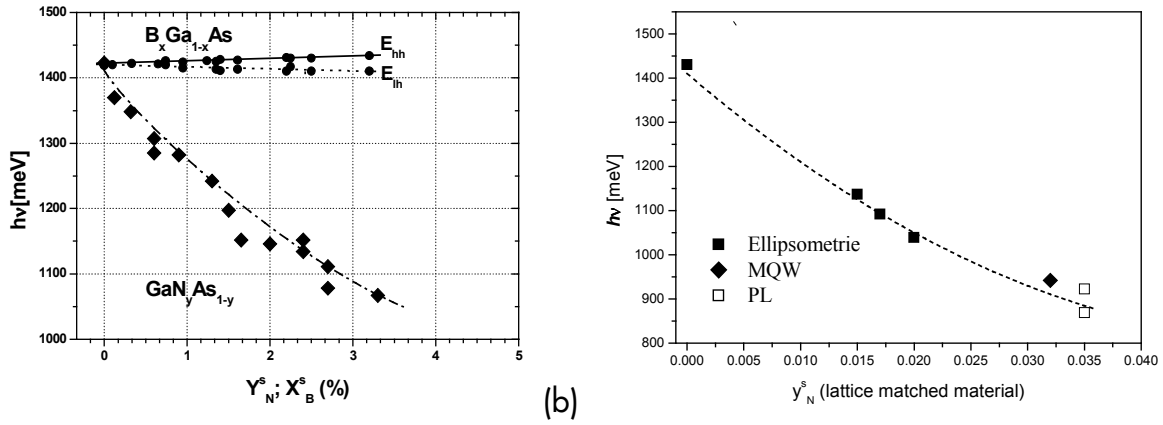

Fig. 1: (a) Room temperature PL-peak energies of $B_xGa_{1-x}As$ and GaN_yAs_{1-y} bulk-like materials as a function of the boron and the nitrogen concentration. (b) Band-gap energies of lattice matched $In_xGa_{1-x}N_yAs_{1-y}$ layers with different N concentrations measured at room temperature.

We have grown nearly lattice matched $B_xGa_{1-x-y}In_yAs$ and $In_xGa_{1-x}N_yAs_{1-y}$ layers with thicknesses ranging from 300 to 800 nm. Fig. 2 shows the dependence of the band-gap energies on the N composition for $In_xGa_{1-x}N_yAs_{1-y}$ layers lattice matched to GaAs. The obtained experimental $E_g(y)$ dependence can be described by $E_g(y) = 1.41 – 22\ y + 200\ y^2$ *[eV]* (dotted line in Fig. 2). From a $B_{0.03}Ga_{0.91}In_{0.06}As$ layer, which is lattice matched to GaAs, we obtained room –temperature PL with a peak energy of 1.36 eV.

[1] V.Gottschalch, G.Leibiger, G.Benndorf, J. Cryst. Growth 248 (2003) 468.
[2] G.Leibiger, V.Gottschalch, G.Benndorf, M.Schubert, J.Sik, in Compound semiconductor heterojunctions: physics and applications by W.Cay and others, Transworld Research Network 2003 (in press).

8.17 MOVPE-Growth of $(B_x)Ga_{1-x-y}In_yAs/GaAs$ laser structures in a wavelength range of 1200 nm

V. Gottschalch*, G. Leibiger*, H. Herrnberger*, G. Benndorf
*Department of Inorganic Chemistry, Semiconductor Chemistry Group, University Leipzig

The boron incorporation in $In_yGa_{1-y}As$ is only little studied and offers new possibilities in band-gap engineering and strain engineering. We have investigated $B_xGa_{1-x-y}In_yAs$ highly strained quantum well structures grown by low-pressure metal-organic vapour-phase epitaxy on (001) GaAs substrates using the precursors triethylboron, trimethylaluminium, trimethylgallium, trimethylindium, and arsine [1,2]. The boron and indium composition of the alloys were varied from $0 \leq x \leq 0.04$ and $0 \leq y \leq 0.35$. We have grown laser structures with three different kinds of active regions: A) double quantum well of (GaIn)As with a tickness of 11 nm embedded in 180 nm GaAs, B) same structure as A, the quantum well material is (BGaIn)As, C) structure with separate strain compensation of the (BGaIn)As quantum wells by surrounding with (BGa)As.

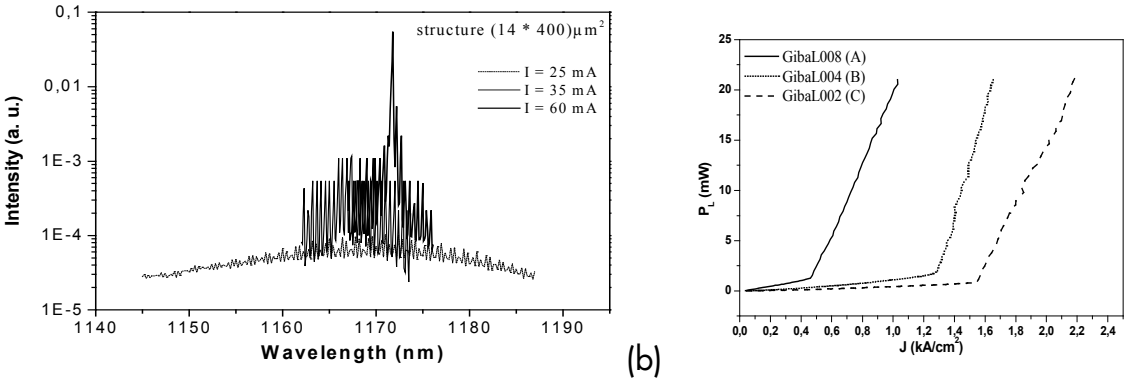

(a) (b)

Fig.1: Emission spectra of a double quantum well (GaIn)As laser diodes (a) and light-current (P_L-j) characteristics of structures A, B, and C (b).

The active region is sandwiched between two $Al_{0.35}Ga_{0.65}As$ layers. The as-grown laser structures were fabricated into oxide stripe lasers with stripe widths (w_s) ranging from 10 to 35 µm and cavity lengths (L_c) of 400, 600, and 800 µm. Devices were measured at room temperature under pulsed operation with a pulse width of 5µs and a frequency of 1 kHz. Lowest threshold current densities (J_{th}^{min} = 250 A/cm^2, λ = 1164 nm with L_c = 800 µm and w_s = 35 µm) were reached for lasers with $In_xGa_{1-x}As/GaAs$ active regions (type A) (Fig.1). The same type of lasers were also measured under cw operation with a maximum output power of 20mW per facet at a fixed temperature of $T_{heatsink}$ = 18°C. Additionally, we measured the temperature dependence of the output-power-versus-current-density (P_L-J) characteristics for all three types of lasers with temperatures ranging from 20 to 70°C. The characteristic temperatures T_0 were 103 K and 80K for structures A and B, C, respectively.

[1] V. Gottschalch, G. Leibiger, G. Benndorf, J. Cryst. Growth 248 (2003) 468 – 473.
[2] V. Gottschalch, G. Leibiger, G. Benndorf, Z. Anorg. Allg. Chem. 628 (2002) 2156.

8.18 High-T_c superconductor science and technology: Large-area PLD $YBa_2Cu_3O_{7-\delta}$ thin films and j_c-scan measurement

M. Lorenz, H. Hochmuth, D. Natusch

High-T_c superconducting $Y_1Ba_2Cu_3O_{7-\delta}$ (YBCO) thin films on low dielectric loss sapphire substrates are expected to be useful for applications as passive microwave components (e.g. bandpass filters) for third generation mobile communication systems.
A highly reproducible PLD process for large-area 4-inch diameter and double-sided YBCO films on sapphire substrates for microwave applications (see Fig. 1) is established and continuously improved at University of Leipzig [1, 2]. In addition, a simple and fast inductive characterization system for the critical current density j_c at 77 K of the double sided HTSC thin films as shown in figure 1 was developed [3]. This so called "j_c-scan Leipzig" system represents the state of the art of HTSC thin film characterization and works now successfully in research institutes in Jena (Germany), Atsugi-shi (Japan), Beijing, and Chengdu (China). Recently, grain boundary effects in HTSC thin films have been investigated and reduced by Ca-doping of YBCO [4].

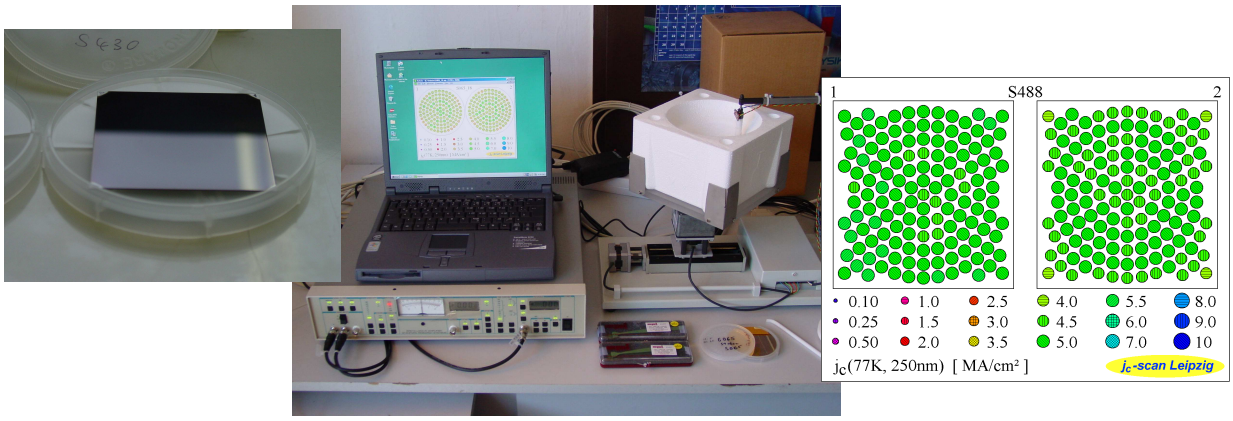

Fig. 1: Large-area and double-sided PLD-YBCO:Ag thin films of size 71 x 75 mm² exhibiting mirrorlike optical (left) and electrical homogeneity (right). The scan of the critical current density at 77 K is measured using the "j_c-scan Leipzig" system (center).

[1] M. Lorenz, H. Hochmuth, D. Natusch, H. Börner, K. Kreher, W. Schmitz, Appl. Phys. Lett. 68 (1996) 3332.
[2] M. Lorenz, H. Hochmuth, D. Natusch, M. Kusunoki, V. L. Svetchnikov, V. Riede, I. Stanca, G. Kästner, D. Hesse, IEEE Transact. Appl. Superconductivity 11 (2001) 3209.
[3] H. Hochmuth, M. Lorenz, Physica C 265 (1996) 335.
[4] M. Lorenz, H. Hochmuth, M. Grundmann, E. Gaganidze, J. Halbritter, to be published in Solid State Electronics, 9th International Workshop on Oxide Electronics 2002, St. Pete Beach, FL, 20-23 Oktober 2002

Supported by the BMBF under Grants No. FKZ 13N6099, 13N6829, 13N7390 and 13N8158.

8.19 Ferroelectric properties of Fe-doped $BaTiO_3$ thin films in dependence on temperature and bias field

M. Lorenz, H. Hochmuth, D. Natusch, G. Ramm, M. Grundmann

Large-area $Ba_xSr_{1-x}TiO_3$ (BSTO-x) thin films, partially Fe-doped, have been grown by pulsed laser deposition on polycrystalline alumina based ceramics. The capacity (dielectric constant ε_r) and Q-factor of planar Pt/BTO:Fe/Pt capacitors were investigated within a temperature range from –35°C to +85°C at a frequency of 1kHz. These investigations have been performed for an industrial partner to qualify the materials base of new tunable electronic devices under outdoor temperature conditions.
Although operating in the ferroelectric state below the Curie temperature, pure $BaTiO_3$ (BTO) thin films showed the smallest variation of ε_r from –35°C to +85°C compared to BSTO-0.6 and BSTO-0.8 (Fig. 1. top left). A homogeneous tunability of the capacity of about 60% was achieved for applied electrical DC voltages resulting in electrical field strengths between 0 and 5V/µm within the whole temperature range (Fig. 1. top right). Furthermore, by Fe-doping of BTO films Q-factors could be increased by a factor of three up to about 70 compared to the undoped films (Fig. 1. bottom right). In addition, the temperature dependence of capacity is considerably influenced by Fe-doping (Fig. 1. bottom left). For further investigations, planar BTO:Fe capacitors with transparent conducting ZnO electrodes have been grown which should show interface dependent polarization and optical properties by spectroscopic ellipsometry.

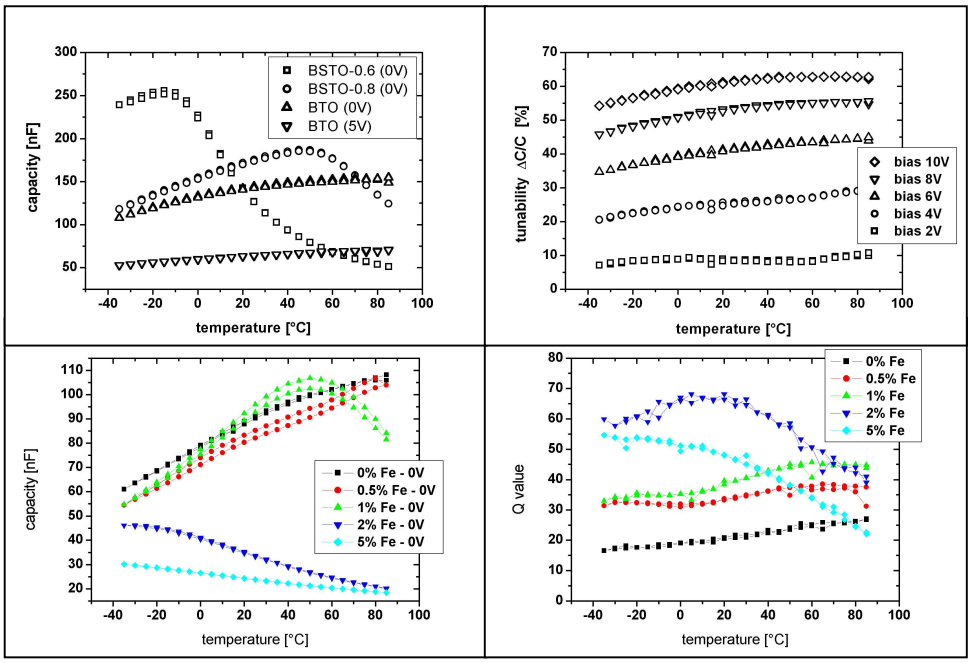

Fig. 1. Capacity of BSTO-x and tunability of BTO capacitors (top left and right), and capacity and Q-factor of Fe-doped BTO capacitors (bottom left and right), in dependence on temperature, DC bias voltage, or Fe-content, respectively.

Supported by the BMBF under Grant No. FKZ 13N8158.

8.20 Nanoscale attachment of peptides to semiconductor surfaces

K. Goede, M. Grundmann

Self-organized hybrid nanostructures of anorganic semiconductors and organic molecules are being increasingly investigated. Understanding of the molecular attachment process is essential for possible future applications, such as bio-sensors, reconcilable prostheses and electronic or optoelectronic devices on a molecular basis. However, many fundamental properties of such hybrid systems are still unkown: How specific with respect to both the molecule and the semiconductor is the attachment? How strong are the binding forces and do they depend on the environment? Can a possible electrical current through such a single molecule be utilized for some kind of data processing? Recent work in our group is focussed on the attachment of artificial peptides which consist of few (here: twelve) amino acids to various III-V and group-IV semiconductor surfaces on the nanometer scale. The peptide selection follows work of [1] where peptides with the highest binding affinity to GaAs were selected from a library of 10^9 peptides. We brought these peptides in aqueous solution into contact with clean, etched and in-liquido cleaved semiconductor surfaces. After applying a standardised washing process (to remove non-bound molecules), clearly varying attachment properties of the different surfaces have been identified, as is shown in Fig. 1.

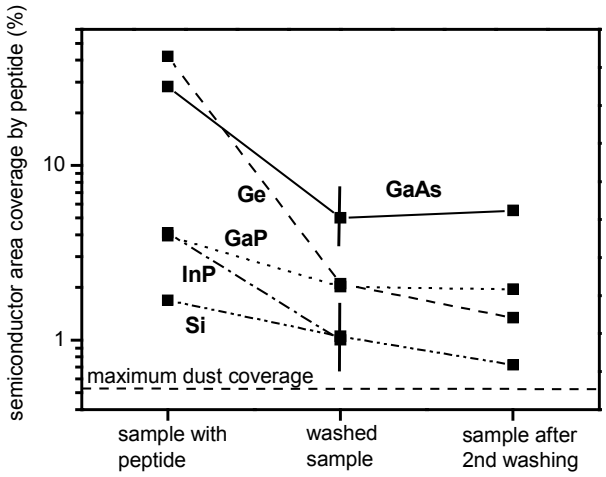

Fig.1: Fraction of surface which is covered by the peptide for different (001)-grown semiconductor surfaces.

Once the sample was "dry" again, we studied its surface by means of atomic force microscopy (AFM) in tapping mode. A subsequent grain analysis was applied to the AFM pictures to extract the values shown in Fig.1. A second washing cycle did not change the area coverage much which indicates that binding of the molecules is present. Additionally, we have shown that the tunnelling current density through these single molecules is comparable to that through the normally doped semiconductor. Thus, electronic applications of such devices are conceivable.

[1] Belcher et al., Nature 405, 665 (2000)

8.21 Funding

Untersuchung der Intersubniveau-Übergänge in selbstordnenden Quantenpunkten, Entwicklung neuartiger Infrarot-Detektoren und -Laser
Investigation of intersub-level transistions in self-organized quantum dots; development of novel infrared detectors and lasers
DFG Gr 1011/7-3

Übertragbarkeit des Kodotierungs-Konzeptes auf ternäres ZnO:(Cd,Mg)
Transferability of the codoping concept to ternary ZnO:(Cd,Mg)
DFG Gr 1011/10-1 im DFG-Schwerpunktprogramm 1136 "Substitutionseffekte in ionischen Festkörpern"

Lichtemitter und Fotodetektoren auf der Basis von III-V-Halbleiter-Nanostrukturen
III-V-Semiconductor Nano-Heterostructures for Advanced Opto-Electronic Devices
BMBF: Bilaterale Zusammenarbeit BRD-Slowakei: SVK 01/001

New gallium phosphide grown by vertical gradient freeze method for light emitting diodes (VGF GaP - LED's) No. IST - 2001-32793
EU-FP5-Projekt und BMBF: Bilaterale Zusammenarbeit BRD-Slowakei: SVK 01/001

PLD von neuartigen dielektrischen und HTSL-Dünnschichten für zukünftige Anwendungen im Richt- und Mobilfunk
PLD of new dielectric and HTSC thin films for future applications in wireless and mobile communication
BMBF-Teilprojekt FKZ 13N8158 innerhalb BMBF-Leitprojekt „Supraleiter und neuartige Keramiken für die Kommunikationstechnik der Zukunft", Förderschwerpunkt Supraleitung und Tieftemperaturtechnik.

Elektronische und optische Eigenschaften, in-situ-Ramanstreuung, in-situ-Ellipsometrie und Ionenstrahlanalytik von flexiblen Cu-(In,Ga)-(Se,S)-Dünnfilm-Solarzellen.
Electronic and optical properties, in-situ Raman scattering, in-situ ellipsometry and ion beam analysis of flexible Cu-(In,Ga)-(Se,S) thin film solar cells.
BMBF-Wachstumskern INNOCIS, Teilprojekt FKZ 03WKI09.

Intraband and interband carrier transitions in type I and type II nanostructures with quantum dots, quantum dot molecules and impurities
Intraband und Interband Übergänge in Typ I und Typ II Nanostrukturen mit Quantenpunkten, Quantenpunkt-Molekülen und Störstellen
INTAS 01-0615

8.22 Organizational Duties

M. Grundmann
Member of Program Committee for QD2002, Tokyo
Vertrauensdozent der Studienstiftung des deutschen Volkes
Direktor des Institut für Experimentelle Physik II
Project Reviewer: Deutsche Forschungsgemeinschaft (DFG), Alexander von Humboldt-Stiftung (AvH), Schweizerischer Nationalfonds zur Förderung der wissenschaftlichen Forschung (FNSNF), Deutsch-Israelische Projektkooperation (DIP), SONS-Program of EU
Referee: Appl. Phys. Lett, Phys. Rev. B, Phys. Rev. Lett., Electr. Lett., Physica E, Europhysics Lett., phys. stat. sol., J. Appl. Phys.

8.23 External cooperations

Academic

A.F. Ioffe-Institut, St. Petersburg
Prof. Zh.I. Alferov, Dr. V.M. Ustinov, Dr. G. Cirlin
Forschungszentrum Karlsruhe, Institut für Materialforschung III
Dr. H. Heidinger, Dr. J. Halbritter
Institute for Metal Physics of National Academy of Sciences of Ukraine, Kiev, Ukraine
Prof. Dr. V. M. Pan
Institut für Oberflächenmodifizierung e.V., Leipzig
Prof. B. Rauschenbach
Universität Leipzig, Fakultät für Biowissenschaften, Pharmazie und Psychologie
Prof. A. Beck-Sickinger
Universität Leipzig, Fakultät für Chemie und Mineralogie
Dr. V. Gottschalch
Max-Planck-Institut für Mikrostrukturphysik, Halle/Saale
Dr. O. Breitenstein, Dr. D. Hesse
St. Petersburg State Technical University
Prof. L. Vorob'jev, Dr. V. Shalygin
Slovak University of Technology, Bratislava, Slovak
Prof. J. Kovác, Dr. F. Uherek
Technische Universität Berlin
Prof. D. Bimberg, Dr. R. Heitz, Prof. N.N. Ledentsov
Universidade de Aveiro, Portugal
Prof. N. Sobolev
Yamagata University, Department of Electrical Engineering, Yonezawa, Japan
Dr. M. Kusunoki
Paul Scherrer Institut, Villingen
Prof. H. Sigg
Université Paris-Sud
Prof. F. Julien
Universität Gießen
Dr. D. Hofmann

Industry
Tesat-Spacecom GmbH & Co KG, Backnang
Dr. T. Kässer
Cryoelectra GmbH Wuppertal und Bergische Universität Wuppertal
Prof. H. Piel
Marconi Communications GmbH Backnang
Dr. M. Schallner
Solarion GmbH, Leipzig
Dr. G. Lippold, Dr. A. Braun
SIEMENS Landis&Staefa electronic GmbH
D. Mrozinski

8.24 Publications

8.24.1 Journals

L. E. Vorobjev, A. V. Glukhovskoy, S. N. Danilov, V. Yu. Panevin, D. A. Firsov, N. K. Fedosov, V. A. Shalygin, A. D. Andreev, B. V. Volovik, N. N. Ledentsov, D. A. Livshits, V. M. Ustinov, A. F. Tsatsul'nikov, Yu. M. Shernyakov, M. Grundmann, A. Weber, F. Fossard, F. H. Julien
Nonequilibrium Spectroscopy of Inter- and Intraband Transitions in Quantum Dot Structures
Materials Science Forum 384-385, pp. 39-42 (2002)

A. Weber
Inter-Sublevel Transitions in Quantum Dots and Device Applications
in *Nano-Optoelectronics: Concepts, Physics and Devices (Springer, Berlin), M. Grundmann, ed., Chap. 16, pp. 371-390, ISBN 3-540-43394-5 (2002)*

Towe E, Pal D, Vorobjev LE, Glukhovskoy AV, Danilov SN, Zerova VL, Panevin VY, Firsuv DA, Shalygin VA, Zegrya GG, Weber A, Grundmann M
Injection lasers based on intraband carrier transitions
ULTRAFAST PHENOMENA IN SEMICONDUCTORS 2001
MATERIALS SCIENCE FORUM
384-3: 209-212 2002

V. Gottschalch, R. Schmidt, B. Rheinländer, D. Pudis, S. Hardt, G. Wagner, R. Franzheld:
Plasma-Enhanced Chemical Vapor Deposition of SiO_x/SiN_x Bragg reflectors
Thin Solid Films **416** (2002) 224-232

D. Pudis, J. Kovac, J. Kovac Jr., J. Jakabovic, A. Vincze, V. Gottschalch, G. Benndorf, B. Rheinländer, R. Schwabe
Stimulated emission from InAs (GaAs) monolayers stacks embedded in $Al_{0,33}Ga_{0,67}As$ active region,
Advances in Electrical and Electronic Engineering **1** (2002) 33-37

M. Lorenz, H. Hochmuth, D. Natusch, M. Grundmann
High-quality reproducible PLD Y-Ba-Cu-O:Ag thin films up to 4-inch diameter for microwave applications
Physica C Superconductivity 372-376 (2002) 587-589.

I. V. Korotash, M. Lorenz
Investigation of the temperature features forming the passband of microwave HTSC bandpass filter
Physica C Superconductivity 372-376 (2002) 529-531.

D. Spemann, J. Vogt, T. Butz, D. Oppermann, M. Lorenz, G. Wagner, K. Bente
Ion beam analysis of $Zn_{2-2x}Cu_xIn_xS_2$ films
Nucl. Instr. Methods in Physical Research B 190 (2002) 667-672.

M. Kusunoki, M. Inadomaru, S. Ohshima, K. Aizawa, M. Mukaida, M. Lorenz, H. Hochmuth,
Dielectric loss tangent of sapphire single crystal produced by edge-defined film-fed growth method.
Physica C Superconductivity 377 (2002) 313-318.

R. Schmidt, C. Bundesmann, N. Ashkenov, B. Rheinländer, M. Schubert, M. Lorenz, E. M. Kaidashev, D. Spemann, T. Butz, J. Lenzner, M. Grundmann
Optical properties of ternary MgZnO thin films
Proceedings of the 26th Int. Conf. on the Physics of Semiconductors (ICPS-26) 2002

C. Bundesmann, M. Schubert, D. Spemann, T. Butz, M. Lorenz, E. M. Kaidashev, M. Grundmann, N. Ashkenov, H. Neumann, G. Wagner
Infrared dielectric functions and phonon modes of wurtzite $Mg_xZn_{1-x}O$ (x<=0.2)
Appl. Phys. Lett. 81, 2376 (2002)

M. Grundmann, R. Heitz, D. Bimberg
Comment on "Problems in recent analysis of injected carrier dynamics in semiconductor quantum dots" [Appl. Phys. Lett. 79, 3912 (2001)]
Appl. Phys. Lett. 81, 565 (2002)

M. Grundmann, ed.
Nano-Optoelectronics, Concepts, Physics and Devices
(Springer, Berlin, 2002), ISBN: 3-540-43394-5

M. Grundmann
Theory of Quantum Dot Lasers
in "Nano-Optoelectronics, Concepts, Physics and Devices" (Springer, Berlin, 2002), pp. 299-316

M. Grundmann, N.N. Ledentsov, F. Hopfer, F. Heinrichsdorff, F. Guffarth, D. Bimberg, V.M. Ustinov, A.E. Zhukov, A.R. Kovsh, M.V. Maximov, Yu.G. Musikhin, Zh.I. Alferov, J.A. Lott, N.D. Zhakarov, P. Werner
Long Wavelength Quantum Dot Lasers
J. of Materials Science: Materials in Electronics 13, 643-647 (2002)

R. Schmidt, B. Rheinländer, M. Schubert, D. Spemann, T. Butz, J. Lenzner, E. M. Kaidashev, M. Lorenz, M. Grundmann
Dielectric functions (1 eV to 5 eV) of wurtzite $Mg_xZn_{1-x}O$ (0 <= x < 0.29) thin films
Appl. Phys. Lett. 82, 2260 (2003)

8.24.2 in press

M. Lorenz, H. Hochmuth, M. Schallner, R. Heidinger, D. Spemann, M. Grundmann.
Dielectric properties of Fe-doped $Ba_xSr_{1-x}TiO_3$ thin films on polycrystalline substrates at temperatures between –35 and +85 °C.
to be published in Solid State Electronics, International Workshop on Oxide Electronics 2002, St. Pete Beach, FL, 20-23 Oktober 2002

M. Lorenz, H. Hochmuth, M. Grundmann, E. Gaganidze, J. Halbritter
Microwave properties of epitaxial large-area Ca-doped $YBa_2Cu_3O_{7-\delta}$ thin films on r-plane sapphire
to be published in Solid State Electronics, 9th International Workshop on Oxide Electronics 2002, St. Pete Beach, FL, 20-23 Oktober 2002

M. Lorenz, E. M. Kaidashev, H. von Wenckstern, V. Riede, C. Bundesmann, D. Spemann,
G. Benndorf, H. Hochmuth, A. Rahm, H.-C. Semmelhack, M. Grundmann.
Optical and electrical properties of epitaxial $(Mg, Cd)_xZn_{1-x}O$, ZnO, and ZnO:(Ga, Al) thin films on c-plane sapphire grown by pulsed laser deposition
to be published in Solid State Electronics, 9th International Workshop on Oxide Electronics 2002, St. Pete Beach, FL, 20-23 Oktober 2002

H. v. Wenckstern, H. Schmidt, R. Pickenhain, M. Grundmann
Conduction band offset of pseudomorphic InAs/GaAs determined by capacitance spectroscopy
Proceedings of the 26th Int. Conf. on the Physics of Semiconductors (ICPS-26) 2002

E. M. Kaidashev, M. Lorenz, H. von Wenckstern, J. Lenzner, G. Benndorf, A. Rahm, H.-C. Semmelhack, K.-H. Han, H. Hochmuth, C. Bundesmann, V. Riede, M. Grundmann
High electron mobility of epitaxial ZnO thin films on c-plane sapphire grown by multistep pulsed-laser deposition
Appl. Phys. Lett. (2003), in press

8.24.3 Conference contributions, Posters, Fairs

M. Lorenz, E. M. Kaidashev, J. Lenzner, H. von Wenckstern, D. Spemann, G. Wagner, C. Bundesmann, V. Riede, M. Grundmann
Electronic and structural properties of n-type Zn(Ga, Al, Mg, Cd) oxide thin films by PLD
Poster HL38.48 DPG-Frühjahrstagung Regensburg 11.-15. März 2002

R. Schmidt, C. Bundesmann, N. Ashkenov, B. Rheinländer, M. Schubert, M. Lorenz, E.M. Kaidashev, D. Spemann, T. Butz, J. Lenzner, A. Rahm, G. Wagner, M. Grundmann
Optical properties of ternary MgZnO thin films
26th International Conference on the Physics of Semiconductors (ICPS), July/August 2002, Edinburgh

R.Schmidt, C. Bundesmann, E.M.Kaidashev, B. Rheinländer, M.Lorenz, H. v. Wenckstern, A. Kasic, M. Schubert and M.Grundmann
Dielektrische Funktion im Bereich der Absorptionskante von ZnO und ZnO-MgO- und ZnO-GaO-Mischkristallen untersucht mittels spektroskopischer Ellipsometrie
66. Frühjahrstagung der DPG, Regensburg, Germany, March 2002

C. Bundesmann, N. Ashkenov, A. Kasic, B. Mbenkum, M. Schubert, M. Lorenz, E. M. Kaidashev, D. Spemann, G. Wagner, M. Grundmann
Phonon modes and free-carrier-properties of ZnO, Zn(Mg,Cd)O and ZnO:Ga thin films
66. Frühjahrstagung der DPG, Regensburg, Germany, March 2002

M. Grundmann, M. Lorenz, H. Hochmuth
Oxidische Dünne Schichten und Messplatz für die kritische Stromdichte von HTSL
Stand Forschungsland Sachsen auf Hannover-Industriemesse 15.-20.04.2002

M. Lorenz
Gepulste Laser-Plasmaabscheidung – ein flexibles Werkzeug zur Synthese hochwertiger dünner Schichten
Eingeladener Vortrag IMF-Seminar FZ Karlsruhe, Institut für Materialforschung III, 11.01.2002

M. Lorenz
PLD von großflächigen supraleitenden, ferroelektrischen und halbleitenden Oxidschichten
Vortrag Tageskolloquium Laser in der Mikrostrukturierung und Schichtabscheidung, IOM Leipzig, 13.05.2002

D. Spemann, J. Vogt, T. Butz, D. Oppermann, M. Lorenz, G. Wagner, K. Bente
Ion beam analysis of $Zn_{2-2x}Cu_xIn_xS_2$ films
Vortrag 15th Internat. Conf on Ion Beam Analysis 15.-20.7.2001 Cairns, Australien

M. Lorenz, H. Hochmuth, M. Schallner, R. Heidinger, D. Spemann, M. Grundmann.
Dielectric properties of Fe-doped $Ba_xSr_{1-x}TiO_3$ thin films on polycrystalline substrates at temperatures between –35 and +85 °C.

Poster at 9th International Workshop on Oxide Electronics 2002, St. Pete Beach, FL, 20-23 Oktober 2002

M. Lorenz, H. Hochmuth, M. Grundmann, E. Gaganidze, J. Halbritter
Microwave properties of epitaxial large-area Ca-doped $YBa_2Cu_3O_{7-\delta}$ thin films on r-plane sapphire
Poster at 9th International Workshop on Oxide Electronics 2002, St. Pete Beach, FL, 20-23 Oktober 2002

M. Lorenz, E. M. Kaidashev, H. von Wenckstern, V. Riede, C. Bundesmann, D. Spemann, G. Benndorf, H. Hochmuth, A. Rahm, H.-C. Semmelhack, M. Grundmann.
Optical and electrical properties of epitaxial $(Mg, Cd)_xZn_{1-x}O$, ZnO, and ZnO:(Ga, Al) thin films on c-plane sapphire grown by pulsed laser deposition
Poster at 9th International Workshop on Oxide Electronics 2002, St. Pete Beach, FL, 20-23 Oktober 2002

L. Roussak, K. Bente, Th. Doering, G. Wagner, J. Lenzner, M. Lorenz
Thin Epitaxial films of ZnCuInTe grown on (001) GaAs substrates by pulsed laser deposition – growth conditions and defect structure
Poster 10. Jahrestagung der DGK, Kiel, 4.-7.3.2002

M. Lorenz
Jc scanning system for HTSC thin films – background, working principle and application
Vortrag Beijing General Research Institute for Non-ferrous Metals, Beijing, China, 16.9.2002

M. Lorenz, H. Hochmuth, D. Natusch, M. Grundmann
High-quality reproducible PLD YBCO : (Ag, Ca) Thin Films up to 4-inch diameter for Microwave Applications
Vortrag First Sino-German Workshop on Superconductor Electronics, Beijing, China, 18 September 2002.

M. Lorenz, H. Hochmuth, D. Natusch, M. Grundmann
High-quality reproducible PLD YBCO : (Ag, Ca) Thin Films up to 4-inch diameter for Microwave Applications
Vortrag Institute of Physics, Chinese Academy of Sciences, Beijing, China, 20 September 2002.

M. Lorenz, E. M. Kaidashev, H. von Wenckstern, V. Riede, C. Bundesmann, D. Spemann, G. Benndorf, R. Schmidt, H. Hochmuth, A. Rahm, H.-C. Semmelhack, M. Schubert, M. Grundmann.
Structural, optical, and electrical properties of epitaxial ZnO, $(Mg, Cd)_XZn_{1-X}O$, and ZnO: (Ga, Al) thin films on sapphire grown by PLD
Vortrag 2002 MRS workshop series: Second International Workshop on Zinc Oxide, Dayton, OH, 25 Oct. 2002

H. von Wenckstern, R. Pickenhain, G. Biehne, M. Lorenz, E. M. Kaidashev,

C. Bundesmann, M. Schubert, M. Grundmann.
Electrical properties of ZnO:(Ga, Al, Cd) thin films on C- and R-plane sapphire substrates and of ZnO single crystals
Vortrag 2002 MRS workshop series: Second International Workshop on Zinc Oxide, Dayton, OH, 25 Oct. 2002

M. Lorenz
SNMS-Analytik an oxidischen, halbleitenden und Mehrfach-Schichtsystemen,
Vortrag SNMS-INA-Anwendertreffen IFOS, Universität Kaiserslautern, 18.11.2002.

8.25 Graduations

8.25.1 Diploma

Daniel Fritsch
Theoretische Untersuchung der elektronischen Eigenschaften binärer Nitride mit Zinkblende bzw. Wurtzit-Struktur unter Verwendung der empirischen Pseudopotential-methode

Dietmar Kitzig
Aufbau und Charakterisierung von cw-tauglichen (Al,Ga)As Laserdioden

Holger von Wenckstern
Electrical Properties of ZnO Thin Films and ZnO Single Crystals

9 Soft Matter Physics — Scientific activities

9.1 General Scientific Goals – Polymers and Membranes in Cells

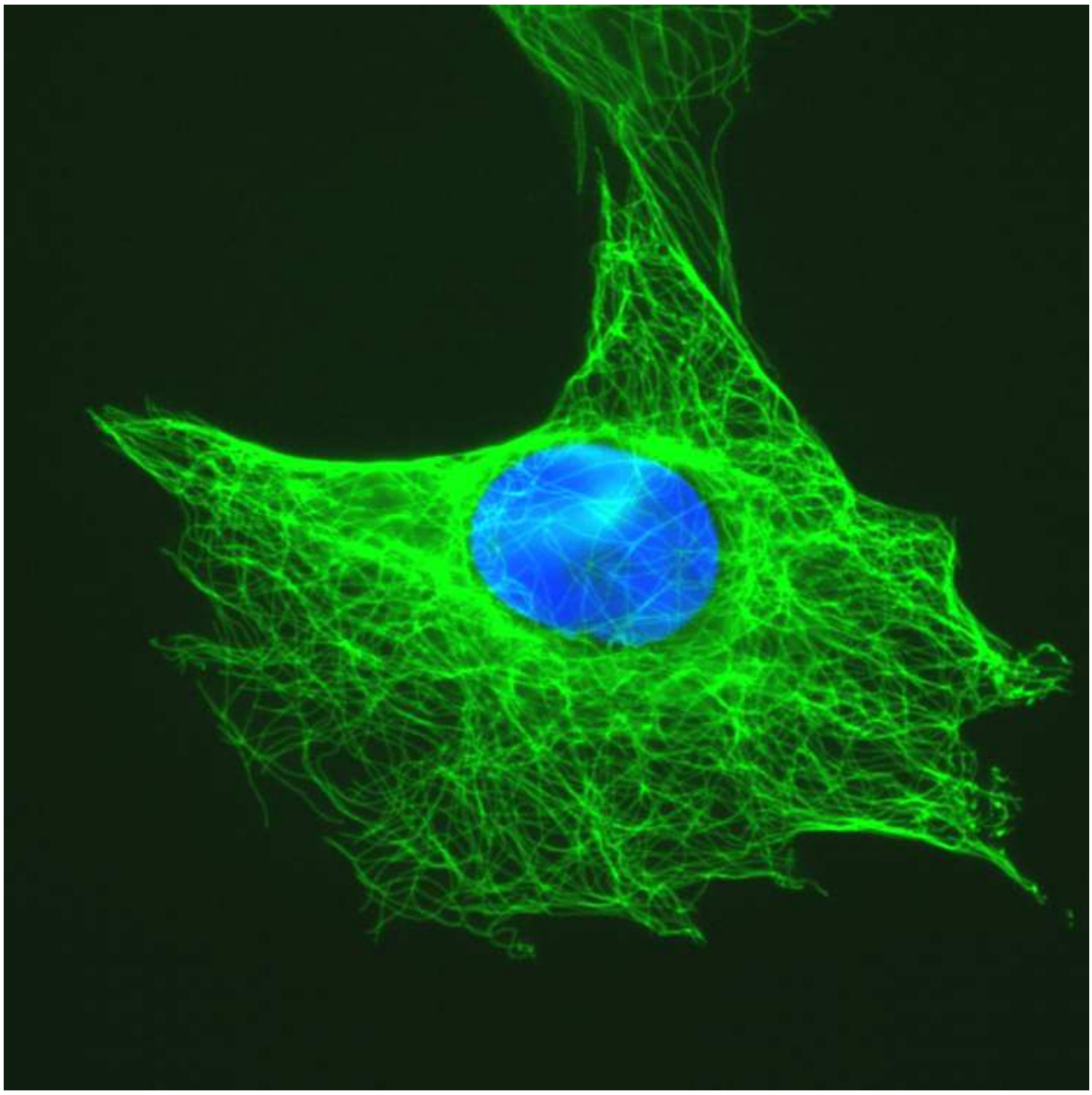

Fig. 1: Picture of a biological cell. The nucleus is represented in blue and the microtubule polymer network in green.

Studies of soft matter physics on the scale of nanometers to tens of microns, i.e., on the scale of proteins and cells, in complex multifunctional biological matter – often far from equilibrium and frequently behaving in a highly nonlinear manner – are the next big challenge for physics. Our research group is based on the idea that a complete understanding of molecular and cell biological systems calls forth a new type of fundamental physics, biological physics, which can describe biological soft matter with active elements and which is adaptive to multipurpose. Over the last decade there has been tremendous progress in molecular biology. Nevertheless, this progress will only impact the design and development of new materials if a novel combination of nanosciences and soft matter

physics is developed – bridging biology and engineering. This synergetic research in physics, chemistry, bioengineering and biology simultaneously advances our fundamental knowledge-base and provides novel applications in biomedicine and materials science.

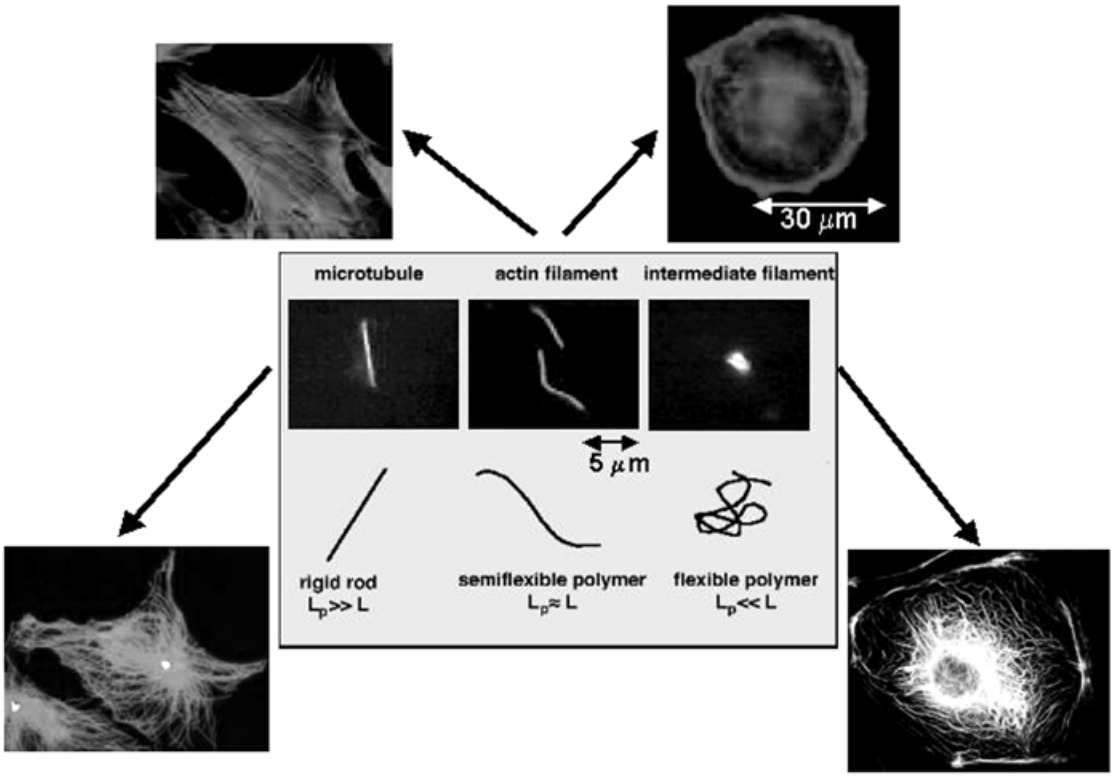

Fig. 2: Elements of the cytoskeleton: Microtubles emanate from the microtubule organizing center close to the nucleus. Intermediate filaments are often co-localized with microtubules. Actin filaments are found in stress fibers (upper left part) and in a homogenous filamentous network underlying the plasma membrane (upper right part). Intermediate filaments are unique to multicellular organisms, and various kinds of differentiated cells usually contain specific types of intermediate filaments. For example, vimentin is expressed in mesenchymal cells (e.g. fibroblasts) and is closely associated with microtubules.

The need for novel soft matter physics is exemplified in the actin cytoskeleton, an active network of protein filaments and molecular machines found in biological cells, and the plasma membrane, a complex liquid crystal material made out a wide variety of lipids and proteins. In contrast to well-described, conventional materials the actin cytoskeleton and the plasma membrane are not a static materials they actively change in response to various cellular functions (e.g. cell motility), conversely mechanical stimuli applied to them directly feedback into cell function (e.g. mechanotransduction). Our division's specific goal is to unravel the biological physics of the actin cytoskeleton and the plasma membrane. This complex soft matter with its active responses unmatched in the inanimate world and with its multiple functions requires an integrated approach which *in vitro* investigates the motions and interactions of actin filaments, molecular motors, and lipids on a single molecule level and *in vivo* measures the collective properties on a cellular level. This guiding principle allowed us over the last years to identify the following key projects described in the next

sections, which clearly illustrate the unparalleled, fundamentally new properties of the actin cytoskeleton and the plasma membrane.

The technical strength of our group lies in the synergetic and unique combination of methods which allows us the study of the actin cytoskeleton and the plasma membrane from a level of individual molecules *in vitro* to *in vivo* studies of the cellular actin cytoskeleton with techniques which integrate novel microrheological techniques, optical nanomanipulation, multiphoton microscopy, single particle tracking in Langmuir monolayers and molecular biology. We have pioneered the study of the polymer dynamics of individual actin filaments in actin networks (e.g. direct visualization of reptation in actin networks). For the first time we just succeeded in visualizing the motions of single molecule in lipid monolayers. We have developed a unique tool box to measure the viscoelastic properties of individual cells locally by AFM-based microrheology as well as globally with a new laser trap, the optical stretcher. These two techniques complement each other by allowing us to obtain very detailed information from single cells as well as to screen large numbers of cells. Furthermore, we have developed novel approaches to use laser light to manipulate cells without touching them as we have demonstrated with the optical stretcher and the optical neuron guidance.

9.2 Active Polymer Dynamics in Cells

David Smith, Vanessa Bell, Brian Gentry, Josef Käs

The molecular motor myosin II has not only the well-known force generating functions in structures such as muscle cells; it can fluidize entangled actin networks by superseding reptation dynamics with myosin-induced filament sliding. This illustrates how molecular motors can overcome conventional polymer dynamics and generate an active material with a new switchable viscoelastic behavior. Up to 40 % of a cell's energy (i.e. ATP) turnover fuel this active, energy-dissipating states of the actin cytoskeleton illustrating the importance for a cell's material properties.

Publications:
1) D. Humphrey, C. Duggan, D. Saha, D. Smith and J. Käs, Active fluidization of polymer networks through molecular motors, *Nature*, **416** 413- 416 (2002)
For background see also:
2) J. Käs, H. Strey and E. Sackmann, Direct imaging of reptation for semiflexible actin filaments, *Nature,* **368**, 226-229 (1994)

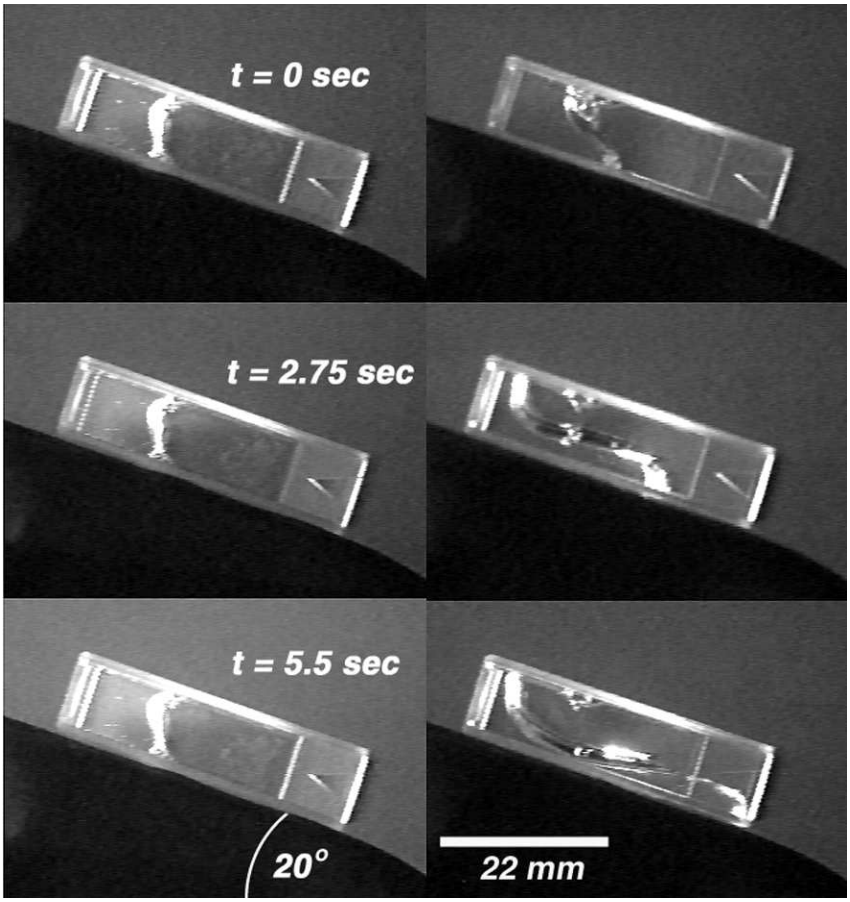

Fig. 3: Comparison of the flow properties of actin networks with inactive (left side) or active (right side) myosin dispersed in them. Under ADP conditions with inactive myosin the samples gelated and behaved like an elastic solid. In the presence of ATP or when caged ATP was released the active motors caused fluid-like flow properties.

9.3 Molecular Motors and Entropic State of Polymer Networks

David Smith, Vanessa Bell, Brian Gentry, Florian Huber, Peter Rödiger, Anatol Fritsch, Angela Stevens, Josef Käs

Besides the well known functions in contractility and transport molecular motors also influence the spatial organization of actin filaments and microtubules. We found that with increasing myosin-to-filament ratio the isotropic actin mesh continuously transforms first into a network of filament bundles which then orders into a pattern of asters and at even higher concentrations of the motor myosin to highly condensed actin coagulates. These assemblies drastically depend on motor activity. Although fully active myosin mini-filaments randomize, i.e. disorder, actin networks, ATP-depletion, which drastically slows down motor function and makes the minifilaments to crosslinkers, cause the association of supramolecular actin filament assemblies. In contrast, Dr. Surrey's and Dr. Nedelec's group at the EMBL in Heidelberg have seen that active motor constructs caused aster formation and ordering in microtubule networks whereas inactive motors resulted in the decay of this ordered structures.

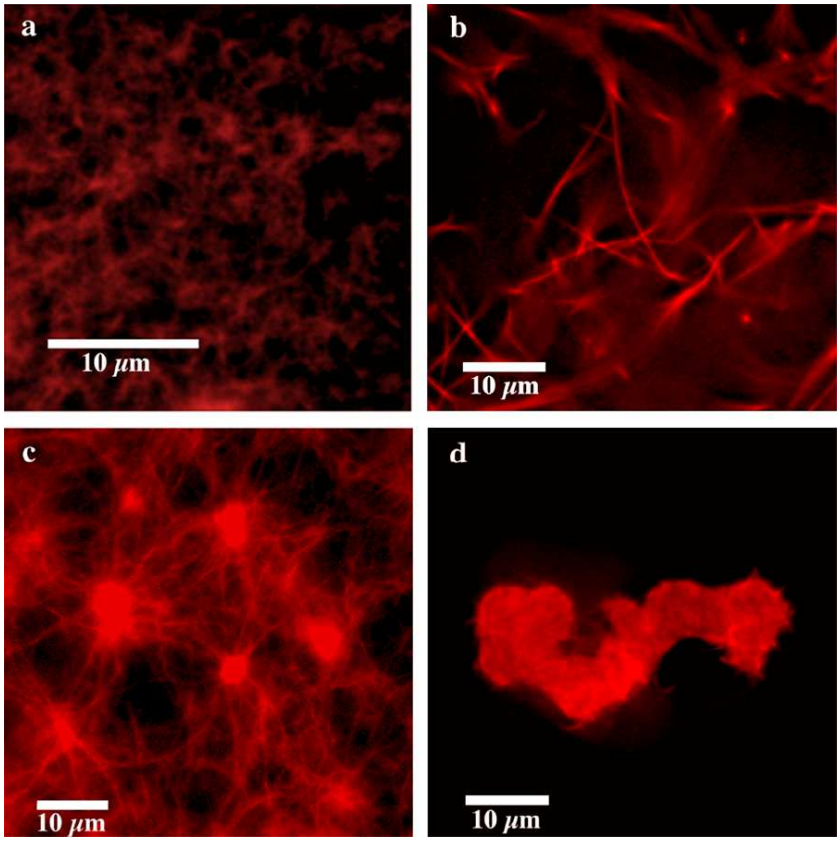

Fig. 4: Fluorescence pictures of spatial patterns formed in actin-myosin networks at different motor concentrations after ATP is used up: a) random mesh at 10 motors/ filament, b) network of actin bundles at 10^2 motors/ filament, c) asters at 10^3 motors/filament, d) strongly condensed phase at 10^4 motors/filament.

Nevertheless, both results clearly illustrate that molecular motor activity impacts the spatial organization of the cytoskeleton. In usual polymer systems order is frequently controlled by temperature as illustrated by thermotropic liquid crystals. Temperature is a fixed parameter in biological cells. Thus, motor activity may be an alternative variable – not known in conventional material science – to control order and disorder. However, in the light of the contrasting effects observed for microtubules and actin a fundamental understanding can be only found in collaboration between the Leipzig and the Heidelberg group considering the differences and common of the two biopolymer systems. Here also the collaboration with Dr. Amblard from Dr. Joanny's laboratory at the Institute Curie will be of great help. He has recently shown that the fragment S1 of the protein myosin, the active subunit of myosin minifilaments, increases the kinetic energy, i.e. the effective temperature, of an actin network when the fragment is activated.

Publications:

1) D. Smith, D. Humphrey, C. Duggan and Josef Käs, Molecular motor induced order disorder transitions in polymer networks, *Nature*, submitted (2002)

For background see also:

2) Nedelec, F.J., Surrey, T., Maggs, A.C. & Leibler, S. Self-organization of microtubules and motors, *Nature* **389**, 305-308 (1997)

9.4 Nonlinear Pattern Formation in Actin Networks

Brian Gentry, David Smith, Vanessa Bell, Florian Huber, Peter Rödiger, Anatol Fritsch, Angela Stevens, Josef Käs

The active nature of the cytoskeleton is synonym to a polymeric state far from thermal equilibrium. This raises the question to what extent the nonequilibrium stabilizes novel assembly states of actin networks, impacts cell elasticity and has been specifically chosen by nature to use instabilities to switch between different cytoskeletal assemblies. Our initial results show that the molecular motor myosin II and treadmilling as active cytoskeletal elements impact network architecture. Due to their polar nature, actin filaments polymerize on one end and depolymerize on the other while hydrolyzing ATP. This treadmilling process does not allow an actin filament alone to reach equilibrium whilst ATP is present. In the isotropic-liquid crystalline coexistence range the treadmilling-based nonequilibrium creates patterns of nematic and random network regions of actin filaments. In the spirit of Alan Touring we investigate to what extent these spatial arrangements are caused by nonlinear pattern formation. Dr. Carlier is a world-leading in the biochemistry of treadmilling. She will advice us on manipulating the treadmilling rates which should result in different patterns.

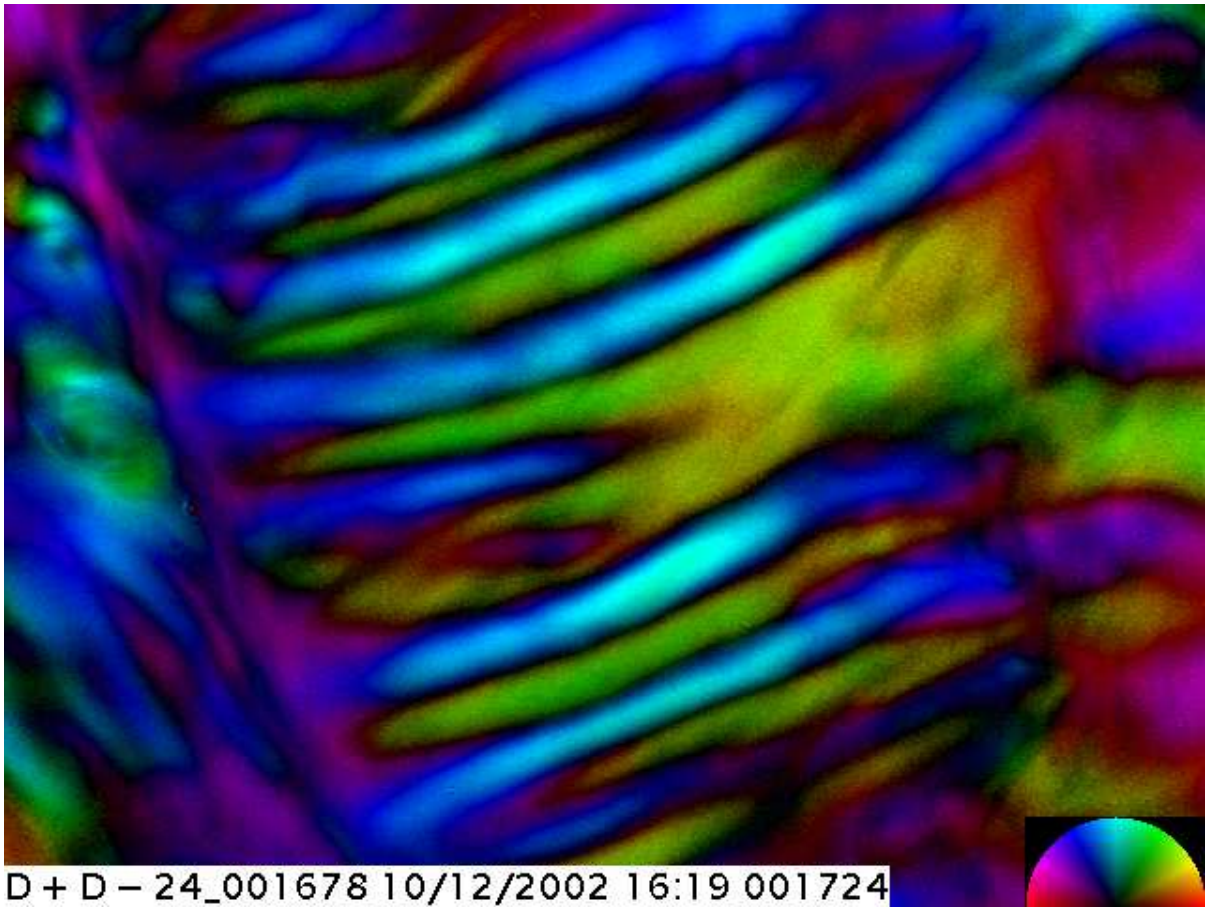

Fig. 5: Nonlinear pattern of nematic stripes of actin filaments.

9.5 AFM-based Microrheology

Soyeun Park, Claudia Brunner, Kristian Franze, Jens Gerdelmann, Josef Käs, Ken Shih

Atomic Force Microscopy (AFM) measurements of cell elasticity have been only of a qualitative nature due to the complex, nonlinear deformation by standard AFM tips, hydrodynamic contributions of the cantilever, and deviations from the Hertz model caused by finite sample thickness. Our new AFM-based microrheology allows us precise quantitative measurements of the spatial distribution of a cell's viscoelastic behavior (i.e. complex shear modulus and Poisson ratio) and adhesive state. In particular, the active lamellipodial regions of a cell show a viscoelastic signature similar to actin networks *in vitro*. Thus, dynamic measurements of the viscoelastic changes will provide an understanding of the actin-based active processes underlying cell motility, which will ultimately provide a template for the design of active polymeric materials.

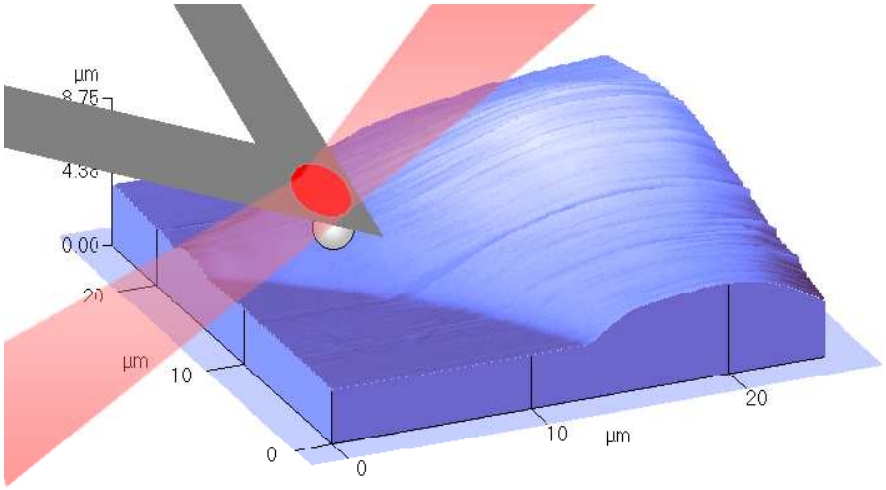

Fig. 6: An AFM cantilever with a polystyrene bead of well-defined diameter is used as a scanning tip to probe the viscoelastic and active responses of cells to deformation forces. The entire AFM is mounted on an inverted microscope equipped for fluorescence and phase contrast microscopy. The AFM is equipped with a temperature controlled wet-cell to assure stable physiologic conditions for the cells.

Publications:

1) R. Mahaffy, S. Park, E. Gerde, J. Käs, and C.K. Shih, Quantitative analysis of the viscoelastic properties of thin regions of fibroblasts using atomic force microscopy, *Biophys. J.*, in press (2003)

For background see also:

2) R. Mahaffy, C.K. Shih, F.C, MacKintosh, and J. Käs, Scanning probe-based, frequency-dependent microrheology of polymer gels and biological cells, *Phys. Rev. Lett.*, **85**(4), 880-883 (2000)

9.6 Mechanotransduction

Claudia Brunner, Kristian Franze, Jens Gerdelmann, Ken Shih, Hubert Wirtz, Thomas Arendt, Josef Käs

One of the most exciting results in cytoskeletal research of the last ten years was that the cytoskeleton is not only involved in cell motility and mitosis by actively organizing the cell, but also senses the cell's mechanical environment and reacts to changes. For this process the term mechanotransduction has been coined. Since the lung is an active organ subjected to various mechanical forces, all cells of the lung have been implicated in mechanotransduction events.

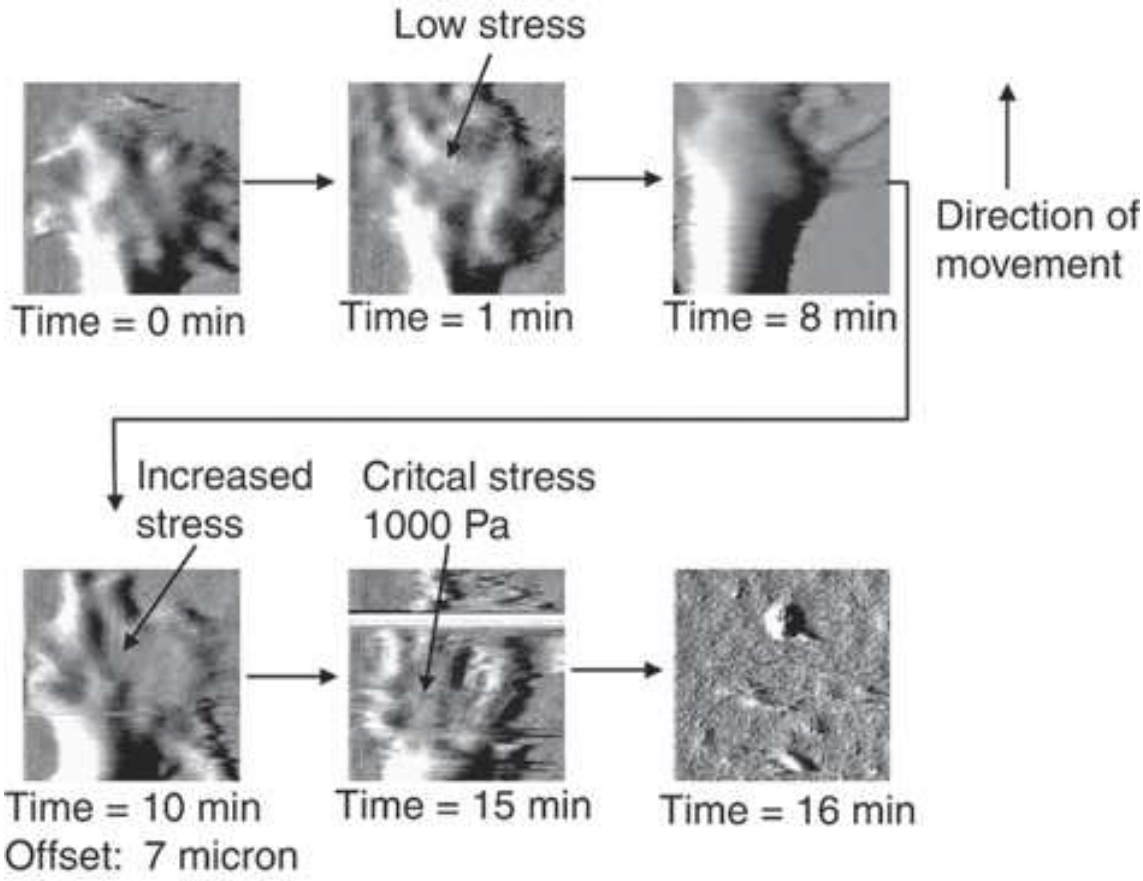

Fig. 7: Time series of a PC12 cell undergoing a critical force measurement by AFM. The first two images demonstrate the negligible effect of the imaging forces on the forward extension of the growth cone (size ≈ 5 µm). Following this, a low force was applied at a single point. Again, no effect was observed on the forward motion of the growth cone, which then moved out of the current imaging range. After the necessary offset, a higher force was applied and resulted in a significant change in the growth cone shape with some withdrawal. At even higher forces the growth cone retracted from view. The critical force corresponds to an approximate deforming stress on the growth cone of approximately 900 Pa. This withdrawal stress was verified on another cell with a value of approximately 1000 Pa. With time, the flat growth cone reformed, thus, demonstrating that although the stresses forced a withdrawal, critical damage was avoided.

A single mechanical stretch of alveolar type II epithelial cells causes a transient increase in cytosolic Ca^{2+} mobilized from intracellular stores and followed by a sustained increased pulmonary surfactant secretion. The specific mechanisms how the mechanical stimuli are transmitted throughout mechanotransduction are not understood. The alveolar type II cells are particularly well suited to study the transduction process since the response is immediate and not an indirect change in gene expression.

AFM-based microrheology will provide a spatial map of the viscoelastic constants of alveolar cells to determine a characteristic dissipation length, which limits the intracellular transmission of mechanical stimuli. By using the same AFM-techniques our laboratory has recently demonstrated that growing neurons retract when opposed to a threshold stress equaling their mechanical strength. For the alveolar cells, the threshold stress for intracellular Ca^{2+}-release and the cellular areas which respond preferred to mechanical stimulation will be determined. These data, which will precisely characterize the initial stimuli in mechanotransduction events, will provide a fundamental understanding how the cytoskeleton as an active polymer network can function as a delicate mechanical sensor.

Publications:
1) M. Lakadamyali, J. Bayer, R.E. Mahaffy, N.L. Peffly, C.K. Shih, and J. Käs, Local mechanosensing by neuronal growth cones, *Nature*, submitted (2002)
For background see also:
2) H. R. Wirtz *et al*, Calcium Mobilization and Exocytosis After One Mechanical Stretch of Lung Epithelial Cells, **250,** 1266-1269, *Science*, 1990

9.7 Optical Deformability as a Cell Marker

Falk Wottawah, Stefan Schinkinger, Bryan Lincoln, Susanne Ebert, Frank Sauer, Frank Emmrich, Anderas Reichenbach, Jochen Guck

To fully comprehend the role the flexible and multifunctional viscoelastic properties of the actin cytoskeleton have for cells it is essential to measure the variability of cell elasticity within and between cell lines. This requires high throughput measurements, which cannot be provided by relatively slow techniques such as our AFM technique (the scans provide precise local data, but need time). To accurately measure the variability of the elasticity of whole cells within and between cell lines we have devised and built an optical tool with an unprecedented force range (pN – nN) to stretch single cells between two laser beams, the optical stretcher. By using a microfluidic setup for the optical stretcher, samples with many cells can easily be handled similar to a flowcytometer. Our results show that cells actively respond to deforming stresses and that optical deformability is a precise cell marker, which allows diagnosing diseases such as cancer in which the cytoskeleton dedifferentiates. Our finding that the elasticity of the actin cytoskeleton is a tightly regulated cellular parameter illustrates the importance of the viscoelastic properties for a cell's state.

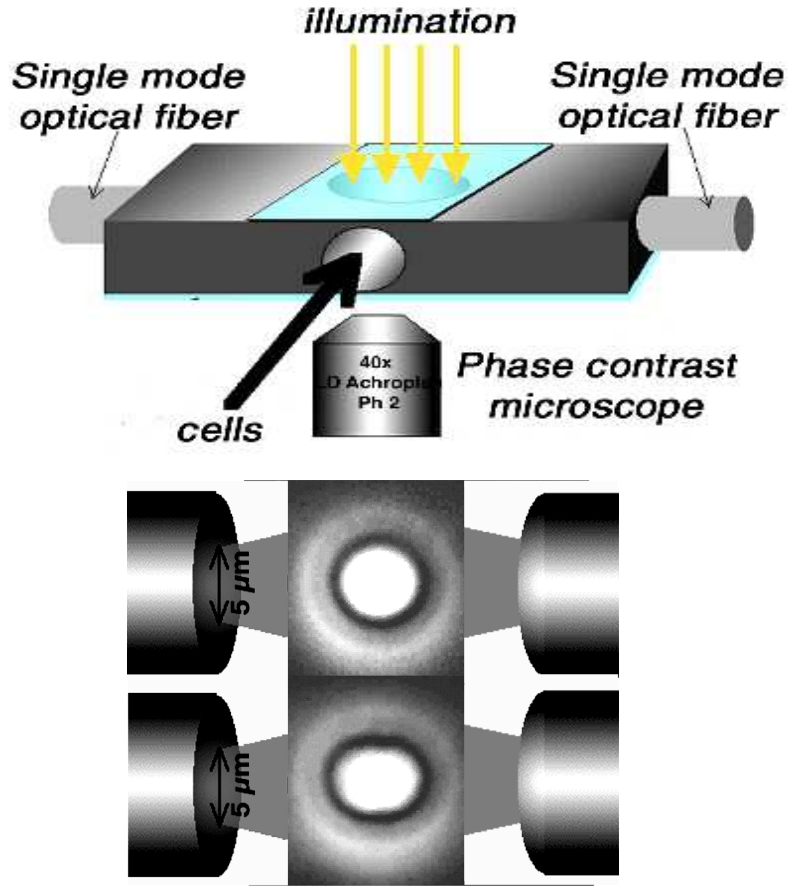

Fig. 8: The optical stretcher. The upper part shows the microfabricated flow chamber. The lower two pictures show the two laser beams stretching a fibroblast (diameter ≈ 30 µm) in phase contrast. Between the upper and the lower picture of the trapped cell, the laser power has been increased from 10 mW to 800 mW. The optical fibers, not drawn to scale, are 150 µm away from the cell. This distance was chosen so that the beam, diverging slightly from a 5 µm waist, illuminates the entire cell.

Publications:

1) J. Guck, H. Erickson, R. Ananthakrishnan, D. Mitchell, J. Bishop, J. Käs, S. Ulvick, C. Bilby, Optical Deformability of Cancer Cells, *Science*, submitted (2002)

2) J. Guck, R. Ananthakrishnan, C.C. Cunningham, and J Käs, The Optical Stretcher - A novel tool to measure cell elasticity, *Jour. of Phys.: Cond. Mat.*, **14** 4843-4856 (2002)

For background see also:

3) J. Guck, R. Ananthakrishnan, T.J. Moon, C.C. Cunningham and J. Käs, Optical deformability of soft dielectric materials, *Phys. Rev. Lett.*, **84**(23), 5451-5454 (2000)

3) J. Guck, R. Ananthakrishnan, T.J. Moon, C.C. Cunningham and J. Käs, The Optical Stretcher - A Novel, noninvasive tool to manipulate biological materials, *Biophys. J.*, **81** 767-784 (2001)

9.8 Biomolecular Machines Based on Active Viscoelasticity

Claudia Brunner, Revathi Ananthakrishnan, Karla Müller, Maren Mielke, Mireille Martin, Falk Wottawah, Stefan Schinkinger, Josef Käs

Due to their inherent elastic properties it is common in materials science that polymers are used to generate well-defined mechanical properties. In cells a fundamental aspect is added to providing structural support. The cytoskeleton is an active structure participating in and responding to cell function. As a general rule, changes in the functioning of a cell are mirrored in cytoskeletal changes. During malignant transformation the cytoskeleton gets less pronounced and more disordered. In cancer metastasis the cytoskeleton transforms from a structural material, to an active machine, which propels a metastatic cell through viscoelastic changes. Thus, precise measurements and a fundamental understanding of the dynamic viscoelastic properties are central to understand the cytoskeleton as a guide for new active materials. For this purpose we measure cell elasticity as a function of cytoskeletal composition and of cellular motility. In particular, we consider the clearly visible active responses of the cytoskeleton to deforming stresses.

To determine the dependence of cell elasticity on the cytoskeletal composition we transfect cells with oncogenes to induce changes in the molecular composition of the cytoskeleton. Using the optical stretcher to measure whole cell elasticity we particularly pick transfected clones which represent the entire spectrum of achievable cell elasticities. The elasticity data are then correlated with cytoskeletal architecture and composition by Western blotting, RNA microarrays and multiphoton microscopy. The cytoskeleton is a complex polymeric compound material which strain hardens, behaves highly nonlinear and can actively respond to deformations. The cytoskeletal transformation to an active cellular machine which is the driving force in cancer metastasis is exemplified when MCF-7 cells, a breast tumor cell line, are treated with phorbolester and become motile. We monitor the time course of the phorbolester-induced cytoskeletal changes by cell elasticity measurements with the optical stretcher, which identifies time points of significant change in cytoskeletal elasticity, and correlate this data with expression data of cytoskeletal proteins obtained by RNA microarrays. Since we assume that these points represent the key molecular events in the development to an actively advancing cell we use our AFM-based microrheology to obtain a temporal and spatial map of the viscoelastic changes in the lamellipodial region, i.e. leading edge of the cell, at these characteristic points. Despite there is great knowledge about the proteins of the cytoskeleton multiple models for cell motility have been proposed. Recent experiments in the Joanny lab at the Institute Curie have shown that cell motility is solely based on the active material properties of the cytoskeleton. Nevertheless, the cytoskeleton is highly redundant. Our experiments have the advantage that they correlate viscoelasticity with molecular architecture and they monitor the changes from a non-motile to a motile cell. This allows us to extract the key elements which allow the cytoskeleton to become an active machine which advances through viscoelastic changes. These data will be cross-fertilized by Dr. Joanny's theoretical work. He currently develops a model of cell motility based on an active viscoelastic material. An experimental proven model of cell motility will be the ideal basis to develop active biomimetic materials.

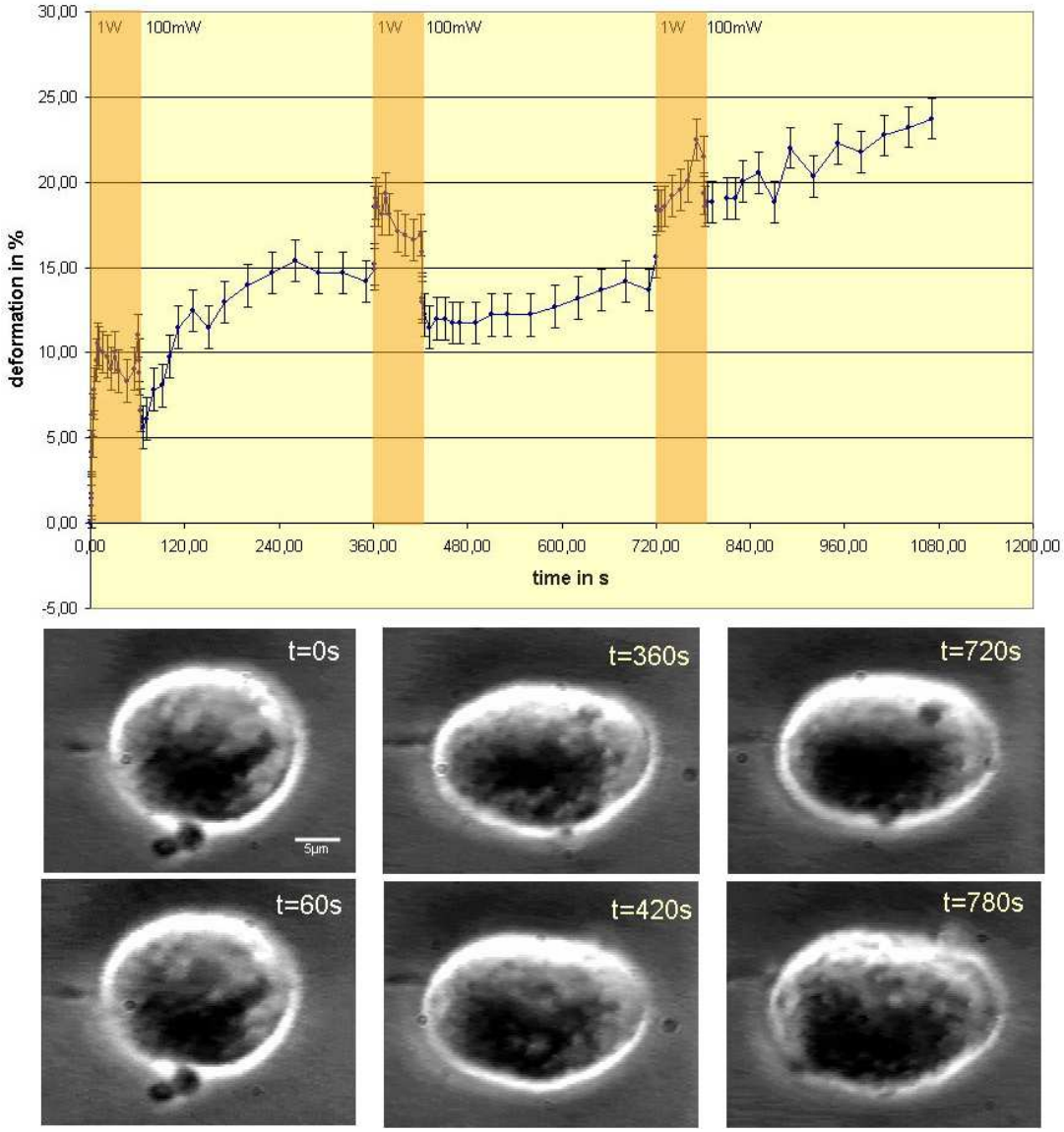

Fig. 9: Active response of a fibroblast to the mechanical stress exerted by the optical stretcher.

Publications:

1) R. Ananthakrishnan, J. Guck, J Käs, and T.J. Moon, The Role of Actin Networks in the Structural Response of Eukaryotic Cells, *Biophys. J.*, submitted (2002)

9.9 Optically Guided Neuronal Growth

Allen Ehrlicher, Timo Betz, Daniel Koch, Bjoern Stuhrmann, Michael Goegler, Mark Raizen, Josef Käs

The highly dynamic, active properties of the actin cytoskeleton require that it is a reaction-diffusion based system which allows quick assembly and disassembly. Guided by this basic property of the cytoskeleton we are therefore using delicate light-induced gradient forces to control biochemical cellular processes (in sharp contrast to the established technique of optical tweezers**,** which holds entire cellular structures with strong gradient forces). Control over neuronal growth is a fundamental objective in neuroscience, cell biology, developmental biology, biophysics, and biomedicine, and is particularly important for the formation of neural circuits *in vitro*, as well as nerve regeneration *in vivo*.

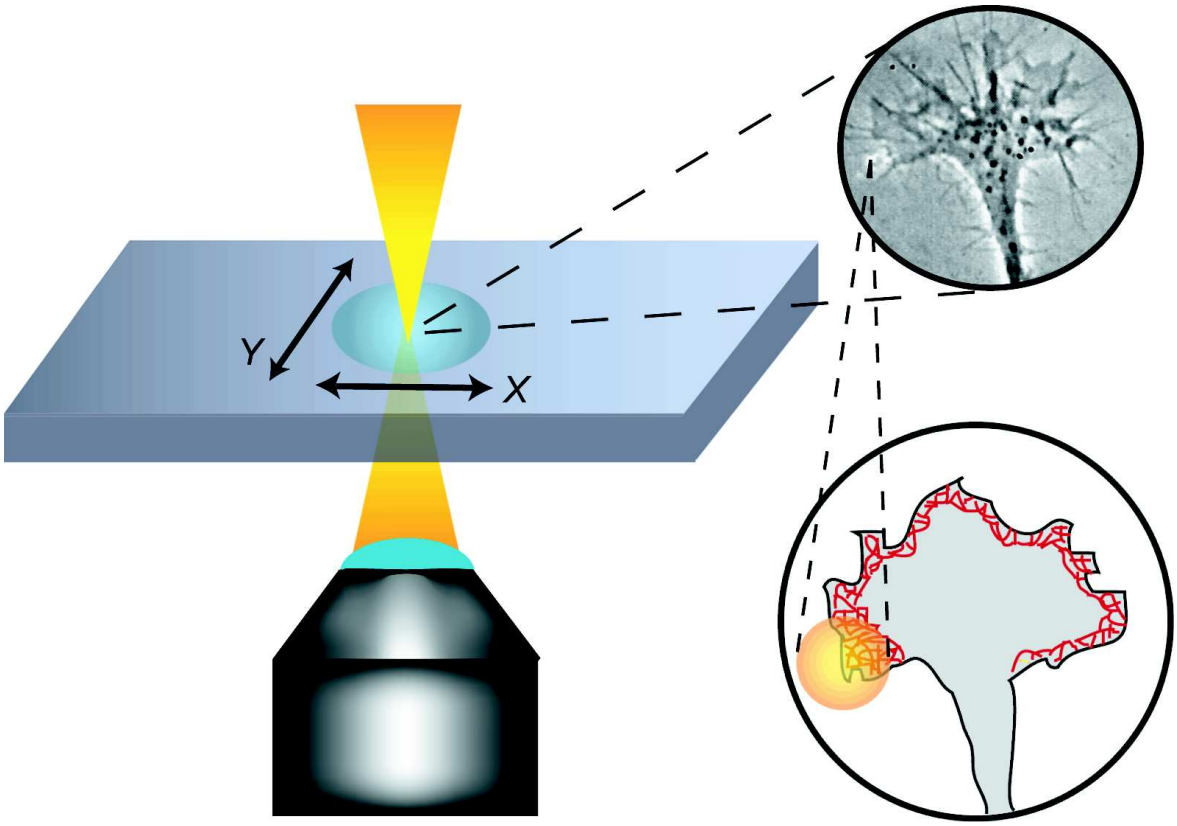

Fig. 10: Experimental setup for the optical guidance of growing neurons. A laser spot (∅ = 2 – 16 µm, power = 20 – 120 mW, λ = 800 nm) was placed with partial overlap in front of an actively extending growth cone. The overlap area was chosen in the direction of the preferred growth and to cover the actin cortex, which directly underlies the plasma membrane and drives the advancement of the leading edge of the nerve.

We have shown experimentally that we can use weak optical forces to guide the direction taken by the leading edge, or growth cone, of a nerve cell. In actively extending growth cones, a laser spot is placed in front of a specific area of the nerve's leading edge, enhancing growth into the beam focus and resulting in guided neuronal turns as well as enhanced growth. The power of our laser is chosen so that the resulting

gradient forces are sufficiently powerful to bias the actin polymerization-driven lamellipodia extension, but too weak to hold and move the growth cone. We are therefore using light to control a natural biological process, in sharp contrast to the established technique of optical tweezers which uses large optical forces to manipulate entire structures. Our results therefore open a new avenue to controlling neuronal growth *in vitro* and *in vivo* with a simple, non-contact technique. We have shown that weak optical dipole forces can be used to bias the molecular process of cell motility so that we can guide neuronal growth. Since we influence lamellipodia extension, a process essential for all motile cells, optical guidance may be extended as a general cell guidance method, and may provide an investigative tool to understand the underlying processes of cell motility. Moreover, we hope that optical guidance will allow us to form controlled neuronal structures *in vitro,* and we can also imagine that optical guidance could find applications in nerve repair *in vivo*.

Publications:

1) A. Ehrlicher, T. Betz, B. Stuhrmann, D. Koch, V. Milner, M. Raizen and J. Käs, Guiding neuronal growth with light, *PNAS*, **99**(25) 16024-16028 (2002)

For background see also:

2) E. J. Furnish, W. Zhou, C.C. Cunningham, J. Käs, and C.E. Schmidt, Increased actin severing via gelsolin overexpression enhances neurite outgrowth*, FEBS Lett.*, **508** 282 - 286 (2001)

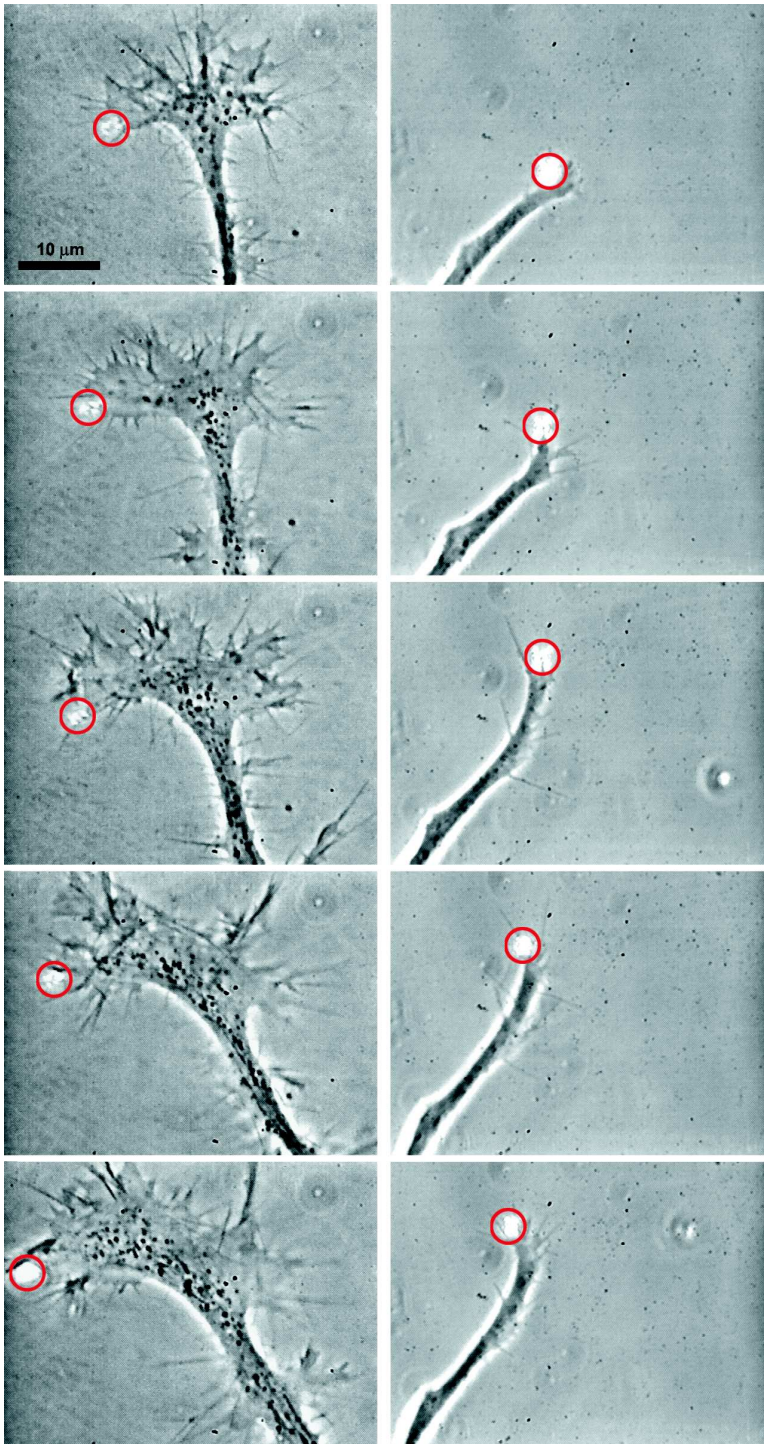

Fig. 11: Time sequences of optically guided turns of neurons and optically enhanced neuronal growth. Optically induced turns are shown for a time period of 40 min (left side) and 20 min (right side). The time interval between successive pictures is 10 min (left side) and 5 min (right side). The power of the laser spot is 100 mW on the left side and 60 mW on the right, and a red circle indicates the position of the laser spot. Optical control was achieved for extensive flat growth cones (left side) as well as for small, tube-like growth cones (right side). Before the laser altered the direction of the growth cone, the nerve was growing upward (left panel) or to the right side (right panel). The growth direction changes on the order of 90° under optical guidance. Note that the apparent change growth direction appears to be smaller since the axon straightens into the new direction.

9.10 Signal Transduction Investigated by Nano-probes

Doug Martin, Martin Forstner, Carsten Selle

Recent experiments by other researchers indicate that diffusive signals in the cell membrane propagate at speeds different from those in Brownian diffusion. The evidence that molecular motion in membranes can be subdiffusive is inconclusive. We have developed a technique using gold nano-particles or fluorescent nano-probes to track transitions between Brownian diffusion and subdiffusion. Under certain conditions, extracellular chemical traces guide the movement of a cell in a particular direction. Extracellular signals are transmitted across the cell membrane by receptors for G protein-mediated signaling pathways. The G-protein signal transduction system regulates the cytoskeleton through the generation of second messengers, such as phospholipids, which activate or inactivate a number of actin binding proteins or cytoskeletal protein kinases. Thus signaling in the cell membrane, a composite of lipids and proteins, affects the cytoskeleton. Since temperature, viscosity, and molecule size cannot control diffusive speed in the membrane, there has been much excitement about recent experiments indicating anomalous diffusion – particularly subdiffusion – in addition to normal diffusion. However, the limited observation space due to cell size (~ 10 μm) leads to statistically inconclusive data. Diffusive transport differs significantly for Brownian or anomalous diffusion due to changes in molecular motion. Whereas normal diffusion is well understood, fundamental questions remain in the physics of anomalous diffusion. For a general study of diffusion in 2-D liquid crystals such as cell membranes, we have developed a lipid monolayer based system with a surface area 100 x larger than that of a cell. By labeling single lipids on a Langmuir monolayer with a gold nano-particle or a fluorescent bead (which can be quantum dot), we can track them individually using darkfield microscopy or fluorescence microscopy. In the fluid-crystalline coexistence phase of the monolayer, our initial results show a transition between normal diffusive regimes with different diffusion coefficients depending on the crystalline fraction. Our final aim is a comprehensive study of lipid diffusion with a special focus on the possibility of inducing transitions between normal diffusion and subdiffusion.

The phospholipid PIP2 down regulates the protein gelsolin. To inhibit the activity of gelsolin it has to bind to two PIP2-molecules. This can only occur if PIP2 forms domains within the cell membrane. It is expected that these domains appear in the membrane locally wherever gelsolin is inhibited. Previously, thermodynamic equilibrium physics was used to explain the domain formation as a phase separation process. However, no experimental evidence could be found that PIP2 phase separation occurs in the cell membrane. We expect that the PIP2-rich domains within the membrane can be explained by nonlinear pattern formation. The signal transduction system, which regulates the cytoskeleton, is a complex reaction-diffusion system in a nonequilibrium steady state. Therefore, it is easy to imagine that controlled instabilities in this system cause biochemical pattern formation. By combining the Langmuir film balance technique with fluorescence microscopy we will explore the possibilities of nonlinear pattern formation in PIP2 containing lipid monolayers.

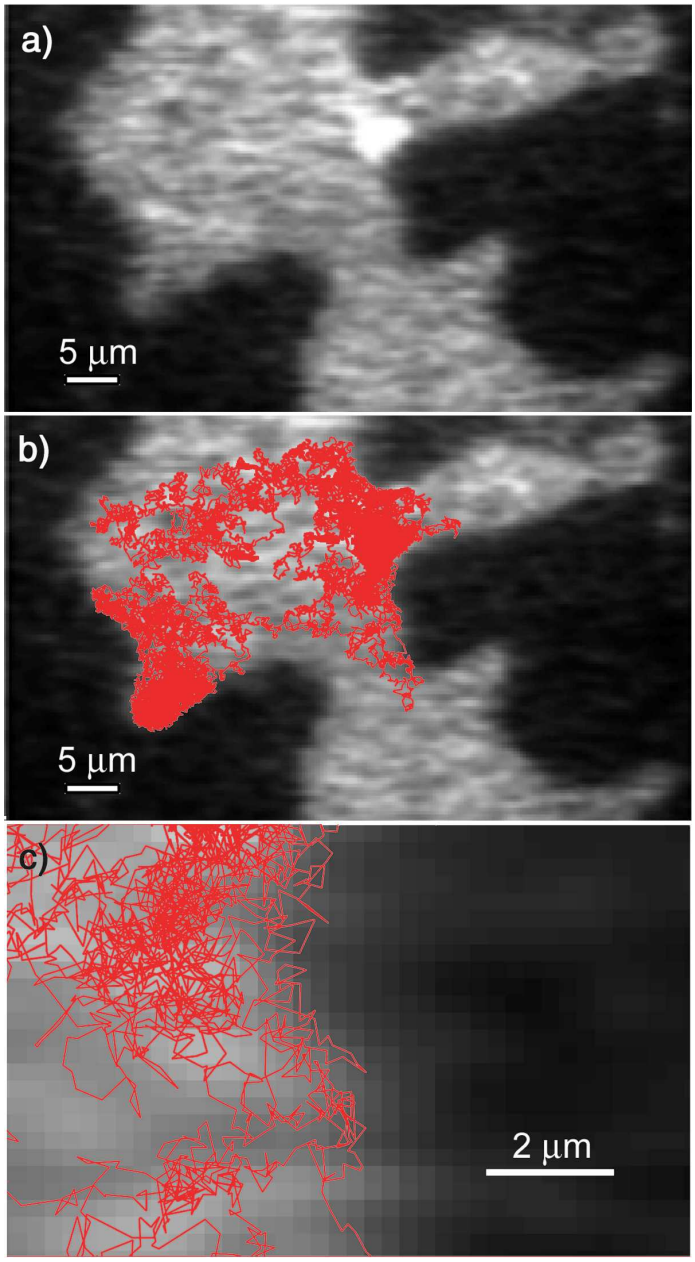

Fig. 12: 200 nm fluorescent polystyrene bead (bright spot marked by the arrow) at the boundary of the liquid expanded (light grey) and the liquid condensed phase (dark grey) of a DMPE lipid monolayer at a surface pressure of 16.0±0.5 mN/m. (b) Overlay of the bead's random walk on the monolayer picture. (c) Magnification of a portion of the random walk close to the domain boundary.

Publications:

1) M. B. Forstner, D.S. Martin, A.M. Navar, J. Käs, Simultaneous Single Particle Tracking and Fluorescence Microscopy on Inhomogenous Lipid Monolayers, *Langmuir*, in press (2003)

2) D. Martin, M. Forstner and J. Käs, Apparent subdiffusion inherent to single particel tracking, *Biophys. J.*, in press (2002)

For background see also:

3) M. Forstner, J. Käs and D. Martin, Single lipid diffusion in Langmuir monolayers, *Langmuir*, **17**(3), 567-570 (2001)

9.11 Interaction of Functionalized Nanoparticles with β-Amyloid Peptides

Herbert Schmiedel, Wolfgang Härtig

The general purpose of the project is the explanation of the structure and the physico-chemical properties of nanoparticles acting as carriers of active ingredients in the treatment of neurodegenerative deseases such as Alzheimer disease (AD). One hallmark of brains in AD is the appearance of extracellular plaques consisting of amyloid-beta-peptide aggregates (Aβ, usually comprising 40 - 42 amino acids). Polymer nanoparticles coated with various agents (see e.g. /1/) were shown to penetrate the blood-brain barrier and might interact with the Aβ plaques. Coated nanoparticles will be chosen for the in vitro interactions between Aβ- aggregates and some of their specific ligands. This study will include nanoparticles surface-labelled with: 1. β-sheet breaking low-molecular-mass substances, 2. Aβ-specific antibodies and 3. Aβ itself (with appropriate spacers). In addition, several types of biotinylated nanoparticles will be developed as well-characterized model polymers. We will then investigate their interactions with streptavidin and subsequently between streptavidin-ensheathed nanoparticles with biotinylated Aβ-peptides or biotinylated antibodies directed against Aβ.Due to the interdisciplinary character of the project largely different methods can be applied to study the interaction of functionalized nanoparticles with Aβ-aggregates. SANS /2/ (Small Angle Neutron Scattering) measurements will be performed to derive the structure of the active layers coating the nanoparticles. QELS (Quasi Elastic Light Scattering) and ITC (Isothermic Titration Calorimetry) measurements will be used to support the SANS results. The distribution of the nanoparticles and its relevant Aβ-targeted compounds in animal tissues will be studied by light and electron microscopy including multiple fluorescence labelling and confocal laser scanning. First electron microscopic data on the delivery of the Aβ-binding model compound thioflavin-T after injection of nanoparticles with encapsulated thioflavin into the hippocampus of mice were recently published. /3/. Nanoparticles optimized by the physico-chemical methods mentioned above should be tested for drug targeting in animal models and might result in carriers for medical applications.

/1/ B.-R. Paulke, W. Härtig, G. Brückner. Synthesis of nanoparticles for brain cell labelling in vivo. Acta Polymerica 43 (1992) 288-291.
/2/ H. Schmiedel, P. Jörchel, M. Kiselev, G. Klose. Determination of structural parameters and hydration of unilamellar POPC/C12E4 vesicles at high water excess from neutron scattering curves unsing a novel method of evaluation. J. Phys. Chem. B 105 (2001) 111-117.
/3/ W. Härtig, B.-R. Paulke, C. Varga, J. Seeger, T. Harkany, J. Kacza. Electron microscopic analysis of nanoparticles delivering thioflavin-T after intrahippocampal injection in mouse: implications for targeting β-amyloid in Alzheimer's disease. Neurosci. Lett. 338 (2003) 174-176.

9.12 Funding

Alexander von Humboldt Foundation, Euro 2.0 Mio, 2002 – 2005, "Molecular structure and function of biopolymer networks, characterized by novel laser trapping tools, nanorheology and single polymer microscopy"

Wechselwirkung beschichteter Nanopartikel mit Amyloid-Peptiden
Interaction of functionalized nanoparticles with β-amyloid peptides
Prof. H. Schmiedel (jointly with Dr. W. Härtig, Paul-Flechsig-Institut für Hirnforschung)
BMBF, 03DUO3LE (from 1/2003, within Bereich Neutronenstreuung)

9.13 Organizational Duties

J.A. Käs
Prize committee, Annual Saxonian Innovation Prize
Advisory committee for nanotechnology in cancer diagnosis, National Institute of Health, USA
Advisory committee for soft matter physics, NASA, USA
Prize committee, "Freundlichste Auslaenderbehoerde", Alexander von Humboldt Foundation
Chair, scientific advisory board, Evacyte Inc., USA
CNRS review committee, Institute Curie, Paris
Organizing committee, Summer School for Soft Matter Physics 2004, Iran
Journal review: Nature, Physical Review Letters, Physical Review E, Biophysical Journal, Biophysica and Biochemica Acta, Biochemistry, Proceedings of the National Academy of Science, European Biophysical Journal, Langmuir
Grant review: National Science Foundation, Div. of Materials Research; National Science Foundation, Div. of Cellular Organization; National Science Foundation, Div. of Computational Biology; National Science Foundation, Div. of Physics, Special Programs; Deutsche Forschungsgemeinschaft, Alexander von Humboldt Foundation, Deutsche Studienstiftung, Centre National de Reserche

9.14 External Cooperations

Academic

Prof. Dr. Michel Follen, MD Anderson Cancer Center, Houston, Texas
Prof. Dr. Harry Swinney, Center for Nonlinear Dynamics, Austin, Texas
Prof. Dr. Ken Shih, University of Texas at Austin
Prof. Dr. Mark Raizen, University of Texas at Austin
Prof. Dr. Tess Moon, University of Texas at Austin
Prof. Jean-Francois Joanny, Institute Curie, Paris
Prof. Dr. Jacques Prost, ESPCI, Paris
Prof. Dr. Marie-France Carlier, Cea Saclay, France
Prof. Dr. Robert Austin, Princeton
Prof. Dr. Walter Zimmermann, University of Saarbruecken

Prof. Dr. Reinhardt Lipowsky, MPI for Colloids, Golm
Prof. Dr. Frank Juelicher, MPI for Complex Systems, Dresden

Industry
Evacyte Inc., Austin Texas
Nimbus GmbH, Leipzig
jpk Instruments, Berlin
EuroPhoton GmbH, Berlin

9.15 Publications

D. Humphrey, C. Duggan, D. Saha, D. Smith and J. Käs, Active fluidization of polymer networks through molecular motors, *Nature*, **416** 413- 416 (2002)

D. Smith, D. Humphrey, C. Duggan and Josef Käs, Molecular motor induced order disorder transitions in polymer networks, *Nature*, submitted (2002)

R. Mahaffy, S. Park, E. Gerde, J. Käs, and C.K. Shih, Quantitative analysis of the viscoelastic properties of thin regions of fibroblasts using atomic force microscopy, *Biophys. J.*, in press (2003)

M. Lakadamyali, J. Bayer, R.E. Mahaffy, N.L. Peffly, C.K. Shih, and J. Käs, Local mechanosensing by neuronal growth cones, *Nature*, submitted (2002)

J. Guck, H. Erickson, R. Ananthakrishnan, D. Mitchell, J. Bishop, J. Käs, S. Ulvick, C. Bilby, Optical Deformability of Cancer Cells, *Science*, submitted (2002)

J. Guck, R. Ananthakrishnan, C.C. Cunningham, and J Käs, The Optical Stretcher - A novel tool to measure cell elasticity, *Jour. of Phys.: Cond. Mat.*, **14** 4843-4856 (2002)

R. Ananthakrishnan, J. Guck, J Käs, and T.J. Moon, The Role of Actin Networks in the Structural Response of Eukaryotic Cells, *Biophys. J.*, submitted (2002)

A. Ehrlicher, T. Betz, B. Stuhrmann, D. Koch, V. Milner, M. Raizen and J. Käs, Guiding neuronal growth with light, *PNAS*, **99**(25) 16024-16028 (2002)
M. B. Forstner, D.S. Martin, A.M. Navar, J. Käs, Simultaneous Single Particle Tracking and Fluorescence Microscopy on Inhomogenous Lipid Monolayers, *Langmuir*, in press (2002)

D. Martin, M. Forstner and J. Käs, Apparent subdiffusion inherent to single particle tracking, *Biophys. J.*, in press (2002)

Invited Talks
22. Aug. 2002
"Self-Assembly and Spatial Structure in Actin Networks", Brian Gentry, Vortrag bei Experimental Chaos Conference, San Diego, USA

23. Sep. 2002
"Order-Disorder Transitions in Polymer Networks Through Molecular Motors ", David M. Smith, Vortrag am Max Planck Institut für Physik komplexer Systeme, Dresden

5. Juni 2002
"Recent Models in Polymer Physics and their Relevance to Cell Elasticity", Revathi Ananthakrishnan, Vortrag am Max Planck Institut für Mathematik, Leipzig

15. Okt. 2002
"Not Just a Light Stretch – Microrheology from Physics to Biomedicine", Dr. Jochen Guck, Physik-Kolloquium, Universität Leipzig

24. Okt. 2002
"Optical Deformability as a Novel Inherent Cell Marker", Dr. Jochen Guck, Seminarvortrag an der University of California (UCSF), San Franzisko, USA

11. Nov. 2002
"Semiflexible Polymer Models - Do They Work for Eukaryotic Cells?", Revathi Ananthakrishnan, Vortrag am Max Planck Institut für Physik komplexer Systeme, Dresden

11. Nov. 2002
"Microrheology with Optically Induced Surface Stresses", Dr. Jochen Guck, Theorie-Seminar am Max Planck Institut für Kolloide und Grenzflächen, Golm

22. Mai 2002
"Laser in der Zellbiologie –von der Krebsfrühdiagnose zu Gehirnen im Reagenzglas", Josef Käs
Tagung zur Biotechnolgie Forschung in Leipzig

10. Juni 2002
"The Physics of the Actin Cytoskeleton: From Molecular Motors to Neuronal Networks", Josef Käs
Kolloquium, Institut Curie, Paris

12. Juni 2002
"The Physics of the Actin Cytoskeleton: From Molecular Motors to Neuronal Networks", Josef Käs
Kolloquium, Applied Mathematics Department, Trinity College, Cambridge

19. Juni 2002
"A Brain in a Bottle goes from the Wild West to the Wild East", Josef Käs
Abendessen, Wolfgang Paul Preis Träger, Berlin

21. Juni 2002
"The Physics of the Actin Cytoskeleton: From Molecular Motors to Neuronal Networks", Josef Käs

Kolloquium, Max Planck Institut für Mathematik, Leipzig

9. Juli 2002
"The Physics of the Actin Cytoskeleton: From Early Cancer Diagnosis to a Brain in a Bottle", Josef Käs
Antrittsvorlesung, Universität Leipzig

29. Juli 2002
"The Physics of the Actin Cytoskeleton: From Early Cancer Diagnosis to a Brain in a Bottle", Josef Käs
Symposium zum 80. Geburtstag von Hans Frauenfelder, Aspen

9. Sept. 2002
"Lasers in Cell Biology – From Early Cancer Diagnosis to a Brain in a Bottle", Josef Käs
Jahrestagung der Deutschen Gesellschaft für Biophysik, Dresden

10. Okt. 2002
"The Physics of the Actin Cytoskeleton: From Early Cancer Diagnosis to a Brain in a Bottle", Josef Käs
SFB269 Symposium, Leipzig

21. Okt. 2002
"Laser-kontrolliertes Nervenwachstum Auf dem Weg zu neuronalen Netzen im Reagenzglas", Josef Käs
Festsymposium, Leipziger Wolfgang Paul Preisträger

30. Okt. 2002
"Polymers in Cells –From Molecular Motors to Neuronal Networks", Josef Käs
Complex Fluids Meeting, Schloss Ringberg, Tegernsee

3. Nov. 2002
"Laser in der Zellbiologie", Josef Käs
Öffentliche Sonntagsvorlesung, Universität Leipzig

9.16 Conference Contributions

(p: poster, t: talk)
17. Okt. 2002
"Order-Disorder Transitions in Polymer Networks through Molecular Motors ", David M. Smith Seminarvortrag, Universität Leipzig (t)

8-10. Sep. 2002
"Order-Disorder Transitions in Polymer Networks Through Molecular Motors ", D. M. Smith, D. Humphrey, J. Käs, Jahrestagung der Deutschen Gesellschaft für Biophysik, Dresden (p)

8-10. Sep. 2002

"Self-Assembly and Spatial Structure in Actin Networks", B. Gentry, J. Käs, Jahrestagung der Deutschen Gesellschaft für Biophysik, Dresden (p)

18. Okt. 2002
"Order-Disorder Transitions in Polymer Networks Through Molecular Motors ", D. M. Smith, D. Humphrey, J. Käs, 1st Leipzig Research Festival for Life Sciences, Leipzig (p)

18. Okt. 2002
"Self-Assembly and Spatial Structure in Actin Networks", B. Gentry, J. Käs 1st Leipzig Research Festival for Life Sciences, Leipzig (p)

17. Mai 2002
"Is there a role of Müller (glial) cells in retinoschisis?" Kristian Franze, UCLA, Jules Stein Eye Institute (t)

02. September 2002
"Mechanical Properties of Murine Müller Cells", K. Franze, J. Käs, A. Reichenbach, Müller Cell Meeting (p)

18. Oktober 2002
"Mechanical Properties of Murine Müller Cells", K. Franze, J. Käs, A. Reichenbach, 1st Leipzig Research Festival for Life Sciences, Leipzig (p)

07. Nov. 2002
"Optical Control of Neuronal Growth", Björn Stuhrmann, Seminarvortrag, Universität Leipzig (t)

8-10. Sep. 2002
"Guiding Cells with Light", A. Ehrlicher, T. Betz, B. Stuhrmann, D. Koch, M. Goegler, F. Schreck, S. Moore, M. Raizen, J. Käs, Jahrestagung der Deutschen Gesellschaft für Biophysik, Dresden (p)

8-10. Sep. 2002
"Optical guidance of growth cones", T. Betz, A. Ehrlicher, B. Stuhrmann, D. Koch, F. Schreck, S. Moore, M. Goegler, M. Raizen, J. Käs, Jahrestagung der Deutschen Gesellschaft für Biophysik, Dresden (p)

18. Okt. 2002
"Guiding Cells with Light"A. Ehrlicher, T. Betz, B. Stuhrmann, D. Koch, M. Goegler, F. Schreck, S. Moore, M. Raizen, J. Käs, 1st Leipzig Research Festival for Life Sciences, Leipzig (p)

18. Okt. 2002
"Optical guidance of growth cones", T. Betz, A. Ehrlicher, B. Stuhrmann, D. Koch, F. Schreck, S. Moore, M. Goegler, M. Raizen, J. Käs, 1st Leipzig Research Festival for Life Sciences, Leipzig (p)

25. – 29. Sep. 2002
"Optical Guidance of Growth Cones", A. Ehrlicher, T. Betz, B. Stuhrmann, D. Koch, F. Schreck, S. Moore, M. Goegler, M. Raizen, J. Käs, Annual Meeting on Axon Guidance & Neural Plasticity, Cold Spring Harbor Laboratories, USA (p)

30. Juni – 5. Juli, 2002
Gordon Research Conference on Complex Fluids, Oxford, GB, "Optical Deformability as a Novel Inherent Cell Marker", B. Lincoln, S. Schinkinger, F. Wottawah, R. Ananthakrishnan, S, Moore, T.J. Moon, H. Erickson, S. Ulvick, C.C. Cunningham, J. Guck (p)

8-10. Sep. 2002
"Optical Deformability of Cells as Inherent Diagnostic Cell Marker", B. Lincoln, S. Schinkinger, F. Wottawah, R. Ananthakrishnan, K. Travis, T.J. Moon, J. Guck, Jahrestagung der Deutschen Gesellschaft für Biophysik, Dresden (p)

8-10. Sep. 2002
"A Microfluidic Optical Stretcher as a Diagnostic Tool", B. Lincoln, S. Schinkinger, F. Wottawah, J. Guck, Jahrestagung der Deutschen Gesellschaft für Biophysik, Dresden (p)

8-10. Sep. 2002
"Optical Microrheology of Whole Cells", S. Schinkinger, F. Wottawah, B. Lincoln, R. Ananthakrishnan, T.J. Moon, J. Käs, J. Guck, Jahrestagung der Deutschen Gesellschaft für Biophysik, Dresden (p)

8-10. Sep. 2002
"The Role of Actin Networks in the Structural Response of Cells", R. Ananthakrishnan, J. Guck, T. J. Moon and J. Käs, Jahrestagung der Deutschen Gesellschaft für Biophysik, Dresden (p)

18. Okt. 2002
"The Role of Actin Networks in the Structural Response of Cells", R. Ananthakrishnan, J. Guck, T. J. Moon and J. Käs, 1st Leipzig Research Festival for Life Sciences, Leipzig (p)

18. Okt. 2002
"A Microfluidic Optical Stretcher as a Diagnostic Tool", B. Lincoln, S. Schinkinger, F. Wottawah, J. Guck, 1st Leipzig Research Festival for Life Sciences, Leipzig (p)

18. Okt. 2002
"Optical Microrheology of Whole Cells", S. Schinkinger, F. Wottawah, B. Lincoln, R. Ananthakrishnan, T.J. Moon, J. Käs, J. Guck, 1st Leipzig Research Festival for Life Sciences, Leipzig (p)

18-20. Okt. 2002
"Optical Deformability as a Novel Inherent Cell Marker", B. Lincoln, S. Schinkinger, F. Wottawah, R. Ananthakrishnan, K. Travis, T.J. Moon, J. Guck, National Academy of Sciences, Arthur M. Sackler Colloquium on Regenerative Medicine, Irvine, USA (p)

9.17 Awards

Prof. Dr. Josef A. Käs

- Wolfgang-Paul Prize awarded by the Alexander von Humboldt Foundation
- Distinguished Lecturer, SigmaXi Academic Honor Society, USA
- Adjunct Professor, Department of Biomedical Engineering, University of Texas at Austin

Dr. Jochen Guck

- Young Scientist Award in Biomedical Photonics awarded by Hamamatsu and the German Cancer Research Center (Deutsches Krebsforschungszentrum, DKFZ, Heidelberg).
- One of three featured scientists at the March Meeting of the American Physical Society. The other two scientists were Prof. Dr. David Grier (UofChicago) and Prof. Dr. Steve Quake (Caltech).

9.18 Patents

Preliminary U.S. Patent # 05670.P005, *Optical Cell Guidance.* Inventors: Josef Käs, Mark Raizen, Valery Milner, Timo Betz, und Allen Ehrlicher. The European and Asian patents are pending.

10 Solid-state Optics and Acoustics — Scientific activities

10.1 Three-dimensional phase-sensitive acoustic imaging by pulsed operation of a conical PVDF transducer

E. Twerdowski, R. Wannemacher, W. Grill

In the continuous mode of operation conical piezoelectric transducers (axicon ultrasonic lenses) produce diffraction-limited acoustic beams that can be described by a Bessel function. This feature can be exploited to achieve a large depth of field represented by a pencil-shaped point spread function. Due to interference of observed acoustic waves reflected at different depths, however, low-quality images are obtained in this way. To overcome this problem and allow for distance selective detection along the axis by electronic means, pulsed excitation with wave packages of about 5 oscillations at a defined centre frequency in combination with adjusted time selective (gated) phase-sensitive detection has been employed, addressed here as temporal apodization. In this scheme focal distance can be electronically selected by appropriate timing, based on gated (boxcar) or time resolved (transient digitiser) detection. For this detection scheme a broadband conical PVDF transducer has been manufactured. Detection of the electrical signals is based on gated averaging of the two quadrature signals derived by mixing with the centre frequency reference. This method has been applied since higher resolution can be achieved as with transient digitisers due to analog processing in the first stage.

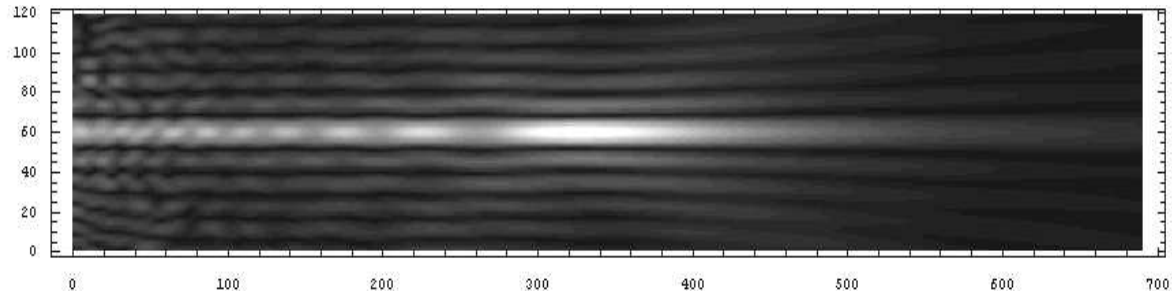

Fig 1. Simulation of the Bessel beam. Image width: 24 mm, heigth 4mm. The source is at the left edge of the image. The width of the main lobe is constant from the left edge till the middle of the image, which corresponds to about 12mm. Sidelobes are pronounced.

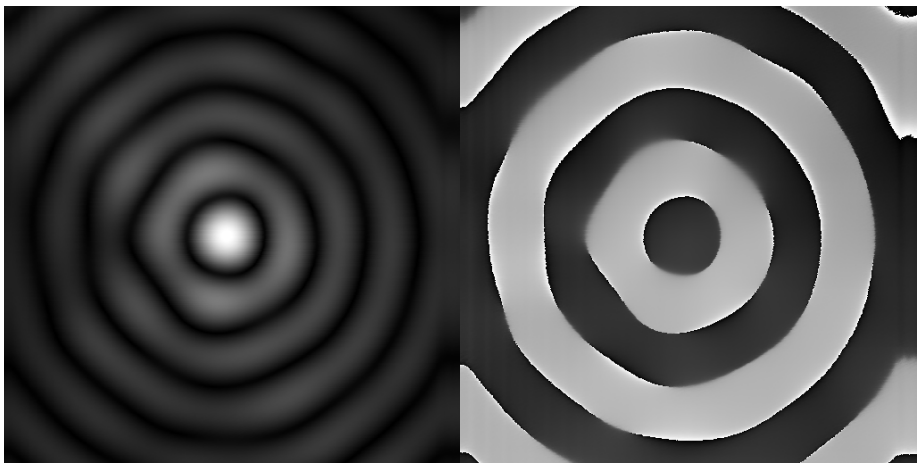

Fig. 2 Experimentally obtained image of the Bessel beam. Cross-section view at 12mm away from the lense surface, 4 MHz, range 4 x 4 mm. Left image: amplitude; right: phase. Theoretically expected $\pi/2$ phase jumps are visible on phase image.

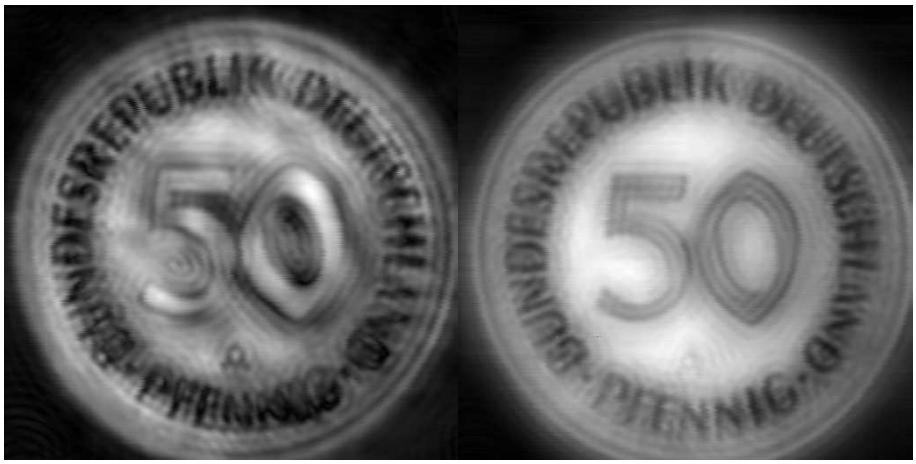

Fig.3 A 50 Pfennig coin imaged in reflection at 4,3 MHz; image range: 20 x 20 mm. Left image: time-selective receiving is not used and is close to CW regime; right image: time gated receiving allowed to improve the imaging properties of the Bessel lens.

10.2 Phase sensitive acoustic microscopy of polymer thin films

W. Ngwa, R. Wannemacher, W. Grill

The three-dimensional images obtained by scanning acoustic microscopy with vector contrast (PSAM), contain significant qualitative and quantitative information that is not easily obtainable by other methods. We employ this technique to examine homopolymer and polymer blend thin films. The complex V(z) functions derived from the images, and the results obtained by image processing and meticulous analysis are employed to render the morphology, composition and micro-mechanical properties of the polymer films. In addition, ways by which the information inherent in the phase images can be extracted are examined. This is highly desirable as the phase images contain very useful additional information.

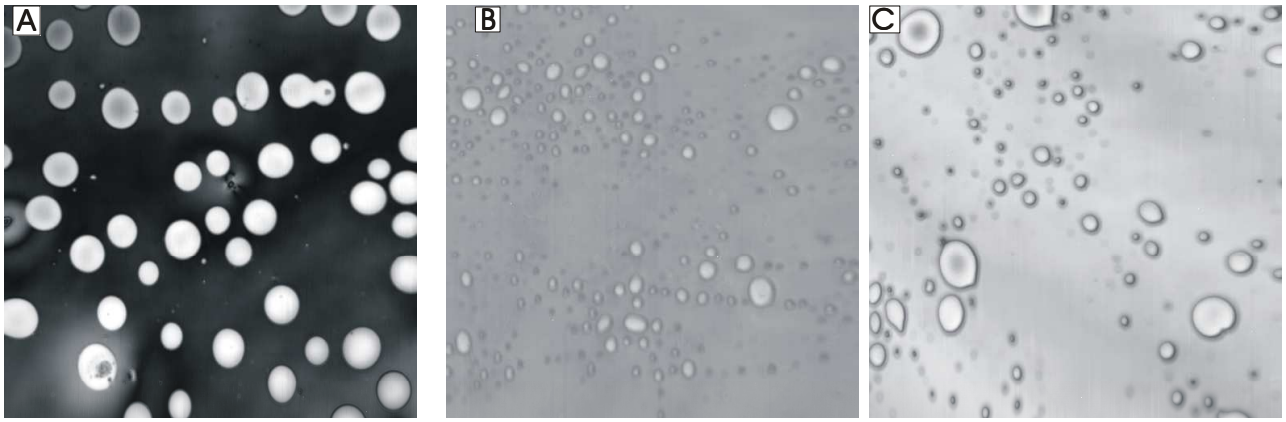

Fig. 4 PSAM images (350 μm x 350 μm) of PS film spun-cast from toluene (solvent) on: (A) a glass substrate thickness 583 nm, and (B) a silicon substrate thickness 159 nm (C) PMMA film, thickness 932 nm, spun-cast on silicon substrate. All the films were annealed for 12 hr.

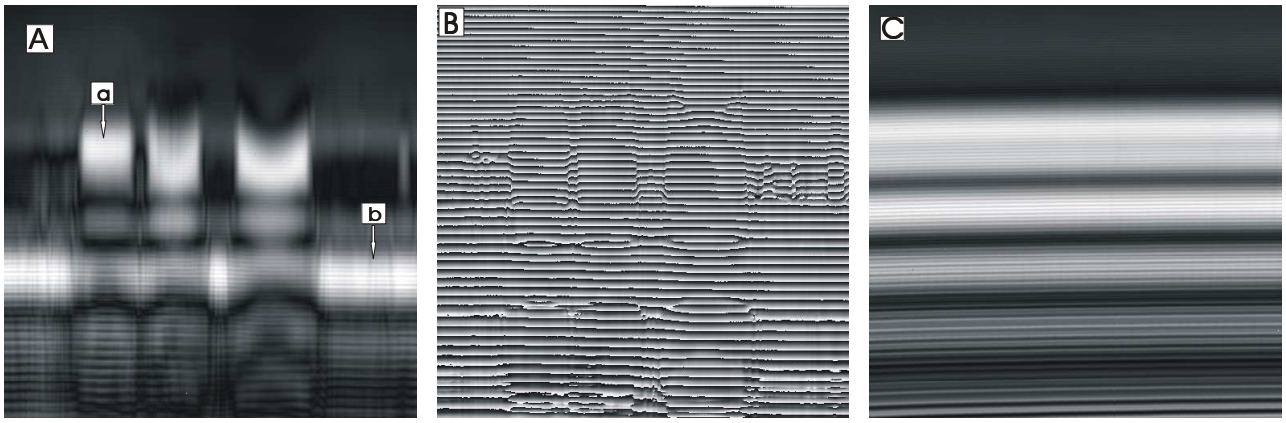

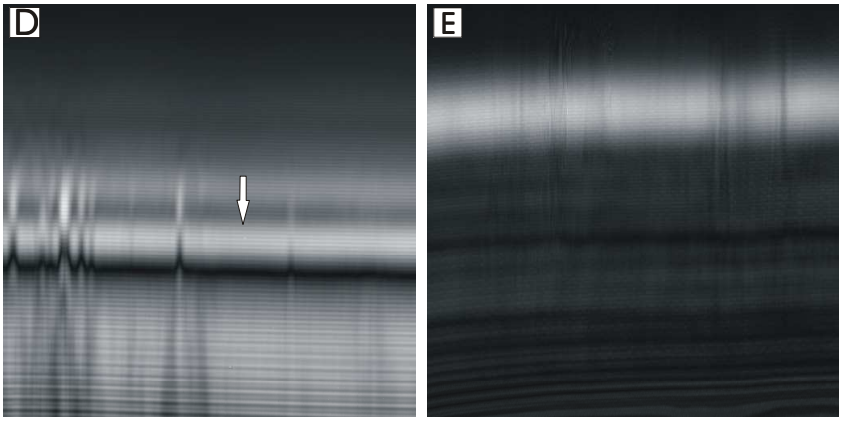

Fig. 5 y-z images (140 μm x 32 μm) of: (A) PS film shown in figures 3D and 4A, (B) Corresponding y-z phase image of A, (C) glass substrate, (D) PS on silicon shown in fig. 2B. (E) PS half-space. The stripes in the lower part of the images are due to cross talk from the phase image. This becomes more evident as one moves into the side maxima away from the focal region.

10.3 GHz acoustic correlation spectroscopy

W. Ngwa, Z. Kojro, R. Wannemacher, W. Grill

The Brownian motion of micro particles and movements of microorganisms in water are investigated by acoustic correlation spectroscopy at 1.2 GHz. An autocorrelation analysis of the time dependent phase and amplitude signals obtained from sound waves scattered from the immersed particles is presented. Due to time gating and the resulting small confocal detection volume of about 2 μm^3, single particle detection can be achieved under favorable circumstances. Very small particles can be detected because of the high acoustic impedance contrast, compared to, e.g., the optical contrast in dynamic light scattering (DLS) experiments. Furthermore, the short wavelength of GHz acoustic excitation is advantageous, in view of scattering cross sections described by Rayleigh's law. Results obtained by a systematic variation of experimental parameters demonstrate the power of this technique, which shows prospects for biological applications.

10.4 Acoustic and optical correlation spectroscopy of aquatic microorganisms

Z. Kojro, Ch. Laforsch, W. Ngwa, M. Helmstedt, W. Grill

Aquatic microorganisms exhibit movements on different time scales, which depend on a large number of external parameters, such as the external light level, temperature, food supply, or the presence of enemies. Such movements are of multiple interest, for example in behavioural studies concerning the formation of swarms, in the study of the ecology and evolution of inducible defences, or for automated phenotype characterisation in comparative genomics and population genomics. Acoustic and optical correlation spectroscopy are two appropriate techniques for rapid characterisation of the movements. Examples will be presented which reveal movements of the organisms as a whole, as well as internal movements of their organic constituents, such as legs or heart. Acoustic correlation spectroscopy offers a number of advantages over its optical counterpart, e.g. the absence of an external perturbation of the animal, or a long acoustic wavelength, which, in many cases, is equivalent to the Rayleigh limit of scattering, and can therefore simplify the analysis of the results.

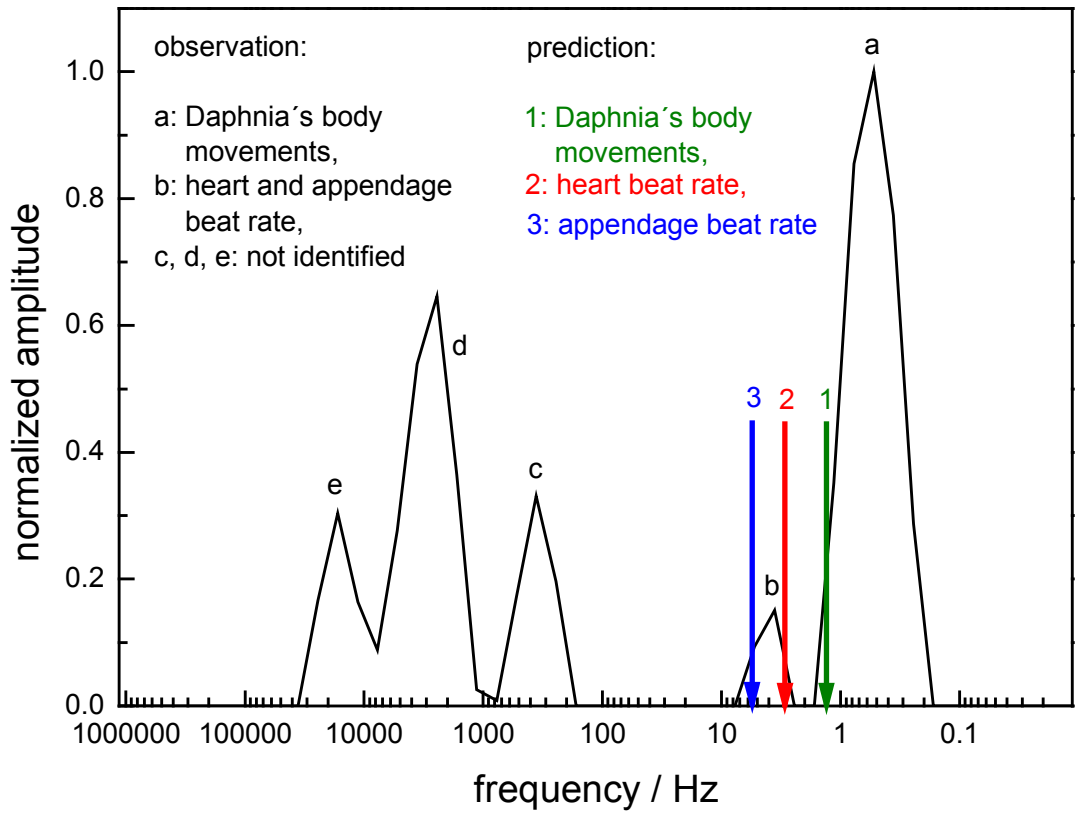

Results of the observation of living *Daphnia* by Photon Correlation Spectroscopy

10.5 Polarisation-Sensitive Confocal Light Microscopy of superlattices

Th. Rudolph, R. Wannemacher, W. Grill

Using a home-built polarisation-sensitive confocal optical microscope buried superlattices have been imaged employing the local optical anisotropy induced by these structures. The size of this anisortopy turned out to be considerably larger than what was calculated from a simple model.

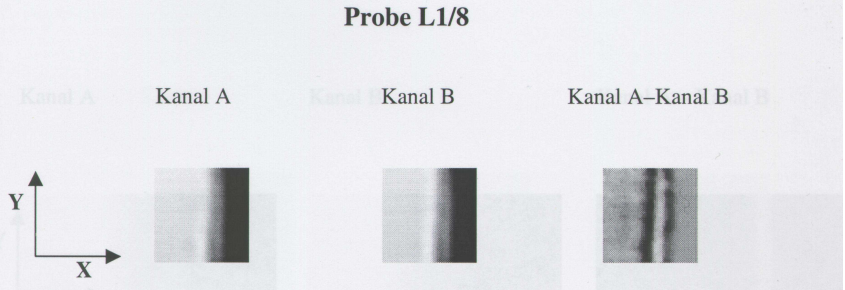

Abb. 2–11: konfokale Abbildung eines Bereiches der Probe L1/8, der Substrat und aufgewachsene Schichten inklusive Übergitter enthält, Polarisationskontrast durch EOM
Kanal A: Laser parallel zur Kante polarisiert
Kanal B: Laser senkrecht zur Kante polarisiert
*Bereich und Skalierung: **x**:1.9 µm (0.039 µm), **y**: 1.9 µm (0.039 µm)*

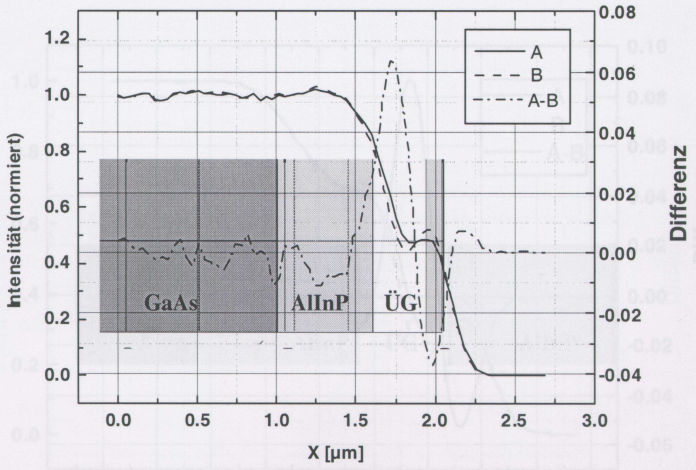

Abb. 2–12: Intensitätsprofile von Kantenscans orthogonaler Polarisation und deren Differenz im Vergleich mit einem maßstäblichen Schema des Probenaufbaus

Diploma thesis of Th. Rudolph

10.6 Polarisation-Sensitive Confocal Light Microscopy of electro-hydrodynamic convection in planar liquid crystal cells

T. Rudolph, R. Wannemacher, W. Grill

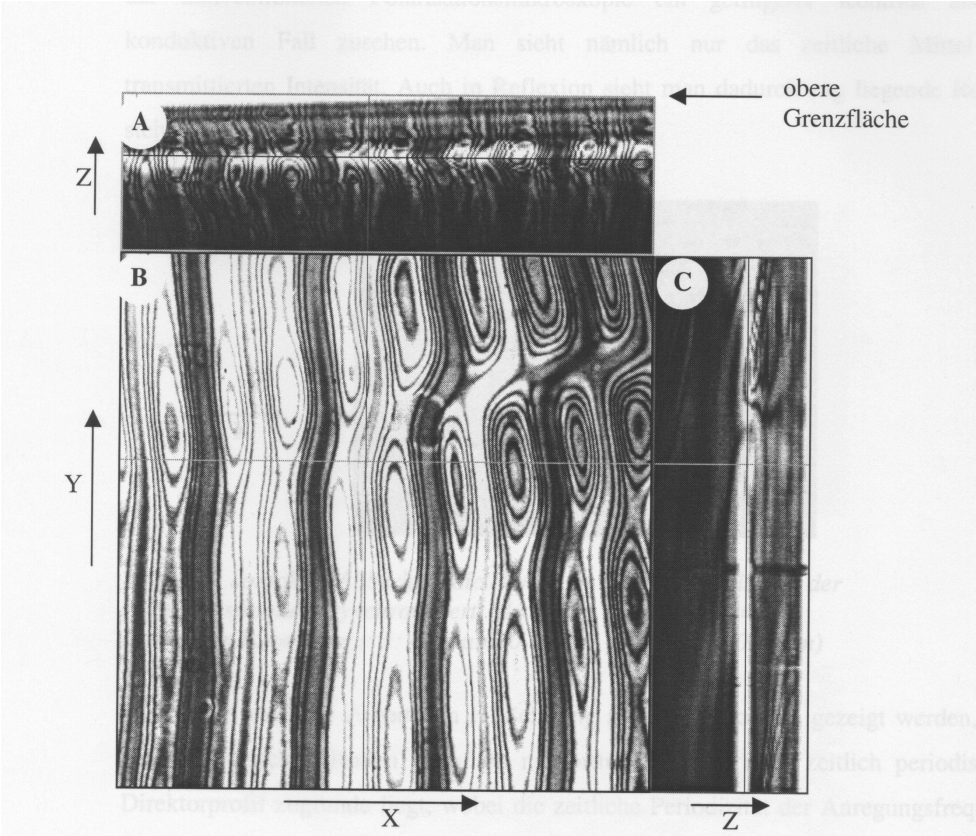

von

*Abb. 5–6: Schnitte durch einen dreidimensionalen Bildstapel von konduktiven Konvektionsrollen, A: x-z-Schnitt, B: Einzelbild aus dem Stapel, C: y-z-Schnitt Bereich und Skalierung: **x** und **y**: 259 µm (0.51 µm),z: 76 µm (1 µm) in Abb. 5–4 ist eine Auswahl der hier verwendeten Aufnahmen zu sehen*

Dynamical convection patterns of nematic liquid crystals contained in planar cells were investigated using a commercial confocal laser scanning microscope. Scanning of the laser beam synchronously with the electrical excitation thereby allows three-dimensional imaging of the time-dependence of these patterns in the dielectric and conductive regimes.

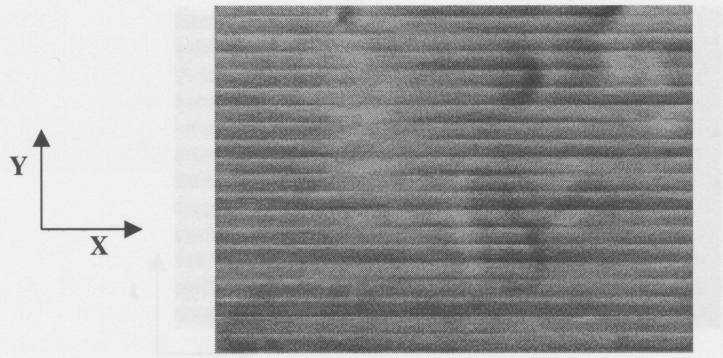

*Abb. 5–7: konfokale Abbildung dielektrischer Rollen, Scan ist mit der Anregungsfrequenz synchronisiert, (d=14 µm, f=20 Hz, V_{pp}=7 V) Bereich und Skalierung: **x**: 42.6 µm (0.19µm), **y**: 30.6 µm (0.19µm)*

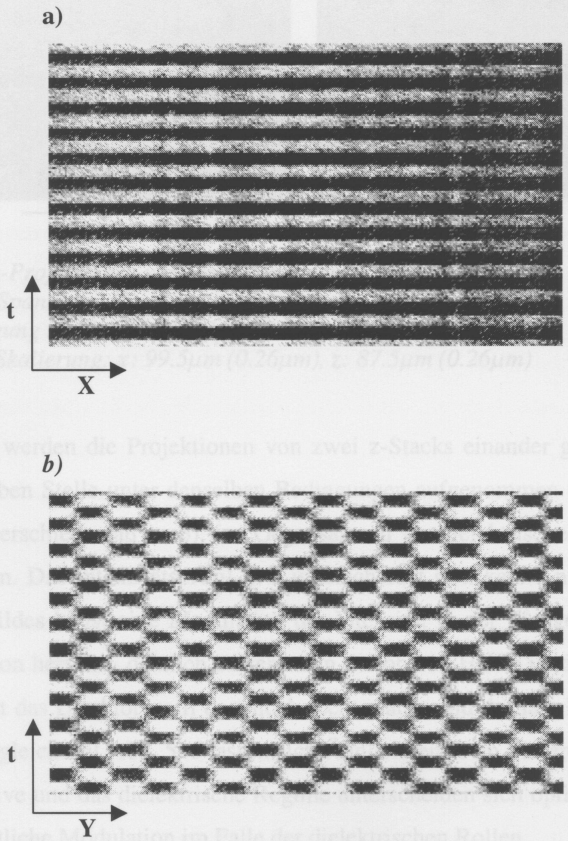

Abb. 5–8: Zeitserie mit 2 ms pro Zeile (d=25.8 µm, f=40,4 Hz, V_{pp}=32.8 Volt)
*a) Linie **parallel** zu den dielektrischen Rollen*
*b) Linie **senkrecht** zu den dielektrischen Rollen*
*Bereich und Skalierung: **x** bzw. **y**: 46.8 µm (0.18 µm), **t**: 300ms (2 ms)*

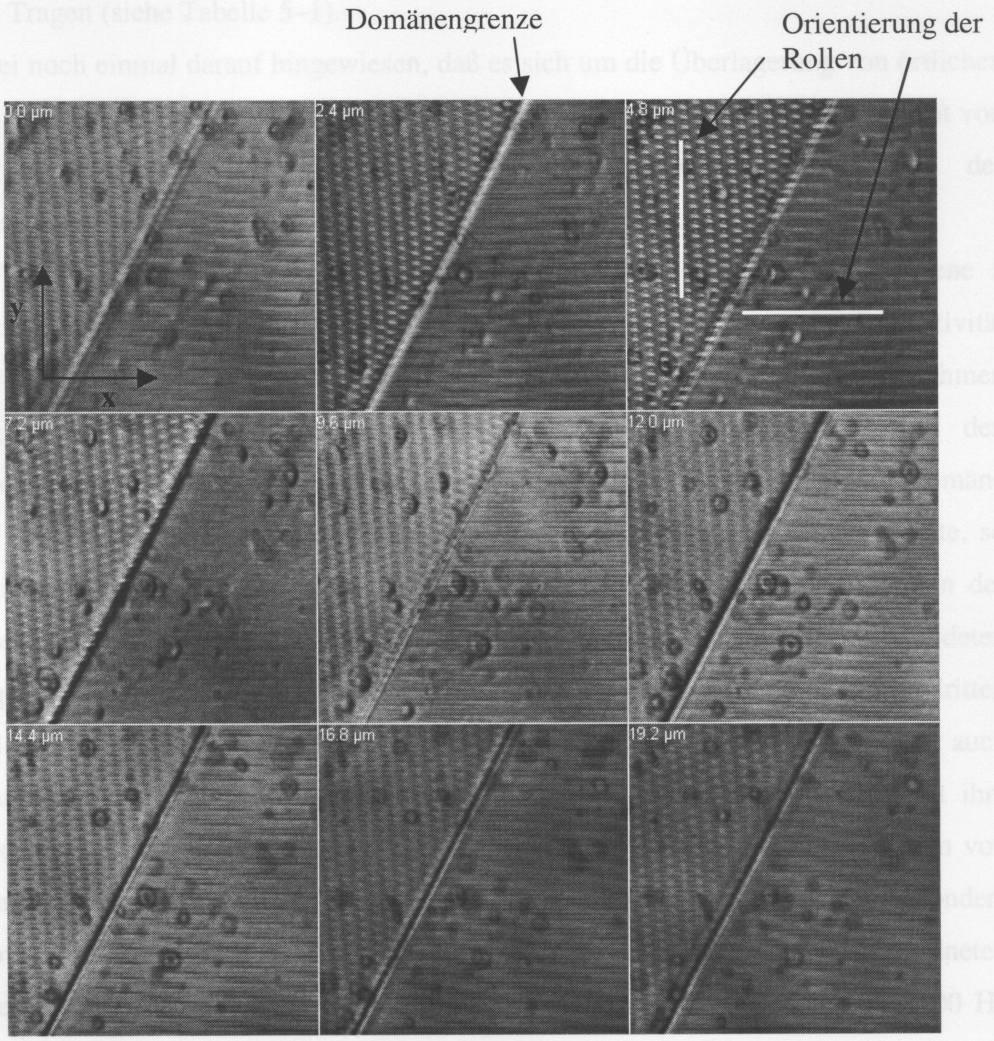

Abb. 5–10: Domänen orthogonaler Orientierung dielektrischer Konvektionsrollen in einer Twist-Zelle (d=14 µm, f=32.8 Hz, V_{pp}=15 V)
*Bereich und Skalierung: **x**: 97 µm (0.19 µm), **y**: 97 µm (0.19 µm), **z**: 19.2 µm (2.4 µm)*

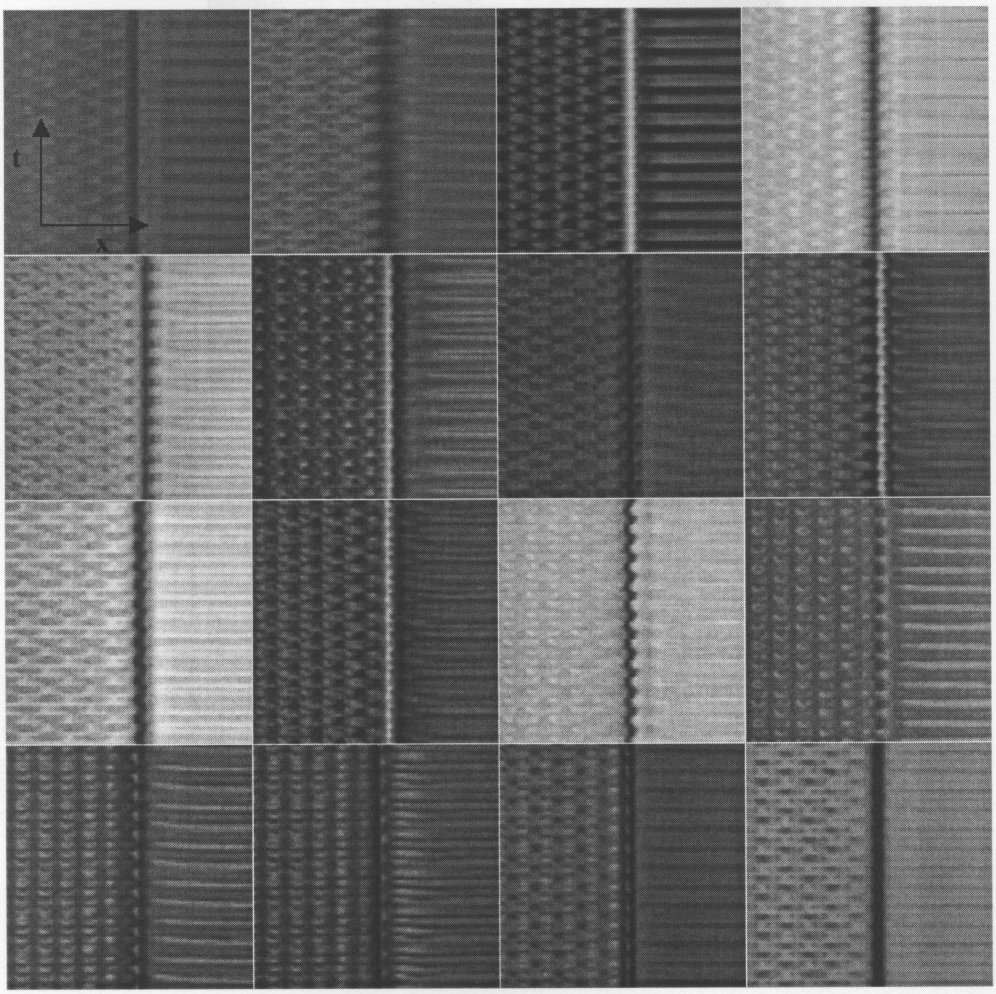

Abb. 5–11: Zeitserien von Linienscans für Fokuspositionen von 0 µm (links oben) bis 30 µm (rechts unten) an einer Domänengrenze in einer Twist-Zelle (d=14 µm, f=32,8 Hz V_{pp}=15 V)
Bereich und Skalierung ***x****: 50.4 µm (0.1 µm),* ***t****: 415.5 ms (2.5 ms),* ***z****: 30 µm (2 µm)*

Diploma thesis Th. Rudolph

10.7 Plasmon Spectroscopy: Propagation of femtosecond light pulses through near-field optical aperture probes

A. Pack, M. Hietschold, R. Wannemacher

The propagation of femtosecond light pulses through near-field optical fiber tips has been modelled numerically in three spatial dimensions by means of the Finite Integration Technique. Ideally conducting as well as real metallic coatings of the tip have been considered, and the influence of surface plasmon polaritons on shape, spectrum, and amplitude of the light pulse in the near and far fields of the tip have been investigated in this way. Special attention has been devoted to the superluminal tunneling of light through the fiber tip. The variation of phase and group velocities along the fiber axis has been characterised for a number of real metals and for different tip angles. A maximum of both velocities in the near field of the tip is characteristic for coatings of finite conductivity. For some tip angles negative values of the phase and/or group velocities are observed, which are caused by the propagation of surface plasmon polaritons on the outer surface of the coating and their conversion into photons. It is shown, that the excitation of surface plasmon polaritons on the metallic coating leads to strongly altered spatial emission characteristics of the tip.

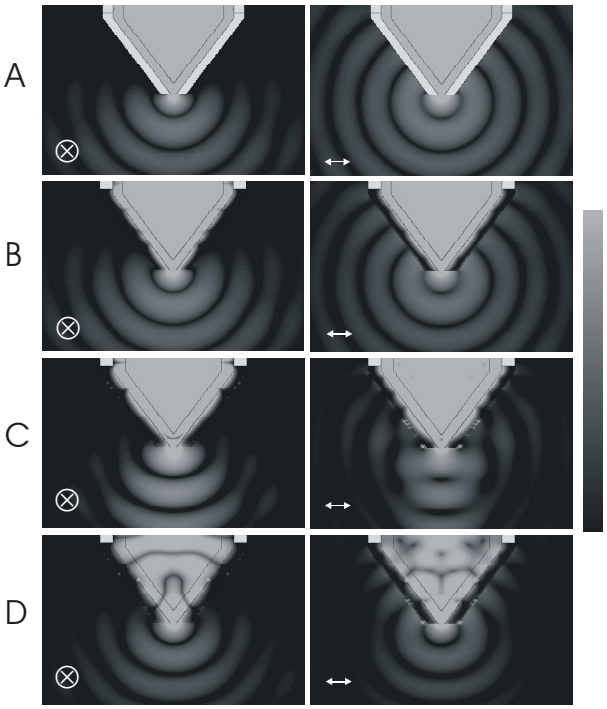

Instantaneous intensities in the vicinity of the probe (tip angle 37.2°) for an ideally conducting coating (A), an aluminum coating (B), and a silver coating (C,D), respectively. The intensities are plotted at the time, when the maximum of the pulse envelope passes the aperture (A,B). In the case of a silver coating the instantaneous intensity is plotted at two times corresponding to the minimum (C) and the second maximum (D) of the double-peaked pulse envelope. The logarithmic grey scales span the ranges 10^{-10}-10^{-6} Wsm^{-3} (A), 10^{-8}-10^{-3} Wsm^{-3} (B), $5 \cdot 10^{-7}$-10^{-4} Wsm^{-3} (C), and $5 \cdot 10^{-7}$-10^{-3} Wsm^{-3} (D), respectively.

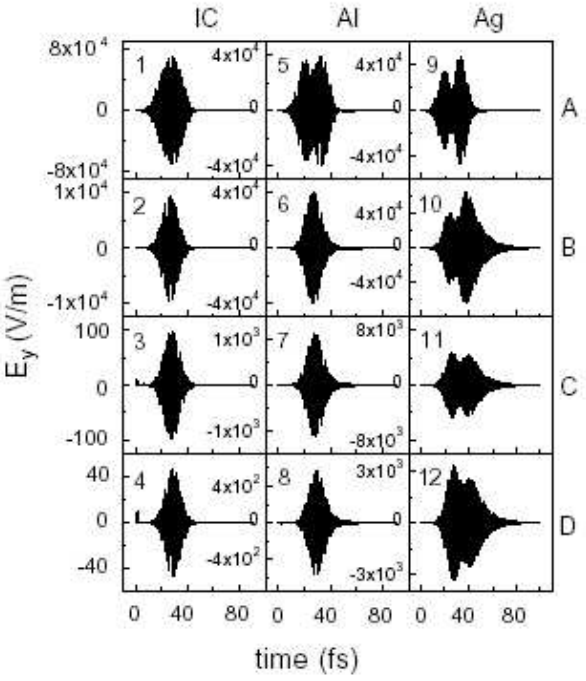

Electric field component $E_y(t)$, parallel to the polarisation of the exciting LP_{01} cylindrical fiber mode, on the axis of a near-field optical fiber probe, tip angle 37.2°, for different coating materials and at different locations in and outside of the fiber tip. IC: ideally conducting coating, Al: aluminum coating, Ag: silver coating. Positions on the fiber axis, for which the time dependence is shown: A: input port, B: in the center of the aperture, C: 400 nm in front of the aperture (in free space), D: 800 nm in front of the aperture. The exciting light pulse is a sine-modulated Gaussian pulse according to eq. (1). Parameters are given in the text and correspond to a center wavelength of 600 nm and a pulse width of 9.85 fs.

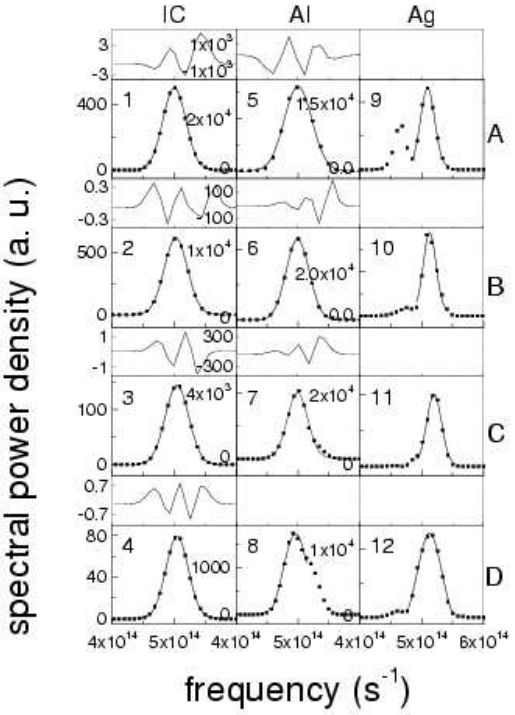

Power spectra obtained by fast Fourier transformation of the pulse shapes shown above. Abbreviations as in fig. 1: (A) input port, (B) within the aperture (c) 400nm in front of the tip (D) 800 nm in front of the tip. IC: ideal conductor, Al: aluminum, Ag: silver. Residues of the Gaussian fits included in the main graphs are given in the smaller graphs, except where they are obvious from the main plots.

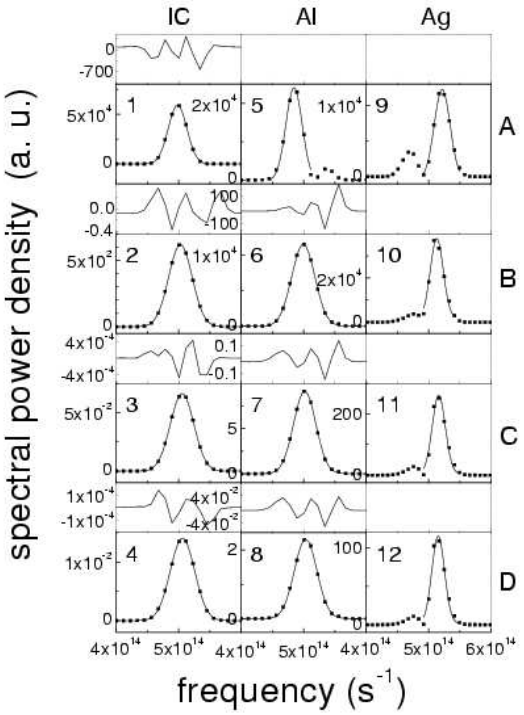

Power spectra obtained by fast Fourier transformation of the pulse shapes in the aperture of several tips with different coating materials and different tip angles. Abbreviations as before: (A) 43.1° (B) 37.2° (C) 31.0° (D) 28.5°.

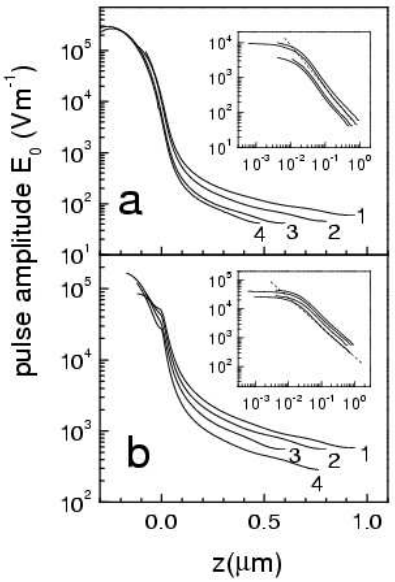

Amplitudes $E_{y,0}$ of the femtosecond light pulses on the axis of the near-field optical probe for four different tip angles (1: 43.1°, 2: 37.2°, 3: 31.0°, 4: 28.5°) and two different coatings: (a): ideally conducting coating, (b): aluminum coating. Inserts: Same as main graphs, but plotted on a double- logarithmic scale. The aperture is located at z=0.

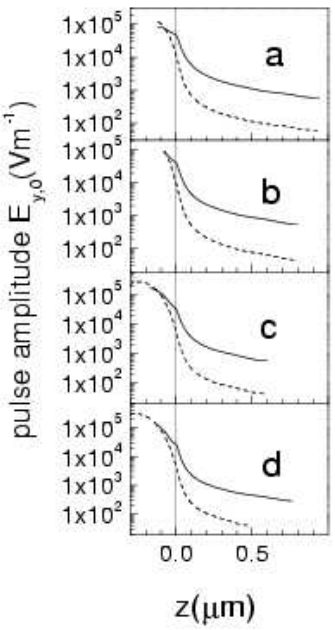

Amplitudes $E_{y,0}$ of the femtosecond light pulses on the axis of the tip as a function of the distance from the aperture and of the tip angle. Same data as in fig. 7, but plotted in a different way in order to facilitate comparison of the transmission behavior of ideally conducting (dashed lines) and real metallic coatings (solid lines).

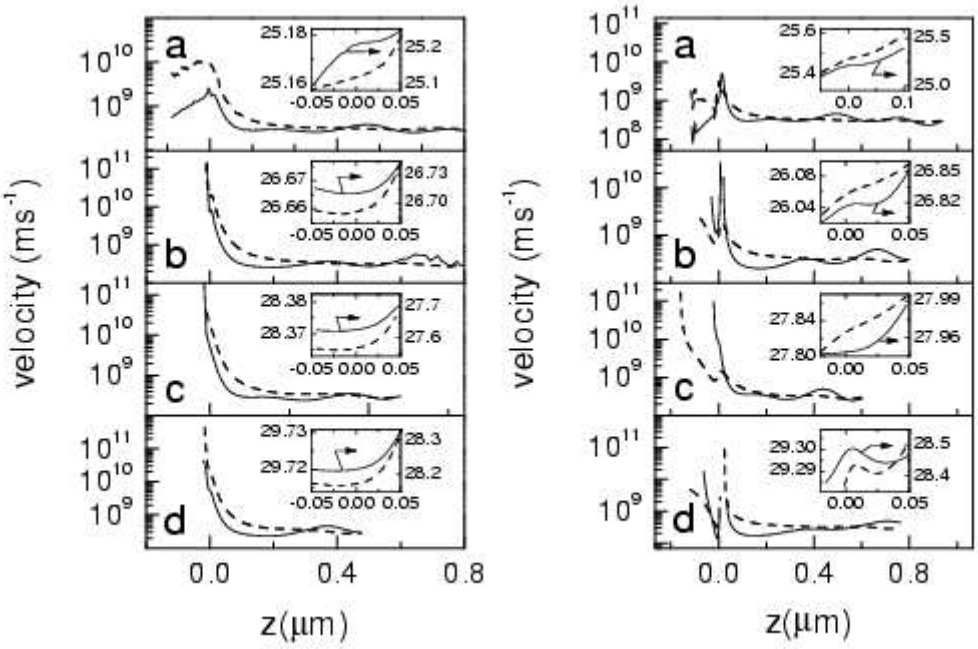

Phase (dashed lines) and group velocities (solid lines) for different tip angles (a: 43.1°, b: 37.2°, c: 31.0°, d: 28.5°). Figure on the left: data for a tip with an ideally conducting coating, Figure on the right: data for an aluminum coated tip. The inserts display the quantities, in femtoseconds, from which the velocities are derived, i.e. the arrival time of the pulse maximum (t_0, compare eq. (1), solid lines) and the phase time of the fit function (t_p dashed lines), in femtoseconds, respectively.

Funding: Project 'Spectroscopy of Plasmons', supported by Deutsche Forschungsgemeinschaft
Related publications in 2002:

A. Pack, M. Hietschold, R. Wannemacher
Propagation of Femtosecond Light Pulses through Near-Field Optical Aperture Probes
Ultramicroscopy 92, 251 (2002)

10.8 Interaction of Semiconductor Nanodots with Microcavities: Mode identification in spherical microcavities doped with quantum dots

B. Möller, M. V. Artemyev, U. Woggon, R. Wannemacher

Using imaging spectroscopy at the diffraction limit, a polarization-sensitive mode mapping allows the experimental identification of transverse electric and transverse magnetic modes for spherical microcavities. The method is applied to microspheres surface covered by CdSe quantum dots. A theoretical estimate of the minimum mode volume excited by a single, anisotropic quantum dot is given with Q/V larger than 1000 mm23 for the parameters of the experimentally studied microcavities.

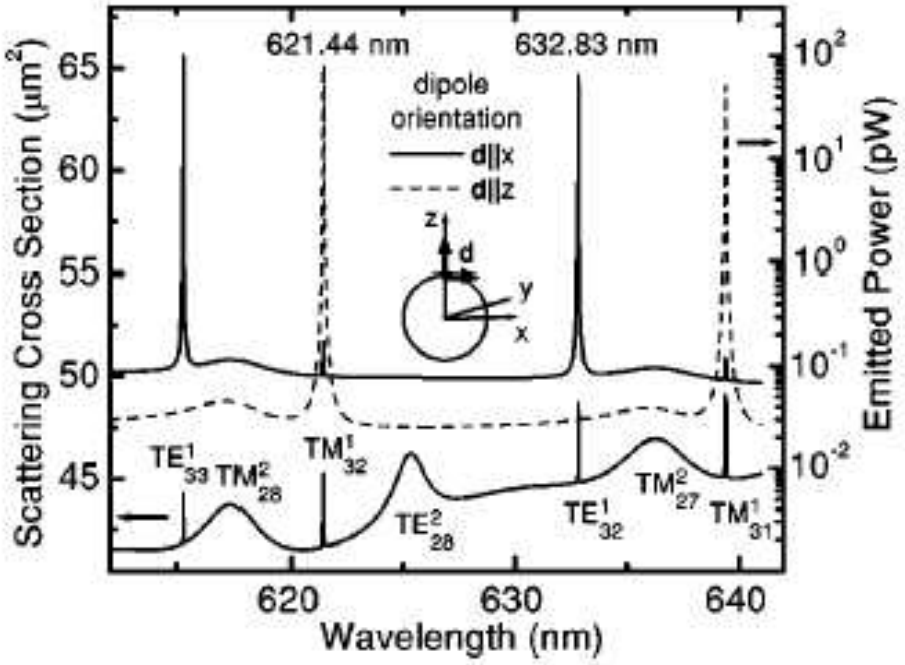

FIG. 1. Scattering spectrum of a microsphere calculated via standard Mie theory for the case of excitation by a plane wave (left-hand side scale, lowest curve) and, calculated by use of the semianalytical MMP method, for the case of excitation by a single dipole with two different orientations (right-hand side scale, logarithmic). The dipole of a strength of $|d|=1$ Debye was positioned at $z=2.3$ μm in a sphere of radius $R=2.5$ μm and refraction index $n=1.5$.

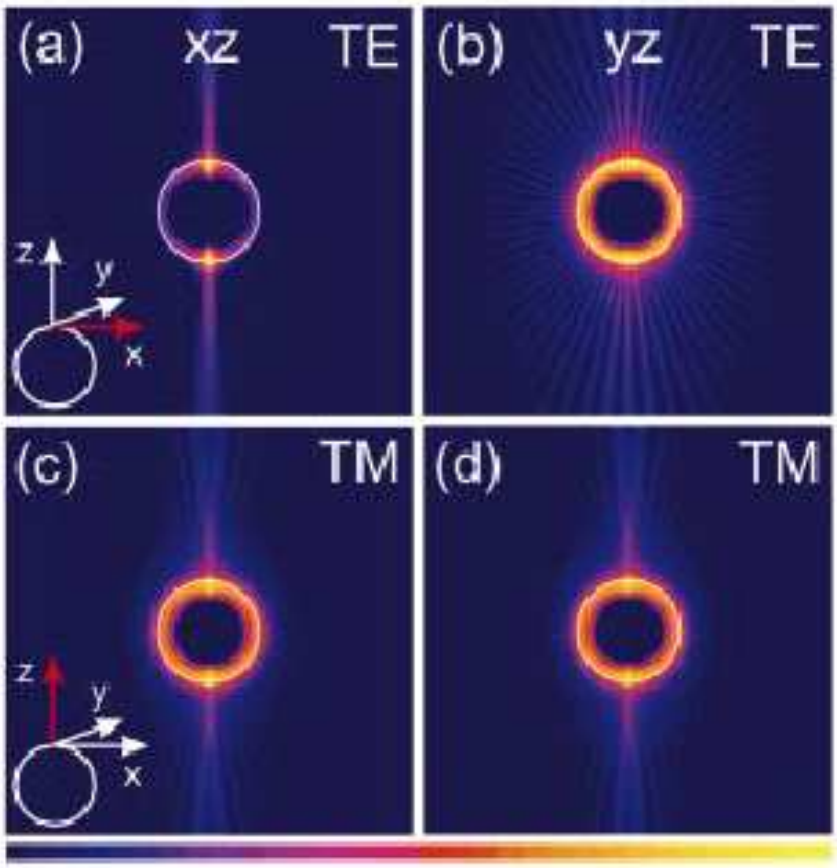

FIG. 2. (Color) Calculated electromagnetic field intensity (E^2) in and outside a spherical microcavity (same parameter as in Fig. 1). The dipole emission is chosen to be resonant either to the TM^1_{32}-mode ($\lambda = 621.44$ nm) or to the TE^1_{32}-mode ($\lambda = 632.83$ nm). Plotted is the intensity in the xz- (a), (c) and yz planes (b), (d) for the dipole oscillating in the x direction (a), (b), and z direction (c), (d), respectively. Each plot represents an area of 20 μm $\times$20 μm. The logarithmic intensity scale covers 60 dB.

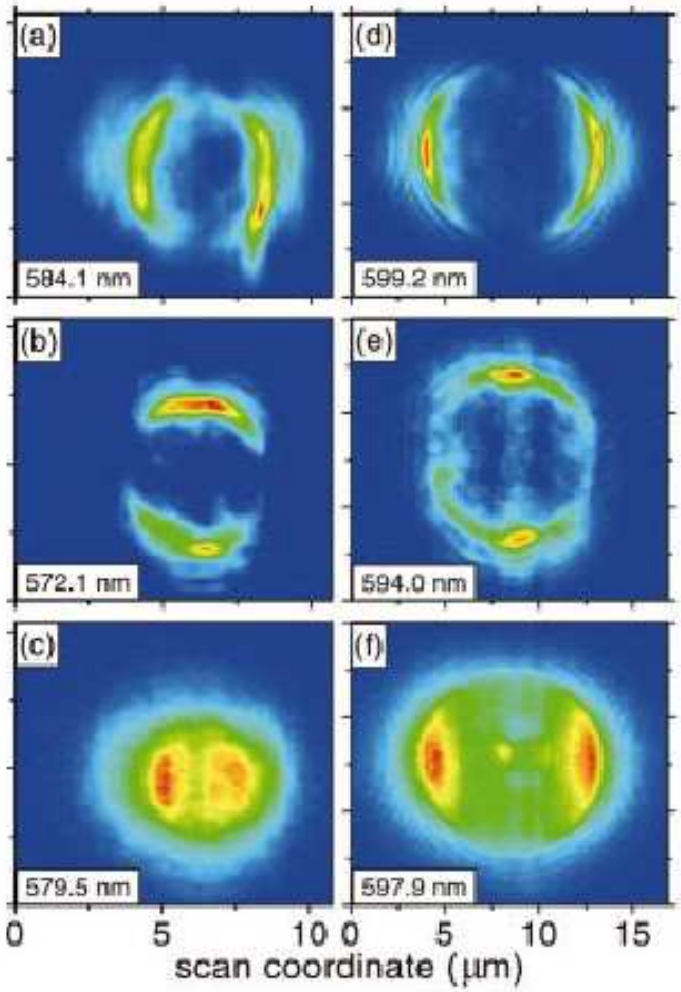

FIG. 4. (Color) Mapping of the emission intensity for two glass microspheres of $R=1.8$ μm (left-hand side) and $R=4$ μm (right-hand side) surface impregnated with CdSe QDs ($R_{QD}\approx 2.5$ nm). The two-dimensional intensity scans are performed at the spectral positions indicated by arrows in Figs. 3 and 5, respectively. In the detection beam, a polarizer is inserted (aligned parallel to the z axis) ensuring polarization-sensitive detection of all emitters with field vectors parallel to the polarizer direction. Small sphere: (a) TE^1_{22}-mode at 584.1 nm, (b) TM^1_{22} mode at 572.1 nm, and (c) background at 579.5 nm. Large sphere: (d) cavity mode at 599.2 nm, (e) cavity mode at 594.0 nm, and (f) background at 597.9 nm. The optical axis is perpendicular to the scan coordinate.

10.9 Phonons, band gaps, and higher-energy interband transitions in group-III nitrides

A. Kasic, M. Schubert

The dielectric functions of binary, ternary, and quaternary group-III nitride compound semiconductors are explored comprehensively from the mid-IR to the vacuum-UV spectral range by ellipsometry. The analysis of the dielectric function leads to the determination of fundamental material quantities, such as lattice phonon mode parameters, free-carrier properties, and interband transition energies. Influences of film strain and composition on frequencies of IR-active phonons can be separated. Information on the crystalline quality and compositional homogeneity of the material are extracted from phonon mode broadening parameters. Longitudinal-optical phonon-plasmon coupling effects are quantified and allow the determination of the free-carrier concentration and mobility, or alternatively of the effective carrier mass. The composition dependences of the energies of the fundamental band gap and of higher-energy interband transitions are obtained and effects of film strain and free-carrier concentration on the transition energies are analyzed.

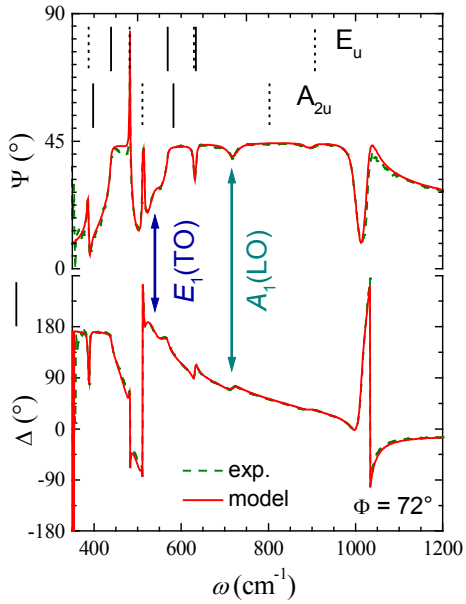

Figure 1: Infrared Ellipsometry spectra of an $In_{0.15}Ga_{0.85}N$ thin film deposited on (0001)Al_2O_3. Vertical arrows indicate the spectral position of the $In_{0.15}Ga_{0.85}N$ phonon modes.

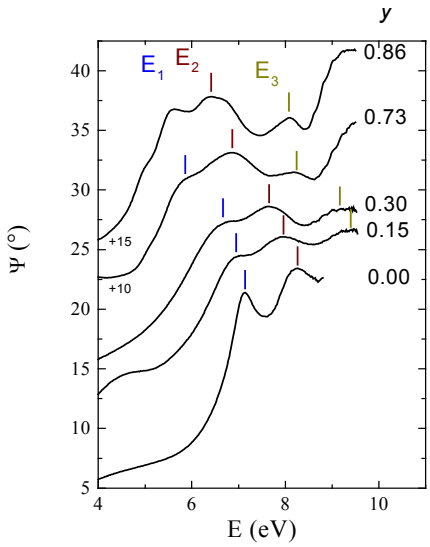

Figure 2: Deep-UV Ellipsometry spectra of $In_yGa_{1-y}N$ thin films. Vertical bars indicate the spectral position of the higher-energy direct band-to-band transitions.

Research supported by DFG Rh 28/3-2

Related publications in 2002: (www.uni-leipzig.de/~hlp/ellipsometrie)

A. Kasic, PhD thesis, University of Leipzig, 2002; M. Schubert, Habil. Thesis, University of Leipzig, 2002; phys. stat. sol. 234, 970 (2002); Rev. B 65, 184302 (2002); Vibrational Spectroscopy 179, 121 (2002); Phys. Rev. B 65, 115206 (2002); Proc. SPIE Vol. 4806, 264 (2002).

10.10 Critical-Point Transitions in $B_xGa_{1-x}As$ and GaN_yAs_{1-y}

G. Leibiger[1], V. Gottschalch[1] and M. Schubert

GaN_yAs_{1-y} alloys have attracted wide interest in the past few years due to their interesting electronic properties and possible device applications, e. g., for 1.3-1.55 µm laser diodes. $B_xGa_{1-x}As$ is a novel material system of fundamental interest, which offers new possibilities in semiconductor-band-gap engineering and, in addition, for optoelectronic devices, such as solar cells [1]. In both alloys, GaAs-host atoms are replaced by much smaller atoms (i. e. B and N for Ga and As, respectively) leading to considerable tensile strain within the ternary layers grown on GaAs. However, as shown in Fig. 1, the influence of B and N on the electronic bandstructure of the GaAs-host lattice is quite different. In GaN_yAs_{1-y}, the electronic states of the host lattice are heavily perturbed by the nitrogen atoms, resulting in a rapid decrease of the band-gap energy with increasing y [2]. This is in contrast to the usual trends within III-V-compound semiconductors, considering that the band-gap energy of cubic GaN is about 3.2 eV. On the other hand, the incorporation of B in GaAs results only in a slight change of all transition energies observed, including the band-gap energy E_0. These results can be understood considering the different nature of the chemical bonds in both alloys. Whereas the Ga-N bonding has a large ionic contribution (ionicity of 0.5 on the Phillips-scale), the B-As bonding is almost purely covalent (ionicity of 0.002 on the Phillips-scale).

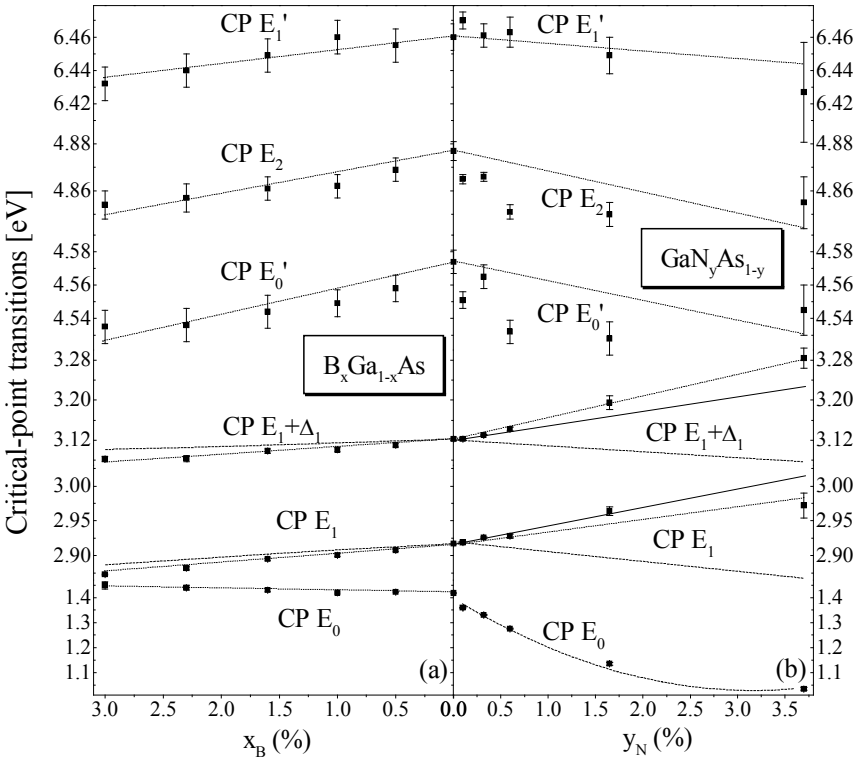

Fig. 1: Critical-point energies (symbols) of direct band-to-band transitions in $B_xGa_{1-x}As$ (a) and GaN_yAs_{1-y} (b) derived by spectroscopic ellipsometry.

[1]Semiconductor-Chemistry Group, Universität Leipzig

Related publications: (www.uni-leipzig.de/~hlp/ellipsometrie)
J. Cryst. Growth 248, 468 (2003); J. Appl. Phys. 89, 4927 (2001). For GaPN see also Phys. Rev. B 65, 245207 (2002).

10.11 Temperature-dependent evolution of bulk and interface polaritons in *n*-GaAs/*i*-GaAs layer structures

T. Hofmann, M. Schubert

The infrared optical response of polar semiconductor layer structures is strongly influenced by resonant excitation of phonon- and plasmon-supported bulk and interface modes (surface polaritons: *SP*, surface guided waves: *SGW*). For *SP* and *SGW* modes electromagnetic radiation is mediated parallel to the interfaces of layer structures. Precise information on semiconductor phonon and plasmon mode parameters can be obtained from measurement and model analysis of the frequency-dependent sample response by ellipsometry. A variable angle-of-incidence (Φ) "rotating-polarizer-sample-rotating-analyzer" configuration far-infrared ellipsometer was built at our laboratory. A sample holder within a magnetocryostat (available magnetizing field strengths of ±6Tesla at the sample and 4K … 293K sample temperature) was attached to the system (Figure 1). The first step was determination of the temperature dependence of bulk-, *SP*-, and *SGW*-mode excitation in *n*-GaAs/*i*-GaAs layer structures (Figure 2). The GaAs TO and LO modes (bulk) are red-shifted (lattice expansion), and so are the *SP* and *SGW* modes. The low-frequency *SGW* mode rises as sharp resonance due to the increase of the free carrier momentum relaxation time (decrease in plasmon broadening), and decrease of the bulk mode broadening. This experiment provides insight into free-charge-carrier properties of semiconductor layer structures.

Figure 1: Far infrared ellipsometer at our laboratory with magnetocryostat (Oxford) attached.

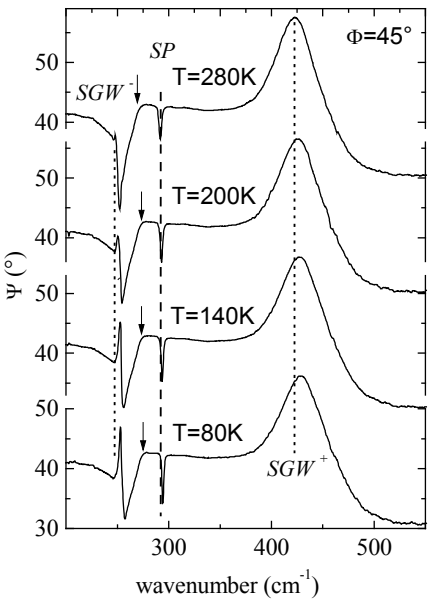

Figure 2: Ψ-spectra from a ~600nm thick undoped (*i*) GaAs buffer layer on *n*-type (*n*) GaAs. Arrows indicate ω_{TO}(GaAs).

Research supported by NSF-DMI 9901510
Special acknowledgement: M. Ziese, P. D. Esquinazi (SUM)
Related publications in 2002: (www.uni-leipzig.de/~hlp/ellipsometrie)

10.12 Far-infrared Magneto-Optic Generalized Ellipsometry: Properties of free-carriers in *n*-type $Al_{0.19}Ga_{0.33}In_{0.48}P$

T. Hofmann, M. Schubert, I. Pietzonka[1]

We demonstrate determination of the free-carrier properties in thin film heterostructures, in particular, for MOCVD-grown *n*-GaAs:Te/*n*-AlGaInP:Te/*i*-GaAs. AlGaInP is the working-horse material for today's high-efficiency LED market. The physical properties of this material can be influenced by alloying, lattice-mismatch-induced strain and atomic ordering. So far, only one report on the effective mass value for AlGaInP exists, and no attention was paid to the degree of ordering, which potentially influences the effective mass value. The heterostructure investigated here consists of a nominally 1900 nm thick Te-doped, *n*-type $Al_{0.19}Ga_{0.33}In_{0.48}P$ layer deposited by MOVPE on an undoped (001) GaAs substrate / buffer layer sequence. The AlGaInP layer is capped by a 70 nm Te-doped GaAs layer. The highly disordered state of the AlGaInP layer was determined from the zero-magnetic-field ellipsometry experiment. Data at high external magnetic fields (Fig. 2) provided the effective mass value for the AlInP layer of $m^* = 0.12m_e$ upon modelling the observed free-charge-carrier induced magneto-optic birefringence, without additional electrical measurements, and by differentiating the effects from all other sample constituents appropriately.

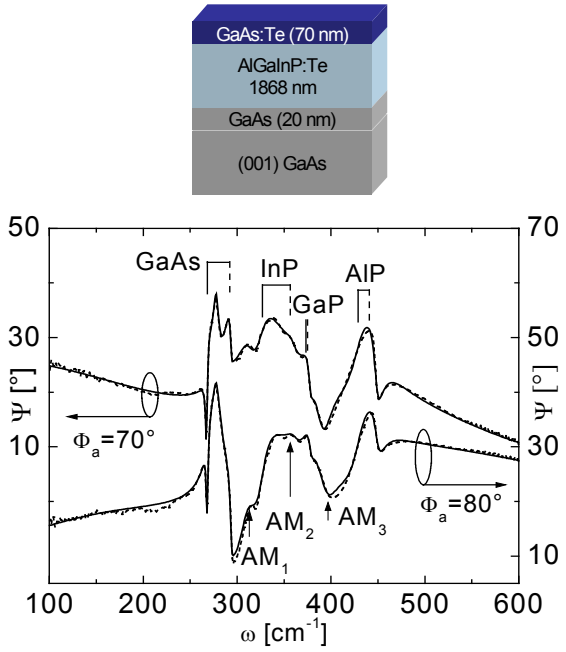

Figure 1. Far-infrared-ellipsometry spectra measured at two different angles of incidence Φ_a on the sample shown above.

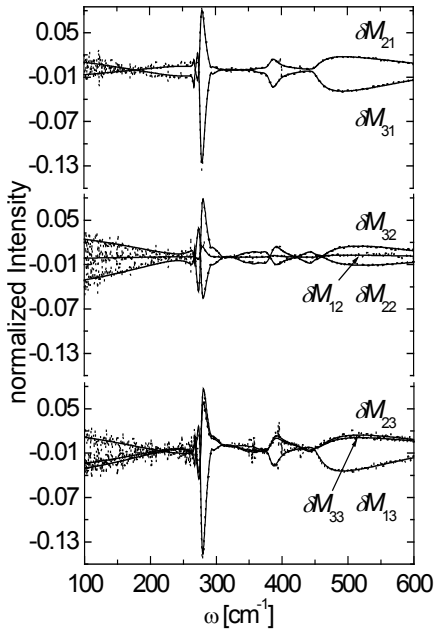

Figure 2. Differences between normalized Mueller matrix spectra taken at $\mu_0 H$ = -2.1T, and $\mu_0 H$ = +2.1T.

[1]Osram Opto Semiconductors, Regensburg; Research supported by NSF-DMI 9901510

Related publications in 2001/02 (www.uni-leipzig.de/~hlp/ellipsometrie)
Proc. SPIE Vol. 4779, 90 (2002); Phys. Rev. B 66, 195204 (2002); Phys. Rev. B 64, 155206 (2001).

10.13 Local vibrational modes in ZnO:(Fe,Sb,Ga,Li) thin films

C. Bundesmann, V. Riede, M. Schubert

ZnO and related compounds are highly ranking materials for next-generation short-wavelength optoelectronic applications, such as solar-blind detectors. Besides incorporation of nitrogen, many pathways are followed to achieve sufficient hole conductivity. Raman spectroscopy provides fast and non-destructive means to study the effect of dopant incorporation, and identify defects and site locations, in conjunction with local mode calculations. Micro Raman measurements on Fe, Sb, Ga and Li doped ZnO thin films grown by pulsed laser deposition on *c*-plane sapphire substrates were performed for the first time. For Fe doped ZnO, additional modes were observed, which were not seen in pure ZnO, but some of which were recently assigned to N incorporation in pure ZnO. However, we find these modes also in Sb, and partly in Ga doped ZnO. We tentatively assign these modes due to host lattice defects, such as vacancies or interstitials. Li doped thin films did not reveal any of the additional modes.

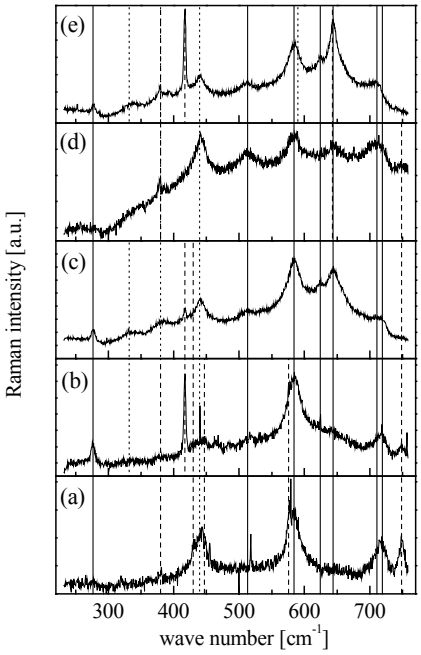

Figure 1: Micro-Raman spectra of ZnO:Fe/(0001)sapphire. The scattering geometries are *z*(*xy*)*z*′ (a), *z*(*xx*)*z*′ (b), *x*(*yy*)*x*′ (c), *x*(*yz*)*x*′ (d), and *x*(*zz*)*x*′ (d). Dotted and dashed lines are ZnO and sapphire modes, respectively. Solid lines indicate the wave numbers of the additional modes.

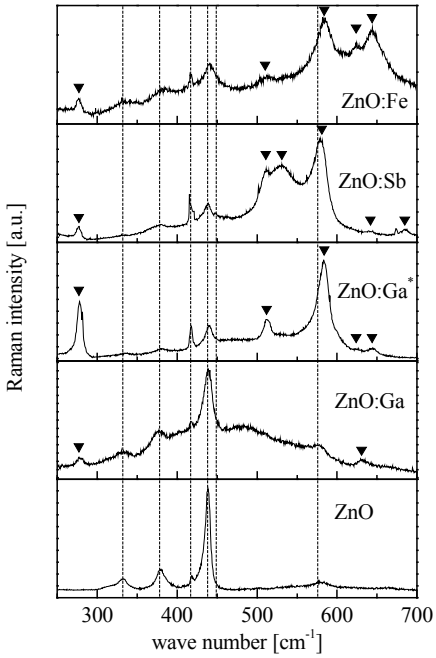

Figure 2: Micro-Raman spectra (z(yy)z′) for undoped, Ga, Sb, and Fe doped ZnO thin films grown in O_2 atmosphere. The ZnO:Ga* film is grown in N_2O atmosphere. ZnO and sapphire modes are indicated by vertical lines. Triangles indicate additional modes.

Research supported by BmbF (INNOCIS)
Related publications: (www.uni-leipzig.de/~hlp/ellipsometrie)
APL 81, 2376 (2002); JAP 93, 126 (2003).

10.14 ZnO band gap energies at elevated temperatures

N. Ashkenov, M. Schubert

A detailed knowledge of the influence of temperature on the fundamental band gap energies of semiconductors is of great importance for many applications in optoelectronic devices that are intended for operation within a large temperature interval. Likewise, knowledge of the dielectric function of materials at their growth temperatures is needed for real-time in-situ monitoring of thin film deposition using spectroscopic ellipsometry. A *c*-plane cut ZnO single crystal at temperatures between 300 K and 1154 K was studied by in-situ spectroscopic ellipsometry for photon energies from 1.25 eV to 3.335 eV. Lineshape analysis of the ZnO dielectric function, determined for polarization perpendicular to the wurtzite *c*-axis, is done using the one-electron interband transition model augmented by Lorentz-broadened excitonic lineshape functions. The strong red-shift of the wurtzite-type direct band gap $E_0^{A,B,C}$ transition energies due to lattice expansion upon increase of temperature is observed. The red-shift of the band gap transition energy can be well described by the empricial Varshni relation. Figure 1 presents the real (a) and imaginary parts (b) of the measured (symbols) and best-fit (solines) pseudodielectric function spectra, respectively. Figure 2 shows the temperature dependence of the $E_0^{A,B,C}$ transition energy values (symbols) along with the empirical Varshni model fit (lines).

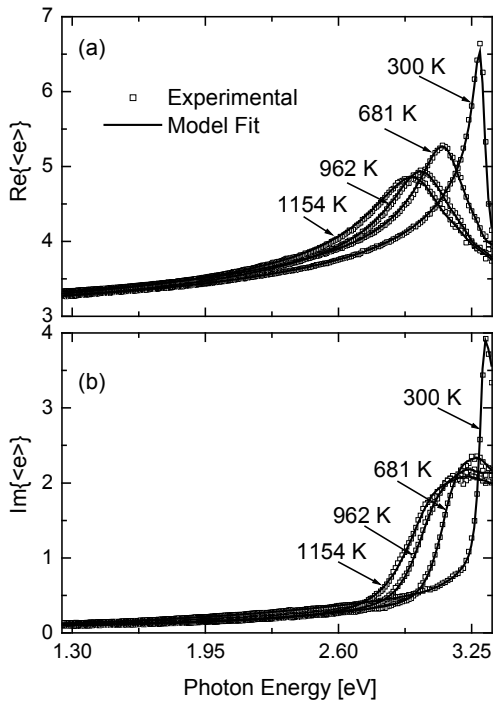

Fig.1: (a) Real and (b) imaginary parts of the pseudodielectric function of bulk ZnO at room and elevated temperatures.

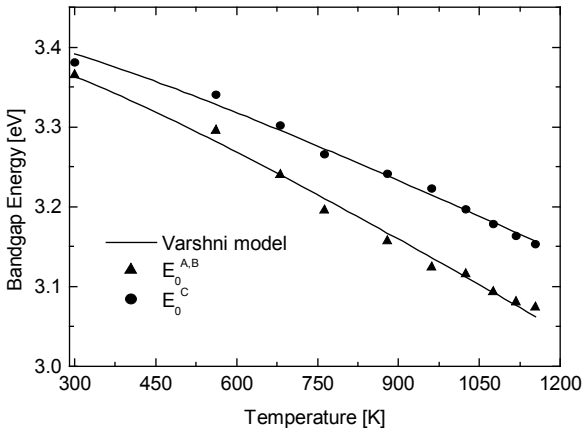

Fig. 2: Shift of the $E_0^{A,B,C}$ transition energies as a function of energy. Solid lines represent the best fit to the Varshni model.

Research supported by BmbF (INNOCIS)
Related publications: (www.uni-leipzig.de/~hlp/ellipsometrie)
J. Appl. Phys. 93, 126 (2003).

10.15 Generalized ellipsometry for orthorhombic absorbing materials: Dielectric functions, and band-to-band transitions of Sb_2S_3

M. Schubert, W. Dollase[1]

There are few, if any, complete and accurate sets of optical constants for biaxial (orthorhombic, monoclinic and triclinic) materials measured over a range of wavelengths. This situation has arisen because (i) most attention has been focused on simple, high-symmetry materials, and (ii) existing methods of measuring the larger number of optical constants of low-symmetry materials were much more difficult, requiring several different, precisely oriented samples, and (iii) no accurate rigorous method exists so far for monoclinic or triclinic absorbing materials. Ellipsometry is a powerful technique for exploration of optical constants. Generalized ellipsometry (GE) is the global extension to anisotropic materials. We report for the first time the three fundamental dielectric function spectra of Stibnite (orthorhombic) obtained by GE from near-infrared to ultra-violet wavelengths (Figure 1), using several, differently cut surfaces from mechanically polished single crystals. We obtain the infrared-active phonon modes, electronic band-to-band transitions, and optical constants data for polarizations along axes *a*, *b*, and *c*, most of which were previously unknown. Herewith we demonstrate the use of low-symmetry surfaces for the GE approach. We further demonstrate the capability of GE to determine the center-of-gravity system of absorbing orthorhombic materials.

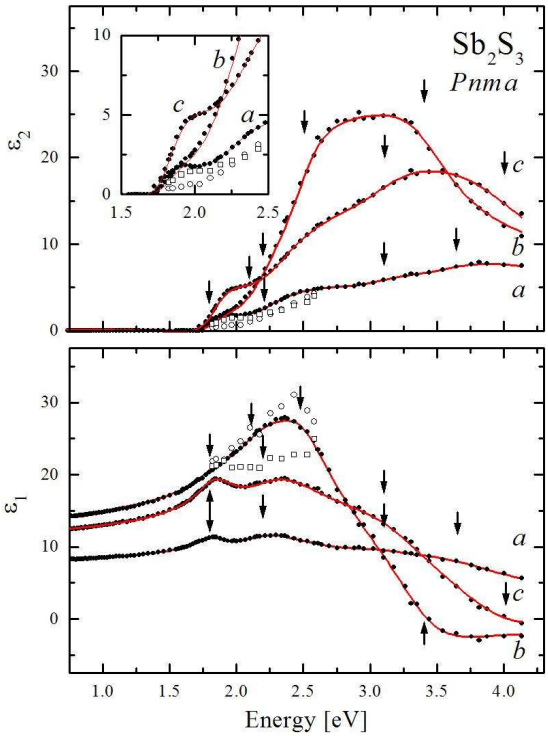

Figure 1. Real (ε_1) and imaginary part (ε_2) of the fundamental dielectric functions of stibnite for polarizations along crystallographic axes *a*, *b*, and *c*, for near-infrared to ultra violet wavelengths. Solid symbols indicate data obtained by the wavelength-by-wavelength inversion approach. Solid lines present best-fit lineshapes using a model dielectric function approach. Vertical arrows indicate identified band-to-band transition energy parameters. The inset enlarges the region of the fundamental band-to-band transitions. Open symbols are data reproduced from Tyndall [Phys. Rev. 21, 162 (1923)] and Drude [Ann. Phys. 34, 489 (1888)].

[1]Department of Earth and Space Sciences, University of California Los Angeles, USA
Research supported by CMOMR, U.S.A.

Related publications in 2002: (www.uni-leipzig.de/~hlp/ellipsometrie)
Opt. Lett. **27**, 2073 (2002); Proc. SPIE Vol. **4806**, 264 (2002).

10.16 Infrared ellipsometry characterization of conducting organic films

M. Schubert, C. Bundesmann, G. Jakopic[1], H. Arwin[2], N.-C. Persson[2], F. Zhang[2], O. Inganäs[2]

Nondestructive determination of conductivity, carrier distribution, and structural properties of individual layers in complex layer structures is a challenge. We report on the optical characterization of conducting organic layers using Infrared Spectroscopic Ellipsometry (IRSE). The in-plane infrared dielectric function of pentacene thin films, deposited by molecular beam epitaxy onto glass substrates, is determined. We find that the pentacene films are optically uniaxial with the optical axis perpendicular to the surface. Frequency, amplitude and broadening parameters of 27 infrared active modes with in-plane polarization component are quantified, consistently for all samples. We have further studied conducting polymer layers (PEDOT:PSS), for which we quantify the dielectric function and 30 characteristic infrared resonance modes. We observe free charge carrier accumulation at the interface between the PEDOT:PSS / Si substrates, tentatively assigned as the result of interface dipole formation. We also study polyfluorene and fullerene layers, and heterostructures thereof. We obtain information on the individual layer thickness and their conductivity behavior, and propose IRSE as useful technique for monitoring of organic device heterostructure properties.

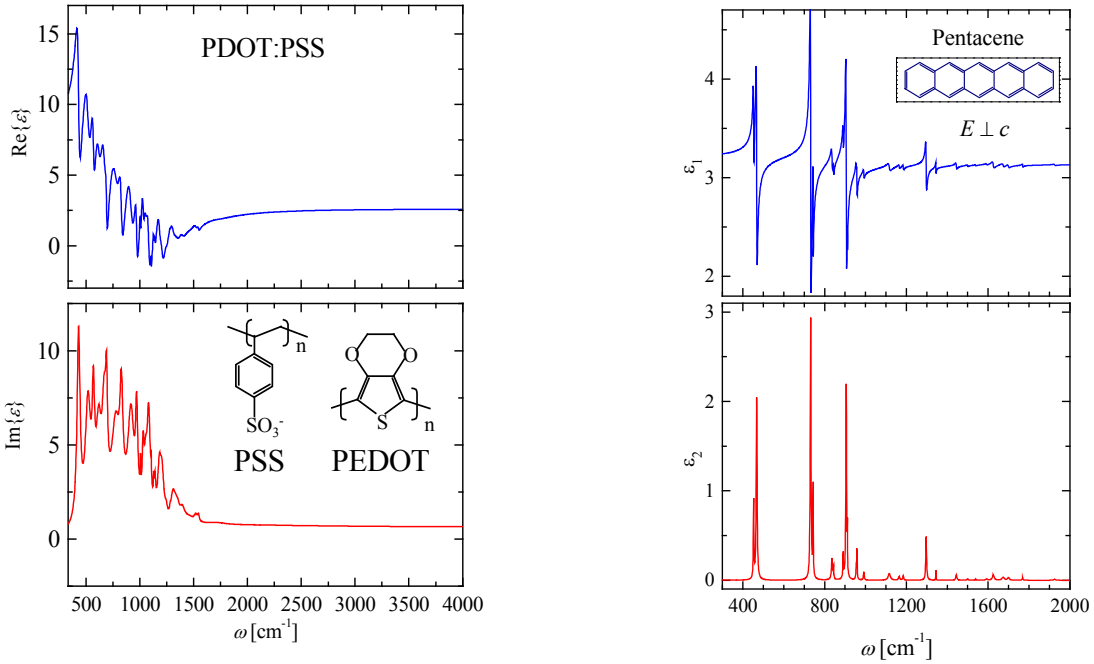

Infrared dielectric function within the "fingerprint" region of carrier-depleted PDOT:PSS (a) and pentacene thin films on glass (b; in-plane response) obtained from multiple-sample analysis.

[1]JOANNEUM Research, Graz, Austria, [2]Department of Physics and Technology, Linköping University, Sweden. Research supported by JOANNEUM and The Swedish Foundation for International Cooperation in Research and Higher Education (STINT).
(www.uni-leipzig.de/~hlp/ellipsometrie)

10.17 Funding

Space Microscope
W. Grill, R. Wannemacher
ESA / ESTEC

Spectroscopy of Plasmons
Ch. v. Borczyskowski, R. Wannemacher, W. Grill
DFG, Bo 935 / 15-1

Research and Development Contract
W. Grill, Z. Kojro
SCHOTT Glas

Research and Development Contract
W. Grill
Heidelberger Druckmaschinen AG

Verallgemeinerte Infarot-Ellipsometrie von Kristallstruktur- und Ladunsgträgereffekten in komplexen Heterostrukturen von Gruppe-III-Nitride
Generalized Infrared Ellipsometry of free-carrier and crystal-structure effects in complex group-III-nitride heterostructures
M. Schubert, B. Rheinländer
Deutsche Forschungsgemeinschaft, Rh 28/3-2

In situ Prozessanalytik mit Hilfe der Ramanstreuung und der spektroskopischen Ellipsometrie für die Kontrolle und Optimierung der optischen Eigenschaften von $Cu(In,Ga)(Se,S)_2$ Dünnschicht-Solarzellen
In-situ-Ramanscattering and in-situ-Ellipsometry of flexible Cu-(In,Ga)-(Se,S)-thin-film solar cells
M. Schubert
Bundesministerium für Bildung und Forschung im Wachstumskern INNOCIS

Bestimmung der Infrarot-dielektrischen Funktion und der Eigenschaften Freier Ladungsträger in organischen Halbleiterdünnschichten
Free-carrier properties and infrared dielectric functions of organic semiconductor layers
M. Schubert
JOANNEUM Research Forschungsgesellschaft mbH, Graz, Österreich

10.18 External Cooperations

Universities and Research Institutes
ACCESS e. V. , Aachen (Ultrasound Monitoring of Solidification Processes)
Fraunhofer Institute for Mechanics of Materials, Halle (Thin Films)
North-Carolina State University, U.S.A., University of California Santa Barbara, U.S.A., Research Center Rossendorf (Focussed Ion Beam Modification of Materials)
Ritsumeikan University, Japan, Universities Bremen, Stuttgart, Magdeburg, Paderborn, and Technical University München (WSI) (group-III Nitrides)
University of California Los Angeles, U.S.A. (low-symmetry optical materials)
University of Dortmund (Nanooptics)
University of Erlangen (Zeolites)
University of Konstanz (Laser Cleaning, Total Internal Reflection Microscopy)
University of Linkoping, Schweden (Organic and inorganic semiconductors)
University of Nebraska-Lincoln, U.S.A. (Infrared spectroscopic Ellipsometry)
University of Technology, Wroclaw, Poland (Ultrasound)
University of the Witwatersrand, Johannesburg, South Africa (Theory of Ultrasound)

Companies (Technology Transfer)
Advanced Acoustix GmbH, Leipzig (ultrasound technology)
Tricat GmbH, Bitterfeld (ultrasound monitoring of zeolite synthesis)
Astrium GmbH, München (ultrasound technology)
Heidelberger Druckmaschinen, Heidelberg (ultrasound sensors and monitoring)
Schott Glas, Mainz (ultrasound sensing)
Solarion GmbH, Leipzig (solar cells)
Honeywell GmbH, Glinde (ultrasound monitoring)
Solarion GmbH, Leipzig (In-situ optical process control of solar cells on flexible substrates)
Joanneum Research mbH, Graz, Austria (free-carrier properties of conducting organic polymers and organic semiconductors)

10.19 Publications

10.19.1 Journals

Scanning acoustic Doppler microscopy and scanning acoustic correlation microscopy
Z. Kojro, J. Jahny, T.-J. Kim, J. Ndop, M. Schmachtl, W. Grill.
J. Ultrasonics 40, 67 (2002).

Propagation of Femtosecond Light Pulses through Near-Field Optical Aperture Probes
A. Pack, M. Hietschold, R. Wannemacher
Ultramicroscopy 92, 251 (2002)

Mode identification in spherical microcavities doped with quantum dots
B. Möller, M.V. Artemyev, U. Woggon, R. Wannemacher,
Appl. Phys. Lett. 80, 3253 (2002)

Optical phonons in hexagonal $Al_xIn_yGa_{1-x-y}N$ ($y \sim 0.12$)
A. Kasic, M. Schubert, J. Off, F. Scholz, S. Einfeldt, D. Hommel
phys. stat. sol. 234, 970 (2002)

Far-infrared dielectric anisotropy and phonon modes in spontaneously CuPt ordered $Ga_{0.52}In_{0.48}P$
T. Hofmann, V. Gottschalch, M. Schubert
Phys. Rev. B 66, 195204 (2002)

Generalized ellipsometry for biaxial absorbing materials: determination of crystal orientation and optical constants of Sb_2S_3
M. Schubert, W. Dollase
Opt. Lett. 27, 2073 (2002)

Infrared dielectric functions and phonon modes of wurtzite $Mg_xZn_{1-x}O$ ($x <= 0.2$)
C. Bundesmann, M. Schubert, D. Spemann, T. Butz, M. Lorenz, E. M. Kaidashev, M. Grundmann, N. Ashkenov, H. Neumann, G. Wagner
Appl. Phys. Lett. 81, 2376 (2002)

Far-infrared Magneto-Optical Generalized Ellipsometry determination of free-carrier parameters in semiconductor thin film structures
T. Hofmann, M. Schubert, C. M. Herzinger
Proc. SPIE Vol. 4779, 90 (2002)

Evolution of the optical properties of III-V Nitride alloys: Band-to-Band transitions in GaPN
G. Leibiger, M. Schubert, V. Gottschalch, G. Benndorf, R. Schwabe
Phys. Rev. B 65, 245207 (2002)

Generalized ellipsometry of complex mediums in layered systems
M. Schubert, A. Kasic, T. Hofmann, V. Gottschalch, J. Off, F. Scholz, E. Schubert, H. Neumann, I. Hodgkinson, M. Arnold, W. Dollase, C. M. Herzinger
Proc. SPIE Vol. 4806, 264 (2002)

Optical phonon modes and interband transitions in cubic AlGaN
A. Kasic, M. Schubert, T. Frey, U. Köhler, D. J. As, C. M. Herzinger
Phys. Rev. B 65, 184302 (2002)

Low-orbit-environment protective coating for all-solid-state electrochromic surface heat radiation control devices
E. Franke, H. Neumann, M. Schubert, C. L. Trimble, J. A. Woollam
Surf. Coat. & Techn. 151-152, 285 (2002)

Infrared spectroscopic ellipsometry - a new tool for characterization of semiconductor heterostructures
A. Kasic, M. Schubert, S. Einfeldt, D. Hommel
Vibrational Spectroscopy 179, 121 (2002)

Effective carrier mass and phonon mode behavior in n-type hexagonal InN
A. Kasic, M. Schubert, Y. Saito, Y. Nanishi, G. Wagner
Phys. Rev. B 65, 115206 (2002)

Interband transitions in [001]-$(GaP)_1(InP)_m$ superlattices
M. Schubert, H. Schmidt, J. Šik, T. Hofmann, V. Gottschalch, W. Grill, G. Böhm, G. Wagner
Mat. Sci. & Eng. B 88, 125 (2002)

Interband transitions and phonon modes in GaB_xAs_{1-x} ($0 \leq x < 0.33$) and GaN_xAs_{1-x} ($0 \leq x < 0.29$)
G. Leibiger, V. Gottschalch, V. Riede, M. Schubert, J. N. Hilfiger, T. E. Tiwald
Phys. Rev. B (in press)

Optical properties of ternary MgZnO thin films
R. Schmidt, C. Bundesmann, N. Ashkenov, B. Rheinländer, M. Schubert, M. Lorenz, E. M. Kaidashev, D. Spemann, T. Butz, J. Lenzner, M. Grundmann
Proceedings of the International Conference on the Physics of Semiconductors (ICPS) 2003 (in press)

Far-infrared magneto-optical generalized ellipsometry determination of free-carrier parameters in semiconductor thin film structures
T. Hofmann, M. Grundmann, C. M. Herzinger, M. Schubert, W. Grill
Mat. Res. Soc. Symp. 744, M5.32.1 (2003)

Far-infrared dielectric functions and phonon modes of spontaneously ordered AlGaInP
T. Hofmann, V. Gottschalch, M. Schubert
Mat. Res. Soc. Symp. 744, M5.33.1 (2003)

Far-infrared-magneto-optic Ellipsometry characterization of free-charge-carrier properties in highly-disordered n-type $Al_{0.19}Ga_{0.33}In_{0.48}P$
T. Hofmann, M. Schubert, C. M. Herzinger, I. Pietzonka
Appl. Phys. Lett. (in press)

Residual strain in HVPE GaN free-standing and re-grown homoepitaxial layers
V. Darakchieva, T. Paskova, P.P. Paskov, B. Monemar, N. Ashkenov, M. Schubert
phys. stat. sol. (a) 195, 516 (2003)

Dielectric functions (1 eV to 5 eV) of wurtzite $Mg_xZn_{1-x}O$ ($0 \leq x < 0.29$) thin films
R. Schmidt, B. Rheinländer, M. Schubert, D. Spemann, T. Butz, J. Lenzner, E. M. Kaidashev, M. Lorenz, M. Grundmann
Appl. Phys. Lett. (in press)

Infrared dielectric functions and phonon modes of high-quality ZnO films
N. Ashkenov, G. Wagner, H. Neumann, B. N. Mbenkum, C. Bundesmann, V. Riede, M. Lorenz, E. M. Kaidashev, A. Kasic, M. Schubert, M. Grundmann, V. Darakchieva, H. Arwin, B. Monemar
J. Appl. Phys. 93, 126 (2003)

Generalized far-infrared magneto-optic ellipsometry for semiconductor layer structures: Determination of free-carrier effective mass, mobility and concentration parameters in n-type GaAs
M. Schubert, T. Hofmann, C. M. Herzinger
J. Opt. Soc. Am. A 20, 347 (2003)

High electron mobility of epitaxial ZnO thin films on *c*-plane sapphire grown by multi-step pulsed laser deposition
E. M. Kaidashev, M. Lorenz , H. von Wenckstern, G. Benndorf, A. Rahm, H.-C. Semmelhack, K.-H. Han, H. Hochmuth, C. Bundesmann, M. Grundmann
Appl. Phys. Lett. (in press)

10.19.2 Invited talks

Generalized ellipsometry of complex mediums in layered systems
M. Schubert
47. Annual SPIE Meeting, Seattle, U.S.A., July 2002

Spectroscopic Ellipsometry of phonon-plasmon-polaritons in III-V-Nitride compound heterostructures
M. Schubert, A. Kasic, G. Leibiger, T. Hofmann, C. M. Herzinger, J. A. Woollam
47. Annual SPIE Meeting, Seattle, U.S.A., July 2002

Generalized Infrared Ellipsometry and polaritons in III-V semiconductor heterostructures
M. Schubert, A. Kasic, G. Leibiger, T. Hofmann
2. Workshop Ellipsometrie des Arbeitskreises Ellipsometrie, Berlin, Februar 2002

10.20 Conference contributions

(T: talk, otherwise poster)

Critical points and phonons in (B,Ga)(N,As) (T)
G. Leibiger, V. Gottschalch, G. Benndorf, V. Riede, M. Schubert
Physics and Technology of Dilute Nitrides for Optical Communications, Istanbul, Türkei, September 2002

Phonons, excitons, band-to-band transitions and optical constants of MgZnO (T)
R. Schmidt, C. Bundesmann, N. Ashkenov, B. Rheinländer, M. Schubert, M. Lorenz, E. M. Kaidashev, D. Spemann, T. Butz, G. Wagner, H.v. Wenckstern, M. Grundmann, C. M. Herzinger

Materials Research Society Fall Meeting, Boston, U.S.A, Dezember 2002

Far-infrared magneto-optic generalized ellipsometry determination of free-carrier parameters in semiconductor thin film structures (T)
T. Hofmann, C. M. Herzinger, M. Schubert
47. Annual SPIE Meeting, Seattle, U.S.A., July 2002

Magneto-optische Ferninfrarot-Spektralellipsometrie: Bestimmung freier Ladungsträger Parameter in Halbleiterheterostrukturen (T)
T. Hofmann, M. Schubert, C. M. Herzinger
German Physical Society Spring Meeting, Regensburg, March 2002

Phonon-modes and free-carrier-properties of Al- and Ga-doped ZnO and (ZnCdMg)O thin films (T)
N. Ashkenov, C. Bundesmann, A. Kasic, B. N. Mbenkum, M. Schubert, M. Lorenz, E. M. Kaidashev, M. Grundmann
German Physical Society Spring Meeting, Regensburg, March 2002

Structural, optical, and electrical properties of epitaxial (Mg, Cd)$_x$Zn$_{1-x}$O, ZnO, and ZnO:(Ga, Al) thin films on sapphire grown by pulsed laser deposition (T)
M. Lorenz, E. M. Kaidashev, H. von Wenckstern, V. Riede, C. Bundesmann, D. Spemann, G. Benndorf, H. Hochmuth, A. Rahm, H.-C. Semmelhack, M. Schubert, M. Grundmann
2002 MRS Workshop Series: 2nd International Workshop on Zinc Oxide, Dayton, USA, October 2002

Electrical properties of ZnO:(Ga, Al, Cd) thin films on *c*- and *r*-plane sapphire substrates and of ZnO single crystals (T)
H. von Wenckstern, R. Pickenhain, G. Biehne, M. Lorenz, E. M. Kaidashev, C. Bundesmann, M. Schubert, M. Grundmann
2002 MRS Workshop Series: 2nd International Workshop on Zinc Oxide, Dayton, USA, October 2002

Optical and electrical properties of epitaxial (Mg, Cd)$_x$Zn$_{1-x}$O, ZnO, and ZnO:(Ga, Al) thin films on *c*-plane sapphire grown by pulsed laser deposition (T)
M. Lorenz, E. M. Kaidashev, H. von Wenckstern, V. Riede, C. Bundesmann, D. Spemann, G. Benndorf, H. Hochmuth, A. Rahm, H.-C. Semmelhack, M. Grundmann
The 9th International Workshop on Oxide Electronics, Florida, USA, October 2002

Optical properties of ternary Mg$_x$Zn$_{1-x}$O ($x<0.3$) thin films (T)
C. Bundesmann, R. Schmidt, N. Ashkenov, B. Rheinländer, M. Schubert, M. Lorenz, E. M. Kaidashev, M. Grundmann
L.O.T. user seminar ellipsometry, Darmstadt, October 2002
IR- and UV-VIS-Ellipsometry of ZnO, ZnMgO, ZnO-GaO thin films (T)
R. Schmidt, C. Bundesmann, N. Ashkenov, B. Mbenkum, B. Rheinländer, M. Schubert, H. v. Wenkstern, A. Kasic, T. Hofmann, M. Lorenz, E. M. Kadaishev, M. Grundmann
Ellipsometry Workshop, BAM Berlin, February 2002

Far infrared magneto-optical generalized ellipsometry determination of free carrier parameters in semiconductor thin film structures
T. Hofmann, C. M. Herzinger, M. Schubert
Materials Research Society Fall Meeting, Boston, U.S.A, Dezember 2002

Far infrared dielectric function and and phonon modes of spontaneously ordered AlGaInP
T. Hofmann, V. Gottschalch, M. Schubert
Materials Research Society Fall Meeting, Boston, U.S.A, Dezember 2002

Critical points and phonons in $B_xGa_{1-x}As$ and GaN_yAs_{1-y}: a comparison
G. Leibiger, V. Gottschalch, V. Riede, A. Kasic, M. Schubert
International workshop on Nitride Semiconductors (IWN 2002), Aachen, Germany, July 2002

Optical phonons in $Al_xIn_yGa_{1-x-y}N$ films
A. Kasic, M. Schubert, S. Einfeldt, D. Hommel, J. Off, F. Scholz, A. P. Lima, O. Ambacher, M. Stutzmann
International Workshop on Nitride Semiconductors (IWN 2002), Aachen, Germany, July 2002

Optical properties of ternary MgZnO thin films
R. Schmidt, C. Bundesmann, N. Ashkenov, B. Rheinländer, M. Schubert, M. Lorenz, E. M. Kadaishev, A. Kasic, T. Hofmann, D. Spemann, G. Wagner, M. Grundmann
26. International Conference on the Physics of Semiconductors, Edinburgh, GB, July 2002

Towards a better understanding of in-situ reflectance transients during MOVPE growth of group-III Nitrides
T. Böttcher, S. Figge, S. Einfeldt, D. Hommel, A. Kasic, M. Schubert
11th International Conference on Metal-Organic Vapour Phase Epitaxy, Berlin, Germany, June 2002

Properties of pulsed-laser-deposited $Zn_{1-x}(Al, Ga, Mg, Cd)_xO$ compound thin films
C. Bundesmann, N. Ashkenov, A. Kasic, V. Riede, M. Schubert, E. M. Kaidashev, M. Lorenz, R. Schmidt, B. Rheinländer, J. Lenzner, H. v. Wenckstern, M. Grundmann
German Physical Society Spring Meeting, Regensburg, March 2002

Dielektrische Funktion im Bereich der Absorptionskante von ZnO und ZnO-MgO- und ZnO-Ga2O3-Mischkristallen untersucht mittels spektroskopischer Ellipsometrie
R. Schmidt, C. Bundesmann, A. Kasic, E. M. Kaidashev, B. Rheinländer, M. Lorenz, M. Schubert, M. Grundmann
German Physical Society Spring Meeting, Regensburg, March 2002

Electronic and structural properties of n-type Zn(Ga, Al, Mg, Cd) oxide thin films by PLD
M. Lorenz, E. M. Kaidashev, J. Lenzner, H. v. Wenckstern, D. Spemann, G. Wagner, C. Bundesmann, V. Riede, M. Grundmann
DPG spring meeting, Regensburg, March 2002

Infrarot-dielektrische Funktion und Phononenmoden in spontan geordnetem $(Al_xGa_{1-x})_{0.52}In_{0.48}P$
T. Hofmann, V. Gottschalch, M. Schubert
German Physical Society Spring Meeting, Regensburg, March 2002

Kritische Punkte und Phononen in $B_xGa_{1-x}As$ und GaN_yAs_{1-y}: Ein Vergleich
G. Leibiger, V. Gottschalch, M. Schubert, V. Riede
German Physical Society Spring Meeting, Regensburg, March 2002

10.21 Graduations

10.21.1 Habilitation (Dr. rer. nat. habil.)

Dr. Mathias Schubert
Infrared Ellipsometry on III-V semiconductor layer structures

10.22 PhD (Dr. rer. nat.)

Dipl.-Phys. Alexander Kasic
Phonons, free-carrier properties, and electronic interband transitions of binary, ternary, and quaternary group-III nitride layers measured by spectroscopic ellipsometry

10.23 Diploma (Dipl.-Phys.)

Thomas Rudolph
Erweiterungen und Anwendungen der konfokalen optischen Mikroskopie

11 SUPERCONDUCTIVITY AND MAGNETISM — SCIENTIFIC ACTIVITIES

The group for Superconductivity and Magnetism is engaged in the study of basic properties of various superconducting and ferromagnetic materials. The present research activities focus on

- the investigation of ferromagnetic and superconducting correlations through different kinds of measurements in carbon-based compounds,
- the study of spin-dependent phenomena in magnetic oxides heterostructures, and
- the electrical and thermal transport in high-temperature superconductors as well as in quasi-2D oriented graphite.

Research highlights of the department SUM for the year 2002

The new research topic "magnetic carbon", started at the department in the year 1999, has continued to provide interesting results. Through an intensive cooperation of three physics departments of the faculty (SUM, NFP and PWM) we have characterized several highly oriented graphite samples, in particular their magnetic properties and ferromagnetic impurity concentration. This work shows for the first time that the measured ferromagnetism cannot be simply attributed to impurities and new physics is necessary to understand the experimental data. The overall results including the characterization by means of magnetic force microscopy in polymerised fullerene indicate that ferromagnetism in systems containing only p- and s-electrons appears to be a reality.

The discovery of a metal-insulator transition in graphite attracts the interest of theoreticians. We could prove that this transition is also observed in the c-axis resistivity. The overall results indicate: (a) The metallic-like behavior of the out-of-plane conductivity of graphite is not intrinsic but is due to a conduction-path mixing mechanism; (b) semiclassical models are inappropriate to understand the electronic transport mechanism in graphite. In a recent work high precision angular measurements reveal that the metal insulator transition in graphite depends only on the normal component to the graphene layers.

The magnetotransport properties of magnetic oxides have attracted an intense research activity in recent years. The scientific activities of our department are focused on the study of magnetic and magnetotransport properties of oxides, especially ferro- and ferrimagnetic films and superstructures. This work is directed towards the study of the fundamental properties of these strongly correlated materials, e.g. the mechanism for colossal magnetoresistance in ferromagnetic oxides of the type $La_{1-x}Ca_xMnO_3$, and towards the exploration of extrinsic magnetotransport phenomena in heterostructures such as ferromagnetic tunnelling junctions, spin-transistors as well as artificially created grain boundaries.

At present our primary interest is in magnetite (Fe_3O_4) and the colossal magnetoresistance manganite $La_{0.7}X_{0.3}MnO_3$ with X = Ca, Sr. According to band-structure calculations both materials are supposed to be fully spin-polarized and should therefore be ideal sources of

spin-polarized currents. Whereas the Curie temperature of the manganites is comparatively low: 270 K (Ca-) and 360 K (Sr-doping), and excludes the use of these materials in room-temperature applications, magnetite has an appreciable Curie temperature of 860 K. Thin oxide films are fabricated in our department using pulsed laser deposition.

Equipment

The group is equipped with a variety of magnetocryostat systems that cover a temperature range between 50 mK to 800 K in magnetic fields up to 11 T. Techniques like SQUID magnetometry, ac susceptibility, Hall effect, electrical and thermal conductivity, μ-Hall sensor array, differential thermal calorimetry and thermogravometry, x-rays and vibrating reed are used for sample characterization and for the study of different phenomena. Thin films and heterostructures are prepared by means of pulsed laser deposition.

11.1 Magnetic and Transport Properties of Graphite and Carbon-based Compounds

11.1.1 Can Carbon be Ferromagnetic ?

R. Höhne and P. Esquinazi

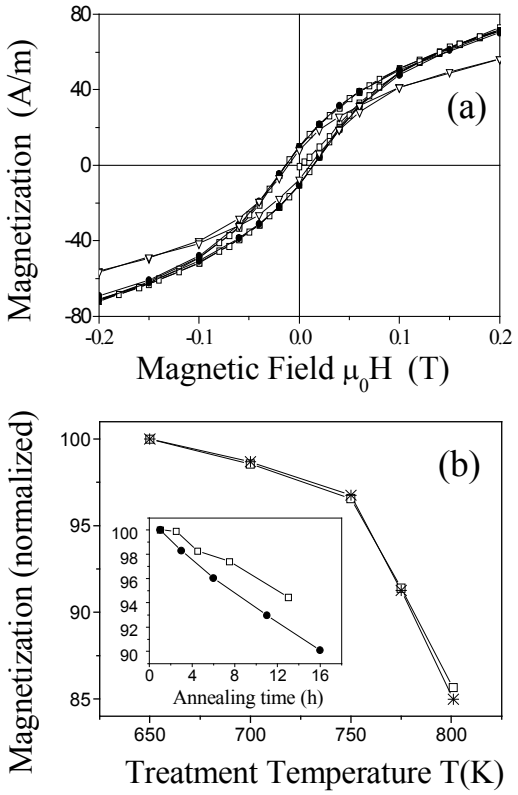

In pure carbon materials, such as fullerenes and highly oriented pyrolitic graphite (HOPG), novel magnetic and electrical properties have recently been discovered. In particular, the discovery of weak ferromagnetism in rhombohedral C_{60} polymers (Rh-C_{60}) has attracted the attention of the scientific community and the press. The main problem one has to show that the weak ferromagnetic signal obtained in several of the carbon-based materials is intrinsic, is due to the contribution of ferromagnetic impurities. An argument against a simple contribution due to the ferromagnetic impurities comes from the observed influence of temperature treatments between 500 and 800 K on the magnetic behavior. A C60 sample (sample 1) was enclosed in an evacuated quartz tube and heat treated in the SQUID magnetometer. After each treatment, the magnetic state was characterized by measurements of the hysteresis loop below the Curie temperature. In the figure expanded views of the loops measured for sample 1 at T = 400 K before and after thermal treatments are shown. There are no changes of the magnetic state after treatments up to 650 K even after 10 hours. After treatment at 700 K the first changes on the magnetic state are observed. After 3 h treatment at 700 K the magnetization (at 400 K and at a field of 1 T) has 98.5 % of the virgin value, decreasing to 79 % after 16 h at 800 K. The magnetic stability depends on the structural stability of each sample, which is influenced by the preparation conditions. For more details see Advanced Materials 14, 753-756 (2002).

11.1.2 Ferromagnetism in Oriented Graphite Samples

P. Esquinazi, A. Setzer, R. Höhne, C. Semmelhack,Y. Kopelevich, D. Spemann, T. Butz, B. Kohlstrunk, M. Lösche

We have studied the magnetization of various, well characterized samples of highly oriented pyrolitic graphite (HOPG), Kish graphite and natural graphite to investigate the recently reported ferromagnetic-like signal and its possible relation to ferromagnetic impurities. The magnetization results obtained for HOPG samples for applied fields parallel to the graphene layers - to minimize the diamagnetic background - show no correlation with the magnetic impurity concentration. Our overall results suggest an intrinsic origin for the ferromagnetism found in graphite. In the figure we show the magnetization at 2 kO2 measured at 10 and 300 K of different graphite samples with different impurity concentration. The results indicate no clear correlation between the two values. The continuous and dashed lines are the magnetization one would obtain if the impurity concentration behaves as pure Fe or pure magnetite, a unlikely assumption due to the small impurity concentration, We discuss possible origins of the ferromagnetic signal. For more details see Phys. Rev. B. 66, 024429-1… -10 (2002).

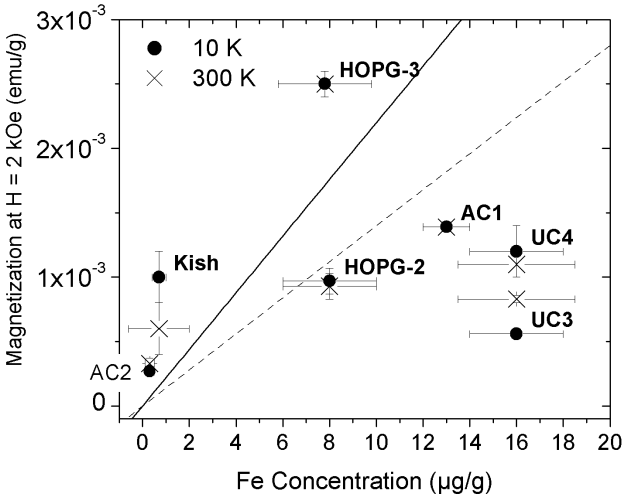

11.2 Thermomagnetic Instabilities versus Phase transitions in the flux line lattice of superconductors

Y. Kopelevich and P. Esquinazi

Thermomagnetic flux-jump instabilities in type-II superconductors reduce the absolute irreversible magnetization relative to the isothermal critical state value at low enough magnetic fields. The recovering of the isothermal critical state with increasing field leads to the ``second magnetization peak" (SMP) in the magnetization curve M(H) as has been unambiguously demonstrated for Nb films. The low-field SMP takes place in many other conventional and unconventional superconductors, and is often attributed to a critical current enhancement associated with a phase transition(s) in the vortex matter. The analysis of most recent experimental results we have performed provides clear evidence that the restoration of the isothermal critical state is responsible for the SMP in both conventional and unconventional superconductors and casts doubts about the interpretation based on phase transition(s) of the vortex matter.

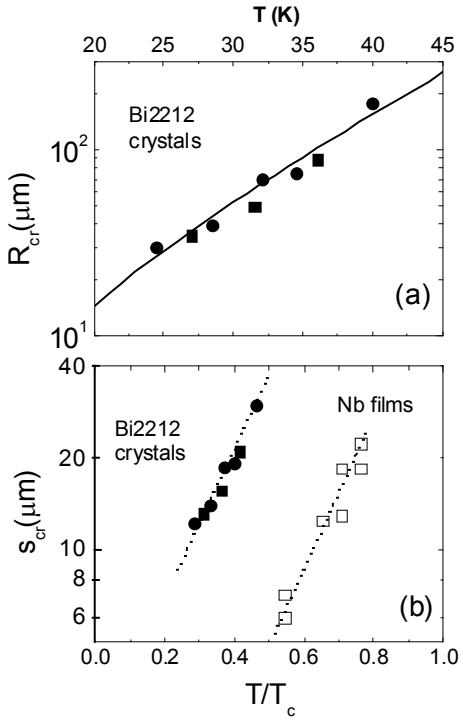

In the figure we show in (a) the temperature dependence of the "critical" sample size for Bi2212 high-temperature superconductor, below which no second magnetization peak is observed. The solid line is obtained from $R_{cr}(T) = A\,T^{3/2}\exp(T/T_0)$ with $A = 0.043\mu m/K^{3/2}$ and $T_0 = 15K$ which follows from the thermomagnetic instability model. (b) Effective sample size vs. reduced temperature obtained for Bi2212 crystals from literature (Tc = 87K) and Nb-films (Tc = 9.2K, our measurements). Dashed lines are only a guide. For more details see Solid State Commun. 122, 33-36 (2002).

11.3 Thermal conductivity tensor in Y123 crystals: Effects of a planar magnetic field

R. Ocaña and P. Esquinazi

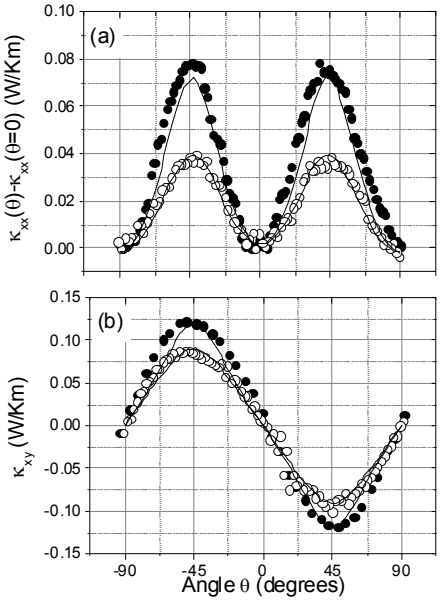

We have measured the thermal conductivity tensor of a twinned $YBa_2Cu_3O_7$ single crystal as a function of angle □ between the magnetic field applied parallel to the CuO_2 planes and the heat current direction, at different magnetic fields and at T=13.8 K. Clear fourfold and twofold variations in the field-angle dependence of k_{xx} and k_{xy} were respectively recorded in accordance with the d-wave pairing symmetry of the order parameter, see left figure. The oscillation amplitude of the transverse thermal conductivity k^0_{xy} was found to be larger than the longitudinal one k^0_{xx} in the range of magnetic field studied 0 □ B □ 9. From our data we obtain quantities that are free from non-electronic contributions and they allow us a comparison of the experimental results with current models for the quasiparticle transport in the mixed state. The continuous lines in the upper figure were calculated using a two-dimensional version of the Bardeen-Rickayzen-Tewordt model assuming the scattering of the quasiparticles by supercurrents (Andreev scattering), which plays a role at high magnetic fields. Our work shows that this model gives a qualitative not

quantitative agreement with experimental results. More details can be seen in Physical Review B 66, 064525 (2002).

11.4 Correlation of Transport and Structure in thin $La_{0.7}Ca_{0.3}MnO_3$ Films on $SrTiO_3$

M. Ziese, K. H. Han, H.-C. Semmelhack

There is a strong coupling between charge, spin and lattice degrees of freedom in colossal magnetoresistance manganites of the type $La_{0.7}Ca_{0.3}MnO_3$ (LCMO). This leads to metallic behavior in the ferromagnetic phase and semiconducting behaviour in the paramagnetic regime; the magnetic transition is accompanied by a metal-semiconductor transition. Especially the strong electron-phonon interaction in colossal magnetoresistance manganites leads to a pronounced dependence of the transport properties on the strain state in thin films. This was investigated in detail on a series of $La_{0.7}Ca_{0.3}MnO_3$ (LCMO) films epitaxially grown on $SrTiO_3$ substrates. The bulk lattice constants are 0.386 nm in case of LCMO and 0.3905 nm in case of $SrTiO_3$, setting the film under a tensile strain of 1.3%.

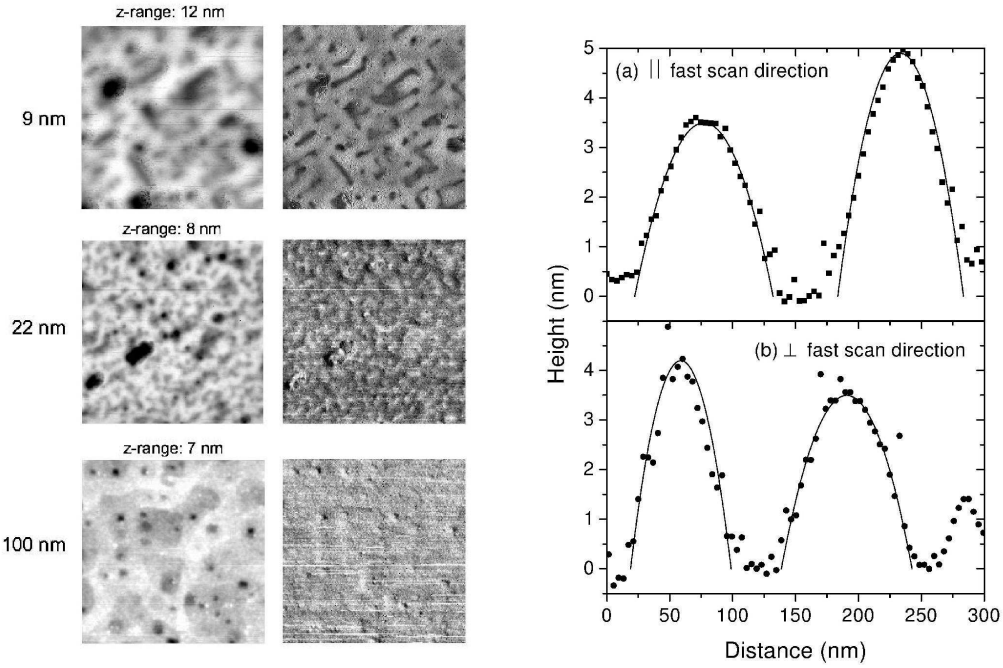

Fig. (left) Height and phase image recorded on three LCMO films on $SrTiO_3$ with thickness 9, 22 and 100 nm, respectively. Scan range was 1x1 μm^2 . (right) Cross section of AFM image of the 9 nm film showing the height variation. Solid lines are fits of an one-dimensional model ("Ling's mound") to the data.

LCMO films were grown on $SrTiO_3$ using pulsed laser ablation. Film thickness was between 5 nm and 300 nm. X-ray diffractometry indicates that the films are under full tensile strain below a thickness of about 30 nm, whereas strain relaxation occurs above this thickness. The surface roughness of the films was investigated by atomic force microscopy (AFM). Typical images are shown in Fig. 1. There are considerable height variations in the thinnest film that induce non-uniform strains. These were analysed within

a one-dimensional model for the elastic strain across a mound of particular shape ("Ling's mound") and a maximum strain of about 2.5% could be estimated.

The magnetotransport properties of the films with a thickness below 30 nm deviate significantly from bulk properties as is illustrated in Fig. 3 showing the zero field resistivity: the 9 nm thick film is insulating even in the ferromagnetic regime. Application of a magnetic field of 8 T drives it back into a metallic state.

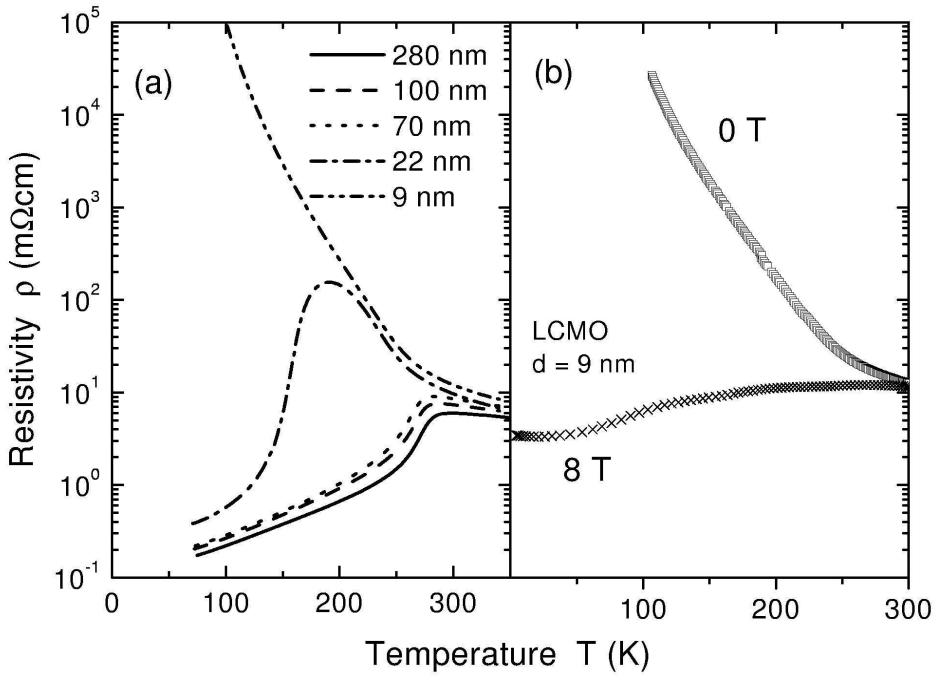

Fig. (left) Zero field resistivity of various LCMO films. (right) Resistivity of the 9 nm LCMO film on $SrTiO_3$ film in applied fields of 0 and 8 T, respectively.

Theoretical calculations of the phase diagram of tetragonally distorted manganites, especially LSMO, show that a transition to an antiferromagnetic insulating state occurs below a lattice constant ratio of c/a = 0.96. From X-ray diffractometry we determined the significantly larger value of c/a = 0.976. The analysis of the strain distribution shows that the insulating state seen in ultrathin manganite films cannot be accounted for by inhomogeneous strains. We concluded that this state arises from orbital order as envisioned in the theoretical calculations. These are, however, not quantitatively correct in the case of LCMO.

11.5 Grain-Boundary magnetoresistance in Magnetite

M. Ziese, R. Höhne, H. Reckentin, and P. Esquinazi

The phenomenon of grain-boundary magnetoresistance in half-metallic oxides has attracted an intense research activity in recent years. There is consensus that this effect – seen mainly in the manganites, $Tl_2Mn_2O_7$ and CrO_2 – can be mainly attributed to spin-dependent tunnelling. The Curie temperature of these ferromagnetic oxides, however, is too low in order to realize magnetoresistive devices operating at room temperature. There is only one notable exception: the half-metallic ferrimagnet magnetite (Fe_3O_4) with a Curie temperature of 858 K. We have investigated the magnetotransport properties of various magnetite films, especially polycrystalline films on Al_2O_3 and films an $MgAl_2O_4$ with artificially created defects due to the presence of step edges. All films were fabricated by pulsed laser deposition from a stoichiometric magnetite target onto substrates heated to about 430°C. Oxygen partial pressure during deposition was between $5x10^{-6}$ mbar and $1x10^{-4}$ mbar.

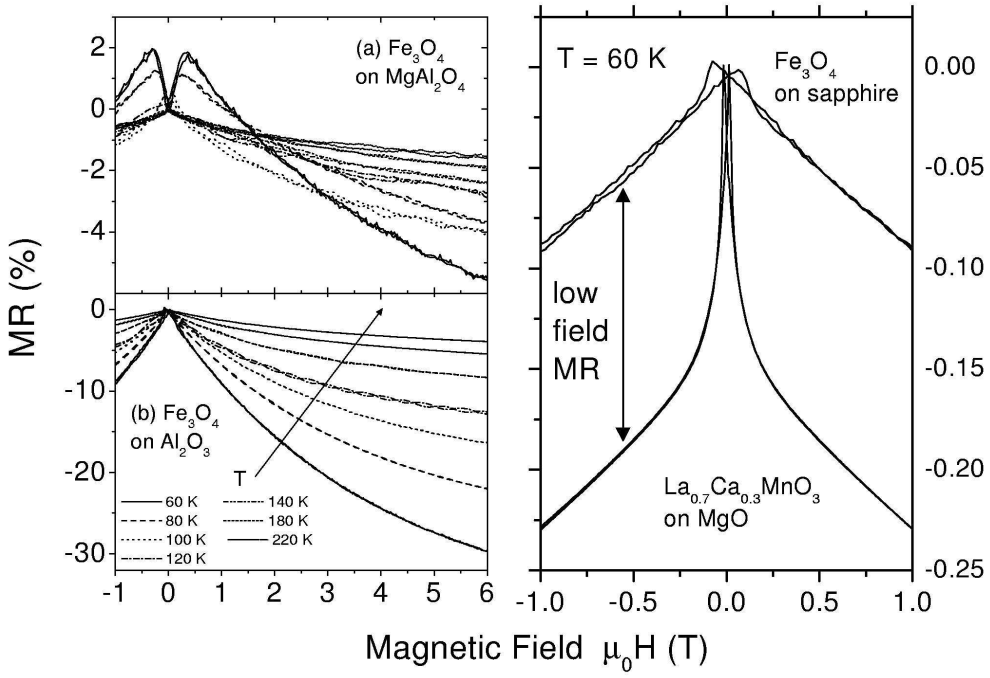

Fig. (left) Magnetoresistance (MR) of (a) an epitaxial and (b) a polycrystalline magnetite film on $MgAl_2O_4$ and Al_2O_3, respectively. (right) Comparison of the magnetoresistance of polycrystalline $La_{0.7}Ca_{0.3}MnO_3$ and magnetite films. The sharp magnetoresistance drop seen for LCMO is due to spin-polarized tunnelling across grain bondaries with high interfacial resistivity.

Polycrystalline films on sapphire are mainly (111) oriented with some (100) orientation present. These films as well as step edge arrays in magnetite show a magnetoresistance that is significantly enhanced compared to the magnetoresistance of epitaxial films on $MgAl_2O_4$ as is shown in Fig. 1. This enhanced magnetoresistance, however, is a high field effect in striking contrast to the behaviour seen in the manganites. This is illustrated in Fig. 2.

We have developed a model for this enhanced magnetoresistance based on the idea of spin-dependent scattering in a thin magnetically disordered interface layer. The magnetic field dependence can be understood within a spin-rotation model. The agreement with experimental curves is satisfactory. We conclude that – in contrast to the situation in other half-metallic oxides – spin-polarized tunnelling is not the dominant transport mechanism across extended defects in magnetite.

11.6 Growth and Characterization of $BaTiO_3$ films on $SrTiO_3$

It is well known that $BaTiO_3$ has three structural transitions at about 183 K, 278 K and 393 K. These can be used to probe the electron-phonon coupling in $La_{0.7}Ca_{0.3}MnO_3$ (LCMO) films incorporated in $BaTiO_3$/LCMO bilayer or multilayer structures. The magnetotransport properties would be expected to show marked anomalies at the structural transitions of $BaTiO_3$ due to the strains induced in the LCMO layers.
As a starting point of such a study, $BaTiO_3$ films were grown on $SrTiO_3$ and $La_{0.7}Ca_{0.3}MnO_3$-buffered $SrTiO_3$ by pulsed laser deposition at a substrate temperature of about 700°C and an oxygen partial pressure of about 0.05 mbar. Film thickness was determined with a profilometer (Frau Ramm, HLP), and was in the range between 10 and 1000 nm. X-ray diffractometry showed textured film growth with FWHM of the (002) rocking curves of 0.4-0.5°. At room temperature the in-plane and out-of-plane lattice constants were determined from the (002) and (013) reflections: the films are nearly cubic with $a_{\parallel}$ = 0.4032(5) nm and $a_{\perp}$ = 0.4021(5) nm. Extensive AFM studies show an island-like morphology with grain sizes of typically 100 nm diameter.
In order to investigate the ferroelectric properties, the capacitance of LCMO/$BaTiO_3$/LCMO trilayer structures was measured as a function of the applied electric field. Most samples appear to be ferroelectric; some variation of the coercive field and dielectric constant was found. Measurements of the dielectric constant between 10 K and room temperature did not show any indication of a phase transition. This might be attributed to the considerable strains imposed by the $SrTiO_3$ substrate on the $BaTiO_3$ films.

11.7 Funding

Wärmeabgabe und Wärmetransport in Supraleitern, Gläsern und magnetischen Materialien bei tiefen Temperaturen
Heat Release and Thermal Transport in Superconductors, Glasses and Magnetic Materials at Low Temperatures
Prof. P. Esquinazi
Deutsche Forschungsgemeinschaft, ES 86/4-3

Lokale und nichtlokale Untersuchungen von Flusslinienbewegungen in Supraleitern
Local and Non-Local Studies of Vortex Dynamics in Superconductors
Prof. P. Esquinazi, Prof. E. Zeldov (Weizmann Inst. Rehovot)
German-Israeli Foundation, G - 553 - 191.14/97

Schermodul des Flusslinengitters und Quanten-Flusskriechen in HTSL
Shear-module of Flux-line-lattice and Quantum Flux-flow in HTSC
Prof. P. Esquinazi, Prof. S. Moehlecke (Universidade Estadual de Campinas)
DAAD-Programme (PROBRAL - Exchange of Scientists with Brazil)

Wechselspiel zwischen Supraleitung und Magnetismus in Graphit und in ungeordneten Metallen
Interplay between Superconductivity and Magnetism in Graphite and Disordered Metals
Prof. P. Esquinazi
Deutsche Forschungsgemeinschaft, ES 86/6-1

Magnetotransport in Oxidschichtsystemen
Magnetotransport in Oxide Thin Film Systems
Project of the Forschergruppe "Oxidische Grenzflächen" with the University of Halle and Max-Planck-Institute for Microstructure Research in Halle
Prof. P. Esquinazi
Deutsche Forschungsgemeinschaft, ES 86/7-1

11.8 Organizational Duties

P. Esquinazi
Dean of Studies of the Faculty for Physics, Meteorology and Geophysics Studies
Project Reviewer: Deutsche Forschungsgemeinschaft, National Science Foundation (USA), German-Israeli Foundation
Referee: Phys. Rev. Lett., Phys. Rev. B, Physica C, Phys. Lett. A, phys. stat. sol., J. Low Temp. Phys.

R. Höhne
Referee: phys. stat. sol. (a), (b)

M. Ziese
Referee: Phys. Rev. Lett., Phys. Rev. B, phys. stat. sol. (b), J. Magn. Magn. Mater., Eur. J. Phys. B, J. Low Temp. Phys.

11.9 External cooperations

Prof. Dr. Yakov Kopelevich, Campinas, Brazil
Prof. Dr. Eli Zeldov, Weizmann Institute of Sciences, Israel
Dr. Tatiana Makarova, Ioffe Institute, St. Petersburg, Russia
Prof. Bertil Sundqvist, Umea University, Sweden
Prof. Dr. Miguel Angel Ramos, Universidad Autónoma de Madrid, Spain
Prof. Dr. Sebastian Vieira, Universidad Autónoma de Madrid, Spain
Prof. Dr. Vladimir Pan, Institute of Metal Physics, Kiev, Ukraine
Dr. K. Zimmer and J. Dienelt, Institute for Surface Modification, Leipzig
Prof. Dr. R. Szargan, Chemistry Department, University of Leipzig
Dr. K.-M. Schindler, Physics Department, University of Halle
Dr. K. Steenbeck, IPHT Jena
Dr. E. Rozenberg, Physics Department, University of the Negev, Beer Sheva, Israel
Prof. J. M. D. Coey, Trinity College Dublin, Ireland
Dr. Mike Cooke, University of Durham, United Kingdom

11.10 Publications

11.10.1 Journals

Esquinazi, P.; Setzer, A.; Höhne, R.; Semmelhack, C.; Kopelevich, Y.; Spemann, D.; Butz, T.; Kohlstrunk, B.; Lösche, M.
Ferromagnetism in oriented graphite samples
Physical Review B **66**, 024429-1 - 024429-10 (2002)

Glaser, A.; Ziese, M.
Grain-boundary capacitance of $La_{0.7}Ca_{0.3}MnO_3$ films
Physical Review B **66**, 094422-1 - 094422-5 (2002)

Höhne, R.; Esquinazi, P.
Can Carbon Be Ferromagnetic?
Advanced Materials **14**, 10, 753 - 756 (2002)

Kempa, H.; Esquinazi, P.; Kopelevich, Y.
Field-induced metal-insulator transition in the *c*-axis resistivity of graphite
Physical Review B **65**, 241101-1 - 241101-4 (2002), Rapid Communications

König, R.; Mrowka, F.; Usherov-Marshak, I.; Esquinazi, P.; Wasserbäch, W.
Influence of sample preparation on the glass-like acoustic properties of pure crystalline tantalum
Physica B **316-317**, 539 - 541 (2002)

König, R.; Ramos, M. A.; Usherov-Marshak, I.; Arcas-Guijarro, J.; Hernando-Mañeru, A.; Esquinazi, P.
Strain dependence of the acoustic properties of amorphous metals below 1 K: Evidence for the interaction between tunneling states
Physical Review B **65**, 180201-1 - 180201-4 (2002), Rapid Communications

Kopelevich, Y.; Esquinazi, P.
Thermomagnetic instability effects vs. vortex matter phase transitions in type-II superconductors
Solid State Communications **122**, 33 - 36 (2002)

Krause, M. K.; Esquinazi, P.; Ziese, M.; Höhne, R.; Pan, A.; Galkin, A.; Zeldov, E.
Out-of-plane stray field at magnetization reversal in epitaxial magnetite thin films
Journal of Magnetism and Magnetic Materials **242-245**, 1097 - 1099 (2002)

Ocaña, R.; Esquinazi, P.
Thermal conductivity tensor in $YBa_2Cu_3O_{7-x}$: Effects of a planar magnetic field
Physical Review B **66**, 064525-1 - 064525-9 (2002)

Ziese, M.
Extrinsic magnetotransport phenomena in ferromagnetic oxides
Reports on Progress in Physics **65**, 143 - 249 (2002)

Ziese, M.
Spin hopping in a discontinuos $La_{0.7}Ca_{0.3}MnO_3$ film
Applied Physics Letters **80**, 2144 - 2146 (2002)

Ziese, M.; Han, K. H.; Esquinazi, P.
Spin hopping in ultrathin La-Ca-Mn-O Films
IEEE Trans. Mag. **38**, 2898 - 2900 (2002)

Ziese, M.; Höhne, R.; Esquinazi, P.; Busch, P.
Micromagnetic studies of magnetite films using μ-Hall sensor arrays
Physical Review B **66**, 134408-1 - 134408-8 (2002)

Ziese, M.; Höhne, R.; Esquinazi, P.; Busch, P.
Step edge magnetoresistance of magnetite films
IEEE Trans. Mag. **38**, 2883 - 2885 (2002)

Ziese, M.; Höhne, R.; Hong, N. H.; Dienelt, J.; Zimmer, K.; Esquinazi, P.
Magnetoresistance at grain boundaries artificially introduced into magnetite films
Journal of Magnetism and Magnetic Materials **242-245**, 450 - 452 (2002)

Ziese, M.; Höhne, R.; Semmelhack, H. C.; Reckentin, H.; Hong, N. H.; Esquinazi, P.
Mechanism of grain-boundary magnetoresistance in Fe_3O_4 films
The European Physical Journal B **28**, 415 - 422 (2002)

Ziese, M.; Semmelhack, H. C.; Busch, P.
Sign reversal of the magnetic anisotropy in $La_{0.7}A_{0.3}MnO_3$ (A = Ca, Sr, Ba) films
Journal of Magnetism and Magnetic Materials **246**, 327 - 334 (2002)

Ziese, M.; Semmelhack, H. C.; Han, K. H., Sena, S. P., Blythe, H. J.
Thickness dependent magnetic and magnetotransport properties of strain-relaxed $La_{0.7}Ca_{0.3}MnO_3$ films
Journal of Applied Physics **91**, 9930 - 9936 (2002)

11.10.2 Invited Talks

P. Esquinazi
"Ferromagnetism in Graphite", Instituto "Nicolas Cabrera",
Universidad Autónoma de Madrid, 22.02.2002, Madrid.

P. Esquinazi
"Phase Transitions in the Vortex Matter or how to publish in Physical Review Letters"
Instituto de Ciencia de Materiales, CSIC, 18.04.2002, Madrid.

P. Esquinazi
"Metal-Insulator-Metal Transitions in Graphite: An overview of the experimental evidence", Universidad Autónoma de Madrid, 22.05.2002, Madrid.

P. Esquinazi
"Mechanism of grain-boundary magnetoresistance in Fe_3O_4 films",
Universidad Nacional del Tucuman, 01.10.2002, Tucuman (Argentine).

M. Ziese
"Spin Electronic devices: Opportunities, Bottlenecks and Challenges",
Chinese-German workshop on “Fundamentals and applications of nanoscience: materials, building blocks, modeling and structuring”, Karlsruhe, July 2002.

M. Ziese
"Fabrication and Characterization of Magnetite Films"
Seminar of the Semiconductor Physics Group, University of Leipzig, October 2002.

M. Ziese
"Fabrication and Characterization of Oxide Films: $BaTiO_3$ and $La_{0.7}Ca_{0.3}MnO_3$"
Seminar of the Surface Science Group, University of Halle, November 2002.

11.10.3 Conference Contributions

(T:talk, P:poster)

Spin hopping in ultrathin $La_{0.7}Ca_{0.3}MnO_3$ films. (T)
M. Ziese, K. H. Han, H.-C. Semmelhack, P. Esquinazi
International Workshop on “Oxide Interfaces“, Wittenberg 2002

Magnetization and magnetotransport measurements on thin magnetite films grown on spinel substrates. (T)
M. Ziese, R. Höhne, N. H. Hong, H.-C. Semmelhack, H. Reckentin, P. Esquinazi
International Workshop on "Oxide Interfaces", Wittenberg 2002

Step-edge magnetoresistance of magnetite films. (P)
M. Ziese, R. Höhne, N. H. Hong, K. H. Han, K. Zimmer, P. Esquinazi
International Workshop on "Oxide Interfaces", Wittenberg 2002

Low temperature magnetotransport properties of $La_{0.7}Ca_{0.3}MnO_3$ films on $SrTiO_3$. (P)
M. Ziese
International Workshop on "Oxide Interfaces", Wittenberg 2002

Spinabhängige Transporteigenschaften von granularen $La_{0.7}Ca_{0.3}MnO_3$ Schichten. (T)
M. Ziese, K. H. Han, H.-C. Semmelhack, P. Esquinazi
Frühjahrstagung des Arbeitskreises Festkörperphysik, Regensburg 2002

Step-edge magnetoresistance of magnetite films. (P)
M. Ziese, R. Höhne, N. H. Hong, K. H. Han, K. Zimmer, P. Esquinazi
Frühjahrstagung des Arbeitskreises Festkörperphysik, Regensburg 2002

Low temperature magnetotransport properties of $La_{0.7}Ca_{0.3}MnO_3$ films on $SrTiO_3$. (P)
M. Ziese
Frühjahrstagung des Arbeitskreises Festkörperphysik, Regensburg 2002

Magnetization and magnetotransport measurements on thin magnetite films grown on spinel substrates. (P)
R. Höhne, M. Ziese, N. H. Hong, H.-C. Semmelhack, H. Reckentin, P. Esquinazi
Frühjahrstagung des Arbeitskreises Festkörperphysik, Regensburg 2002

Mikromagnetische Charakterisierung von Magnetitschichten mittels µ-Hall-Sensoren. (P)
M. Ziese, R. Höhne, P. Busch* und P. Esquinazi
Frühjahrstagung des Arbeitskreises Festkörperphysik, Regensburg 2002

Step-edge magnetoresistance of magnetite films. (T)
M. Ziese, R. Höhne, P. Esquinazi, K. H. Han, K. Zimmer
INTERMAG, Amsterdam 2001

Spin hopping in ultrathin $La_{0.7}Ca_{0.3}MnO_3$ films. (P)
M. Ziese, K. H. Han, P. Esquinazi
INTERMAG, Amsterdam 2001

$La_{0.7}Ca_{0.3}MnO_3$ Films on SrTiO3: Small Polarons, Stripe Domains and Metal-Insulator Transitions. (P)
M. Ziese
INTERMAG, Amsterdam 2001

11.11 Graduations

11.11.1 Diploma Theses

Name: Heiko Reckentin
Title: Herstellung oxidischer Mehrschichtsysteme und Charakterisierung ihrer Magnetotransporteigenschaften
Submission date: 1. August 2002 Diploma Theses

11.12 Guests

Dipl.-Phys. Yuriy Cherpak
Institute for Metal Physics, Academy of Sciences of Ukraine, Kiev
23.06.2002 - 21.07.2002

Prof. Dr. Yakov Kopelevich
Instituto de Fisica, Universidade Estadual de Campinas, Brazil
27.08.2002 - 10.09.2002

Prof. Dr. Jorge Ossandón
Depto. de Ciencias de la Ingeniería, Universidad de Talca, Chile
18.08.2002 - 15.02.2003

Dipl.-Phys. Oleksiy Pronin
Institute for Metal Physics, Academy of Sciences of Ukraine, Kiev
23.06.2002 - 21.07.2002

Prof. Dr. Sebastian Vieira
Facultad de Ciencias, Universidad Autonoma de Madrid, Spain
18.11.2002 - 21.11.2002

12. Introduction

The aim of the research at the Institute for Theoretical Physics (ITP) is to explore the theoretical and mathematical fundamentals of physics. The key areas of research are the theory of elementary particles and the theory of condensed matter, which synergistically augment each another. Fundamental problems of the structure of space, time and matter (from the smallest conceivable unit of length up to cosmic dimensions) are examined and practical problems of complex physical systems with mesoscopic dimensions are tackled.

The institute consists of the following research groups:

- **Quantum Field Theory (QFT)** – fundamental problems of mathematical physics, general structure of gauge theories, primary and effective interactions of elementary particles.
- **Particle Physics Group (TET)** – quantum field theory of elementary particles, supersymmetrical theories, quantum chromodynamics, lattice gauge theory.
- **Theory of Condensed Matter (TKM)** – noise-induced phenomena, structure formation in liquid crystals, non-linear dynamics in biological models, immune system, strongly coupled electron systems.
- **Computer-Oriented Quantum Field Theory (CQT)** – computer simulations of phase transitions and critical phenomena, physics of soft matter and disordered systems, quantum magnets.
- **Molecule Dynamics/Computer Simulation (MDC)** – computer simulations of molecules at interfaces, computations of structural data, studies of thermodynamic parameters and transport coefficients.
- **Statistical Physics (STP)** – interacting many-particle systems, statistical and quantum-field theoretical methods.

In Section 3, for each group a short overview of the research profile is followed by extended abstracts describing their most relevant current projects. Added is a subsection devoted to the Graduate Studies Programme "Quantum Field Theory", which plays an important integrating rôle not only within the ITP, but also for the scientific interaction with the Department of Mathematics and Computer Sciences and the Max-Planck Institute for Mathematics in the Sciences (MIS). In addition the research groups of the ITP take part in many of the interdisciplinary research projects of the Centre for Theoretical Sciences (NTZ) which is part of the Centre of Advanced Studies (ZHS) of the University of Leipzig. In Section 4, the publications of members of the ITP of the year 2001 are listed. Sections 5 and 6 give an overview of talks and organizational activities of ITP members.

K. Sibold

March 2003

13. Members of the ITP

Name	*Status*	*Room*	*Phone*	*Fax*
Director				
Prof. Dr. Sibold, Klaus		1L18	97-32424	97-32425
Quantum Field Theory (QFT)				
Prof. Dr. Rudolph, Gerd	spokesperson	1R24	97-32426	
Prof. Dr. Geyer, Bodo	professor em.	1R23	97-32422	
Prof. Dr. Uhlmann, Armin	professor em.	2L10	97-32421	
Prof. Dr. Weller, Wolfgang	professor em.	2L10	97-32421	
PD Dr. Bordag, Michael	staff member	1R19	97-32427	
Dr. Richter, Olaf	staff member	1R17	97-32461	
Dr. Schmidt, Matthias	staff member	1R22	97-30293	
Dr. Fleischhack, Christian	associated member	1R17	97-32431	
Dr. Vassilevich, Dimitri	staff member	2L21	97-32462	
Neumeier, Stefan	PhD student	2L17	97-30436	
Drosdow, Igor	PhD student	2L21	97-32462	
Eilers, Jörg	PhD student	2L17	97-30436	
Krähmer, Ulrich	PhD student	2L15	97-32432	
Fischer, Tobias	Diploma student	2L14	97-32453	
Theory of Elementary Particles (TET)				
Prof. Dr. Sibold, Klaus	spokesperson	1L18	97-32424	97-32425
PD Dr. Kirschner, Roland	staff member	1L19	97-32441	
PD Dr. Schiller, Arwed	staff member	1L22	97-32446	
Dr. Liao, Yi	staff member	2L22	97-32464	
Dehne, Christoph	PhD student	1R16	97-32444	
Ivanov, Alexander	PhD student	2L15	97-32432	
Zhang, Yong	PhD student	2L18	97-30292	
Theory of Condensed Matter (TKM)				
Prof. Dr. Ihle, Dieter	spokesperson	1L15	97-32433	
Prof. Dr. Behn, Ulrich	professor	1L20	97-32434	
Prof. Dr. Kühnel, Adolf	professor em.	1L16	97-32423	
PD Dr. Kolley, Wilfried	staff member	1R18	97-32435	
Brede, Markus	PhD student	2L15	97-32432	
John, Thomas[1]	PhD student		97-32566	
Junger, Iren	PhD student	1R15	97-32437	
Krieger-Hauwede, Micaela	PhD student	2L15	97-32432	
Martin, Edgar	Diploma student	2L15	97-32432	

Computer-Oriented Quantum Field Theory (CQT)

Prof. Dr. Janke, Wolfhard	spokesperson	2L21	97-32725	97-32747
Dr. Bachmann, Michael	staff member	1R20	97-32443	
Dr. Bittner, Elmar	staff member	1R21	97-32429	
Dr. Weigel, Martin	staff member	2L16	97-32450	
Kaehler, Götz	Diploma student	2L16	97-32450	
Krinner, Axel	Diploma student	2L14	97-32453	
Nußbaumer, Andreas	Diploma student	2L16	97-32450	
Schiemann, Reinhard	Diploma student	2L14	97-32453	
Vogel, Thomas	Diploma student	2L14	97-32453	
Wenzel, Sandro	Diploma student	2L14	97-32453	

Molecule Dynamics/Computersimulations (MDC)[2]

Dr. Fritzsche, Siegfried	staff member	P 9.1/201	235-2261	235-2307
Prof. Dr. Haberlandt, Reinhold	staff member	P 9.1/216	235-2280	
Dr. Vörtler, Horst-Ludger	staff member	P 9.1/213	235-2435	
Dr. Kormilets, Viatcheslav	staff member	P 9.1/214	235-2589	
Loisrangsin, Arthorn	PhD student	P9.1/214	234-2589	

Statistical Physics (STP)

Prof. Dr. Salmhofer, Manfred	spokesperson	1L17	97-32468	
Dr. Lauscher, Oliver	staff member	1R15	97-32437	
de Siqueira Pedra, Walter	PhD student	1R15	97-32437	
Husemann, Christoph	Diploma student	2L14	97-32453	

Library

Thiele, Elfriede		1R13	97-32440	

Secretariat

Voigt, Lea		1L24	97-32420	97-32548
Salzer, Gloria		1L24	97-32430	

[1] Linnéstr., PAF group.
[2] Building Permoserstr. 15, 04318 Leipzig.

14. Research Projects

14.1. Quantum Field Theory (QFT)

The "Mathematical Physics" group works on mathematical structures of gauge theories (investigation of gauge models in terms of gauge invariants, structure of the gauge orbit space, anomalies, lattice approximation), certain aspects of noncommutative geometry (basic structures, model building, quantum groups) and dimensional reduction of gauge theories (model building, exact solutions of Einstein-Yang-Mills systems – including systems with coupled fermions). Following these lines of research, methods of differential geometry, Lie groups and Lie algebras, algebraic topology and – in the context of noncommutative geometry – also *-algebras are used. There are relations both to research in quantum field theory and elementary particle physics performed at the Institute for Theoretical Physics and mathematical research performed at the Institute of Mathematics and the Max-Planck-Institute for Mathematics in the Sciences. There is a lecture course on Mathematical Physics (differentiable manifolds, Lie groups, Hamiltonian systems, fibre bundles and connections, applications to Yang-Mills theory and the theory of gravity), which is regularly delivered. We are collaborating with colleagues from Warsaw and Moscow and have good scientific contacts with many other research centres.

The group "Relativistic Quantum Field Theory" works on the theory of elementary particles, their primary and effective interactions, mainly based on the Standard Model of strong and electroweak interactions and its extensions, and on the influence of external conditions (boundaries, classical fields and background configurations). In the centre of current interest are the structure of general gauge theories, special models taking into account external fields and curved spacetime, two-dimensional gravity, the polarized lepton-nucleon scattering and other hard hadronic processes, the role of vacuum energy (general Casimir effects) and finite temperature. The applied methods include: various quantization and renormalization procedures, effective action approach, application of functional integration, heat kernel expansion, theory of Lie groups and functional analysis. – This basic research contributes to the understanding of the fundamental constituents of matter and of the universe as a whole. It also is related to and has applications in solid state and statistical physics. The group has close connections to the mathematical physics and elementary particle groups at ITP, and cooperations with DESY (Zeuthen) as well as various international institutions, e.g., in Russia, Austria, Brazil and Great Britain. – There are lecture courses on special aspects of quantum field theory which are regularly offered by the Graduate Studies Programme "Quantum Field Theory" whose speaker is a member of this group.

14.1.1. Quantum Field Theory under the Influence of External Conditions

M. Bordag, K. Kirsten (MPI, Leipzig), D. V. Vassilevich, V. Skalozub (National University, Dnepropetrovsk) and I. Drosdow

The vacuum of quantum fields shows a response to changes in external conditions with measurable consequences. The investigation of the electromagnetic vacuum in the presence of dielectric bodies is of actual interest in view of the rapid progress in measurements. The investigation of the vacuum energy and of the ultraviolet divergences which appear in this kind of problems has been continued. Results are obtained on the physical significance of vacuum energy for a single dielectric body [1].

The heat kernel methods are of prime importance for the understanding of the structures of the ultraviolet divergences. In the case of non smooth backgrounds the general recursive Seeley methods does not work. As an alternative approach the multiple reflection expansion had been proposed and its use was demonstrated in more complicated examples in [2]. High temperature expansions in terms of heat kernel coefficients had been studied in [3]. In two overview articles we reviewed applications of the heat kernel to strings [4] and recent developments in spectral geometry for "exotic" boundary value problems [5].

Field theory at finite temperature can be described by periodic boundary conditions in the imaginary time. Questions related to the temperature induced phase transition are investigated in the symmetric $O(N)$-model [6]. A new non-analytic expansion parameter was found [7,8].

The zeta functional methods has been applied to the mass of the supersymmetric kink clarifying the role of the boundary contributions [9].

Dilaton gravity models in two dimensions play an important role in understanding quantum gravity effects and the black hole dynamics. The paper [10] reviews developments in this field over the last decade.

References

[1] M. Bordag and K. Kirsten, Int. J. Mod. Phys. A **17**, 813 (2002).

[2] M. Bordag, H. Falomir, E. M. Santangelo and D. V. Vassilevich, Phys. Rev. D **65**, 064032 (2002).

[3] M. Bordag, V. V. Nesterenko and I. G. Pirozhenko, Nucl. Phys. Proc. Suppl. **104**, 228 (2002).

[4] D. V. Vassilevich, Nucl. Phys. Proc. Suppl. **104**, 208 (2002).

[5] P. Gilkey, K. Kirsten, J. H. Park and D. Vassilevich, Nucl. Phys. Proc. Suppl. **104**, 63 (2002).

[6] M. Bordag and V. Skalozub, Theor. Mat. Phys. **131**, 450 (2002) (translated from Teor. Mat. Fiz. **131** 4 (2002)).

[7] M. Bordag and V. Skalozub, Phys. Rev. D **65**, 085025 (2002).

[8] M. Bordag and V. Skalozub, Phys. Lett. B **533**, 182 (2002).

[9] M. Bordag, A. Scharff Goldhaber, P. van Nieuwenhuizen and D. Vassilevich, Phys. Rev. D **66**, 125014 (2002).

[10] D. Grumiller, W. Kummer and D. V. Vassilevich, Phys. Rep. **369**, 327 (2002).

14.1.2. Casimir Effect and Real Media

M. Bordag, B. Geyer, G. L. Klimchitskaya and V. M. Mostepanenko (St. Petersburg)

The vacuum of quantum fields shows a response to changes in external conditions with measurable consequences. The investigation of the electromagnetic vacuum in the presence of real media is of actual interest in view of current experiments. During the past years the Casimir effect has been measured with high accuracy. This required a detailed investigation of the influence of real experimental structures on the corresponding force. This allows for new constraints on hypothetical long range interactions which are predicted by supersymmetric extensions of the standard model. In [1] a detailed investigation of these constraints taking into account the real experimental structures has been done.

References

[1] B. Geyer, G. L. Klimchitskaya and V. M. Mostepanenko, Phys. Rev. A **65**, 062109 (2002).

14.1.3. Light-Cone Dominated Hadronic Processes

B. Geyer, J. Eilers, M. Lazar (MPI MiS, Leipzig), J. Blümlein (DESY-IfH, Zeuthen) and D. Robaschik (BTU, Cottbus)

Light-cone dominated (polarized) hadronic processes at large momentum transfer Q factorize into process-dependent hard scattering amplitudes and process-independent non-perturbative distribution amplitudes, whose Q^2–evolution is perturbatively determined. Growing experimental accuracy requires the entanglement of various twist as well as (target) mass contributions and radiative corrections. A quantum field theoretic prescription of these processes is based on the nonlocal light-cone expansion [1].

The group-theoretical procedure allowing for the decomposition of nonlocal tensor-valued light-ray operators into (tensorial) harmonic operators with well-defined (geometric) twist (= dimension − spin), thereby taking trace terms correctly into account [2], has been studied further and applied to new processes:

(1) Concerning special processes, former investigations of the polarized virtual Compton scattering at leading twist in the generalized Bjorken region [3] have been extended to the case with an additional (scalar) meson in the final state [4]. Thereby, triple-valued off-forward parton distribution amplitudes have been introduced. The related one-valued amplitudes, obtained by decomposing the Compton amplitude into collinear and non-collinear components, obey Wandzura-Wilczek and Callan-Gross like relations. The evolution of these distribution amplitudes has been determined.
In another study [5], in the spirit of [3], analogous considerations have been made for the case of polarized deep inelastic diffractive electron-proton scattering near the light-cone. Evolution equations of the diffractive hadronic matrix elements were derived for leading twist and compared with those of the (inclusive) deep-inelastic forward scattering (DIS). Diffractive parton densities are obtained as projections of two-variable parton distributions. Also Wandzura-Wilczek relations, similar to DIS, have been obtained.

(2) With the aim to take into account also target mass corrections for the above mentioned processes the twist decomposition on the light-cone [2] has been extended to the relevant off-cone operators [6]. Then, the non-forward matrix elements of the off-cone quark operators of definite twist (up to infinite twist in the case of scalar operators and up to twist 2 and 3 for tensor operators of mixed symmetry) in configuration space – leading to general off-diagonal distribution amplitudes – and their power resp. mass corrections have been given in terms of Bessel functions and, in the case of their moments, in terms of Gegenbauer polynomials. In addition, these results have been applied to the power corrections of the vector meson distribution amplitudes. – Now, these considerations will be continued up to infinite twist also in the case of vector operators and tensor operators of second order.

(3) The application of the foregoing results to virtual Compton scattering in the generalized Bjorken region and deep virtual Compton scattering requires, after a Fourier transformation, the convolution with the propagator in momentum space. Here, earlier work at leading twist [7] has to be extended to higher twist. A first step has been performed for the scalar operators showing that, after truncating with the relevant parts of the propagator, only a finite number of contributions of definite twist survives [8]. At present, the extension to the case of tensor

operators up to second order is under consideration.

References

[1] S. A. Anikin and O. I. Zavialov, Ann. Phys. (N.Y.) **116**, 135 (1978).
D. Müller, D. Robaschik, B. Geyer, F.-M. Dittes and J. Hořejši, Fortschr. Phys. **42**, 101 (1994), Preprint hep-th/9812448.

[2] B. Geyer, M. Lazar and D. Robaschik, Nucl. Phys. **B559**, 339 (1999).
B. Geyer and M. Lazar, Nucl. Phys. **B 581**, 341 (2000); Phys. Rev. **D 63**, 094003 (2001).

[3] J. Blümlein, B. Geyer and D. Robaschik, Nucl. Phys. **B560**, 283 (1999).
J. Blümlein and D. Robaschik, Nucl. Phys. **B581**, 449 (2000).
J. Blümlein, B. Geyer, M. Lazar and D. Robaschik, Nucl. Phys. B (Proc. Suppl.) **89**, 155 (2000).

[4] J. Blümlein, J. Eilers, B. Geyer and D. Robaschik, Phys. Rev. **D 65**, 054029 (2002), Preprint hep-ph/0108095.

[5] J. Blümlein and D. Robaschik, Phys. Rev. D **65**, 096002 (2002), Preprint hep-ph/0202077; Nucl. Phys. A **711**, 228 (2002), Preprint hep-ph/0207250.

[6] B. Geyer, M. Lazar and D. Robaschik, Nucl. Phys. **B 618**, 99 (2001).

[7] A.V. Belitzky and D. Müller, Phys. Lett. B **507**, 173 (2001).

[8] J. Eilers and B. Geyer, Phys. Lett. **B 546**, 78 (2002), Preprint hep-ph/0207104.

14.1.4. Quantum Symmetries of General Gauge Theories

B. Geyer, D. Mülsch (Wissenschaftszentrum Leipzig e.V.), D. M. Gitman and P. Yu. Moshin (U São Paulo), P. M. Lavrov (PU Tomsk), A. P. Nersessian (Yerevan State U) and I. V. Tyutin (Lebedev Inst., Moscow)

General gauge theories are characterized by local symmetries whose generators, in contrast to the well-known Yang-Mills theories, not necessarily obey a Lie algebra structure. Their gauge algebra may be open, i.e., close only up to the equations of motion, and, in addition, may be reducible (up to any finite order of reducibility) requiring for the introduction of various extra ghost and auxiliary fields. Nevertheless, the quantum symmetries of such theories [containing, e.g., higher dimensional and extended supersymmetric Yang-Mills theories, (super) string theories and topological field theories] are governed by (extended) BRST operations. Furthermore, these theories may be considered in external as well as composite (or condensate) fields and various background configurations.

Three different areas of research are to be reported:

(1) Given an arbitrary Lagrangian it is, in general, very difficult to find all its (gauge) symmetries. In order to attack this problem the structure of the Euler-Lagrange equations (ELE) for a general Lagrangian theory with finite degrees of freedom (having singular or nonsingular Lagrangian with higher derivatives of arbitrary order, with degenerate coordinates as well as external fields) has been studied [1]. Generalizing former results [2] for the ELE a reduction procedure to the so-called canonical form was presented where the equations are solved with respect to highest-order derivatives of non-gauge coordinates, whereas gauge coordinates and their derivatives enter in the right hand sides of the equations as arbitrary functions of time. This reduction procedure reveals the constraints in the Lagrangian formulation of singular systems and, in that respect, is similar to the Dirac procedure in the Hamiltonian formulation [3]. Thereby, for the first time, a constructive way of revealing the gauge identities between the ELE and, thus, finding all the gauge generators within the (covariant) Lagrangian formulation was presented. For local theories all the gauge generators are local in time operators. An extension to field theory is under consideration.

References

[1] B. Geyer, D. M. Gitman and I. V. Tyutin, *Canonical form of Euler-Lagrange equations and gauge symmetries,* Preprint hep-th/0212289; *Reduction of Euler-Lagrange equations in gauge theories*, Proc. Second Londrina Winter School: "Mathematical Methods in Physics", August 25-30, 2002, Londrina, Parana (Brazil), to appear: Int. J. Mod. Phys. **A** (2003).

[2] D. M. Gitman and I. V. Tyutin, *Quantization of Fields with Constraints* (Springer, Berlin 1990); *Constraint reorganization consistent with Dirac procedure,* Preprint hep-th/0112103; *Multiple Facets of Quantization and Supersymmetry*, in: *Michael Marinov Memorial Volume* (World Publishing, Singapore, 2002); Nucl. Phys. B **630**, 509 (2002), Preprint hep-th/0201143.

[3] P. A. M. Dirac, *Lectures on Quantum Mechanics* (Belfer Graduate School of Science, Yeshiva University, New York, 1964).

(2) There exist various (related) methods of covariant Lagrangian quantization of general gauge theories which generalize the field-antifield approach of Batalin & Vilkovisky (BV) [1]. Two of

them, the $Sp(2)-$symmetric approach of Batalin, Lavrov & Tyutin (BLT) [2] and the (modified) triplectic quantization (TQ) [3,4] have been applied and considered in detail.
First, continuing our former study of W_2-gravity [5], we considered the model of W_3-gravity [6] – possibly the simplest one with open gauge algebra – within the BV-formalism to study the arbitrariness in the realization of the gauge algebra. We obtained a one-parametric non-analytic extension of the gauge algebra, and a corresponding solution of the classical master equation, related via an anti-canonical transformation to a solution corresponding to an analytic realization. Motivated by this result, we investigated the possibility of getting closed solutions of the classical master equation in the BLT-formalism and showed that such solutions do not exist in the approximation up to the third order in ghost and auxiliary fields.
Second, we looked for a formulation of (modified) TQ in general coordinates [7,8] and showed that the specific operators V^a appearing in TQ can be viewed as anti-Hamiltonian vector fields generated by a second-rank irreducible $Sp(2)$ tensor. This allowed for an explicit realization of the triplectic algebra being constructed from an arbitrary Poisson bracket on the space of the fields, equipped by the flat Poisson connection. In addition, the whole space of fields and antifields can be equipped by an even supersymplectic structure, when the Poisson bracket is non-degenerate. This opened the possibility to provide the BRST/antiBRST path integral by a well-defined integration measure, as well as to establish a direct link between the BLT- and the Hamiltonian BRST quantization schemes. Furthermore, we found [8] that the primary version of TQ [3] and its modified form [4] are special examples of 3-parametric class of quantization procedures.

References

[1] I. A. Batalin and G. A. Vilkovisky, Phys. Lett. B **102**, 27 (1981); Phys. Rev. D **28**, 2567 (1983) [E: **30**, 508 (1984)]; Nucl. Phys. B **234**, 106 (1984).

[2] I. A. Batalin, P. M. Lavrov and I. V. Tyutin, J. Math. Phys. **31**, 1487 (1990); *ibid.* **32**, 532 (1990); *ibid.* **32**, 2513 (1990).

[3] I. A. Batalin and R. Marnelius, Phys. Lett. B **350**, 44 (1995); Nucl. Phys. B **465**, 521 (1996).
I. A. Batalin, R. Marnelius and A. M. Semikhatov, Nucl. Phys. B **446**, 249 (1995).

[4] B. Geyer, D. M. Gitman, and P. M. Lavrov, Mod. Phys. Lett. A **14**, 661 (1999); Theor. Math. Phys. **123**, 813 (2000).

[5] B. Geyer, P. M. Lavrov and P. Yu. Moshin, Int. J. Mod. Phys. A **16**, 4297 (2001).

[6] B. Geyer, D. M. Gitman, P. M. Lavrov and P. Yu. Moshin, *On problems of the Lagrangian quantization of W_3-gravity*, Preprint hep-th 0301060, submitted to: Int. J. Mod. Phys. A.

[7] B. Geyer, P. M. Lavrov and A. P. Nersessian, Phys. Lett. B **512**, 211 (2001).

[8] B. Geyer, P. M. Lavrov and A. P. Nersessian, Int. J. Mod. Phys. A **17**, 349 (2002).

(3) Topological quantum field theories (TQFT) are the simplest QFT's with the defining property that their Green functions are independent of the local Riemannian structure of the underlying manifold. There are two classes of TQFT [1], namely (i) Schwarz type topological theories, which are manifestly free of any metric dependence, and (ii) Witten type or cohomological topological theories, where the stress tensor as well as the partition and correlation functions are independent of the choice of the metric.
Concerning our investigation of topological field theories we introduced a new type of topological matter interactions involving second-rank tensor matter fields with an underlying $N_T \leq 1$ topological supersymmetry [2]. The example of the 4-dimensional $N_T = 1$ super BF model and

the $N_T = 2$ topological B-model with tensor matter has been explicitly worked out.
In addition, we constructed various non-abelian examples of cohomological gauge theories of Hodge type, i.e., theories where the generators of the topological shift, co-shift and gauge symmetry together with a discrete Hodge-type $\star-$operation obey a complex being completely analogous to the de Rham complex. In these theories the physical states are 'harmonic' in that terminology. First, by dimensional reduction of the Blau-Thompson model [3] from 3 to 2 dimensions we obtained a $N_T = 4$ Hodge-type theory with global symmetry group $SU(2)$ [4] which can also be obtained by the 'novel' twist of the $N = 8, D = 2$ super Yang-Mills theory. Second, by constructing a 5-dimensional analogue of the Blau-Thompson model and reducing it to $D = 2$ dimensions we obtained a $N_T = 8$ Hodge-type theory with global symmetry group $SU(4)$ [5] which can also be obtained by the 'novel' twist of the $N = 16, D = 2$ super Yang-Mills theory.

References

[1] E. Witten, Commun. Math. Phys. **117**, 353 (1988); *ibid.* **121**, 351 (1989); Int. J. Mod. Phys. A **6**, 2775 (1991).
D. Birmingham, M. Blau, M. Rakowski and G. Thompson, Phys. Rep. **209**, 129 (1991).
O. Piguet, *Introduction to supersymmetric gauge theories*, Preprint hep-th/9710095.
F. Fucito, A. Tanzini, O. S. Ventura, L. C. Q. Vilar and S. P. Sorella, *Algebraic renormalization: Perturbative considerations on topological Yang-Mills theory and on $N = 2$ supersymmetric gauge theories*, Preprint hep-th/9707209.

[2] B. Geyer and D. Mülsch, Phys. Lett. B **535**, 349 (2002).

[3] M. Blau and G. Thompson, Nucl. Phys. B **492**, 545 (1997).

[4] B. Geyer and D. Mülsch, Phys. Lett. B **518**, 181 (2001); Int. J. Mod. Phys. A **17**, 4425 (2002).

[5] B. Geyer and D. Mülsch, $N_T = 8, D = 2$ *Hodge-type cohomological gauge theory with global $SU(4)$ symmetry,* Preprint hep-th/0210268; *Higher dimensional analogue of the Blau-Thompson model and $N_T = 8, D = 2$ Hodge-type cohomological gauge theories,* Preprint hep-th/0211061.

14.1.5. Algebro-Geometric Solutions to the Ernst Equation and Twistor Theory

S. Kolditz and O. Richter

In general relativity the class of stationary and axisymmetric space-times is of particular importance. The interest comes from the fact that the space-times of isolated bodies of revolution are usually supposed to be stationary and axisymmetric. The field corresponding field equations are equivalent to one nonlinear complex differential equation, the Ernst equation. This equation has some mathematically interesting features. First, it belongs to the class of completely integrable equations, for which the inverse spectral method can be applied successfully, see [1]. Second, it is a symmetry reduction of the anti-self dual Yang-Mills equations. It is well known that the anti-self dual solutions to the Yang-Mills equations are related via the Penrose transform to algebraic bundles over the projective twistor space $\mathbb{C}\mathrm{P}^3$. Similarly, Mason and Woodhouse were able to show that solutions to the Ernst equation can be interpreted in terms of bundles over some reduced twistor space, see [2].

For a class of solutions to the Ernst equation with physically reasonable properties, see [3], the corresponding metric functions may be expressed in terms of theta functions on hyperelliptic Riemann surfaces. We were able to characterize explicitly the holomorphic vector bundles over the reduced twistor space in terms of patching matrices.

This allows us to give a geometrical interpretation of the analytic solutions of [3] in terms of holomorphic bundles over the reduced twistor space, see [4]. With the local data encoded in the patching matrices at hand it should now be possible to determine the corresponding invariants of the bundles, e.g. characteristic classes, in order to get a better geometrical understanding of the solutions found.

References

[1] D. A. Korotkin, Theor. Math. Phys. **77**, 1018 (1989).

[2] N. M. J. Woodhouse and L. J. Mason, Nonlinearity **1**, 73 (1988).

[3] C. Klein and O. Richter, Phys. Rev. D **58**, 124018 (1998).

[4] O. Richter, *Proceedings of GR16* (Durban, 2001).

14.1.6. Structure of the Gauge Orbit Space and Study of Gauge Theoretical Models

G. Rudolph, C. Fleischhack, P. Jarvis (Hobart), J. Kijowski (Warsaw), M. Schmidt and I. P. Volobuev (Moscow)

The results concerning the structure of the gauge orbit space obtained in recent years, together with an invited review, were published [1,2]. The programme for investigating the role of non-generic strata for quantum gauge theory has been pushed forward. There are first results on singular Marsden-Weinstein reduction [3] and geometric quantization [4] for the model space $SU(3)$. Neglecting, for the time being, some delicate mathematical aspects, the analogous problem for full Yang-Mills theory on compact manifolds is under investigation, too.

The study of non-perturbative aspects of gauge theories on the lattice in terms of gauge invariant fields was continued. Applying similar techniques as for spinorial lattice QED [5], the observable algebra and the charge superselection structure of scalar lattice QED was clarified, see [6]. An analogous, but much more complicated analysis of lattice QCD [7] was essentially pushed forward (with a couple of publications being in preparation).

Christian Fleischhack continued the study of gauge theories within the Ashtekar approach, with special emphasis on noncompact structure groups and applications in quantum gravity.

The project was supported by the Max-Planck Institute for Mathematics in the Sciences, by the Alexander-von-Humboldt Foundation and by DFG.

References

[1] G. Rudolph, M. Schmidt and I. P. Volobuev, J. Math. Phys. Anal. Geom. **5**, 201 (2002); J. Geom. Phys. **42**, 106 (2002).

[2] G. Rudolph, M. Schmidt and I. P. Volobuev, J. Phys. A: Math. Gen. **35**, R1 (2002).

[3] R. Sjamaar, E. Lerman, Ann. Math. **134**, 375 (1991).

[4] J. Huebschmann, J. Reine Angew. Math. **408**, 57 (1990); Preprint math.dg/0104213; Preprint math.sg/0207166.

[5] J. Kijowski, G. Rudolph and A. Thielmann, Commun. Math. Phys. **188**, 535 (1997).

[6] J. Kijowski, G. Rudolph and C. Śliwa, Preprint hep-th/0203214.

[7] J. Kijowski, G. Rudolph, J. Math. Phys. **43**, 1796 (2002).

14.1.7. Noncommutative Geometry

G. Rudolph, D. Calow, P. Hajac (Warsaw), R. Matthes (Clausthal), O. Richter and W. Szymanski (Newcastle)

The study of the theory of foliations in the sense of Connes [1] was continued. In particular, several spectral triples related to the Kronecker foliation of the 2-torus have been constructed [2]. Moreover, the associated differential calculi were studied and for one spectral triple the topological invariant (Chern character) was calculated. The study of the Hopf algebra, associated to a foliation, was initiated.

The study of quantum principal bundles in the sense of Budzyński and Kondracki was continued [3,4]. It was shown that the interpretation of the quantum disc and the quantum real projective space as quotients of Podles quantum spheres can be understood in terms of graph C^*-algebras [5]. Concerning the study of quantum Hopf bundles, Chern-Connes pairings between traces on the basis algebra and the K^0-classes for projectors of line bundles associated with a quantum Hopf bundle were calculated. This way, one obtains the winding numbers of these line bundles and one can conclude the topological non-triviality of the quantum Hopf bundle. A paper on this subject is in preparation.

The projects were supported by the Max-Planck-Institute for Mathematics in the Sciences and DFG.

References

[1] A. Connes and H. Moscovici, GAFA **5** (2), 174 (1995).

[2] R. Matthes, O. Richter and G. Rudolph, Preprint math-ph/0201066, to appear in J. Geom. Phys.; *Spectral triples for the Kronecker foliation*, to appear in: *Proceedings 2nd Symposium on Quantum Theory and Symmetries* (Krakow, 2001).

[3] D. Calow and R. Matthes, J. Geom. Phys. **41**, 114 (2002).

[4] R. Matthes, Preprint math.qa/0210199.

[5] P. M. Hajac, R. Matthes and W. Szymański, Preprint math.qa/0209268.

14.1.8. Contributions to Quantum Informatics

A. Uhlmann, P. Alberti, B. Crell and J. Dittmann (IMath)

The following problems were studied: representation and properties of the fidelity of density operators and related quantities [1,2], differential geometry of monotonous metrics on the space of states, in particular, of Bures' metric, properties of purifying lifts, transport of states, and geometrical phases [3], refinements of Bures' metric (partial fidelities, decomposition of pairs of states), operators and mappings related to Einstein-Podolski-Rosen channels and quantum teleportation [4]. Furthermore, characteristic parameters (entropy, channel capacity) for quantum channels of length two were calculated. The use of anti-linearity in quantum information and possible connections with k-positivity were discussed. Algebraic formulations of some basic concepts of quantum information theory, i.e. entanglement, asymptotic conversibility, and their relation to partial orderings of states were developed.

References

[1] P. Alberti and A. Uhlmann, Acta Applicandae Mathematica **60**, 1 (2000).

[2] A. Uhlmann, Preprint quant-ph/9909060; Preprint quant-ph/9912114.

[3] J. Dittmann and A. Uhlmann, J. Math. Phys. **40**, 3246 (1999).

[4] A. Uhlmann, in: *Fin De Siecle*, LNP 539 (Springer, Berlin, 2000), p. 93; in: *Trends in Quantum Mechanics* (World Scientific, Singapore, 2000), p. 128.

14.1.9. One-Particle Properties of Quasiparticles in the Half-Filled Landau Level

W. Weller and W. Apel (PTB Braunschweig)

Using field theoretical methods, two-dimensional electron systems in strong magnetic fields were studied. The investigations were concentrated on the half-filled lowest Landau level.

The theory for the half-filled lowest Landau level of Halperin *et al.* [1] transforms from the electrons to Chern–Simons fermions by eliminating the external magnetic field. The theory leads to an infrared divergent energy. It was shown [2] that this is due to missing diagrams and to the fact that in [1] the ordering of the operators in the path integral was changed. The correct formulation yields a three-particle interaction. For this interaction, a path integral representation was developed [2] with correct ordering of the operators by using time steps with intermediate times.

The energy was computed by evaluating the path integral in various approximations. The calculated energies are convergent and agree well with numerical simulations. The idea of the Singwi–Sjölander approach to the 3d Coulomb problem was extended to the Chern–Simons theory [3] with even better results for the energies.

An approximation scheme was developed conserving the particle number and the constraints. Now, the conserving Hartree–Fock approximation is being numerically evaluated. The self energy of the Chern–Simons fermions is until now infrared divergent. For the solution of that problem we started investigations based on a transformation introduced by Bohm and Pines and by Shankar and Murthy [4]; that transformation transforms from the Chern–Simons fermions to the composite fermions (CF), which include the correlation hole. The conserving approximations are extended to the CF.

The project was supported by DFG (Schwerpunktprogramm "Quanten-Hall-Systeme", WE 480/3-2)

References

[1] B. I. Halperin, P. A. Lee and N. Read, Phys. Rev. B **47**, 7312 (1993).

[2] W. Weller, J. Dietel, Th. Koschny and W. Apel, in: *Proceedings 6th Int. Conf. on Path Integrals*, eds. R. Casalbuoni *et al.* (World Scientific, Singapore 1999), p. 466.

[3] J. Dietel and W. Weller, Phys. Rev. B **64**, 195307 (2001).

[4] R. Shankar and G. Murthy, Phys. Rev. Lett. **79**, 4437 (1997).

14.2. Theory of Elementary Particles (TET)

The Particle Physics Group performs basic research in the quantum field theoretic description of elementary particles and in phenomenology. Topics of current interest are conformal symmetry and its breaking in the context of supersymmetric theories, renormalization problems, electroweak matter at finite temperature and the derivation of Regge behaviour of scattering amplitudes from Quantum Chromodynamics. Perturbative and non-perturbative methods are applied to answer the questions. In perturbation theory the work is essentially analytical using computers only as a helpful tool. Lattice Monte Carlo calculations as one important non-perturbative approach however are based on computers as an indispensable instrument. Correspondingly the respective working groups are organized: in analytical work usually very few people collaborate, in the lattice community rather big collaborations are the rule. Our group is involved in many cooperations on the national and international level (DESY, Munich; France, Russia, Armenia, USA, Japan). Since elementary particles are very tiny (of the order of 10^{-15} m) and for the study of their interactions large accelerators producing enormously high energy are needed, it is clear that results in this direction of research do not have applications in daily life immediately. To clarify the structure of matter is first of all an aim in its own and is not pursued for other reasons. But particle theory has nevertheless a very noticeable impact on many other branches by its power of providing new methodological insight. Similarly for the student specializing in this field the main benefit is her/his training in analysing complex situations and in applying tools which are appropriate for the respective problem. As a rule there will be no standard procedures which have to be learned and then followed, but the student has to develop her/his own skill according to the need that arises. This may be a mathematical topic or a tool in computer application. Jobs which plainly continue these studies are to be found at universities and research institutes only. But the basic knowledge which one acquires in pursuing such a subject opens the way to many fields where analytical thinking is to be combined with application of advanced mathematics. Nowadays this seems to be the case in banks, insurance companies and consulting business.

14.2.1. Quantum Field Theory on Noncommutative Spacetime

C. Dehne, Y. Liao and K. Sibold

Quantum field theory on noncommutative (NC) spacetime as formulated in Ref. [1] has been shown to violate the unitarity of S matrix [2]. The main feature in this formalism as compared to ordinary theory is the appearance of phases involving the NC parameter and relevant momenta. Doubts on it have been raised recently in Ref. [3] by reformulating in φ^3 theory the equation of motion in terms of the Yang-Feldman equation. Its solution is found to be manifestly Hermitian, hence the theory must be unitary even if time-space NC is nonvanishing, in accord with general considerations of Ref. [4]. But this does not yet explain why one arrives at violation of unitarity in the same model when using the formalism of Ref. [1]. Starting from some standard assumptions about perturbation theory, we have shown [5] that the answer is very simple. When performing field contractions properly according to Wick's theorem, one can never combine the contraction functions of positive and negative frequency to the causal Feynman propagator. This arises because when time does not commute with space, the time-ordering procedure does not commute with the star multiplication either. The formalism in terms of Feynman propagators is thus not well founded in this case. Instead, the correct procedure of doing perturbation in NC field theory is just the time-ordered perturbation theory extended to the NC case. The NC phases in this framework involve exclusively on-shell momenta which makes the analyticity properties of Green functions considerably different from those following the approach of Ref. [1]. The unitarity is shown to be preserved as long as the interaction Lagrangian is explicitly Hermitian [6]. As the picture of perturbation theory has been changed already at tree level, phenomenological results obtained previously will be modified accordingly, some of which have been worked out in Ref. [7] for future linear colliders.

We have also studied the spectral representation and dispersion relations that follow from some basic assumptions and the reduced spacetime symmetries on noncommutative (NC) space [8]. We found that kinematic variables involving the NC parameter appear naturally as parametric variables in this analysis. When subtractions are necessary to remove ultraviolet divergences, they are always made at the fixed values of these NC variables. Our analysis of the reduced spacetime symmetries suggests a weaker microcausality requirement. Starting from it, we made a first attempt at dispersion relations for forward scattering. It turns out that the attempt is hampered by a new unphysical region specified by a given motion in the NC plane which does not seem to be surmountable using the usual tricks.

The project is supported by a grant from DESY in Zeuthen.

References

[1] T. Filk, Phys. Lett. B **376**, 53 (1996).
[2] J. Gomis and T. Mehen, Nucl. Phys. B **591**, 265 (2000).
[3] D. Bahns *et al.*, Phys. Lett. B **533**, 178 (2002).
[4] S. Doplicher, K. Fredenhagen and J. E. Roberts, Commun. Math. Phys. **172**, 187 (1995).
[5] Y. Liao and K. Sibold, Eur. Phys. J. C **25**, 469 (2002).
[6] Y. Liao and K. Sibold, Eur. Phys. J. C **25**, 479 (2002).
[7] Y. Liao and C. Dehne, Preprint hep-ph/0211425.
[8] Y. Liao and K. Sibold, Phys. Lett. B **549**, 352 (2002).

14.2.2. Supersymmetric Yang-Mills Theory with Local Coupling: The Supersymmetric Gauge

K. Sibold, E. Kraus (Bonn) and Ch. Rupp (Karlsruhe)

When one introduces within supersymmetric Yang-Mills theory a local, i.e. space-time dependent coupling (which for consistency has to be a chiral superfield) one encounters an anomaly. This has first been detected in the Wess-Zumino gauge where the anomaly has a natural place in the supersymmetry transformation of this coupling function. In a formulation where supersymmetry is realized linearly its place changes. It may now appear in either one of two identities: the first one describes the non-renormalization of the topological term, the second relates the renormalization of the gauge coupling to the renormalization of the complex supercoupling. Only one of the two equations can be maintained in perturbation theory. The two possibilites are discussed and the respective β-function of the local coupling is derived. It is non-holomorphic in the first version, but directly related to the coupling renormalization. It is holomorphic in the second version, but has a non-trivial, i.e. anomalous relation to the β-function of the gauge coupling.
The physical consequences of this anomaly have still to be found. They may either refer to an interesting relation between scaling and topological properties as indicated by the above formulation where supersymmetry is manifest or they may point to breaking of supersymmetry as indicated by the Wess-Zumino gauge formulation. In any case it is clear that the consequences must be identical when formulated for truly physical quantities.
In the context of string theory the question whether the gauge coupling when extended to a local field gets renormalized in a holomorphic or non-holomorphic fashion has quite some importance. It is to be noted however that usually the extension is not to a superfield which from the start causes inconsistencies. In any case it is clear that the above findings clarify the situation completely.

References

[1] E. Kraus, Ch. Rupp and K. Sibold, Preprint hep-th/0212064.

[2] E. Kraus, Nucl. Phys. B **620**, 55 (2002), Preprint hep-th/0107239.

[3] E. Kraus, Phys. Rev. D **65**, 115012 (2001), Preprint hep-ph/0110323.

[4] O. Piguet and K. Sibold, *Renormalized Supersymmetry. The Perturbation Theory Of N=1 Supersymmetric Theories In Flat Space-Time* (Birkhäuser, Boston, 1986).

14.2.3. Confinement, Deconfinement and the Photon Propagator in 3D cQED on the Lattice

M. N. Chernodub (ITEP Moscow/Kanazawa University), E.-M. Ilgenfritz (Humboldt-Universität zu Berlin) and A. Schiller

Three–dimensional compact electrodynamics ($cQED_3$) shares two essential features with QCD, confinement [1] and chiral symmetry breaking. Confinement of electrically charged particles is caused by a plasma of monopoles which emerge due to the compactness of the gauge field. Here we study the lattice gauge boson propagator of 3D compact QED in Landau gauge at zero and non-zero temperature [2,3].

In order to discuss the form of the propagator from the monopole plasma point of view, we decompose the gauge fields links into singular (monopole) and regular (photon) contributions. Once that decomposition is done, one is free to define the the decomposition of the propagator into monopole, photon and mixed contributions.

Non-perturbative effects are reflected by the generation of a mass m, by an anomalous dimension α and by the photon wave function renormalization Z. These effects can be attributed to monopoles: they are absent in the propagator of the regular (photon) part of the gauge field. The rôle of Gribov copies is carefully investigated.

A typical propagator behaviour at zero temperature is visualized in Fig. 1(a), results for α and m are shown in Fig. 1(b), the extracted nonperturbative mass is compared to a theoretical prediction.

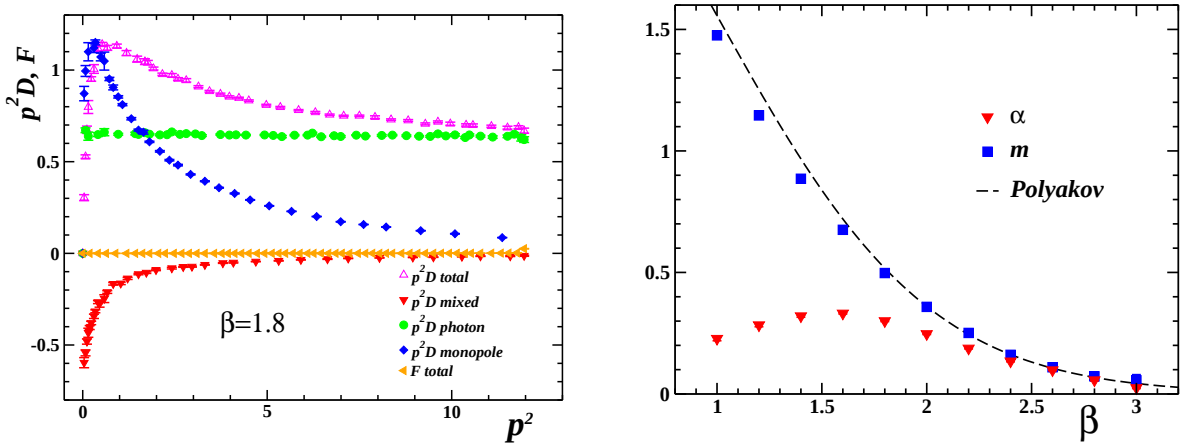

(a) (b)

Figure 1. (a) The transverse propagator p^2D and its contributions, as well as the (vanishing) longitudinal propagator F vs. p^2 at $\beta = 1.8$. (b) Fitted α and m vs. β for D.

References

[1] A. M. Polyakov, Nucl. Phys. B **120**, 429 (1977).

[2] M. N. Chernodub, E. M. Ilgenfritz and A. Schiller, Phys. Rev. Lett. **88**, 231601 (2002).

[3] M. N. Chernodub, E. M. Ilgenfritz and A. Schiller, Preprint hep-lat/0208013, to be published in Phys. Rev. D.

14.2.4. String Breaking and the Photon Propagator in the 3D Lattice Abelian Higgs Model

M. N. Chernodub (ITEP Moscow/Kanazawa University), E.-M. Ilgenfritz (Humboldt-Universität zu Berlin) and A. Schiller

Nowadays, the interest in the lattice Abelian Higgs model with compact gauge field (cAHM) in three dimensions has grown because of its relation to high energy physics [1,2] and its applications in condensed matter physics [3].

We have studied on the lattice the breaking of the string spanned between test charges in the three dimensional Abelian Higgs model with compact gauge field and fundamentally charged Higgs field at zero temperature in the London limit [4]. In agreement with current expectations we demonstrate that string breaking is associated with pairing of monopoles. However, the string breaking is not accompanied by an ordinary phase transition.

In addition we have studied the Landau gauge photon propagator in that model [5]. The total gauge field is split into singular and regular parts. On the confinement side of the string breaking crossover the momentum dependence of the total propagator is characterized by an anomalous dimension similarly to 3D compact QED. At the crossover and throughout the Higgs region the anomalous dimension disappears. This result perfectly agrees with recent observations that the monopole–antimonopole plasma leads to nonzero anomalous dimension and the presence of the matter fields causes monopole pairing into dipole bound states. The Yukawa mass characterizing the propagator part from regular gauge fields is non-vanishing at the Higgs side and coincides with the mass found for the total propagator. The regular gauge field without anomalous dimension becomes massless at the crossover and in the confinement region.

References

[1] E. H. Fradkin and S. H. Shenker, Phys. Rev. D **19**, 3682 (1979).

[2] M. B. Einhorn and R. Savit, Phys. Rev. D **17**, 2583 (1978); *ibid.* **19**, 1198 (1979).

[3] H. Kleinert, F. S. Nogueira and A. Sudbø, Phys. Rev. Lett. **88**, 232001 (2002), Preprint hep-th/0209132.

[4] M. N. Chernodub, E. M. Ilgenfritz and A. Schiller, Phys. Lett. B **547**, 269 (2002), Preprint hep-lat/0207020.

[5] M. N. Chernodub, E. M. Ilgenfritz and A. Schiller, Phys. Lett. B **555**, 206 (2003), Preprint hep-lat/0212005.

14.2.5. High Energy Asymptotics and Integrable Quantum Systems

D. Karakhanyan (Yerevan, Armenia) and R. Kirschner

Aim of the project

The main aim of this project is to develop methods for treating the Regge and Bjorken limits in gauge theories like QCD. We rely on the idea of the high-energy effective action [1] which we have shown in recent years to be a useful tool for analyzing the asymptotics of scattering amplitudes. In the Regge case the action describes the scattering by the exchange of reggeized quarks and gluons. The reggeon and parton interactions exhibit remarkable symmetry properties and can be related to integrable quantum systems.

Collaboration

In 2002 on this project have been working R. Kirschner and D. Karkhanyan (Yerevan, visit supported by BMBF/IB). There is a collaboration with L. N. Lipatov (St. Petersburg), L. Szymanowski (Warsaw, Paris-Palaiseau) and G. K. Korchemsky (Paris-Orsay).

Results

The leading parton interaction in the Bjorken asymptotics has been studied in the effective action formulation. The conformal representation of the interaction has been derived in a direct way avoiding the conventional momentum representation [2] .

We have constructed the spectral and integral forms of the universal Yang-Baxter operators with one-dimensional q-deformed conformal ($sl(2)$)) symmetry [3] in a representation related to the one appearing in the treatment of the QCD Bjorken asymptotics.

References

[1] L. N. Lipatov, Nucl. Phys. B **365**, 614 (1991).
R. Kirschner, L. N. Lipatov and L. Szymanowski, Nucl. Phys. B **452**, 579 (1994); Phys. Rev. D **51**, 838 (1995).
L. N. Lipatov, Nucl. Phys. B **452**, 369 (1995).
R. Kirschner and L. Szymanowski, Phys. Rev. D **52**, 2333 (1995); Phys. Lett. B **419**, 348 (1998); Phys. Rev. D **58**, 014004 (1998).

[2] R. Kirschner, *Parton interactions in the Bjorken asymptotics*, Preprint NTZ 09/2002, to appear in the proceedings of the 36th Winter School of St. Petersburg Nucl. Phys. Institute, Preprint hep-ph/0212248.

[3] D. Karakhanyan, R. Kirschner and M. Mirumyan, Nucl. Phys. B **636**, 529 (2002), Preprint nlin.si/0111032.

14.2.6. The Spin Structure of the Λ Hyperon in Lattice QCD

M. Göckeler, R. Horsley (University of Edinburgh), D. Pleiter (John von Neumann–Institut für Computing NIC, Zeuthen), P. E. L. Rakow (University of Liverpool), S. Schaefer (Universität Regensburg), A. Schäfer (Universität Regensburg) and G. Schierholz (John von Neumann–Institut für Computing NIC, Zeuthen, and DESY, Hamburg)

The investigation of the nucleon spin structure during the last few years has stimulated a large number of efforts to understand the results with quark models of various kinds. It turned out that the breaking of SU(3) flavour symmetry is of central importance for any such effort. The Λ spin structure is especially sensitive to flavour SU(3) breaking (see, e.g., Refs. [1,2]). While in the naive SU(6) quark model the spin of the Λ is carried exclusively by the s quarks, the SU(3) rotated results for the nucleon spin structure suggest that the s and $\bar{s}$ quarks carry only $\approx 60\%$ of the Λ spin while u, $\bar{u}$, d and $\bar{d}$ quarks quarks contribute $\approx -40\%$.

Thus, there is ample motivation to perform lattice calculations which provide information on the internal Λ structure, and we have performed such calculations in the valence approximation on a lattice with a lattice spacing of $\approx 0.1\,\mathrm{fm}$ [3]. We worked with nine combinations of bare quark masses $m_u = m_d$, $m_s \in \{166, 112, 58\}$ MeV (approximately), parametrised by the corresponding hopping parameters $\kappa_u = \kappa_d$, κ_s. So we could *extra*polate to the chiral limit κ_c in $\kappa_u = \kappa_d$ and *inter*polate in κ_s to the physical value κ_s^*. From the Λ masses at our nine combinations of κ_d, κ_s we have computed Λ masses at $\kappa_d = \kappa_c$ by linear extrapolation of M_Λ^2 in $1/\kappa_d$. These 12 masses are plotted in Fig. 1. At κ_s^* the ratio $M_\Lambda/M_p = 1.19$ is reproduced quite accurately. The plot shows clearly the breaking of the SU(3) flavour symmetry. In particular, the dependence of the masses on κ_d is rather pronounced.

Matrix elements of various two-quark operators in the Λ were computed from ratios of three-point functions over two-point functions (for a recent review of the method and further results see Ref. [4]). In particular, we studied the axial-vector current $\bar{q}\gamma_\mu\gamma_5 q$, whose expectation values in a polarised Λ are proportional to Δq, the fraction of the spin carried by the quarks (and antiquarks) of flavour q. In contrast with the case of M_Λ/M_p, the dependence on κ_d turned out to be rather weak. Values corresponding to $\kappa_d = \kappa_c$ were obtained by extrapolating the matrix elements linearly in $1/\kappa_d$. Finally, by interpolating the matrix elements for $\kappa_d = \kappa_c$ linearly in $1/\kappa_s$ to $1/\kappa_s^*$ we obtained the desired Λ matrix elements with the result: $\Delta u_\Lambda = \Delta d_\Lambda = -0.02(4)$, $\Delta s_\Lambda = 0.68(4)$.

Let us discuss these results in more detail. Applying flavour SU(3) to Monte Carlo results for Δq in the proton, which suffer from similar uncertainties as discussed above, one finds $\Delta u_\Lambda = \Delta d_\Lambda = -0.016(9)$, $\Delta s_\Lambda = 0.65(2)$ in good agreement with the matrix elements computed directly in the Λ. This implies again that the flavour symmetry breaking effects in the matrix elements are rather small. As the mass difference between the light quarks and the strange quark was consistently taken into account this provides a strong argument that the Λ and proton spin structures are, in good approximation, simply related by an SU(3) transformation. Consequently, the values $\Delta u_\Lambda = \Delta d_\Lambda = -0.17(3)$, $\Delta s_\Lambda = 0.63(3)$, which were computed from the proton spin structure under the assumption of flavour SU(3)(see, e.g., [2]), should be quite reliable.

Because we worked in the valence approximation it might be more consistent to compare our results to the prediction for the valence quark contribution, e.g. by Ashery and Lipkin [2]. They obtained $\Delta u_\Lambda = \Delta d_\Lambda = -0.07(4)$, $\Delta s_\Lambda = 0.73(4)$. Notice that all results differ markedly from the predictions of the (naive) quark model $\Delta u_\Lambda = \Delta d_\Lambda = 0$, $\Delta s_\Lambda = 1$.

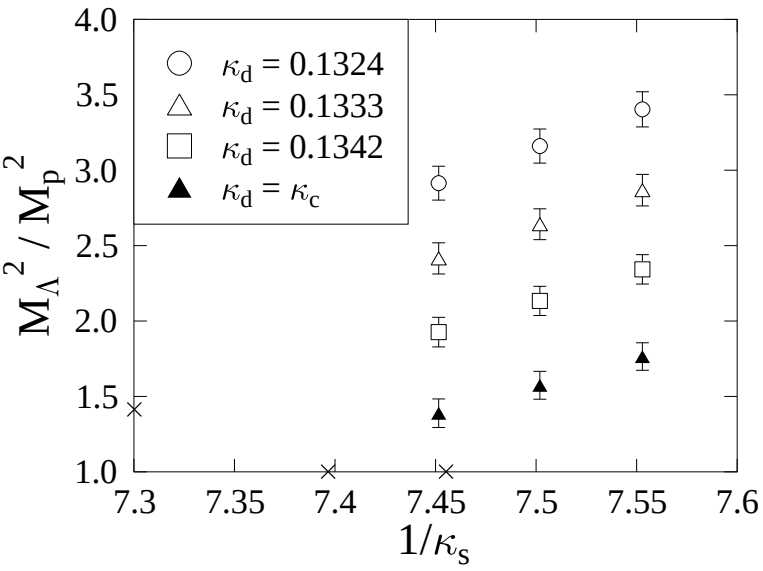

Figure 1. The square of the ratio M_Λ/M_p with the proton mass M_p taken in the chiral limit versus $1/\kappa_s$. The different symbols correspond to the different values of κ_d including the chiral limit. The crosses (left to right) indicate the physical value of M_Λ/M_p, $1/\kappa_c$, and $1/\kappa_s^*$, respectively.

This work was supported in part by the Deutsche Forschungsgemeinschaft, by BMBF and by the European Community's Human Potential Program. The numerical calculations were performed on the Quadrics computers at DESY Zeuthen. We wish to thank the operating staff for their support.

References

[1] M. Burkardt and R. L. Jaffe, Phys. Rev. Lett. **70**, 2537 (1993).
R. L. Jaffe, Phys. Rev. D **54**, 6581 (1996).

[2] D. Ashery and H. J. Lipkin, Phys. Lett. B **469**, 263 (1999).

[3] M. Göckeler, R. Horsley, D. Pleiter, P. E. L. Rakow, S. Schaefer, A. Schäfer and G. Schierholz, Phys. Lett. B **545**, 112 (2002).

[4] M. Göckeler, R. Horsley, D. Pleiter, P. E. L. Rakow, A. Schäfer and G. Schierholz, Preprint hep-lat/0209160.

14.3. Theory of Condensed Matter (TKM)

The topics of research in the Theory of Condensed Matter group are stochasticity and disorder as well as structure formation in soft condensed matter and solids, models of complex biological systems, strongly correlated electron systems, and superconducting materials. Investigations using modern analytic methods and computer applications complement and stimulate each other. Research is performed in cooperation with mathematicians as well as with theoretical and experimental physicists, biologists and researchers in medicine. There are well established collaborations with research groups in France, Germany, Italy, Russia, Switzerland, UK, and USA.

Noise induced phenomena are studied in a number of different systems. Structure formation, stochastic stability, and on-off intermittency is investigated in liquid crystals driven by stochastic electric fields (Cooperation with the Institute for Experimental Physics I). Noise induced non-equilibrium phase transitions are studied in coupled arrays of stochastically driven nonlinear systems. The statistics of first passage times and self-organized criticality is investigated in stochastic nonlinear systems with time delay.

Mathematical modelling of the immune system. Using methods of nonlinear dynamics and statistical physics, we study the architecture and the random evolution of the idiotypic network of the B-cell subsystem and describe the regulation of balance of Th1/Th2-cell subsystems, its relation to allergy and the hyposensitization therapy (Cooperation with the Institute for Clinical Immunology and Transfusion Medicine).

Strongly correlated electron systems. The unconventional magnetic properties of transition metal oxides, such as the mixed-valency manganites, are investigated on the basis of correlation models including anisotropic Heisenberg-type exchange interactions. Using Green's function techniques the effects of magnetic short-range order at arbitrary temperatures are studied in comparison with experiments.

Superconductors. Conventional and high-temperature superconductivity are studied within a gauge field theory by drawing parallels between an Abelian Higgs-like model in the isotropic case and a time-dependent Lawrence-Doniach model for layered high-T_c cuprates. The aim is the macroscopic derivation of an effective action to describe the dynamics of the superconducting condensate at zero temperature in the presence of electromagnetism.

14.3.1. Nonlinear Dynamics and Statistical Physics of the Immune System

U. Behn, M. Brede and J. Richter

The immune system is a hierarchically organized natural adaptive system built by a macroscopic number of constituents which shows a very complex behaviour on several scales of temporal, spatial, and functional organization. It is thus naturally a subject of modelling with methods of statistical physics and nonlinear dynamics, for recent reviews see, e.g., [1–3]. We investigate models describing the architecture of the idiotypic network formed by the subsystem of B-lymphocytes and the regulation of the Th1-Th2 balance of the T-lymphocyte subsystem.

B-cells express on their surface receptors (antibodies) of a given specificity (idiotype). Cross-linking these receptors by complementary structures (antigen or antibodies) stimulates the lymphocyte to proliferate. Thus even without antigen there is a large functional network of interacting lymphocytes, the idiotypic network. Both the potential repertoire and the number of idiotypes expressed by an individual at a given time (the expressed repertoire) are of macroscopic order. In the frame of a simple bit-string model we investigate the architecture of a randomly generated idiotypic network [3–5]. We identify a working regime above the percolation transition where a giant cluster coexists with many small clusters, such that immunological demands as the completeness of the repertoire and a persistent immunological memory preserved by the internal image of antigen can be fulfilled [4]. The dynamics of the idiotypic network is driven by the influx of new idiotypes randomly produced in the bone marrow and by the population dynamics of the lymphocytes themself. Modelling this dynamics by simple cellular automata rules we describe the architecture of the idiotypic network as the highly organized product of a random temporal evolution [5].

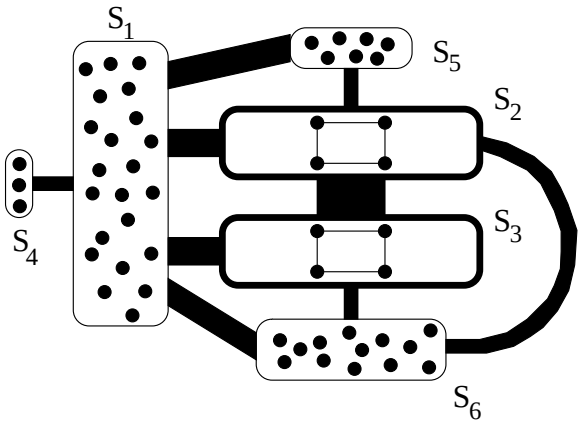

Figure 1. Visualization of the network structure of the idiotypic network. The squares indicate many connections of vertices of a group among themselves, isolated circles in a group visualize that it consists of singletons. The thickness of the connecting lines gives a measure of the number of links connecting elements of different groups. Larger boxes correspond to larger groups. From [5].

T-helper lymphocytes have subtypes which differ in their spectrum of secreted cytokines. These cytokines have autocrine effects on the own subtype and cross-suppressive effects on the other subtype and regulate further the type of immunoglobulines secreted by B-lymphocytes. The balance of Th1- and Th2-cells is perturbed in several diseases. For example, in allergy the response to allergen is Th2-dominated. A widespread and successful therapy consists in the injection of increasing doses of allergen following empirically justified protocols of administration. We seek an explanation of this therapy studying the nonlinear dynamics of a nonautonomous system of few variables which describes the Th1/Th2 populations in the sense of a mean field theory [6,7]. Indeed, the system is driven by proper injections of allergen towards new attractors, where the response is Th1-dominated as for healthy individuals. The target of the initial phase of the therapy with increasing doses of allergen is in our view not primarily the T-cell system but it is to desensitize mast cells and basophils, so that the larger doses during the maintenance phase of the therapy do not cause allergic symptoms. This is corroborated by a model describing the dynamics of the mast cell stimulation and the intracellular Calcium response that triggers the release of inflammatory mediators [6,7]. These investigations are performed in collaboration with Prof. G. Metzner (Institute of Clinical Immunology and Transfusion Medicine).

The project is supported by the Graduiertenförderung des Freistaates Sachsen.

References

[1] A. S. Perelson and G. Weisbuch, Rev. Mod. Phys. **69**, 1219 (1997).

[2] U. Behn, F. Celada and P. E. Seiden, in: *Frontiers of Life*, Vol. II, Part Two: *The Immunological System*, eds. A. Lanzavecchia, B. Malissen and R. Sitia (Academic Press, London, 2001), p. 611.

[3] K. Lippert and U. Behn, in: *Annual Reviews of Computational Physics*, ed. D. Stauffer, vol. V (World Scientific, Singapore 1997), p. 287.

[4] M. Brede and U. Behn, Phys. Rev. E **64**, 011908 (2001).

[5] M. Brede and U. Behn, *Patterns in randomly evolving networks: Idiotypic networks*, Preprint cond-mat/0208246, to appear in Phys. Rev. E.

[6] J. Richter, G. Metzner and U. Behn, J. Theor. Med. **4**, 119 (2002).

[7] J. Richter, *Nonlinear Dynamics of Models Describing Th1/Th2 Regulation, Allergy and Venom Immunotherapy*, PhD thesis, University of Leipzig, 2002.

14.3.2. On-Off Intermittency in Nematic Liquid Crystals Driven by Multiplicative Noise

U. Behn, T. John and R. Stannarius

Electrohydrodynamic convection (EHC) in liquid crystals is a well investigated phenomenon of pattern formation, its physical mechanism is understood and it is easily accessible to experimental control and observation. This allows a quantitative comparison of theoretical models with experimental results; for a recent review see [1]. We investigate on-off intermittency [2] in electrohydrodynamic convection of nematic liquid crystals driven by a stochastic dichotomous electric voltage.

If the characteristic times of the system are well separated from the correlation time of the noise, the onset of the roll pattern is sharp, similar to the case of deterministic driving. If these times are of the same order as it is typical for pure stochastic driving one observes outbursts of spatially regular roll pattern which interrupt quiescent (laminar) periods. The phenomenon is related to the persistence problem of a suitable random walk. At the sample stability threshold [3] the probability distribution of laminar periods is a power law with exponent -3/2 over several decades. We found a quantitative agreement of experiment, analytical results, and simulations of the nemato-electrohydrodynamic equations of the basic model. The phenomenon represents thus a first example of on-off intermittency in a spatially extended dissipative system [4].

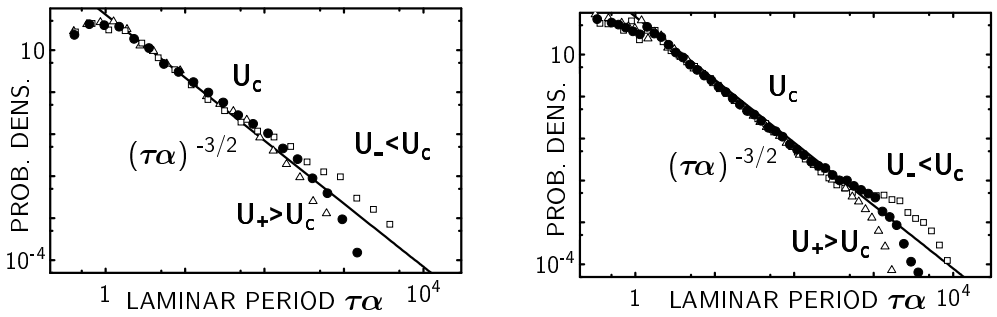

Figure 1. Distribution of laminar periods (in units of $1/\alpha$) in the conductive regime. Experiment (left) vs. theory (right). Shown are the results at the threshold voltage U_c V and at voltages 6% below and above the threshold, U_- and U_+. The solid line indicates a $\tau^{-3/2}$ power law. At the threshold the power law holds over more than three orders of magnitude.

In addition to the previous experiment based on orthoscopic microscopy the distribution of laminar periods and other statistical characteristics of the stochastic signal as the distribution of amplitudes and the power spectrum are determined by laser scattering techniques [5] and compared with theoretical results and simulations [6,7]. Again, at the stochastic stability threshold universal scaling laws are found over several orders of magnitude. Using laser scattering technique first explorations of noise induced wave number selection have been performed.

The project is supported by the Deutsche Forschungsgemeinschaft (BE 1417/4-2).

References

[1] W. Pesch and U. Behn, in: *Evolution of Spontaneous Structures in Dissipative Continuous Systems*, eds. F. H. Busse and S. C. Mueller (Springer, Berlin, 1998), p. 335.

[2] H. Fujisaka and T. Yamada, Progr. Theor. Phys. **74**, 918 (1985).
N. Platt, E. A. Spiegel and C. Tresser, Phys. Rev. Lett. **70**, 279 (1993).
J. F. Heagy, N. Platt and S. M. Hammel, Phys. Rev. E **49**, 1140 (1994).

[3] U. Behn, A. Lange and T. John, Phys. Rev. E **58**, 2047 (1998).

[4] T. John, R. Stannarius and U. Behn, Phys. Rev. Lett. **83**, 749 (1999).

[5] T. John, U. Behn and R. Stannarius, *Laser diffraction by periodic dynamic patterns in anisotropic fluids*, Preprint cond-mat/0209583, submitted to Europhys. J. B.

[6] U. Behn, T. John and R. Stannarius, *On-off intermittency and stochastically driven convection in nematic liquid crystals*, in: *Proc. 6th Experimental Chaos Conference, 22-26 July 2001, Potsdam, Germany*, eds. S. Boccaletti, B. J. Gluckman, J. Kurths, L. M. Pecora and M. L. Spano, AIP Conference Proceedings **622** (American Institute of Physics, Melville, New York, 2002), p. 381.

[7] T. John, U. Behn and R. Stannarius, Phys. Rev. E **65**, 046229 (2002).

14.3.3. Noise Induced Phenomena in Nonlinear Systems

U. Behn, A. Kühnel, M. Krieger-Hauwede, J. Przybilla and A. Traulsen

We describe non-equilibrium phase transitions [1] in arrays of spatially coupled dynamical systems with cubic nonlinearity driven by multiplicative Gaussian white noise (Stratonovich models). Depending on the sign of the harmonic spatial coupling we observe transitions from a state with zero order parameter to a ferromagnetic [2] or an antiferromagnetic stationary state varying the control parameter. Antiferromagnetic ordering is considered for the first time in this class of models. We determine the phase diagram, the order of the transitions [3], and the critical behaviour for both global coupling and nearest neighbour coupling on simple cubic lattices comparing analytical results in mean field approximation and numerical simulations. In mean field approximation we give an analytical result for the critical exponent of the magnetization which exhibits a transition from the classical universal value 1/2 to a non-universal behaviour with increasing ratio of noise strength and magnitude of the spatial coupling [4]. The critical exponent of the magnetization as a function of the strength of the spatial coupling has been determined. Similar results can be obtained for models with other nonlinearities, universality classes have been determined [5].

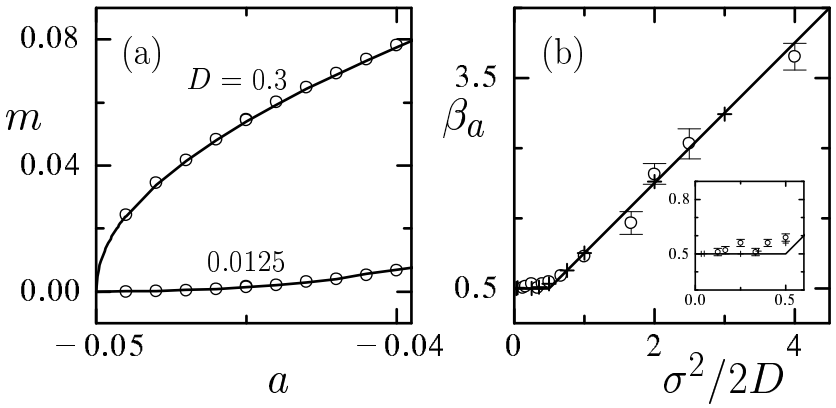

Figure 1. Critical behaviour of the globally coupled Stratonovich model. (a) Order parameter m vs. control parameter a for different strengths of the spatial coupling D and noise strength $\sigma^2 = 0.1$. (b) Critical exponent β_a vs. $\sigma^2/(2D)$. The solid line is the analytical result, the symbols result from simulations. From [4].

Spatially coupled stochastically driven systems are considered in the continuum limit which leads to stochastic partial differential equations. We show that it is preferable to use spatiotemporal colored noise in order to avoid unphysical divergencies in this limit. A generalization of the Ornstein-Uhlenbeck process in $1 + 1$ dimensions is proposed [6].

For a class of stochastically driven nonlinear systems with delayed time argument we investigated the persistence problem and determined the probability density of first passage times. For systems spontaneously evolving to a marginally stable state the density is a power law over

several decades in close analogy to self-organized criticality in spatially extended systems. The marginally stable linear system was considered in the parameter range where the instability is towards oscillating solutions and the corresponding characteristic exponent was determined.

The project is supported by the Graduiertenförderung des Freistaates Sachsen.

References

[1] C. Van den Broeck, J. M. R. Parrondo and R. Toral, Phys. Rev. Lett. **73**, 3395 (1994).

[2] W. Genovese and M. A. Muñoz, Phys. Rev. E **60**, 69 (1999).

[3] R. Müller, K. Lippert, A. Kühnel and U. Behn, Phys. Rev. E **56**, 2658 (1997).

[4] T. Birner, K. Lippert, R. Müller, A. Kühnel and U. Behn, Phys. Rev. E **65**, 046110 (2002).

[5] J. Przybilla, *Kritisches Verhalten in global gekoppelten rauschgetriebenen nichtlinearen Systemen*, Diploma thesis, University of Leipzig (2002), unpublished.

[6] A. Traulsen, *Coupled stochastically driven systems in the continuum limit*, Diploma thesis, University of Leipzig (2002), unpublished.

14.3.4. Spin Correlations in Manganites

D. Ihle, I. Junger and H. Fehske (Universität Greifswald)

The manganites $R_{1-x}A_xMnO_3$ ($R = La, Pr, Nd$ and $A = Sr, Ca, Ba, Pb$) have attracted renewed attention when the phenomenon of colossal magnetoresistance near the phase transition from the ferromagnetic metallic to the paramagnetic insulating phase was discovered [1,2]. It is important to understand first of all the observed magnetic and orbital order and the low-energy excitations in the undoped insulating compound $LaMnO_3$. Neutron-scattering experiments [2] yield strong evidence for a pronounced ferromagnetic short-range order (SRO) in the paramagnetic phase. To provide a good description of SRO at arbitrary temperatures, the standard spin-wave approaches cannot be adopted.

In this project, an effective extended Heisenberg model for the $S = 2$ spin system $LaMnO_3$ including a ferromagnetic intraplane and an antiferromagnetic interplane exchange interaction as well as a single-ion easy-axis spin anisotropy [2] is considered. The aim is to develop a Green's-function theory along the lines indicated in Refs. [3] and [4] (second-order decoupling scheme) which describes the influence of spatial and spin anisotropies on the magnetic order. It turned out that for $S > 1/2$ an additional vertex parameter has to be introduced as compared with the case $S = 1/2$ considered previously [3,4]. For the two-dimensional Heisenberg ferromagnet a good agreement of the spin correlation length with series-expansion results [5] was obtained. To clarify the methodical problems in the description of single-site spin anisotropy effects, a second-order Green's-function theory for the two-dimensional $S = 1/2$ Heisenberg model in a magnetic field was developed. The magnetization and the isothermal susceptibility were calculated in good agreement with Monte Carlo data [6] and Landau's theory [7], respectively.

The project is supported by the DFG through the Graduiertenkolleg "Quantenfeldtheorie".

References

[1] A. P. Ramirez, J. Phys.: Condens. Matter **9**, 817 (1997).
E. L. Nagaev, Phys. Rep. **346**, 387 (2001).

[2] F. Moussa *et al.*, Phys. Rev. B **54**, 15149 (1996).
K. Hirota, N. Kaneko, A. Nishizawa and Y. Endoh, J. Phys. Soc. Jpn. **65**, 3736 (1996).

[3] S. Winterfeldt and D. Ihle, Phys. Rev. B **56**, 5535 (1997); **59**, 6010 (1999).

[4] D. Ihle, C. Schindelin and H. Fehske, Phys. Rev. B **64**, 054419 (2001).

[5] N. Elstner, Int. J. Mod. Phys. B **11**, 1753 (1997).

[6] P. Henelius, A. W. Sandvik, C. Timm and S. M. Girvin, Phys. Rev. B **61**, 364 (2000).

[7] J. Sznajd, Phys. Rev. B **64**, 052401 (2001).

14.3.5. Magnetic Systems with Frustration

J. Richter (Universität Magdeburg), D. Schmalfuss (Universität Magdeburg) and D. Ihle

The exciting magnetic properties of several low-dimensional quantum spin systems with frustration, such as the layered copper oxychlorides $M_2Cu_3O_4Cl_2$ ($M = Ba, Sr$) [1] containing two interpenetrating antiferromagnetic $Cu(A)$ and $Cu(B)$ subsystems with a frustrating ferromagnetic coupling and the Kagomé antiferromagnet [2], have attracted much attention. To describe the magnetic short-range order at arbitrary temperatures, especially in the spin-liquid phase, and the influence of the interplane coupling on the stabilization of long-range order, one has to go beyond the usual spin-wave approaches [3]. Previously, it was shown that frustration effects in the two-dimensional Heisenberg model with antiferromagnetic nearest- and next-nearest-neighbor couplings ($J_1 - J_2$ model) may be described successfully by a spin-rotation-invariant Green's-function theory [4,5].

In this project, the Green's-function approach of Refs. [4] and [5] (second-order decoupling scheme) was extended to a theory for frustrated spin lattices with basis, where the formal structure of the theory turned out to be of much higher complexity as compared with previous situations [4,5]. The obtained ground-state results improve those obtained by other authors [6] and provide a basis for the investigation of the finite-temperature properties.

References

[1] H. Rosner, R. Hayn and J. Schulenburg, Phys. Rev. B **57**, 13660 (1998).
J. Richter, A. Voigt, J. Schulenburg, N. B. Ivanov and R. Hayn, J. Magn. Magn. Mat. **177-181**, 737 (1998).

[2] J. Schulenburg, A. Honecker, J. Schnack, J. Richter and H. J. Schmidt, Phys. Rev. Lett. **88**, 167207 (2002).

[3] A. B. Harris *et al.*, Phys. Rev. B **64**, 024436 (2001).

[4] L. Siurakshina, D. Ihle and R. Hayn, Phys. Rev. B **64**, 104406 (2001).

[5] S. Winterfeldt and D. Ihle, Phys. Rev. B **56**, 5535 (1997); **59**, 6010 (1999).

[6] W. Yu and S. Feng, Eur. Phys. J. B **13**, 265 (2000).

14.3.6. Energy-Momentum Tensor in Superconductivity

W. Kolley

The spacetime symmetry of a bosonic quantum field theory for conventional superconductivity at zero temperature is related to the conservation law for the energy-momentum tensor (EMT). The Galilei invariance of the Lagrange density for the pair field of condensed matter can be established [1] by a constraint onto the EMT. This constraint can be microscopically justified [2] by a bosonization of the non-relativistic BCS or Gorkov models.

Here we restrict ourselves to low-energy quantum fluctuations around the superconducting ground state, where the Galilei invariance is lost. Including a dynamical gauge field, in the presence of a neutralizing ionic background, one gets a Lagrangian whose kinematical matter part is not Lorentz invariant. This is in contrast to the Abelian Higgs model, but more realistic for superconductivity. Using such a Lagrangian on microscopic footing
(i) the canonical EMT and the corresponding local conservation law are derived via the Noether theorem;
(ii) the gauge-invariant EMT and its conservation law are found on combining infinitesimal spacetime translations and U(1) gauge transformations in the sense of [3];
(iii) the metric EMT (see, e.g., [4]) is given, for comparison, within a covariant formalism involving the sound velocity (as simplification of an acoustic metric [5]).

References

[1] M. Greiter, F. Wilczek and E. Witten, Mod. Phys. Lett. B **3**, 903 (1989).
[2] A. M. J. Schakel, Mod. Phys. Lett. B **4**, 927 (1990).
[3] R. Jackiw and N. S. Manton, Ann. Phys. (N.Y.) **127**, 257 (1980).
[4] V. Borokhov, Phys. Rev. D **65**, 125022 (2002).
[5] G. E. Volovik, Physics Reports **351**, 195 (2001).

14.4. Computational Quantum Field Theory (CQT)

The Computational Physics Group performs basic research in classical and quantum statistical physics with special emphasis on phase transitions and critical phenomena. In the centre of interest are currently diluted magnets, spin glasses and other physical systems with random, quenched disorder, fluctuating geometries with applications to quantum gravity (e.g., dynamical triangulations), soft condensed matter physics (e.g., membranes and interfaces), and biologically motivated problems (e.g., lattice models for protein folding).

The methodology is a combination of analytical and numerical techniques. The numerical tools are currently mainly Monte Carlo computer simulations and high-temperature series expansions. The computational approach to theoretical physics is expected to gain more and more importance with the future advances of computer technology, and will probably become the third basis of physics besides experiment and analytical theory. Already now it can help to bridge the gap between experiments and the often necessarily approximate calculations of analytical work. To achieve the desired high efficiency of the numerical studies we develop new algorithms, and to guarantee the flexibility required by basic research all computer codes are implemented by ourselves. The technical tools are Fortran, C, and C++ programs running under Unix or Linux operating systems and computer algebra using Maple or Mathematica. The software is developed and tested at the Institute on a cluster of PC's and workstations, where also most of the numerical analyses are performed. Large-scale simulations requiring vast amounts of computer time are attacked at a recently installed Beowulf cluster with 40 Athlon MP1800+ CPU's and at national supercomputing centres on T3E and Hitachi parallel computers. This combination gives good training opportunities for the students and offers promising job perspectives for their future career.

The research is embedded in a wide net of national and international collaborations funded by network grants of the European Commission and the European Science Foundation, and by binational research grants with scientists in Great Britain, France, and Israel. Close contacts are also established with research groups in Armenia, Austria, Italy, Russia, Spain, Taiwan, and the United States.

14.4.1. Multi-Overlap Monte Carlo Simulations of Spin Glasses

B. A. Berg (Florida State University, Tallahassee), A. Billoire (CEA/Saclay, Gif-sur-Yvette), W. Janke and A. Nußbaumer

Spin glasses are examples for an important class of materials with random and competing interactions between magnetic moments [1]. As a consequence, no unique spin configuration is favoured by all interactions ("frustration") and the free energy exhibits a rugged landscape with many minima and maxima separated by barriers. Among the main objectives of the project are investigations of the scaling behaviour of those barriers with system size using multi-overlap Monte Carlo simulations [2], which can be optimally tailored [3] for the sampling of rare-events. We focused first on the free-energy barriers F_B^q in the probability density $P_{\mathcal{J}}(q)$ of the Parisi overlap parameter q [4] which can be defined in terms of the autocorrelation times τ_B^q of auxiliary Markov chains. In both three and four dimensions [5] we found that the numerically obtained scaling behaviour is quite far off the $D \to \infty$ mean-field prediction.

We further analyzed the tails of the averaged probability density $P(q)$ in the limit $q \to \pm 1$. Again the consistency of the data with mean-field predictions is at best qualitative [6]. On the other hand, in 3D at and below the critical temperature, we obtained striking agreement over about 80 orders of magnitude with the statistics of extremes [7–9], which predicts a characteristic large x fall-off behaviour of the form $f(x) \sim \exp(-a\, e^x)$, $a > 0$ (Gumbel's law) for the tails. This result seems to be specific to spin glasses, since a completely analogous simulation study for the 3D Ising model (measuring also $P(q)$) [10] led to a much better description of the tails in terms of standard Boltzmann scaling.

Currently we are developing further improvements of the multi-overlap method which will eventually enable us to study the spin-glass phase at lower temperatures than previously.

Work partially supported by the German-Israel-Foundation (GIF) under grant No. I-653-181.14/1999, and by computer-time grants at NIC Jülich and CEA Grenoble.

References

[1] K. H. Fischer and J. A. Hertz, *Spin Glasses* (Cambridge University Press, 1991).

[2] B. A. Berg and W. Janke, Phys. Rev. Lett. **80**, 4771 (1998).

[3] W. Janke, B. A. Berg and A. Billoire, Ann. Phys. (Leipzig) **7**, 544 (1998); Comp. Phys. Comm. **121-122**, 176 (1999).

[4] G. Parisi, Phys. Rev. Lett. **43**, 1754 (1979).

[5] B. A. Berg, A. Billoire and W. Janke, Phys. Rev. B **61**, 12143 (2000).

[6] W. Janke, B. A. Berg and A. Billoire, in: *Multiscale Computational Methods in Chemistry and Physics*, eds. A. Brandt, J. Bernholc and K. Binder (IOS Press, Amsterdam, 2001), p. 198; in: *Non-Perturbative Methods and Lattice QCD*, eds. X.-Q. Luo and E. B. Gregory (World Scientific, Singapore, 2001), p. 242.

[7] B. A. Berg, A. Billoire and W. Janke, Phys. Rev. E **65**, 045102 (2002).

[8] W. Janke, B. A. Berg and A. Billoire, in: *NIC Symposium 2001*, eds. H. Rollnik and D. Wolf, John von Neumann Institute for Computing, Jülich, NIC Series, Vol. **9**, 301 (2002) [http://www.fz-juelich.de/nic-series/volume9/janke.pdf].

[9] B.A. Berg, A. Billoire and W. Janke, Physica A **321**, 49 (2003).

[10] B.A. Berg, A. Billoire and W. Janke, Phys. Rev. E **66**, 046122 (2002), Preprint cond-mat/0205377.

14.4.2. Monte Carlo Simulations of Disordered Magnets

B. Berche (Université Nancy), P.-E. Berche (Université Rouen), C. Chatelain (Université Nancy) and W. Janke

The influence of quenched, random disorder on phase transitions has been the subject of exciting experimental, analytical and numerical studies in the past few years. To date most analytical and numerical studies have concentrated on two-dimensional (2D) models with site- or bond-dilution or bond-disorder [1]. Generically one expects that, under certain conditions, a first-order phase transition of the pure system is softened by quenched randomness to a second-order transition and that the critical behaviour associated with a second-order phase transition is modified (Harris criterion) [2]. The softening effect has been observed experimentally for the isotropic-nematic transition of liquid crystals confined into the pores of aerogels consisting of multiply connected internal cavities [3]. While experimentalists [3] tend to explain the softening by the influence of random fields or random uniaxial anisotropies, the random disorder chosen in an exploratory Monte Carlo (MC) simulation [4] is coupled to the energy density and thus more akin to bond-dilution.

In three dimensions (3D), numerically mainly the critical behaviour of the Ising model with site-dilution [5] has been studied and found in good agreement with extensive field theoretic calculations. For systems exhibiting a first-order phase transition in the pure case, large-scale simulations have only been performed for the 3-state Potts model with site-dilution [6]. In 3D one expects that the first-order nature persists for small dilutions up to a (tricritical) dilution from where on the softening to a second-order transition should be observed, until the transition completely vanishes at the percolation point.

Since the undiluted 3D 3-state Potts model exhibits a very *weak* first-order transition [7], the observed softening from a certain dilution threshold on did not appear very stringent. We therefore chose the 4-state Potts model where the transition is known to be *strongly* of first order in the pure case. And in order to be able to compare with other techniques such as series expansions applied to the same model, we considered bond-dilution instead of site-dilution. In a first step the phase diagram in the dilution-temperature ($p-T$) plane was determined from the location of the susceptibility maxima for a moderate system size (16^3) [8], in good agreement with complementary analyses of high-temperature series expansions [9] and with an "effective medium" approximation [10]. A more detailed comparison with the series expansions as well as analyses of autocorrelation times gave a first estimate of the boundary between the regimes of first- and second-order phase transitions, i.e., the location of the tricritical point. By using multicanonical resp. multibondic simulations the regime of first-order transitions was studied quantitatively by determining the latent heat and interface tension. In the regime of second-order transitions the Swendsen-Wang cluster MC update algorithm was used for FSS analyses at two selected dilutions. Since the fluctuations between different disorder realizations turned out to be quite large (see Fig. 1), many different realizations (1 000 – 5 000) had be be averaged. The properties of the disorder distributions (average vs. medium values, long-tail behaviour, (non-) self-averaging etc.) have also been studied and compared with scaling predictions. Presently we are investigating the correlations of thermodynamic quantities such as the susceptibility with the clustering properties of the underlying random bond configurations.

Preliminary results of a comparative MC study of the bond-diluted 3D Ising model are reported in Ref. [11].

The project is partially supported by the DAAD through a collaborative PROCOPE re-

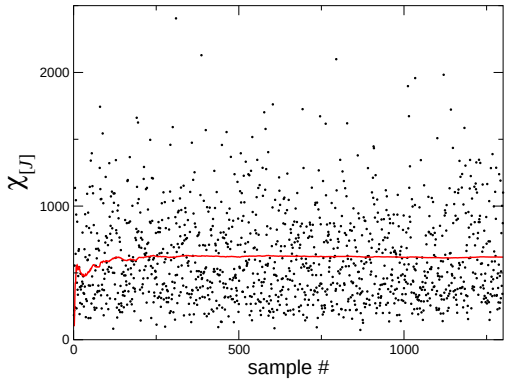

Figure 1. Distribution of susceptibility measurements on a 96^3 lattice at $T_{\rm sim} \approx T_{\chi_{\rm av}^{\rm max}}$ for dilution $p = 0.56$.

search grant, by the German-Israel-Foundation (GIF) under grant No. I-653-181.14/1999, the EU-Network HPRN-CT-1999-000161 "Discrete Random Geometries: From Solid State Physics to Quantum Gravity", the ESF-Network "Challenges in Molecular Simulations: Bridging the Length- and Time-Scale Gap (SIMU)", and the computer-time grants hlz061 of NIC, Jülich, h0611 of LRZ München, C2000-06-20018 of CINES and C2000015 of CRIHAN.

References

[1] B. Berche and C. Chatelain, Preprint cond-mat/0207421.

[2] A. B. Harris, J. Phys. C **7**, 1671 (1974).
Y. Imry and M. Wortis, Phys. Rev. B **19**, 3580 (1979).
M. Aizenman and J. Wehr, Phys. Rev. Lett. **62**, 2503 (1989).

[3] X. I. Wu, W. I. Goldburg, M. X. Liu and J. Z. Xue, Phys. Rev. Lett. **69**, 470 (1992).
T. Bellini, N. A. Clark, C. D. Muzny, L. Wu, C. W. Garland, D. W. Schaefer and B. J. Oliver, Phys. Rev. Lett. **69**, 788 (1992).
G. S. Iannacchione, G. P. Crawford, S. Žumer, J. W. Doane and D. Finotello, Phys. Rev. Lett. **71**, 2595 (1993).

[4] K. Uzelac, A. Hasmy and R. Jullien, Phys. Rev. Lett. **74**, 422 (1995).

[5] H. O. Heuer, J. Phys. A **26**, L333 (1993).
S. Wiseman and E. Domany, Phys. Rev. Lett. **81**, 22 (1998); Phys. Rev. E **58**, 2938 (1998).
H. G. Ballesteros, L. A. Fernández, V. Martín-Mayor, A. Muñoz Sudupe, G. Parisi and J. J. Ruiz-Lorenzo, Phys. Rev. B **58**, 2740 (1998).

[6] H. G. Ballesteros, L. A. Fernández, V. Martín-Mayor, A. Muñoz Sudupe, G. Parisi and J. J. Ruiz-Lorenzo, Phys. Rev. B **61**, 3215 (2000).

[7] W. Janke and R. Villanova, Nucl. Phys. B **489**, 679 (1997).

[8] C. Chatelain, B. Berche, W. Janke and P.-E. Berche, Phys. Rev. E **64**, 036120 (2001).
C. Chatelain, P.-E. Berche, B. Berche and W. Janke, Comp. Phys. Comm. **147**, 431 (2002); Nucl. Phys. B (Proc. Suppl.) **106&107**, 899 (2002).

[9] M. Hellmund and W. Janke, Nucl. Phys. B (Proc. Suppl.) **106&107**, 923 (2002); Phys. Rev. E **67**, 026118 (2003).

[10] L. Turban, Phys. Lett. A **75**, 307 (1980); J. Phys. C **13**, L13 (1980).

[11] C. Chatelain, P.-E. Berche, B. Berche and W. Janke, Comp. Phys. Comm. **147**, 427 (2002).

14.4.3. Series Expansions for Random-Bond Models and Spin Glasses

M. Hellmund and W. Janke

Despite considerable efforts there are still many open problems in the physics of disordered systems. One alternative to large-scale numerical simulations are systematic series expansions. Such expansions for statistical models defined on a lattice are a well-known method to study phase transitions and critical phenomena [1]. The extension of this method to disordered systems [2] demands the development of new graph theoretical and algebraic algorithms.

Using the method of "star graph expansion", we calculate, e.g., free energies and susceptibilities for disordered q-state Potts models on d-dimensional hypercubic lattices. The probability distribution of couplings is parametrized by $P(J_{ij}) = p\delta(J_{ij} - J_0) + (1-p)\delta(J_{ij} - RJ_0)$, which includes spin glasses, diluted ferromagnets, random-bond models and transitions between them. First results for the random-bond Ising [3] and Potts [4] model demonstrate the feasibility of the method to complement Monte Carlo [5] and field theoretic studies of phase transitions in disordered systems.

For the bond-diluted 4-state Potts model in three dimensions, which exhibits a rather strong first-order phase transition in the undiluted case, we obtained results [6] for the transition temperature and the effective critical exponent γ as a function of p from analyses of susceptibility series up to order 18. A comparison with recent Monte Carlo data [5] shows signals for the softening to a second-order transition at finite disorder strength.

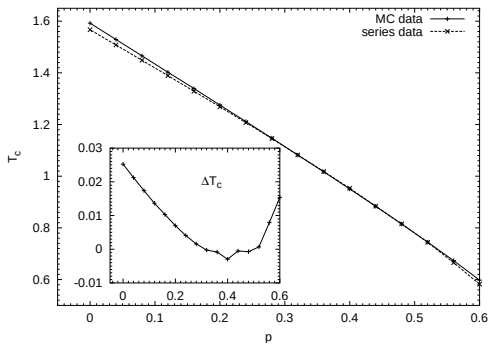

Critical temperature for different dilutions p as obtained from Monte Carlo (MC) simulations [5] and DLog-Padé series analyses [6]. The inset shows the difference between the two estimates.

Support by DFG grant No. JA 483/17-1 and partial support from the German-Israel-Foundation (GIF) under grant No. I-653-181.14/1999 is gratefully acknowledged.

References

[1] C. Domb and M. S. Green, eds, *Phase Transitions and Critical Phenomena*, Vol. 3 (Academic Press, New York, 1974).

[2] R. R. P. Singh and S. Chakravarty, Phys. Rev. B **36**, 546 (1987).

[3] M. Hellmund and W. Janke, Comp. Phys. Comm. **147**, 435 (2002).

[4] M. Hellmund and W. Janke, Nucl Phys. B (Proc. Suppl.) **106/107**, 923 (2002).

[5] C. Chatelain, B. Berche, W. Janke and P. E. Berche, Phys. Rev. E **64**, 036120 (2001).

[6] M. Hellmund and W. Janke, Phys. Rev. E **67**, 026118 (2003).

14.4.4. Effects of Connectivity Disorder on the Potts Model

W. Janke, M. Weigel and A. Wernecke

In the context of quenched disorder, the influence of uncorrelated, geometrically regular types of disorder such as the random dilution of bonds or sites or the random variation of coupling strengths found in spin glasses has been extensively explored, see, e.g., [1,2]. On the other hand, systems subject to *geometrical* disorder, which differs from the former type of randomness first of all in the strong correlation of the disorder degrees of freedom, have not received comparable attention.

In the case of quasi-crystals, the relevance of these types of disorder for the (critical) behaviour of matter models coupled to such random lattices can be judged by means of the so-called Harris-Luck criterion [3,4]. We consider two types of lattices with connectivity disorder, so-called Voronoï-Delaunay random lattices and the planar ϕ^3 random graphs occurring in discrete approaches to quantum gravity. By means of numerical methods, we determine the *wandering exponent* [4] of these lattice types, which is an essential input of the Harris-Luck criterion.

For the three-state Potts model, this analysis implies that disorder of the Voronoï-Delaunay type should be relevant, which is in contrast to previous observations [5]. Extensive investigations of this system by means of Monte Carlo simulations show that the predictions of the Harris-Luck criterion are correct. The contradiction to the prior results of Ref. [5] are tracked down to the much smaller lattices used there, since in this system the crossover from the pure to the disorder fixed point occurs only very close to the critical point.

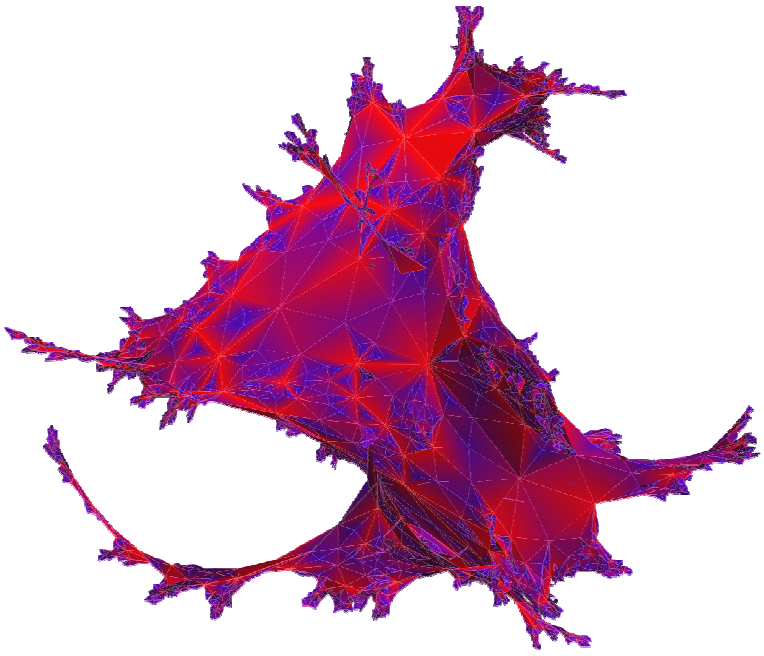

Figure 1. Example of a triangulation dual to the planar ϕ^3 random graphs.

Parallel to the study of the Voronoï-Delaunay case we have also investigated the three-state Potts model on quenched, random ϕ^3 graphs (see Fig. 1), where the Harris-Luck criterion sug-

gests a stronger influence of the connectivity disorder. This expectation is clearly supported by the simulational results [6]. Already for moderate system sizes we obtain significantly altered critical exponents as compared to the pure case. In addition self-averaging properties of geometric and thermodynamic quantities are carefully measured and analyzed within the framework of recent finite-size scaling theories.

This work was supported through the EC network HPRN-CT-1999-000161 "Discrete Random Geometries: From Solid State Physics to Quantum Gravity" and the ESF network "Geometry and Disorder: From Membranes to Quantum Gravity". MW was supported by the DFG through the Graduiertenkolleg "QFT".

References

[1] K. Binder and A. P. Young, Rev. Mod. Phys. **58**, 801 (1986).

[2] *Spin Glasses and Random Fields*, ed. A. P. Young (World Scientific, Singapore, 1997).

[3] A. B. Harris, J. Phys. C **7**, 1671 (1974).

[4] J. M. Luck, Europhys. Lett. **24**, 359 (1993).

[5] F. W. S. Lima, U. M. S. Costa, M. P. Almeida and J. S. Andrade, Eur. Phys. J. B **17**, 111 (2000).

[6] A. Wernecke, Diploma thesis, University of Leipzig, 2002.

14.4.5. Ising Model on "Fat" and "Thin" Random Graphs

B. P. Dolan (National University of Ireland, Maynooth), W. Janke, D. A. Johnston (Heriot-Watt University, Edinburgh) and M. Stathakopoulos (Heriot-Watt University, Edinburgh)

For the Ising model on fluctuating planar ("fat") ϕ^4 random graphs and their dual quadrangulations we show that in the thermodynamic limit the locus of Fisher zeroes [1] can be determined exactly [2,3] by matching up [4] the analytically known [5] real part of the high- and low-temperature branches of the free energy. We also point out that results for the zeroes on finite graphs may be obtained with rather less effort than might appear necessary at first sight [6] by simply reverting the series expansion of a function $g(z)$ which appears in the solution [5] and taking a logarithm [2]. Unlike regular 2D lattices where numerous unphysical critical points exist with non-standard exponents, on planar ϕ^4 graphs the Ising model displays only the physical transition at $c = \exp(-2\beta) = 1/4$ and a mirror transition at $c = -1/4$ both with KPZ/DDK exponents ($\alpha = -1, \beta = 1/2, \gamma = 2$). The relation between the ϕ^4 locus and that of the dual quadrangulations is akin to that between the (regular) triangular and honeycomb lattices since there is no self-duality. By exploiting the fact that the Ising model on dynamical "fat" graphs has also been solved in the presence of an external magnetic field [5], we furthermore discuss the so-called Kertész line [7].

Moreover, using a similar approach, we calculated the Fisher zeroes for Ising and Potts models on non-planar ("thin") random graphs and noted that the locus of Fisher zeroes is identical to that on a Bethe lattice [8]. Since the number of states q of the Potts model appears as a parameter in the solution, the limiting locus of chromatic zeroes is accessible as well [8]. And along similar lines also the Lee-Yang zeroes have recently been discussed [9].

Work partially supported by the DAAD grant 313-ARC-XII-98/41, the EU-Network HPRN-CT-1999-000161 "Discrete Random Geometries: From Solid State Physics to Quantum Gravity", and the ESF-Network "Geometry and Disorder: From Membranes to Quantum Gravity".

References

[1] M. Fisher, in: *Lectures in Theoretical Physics* **VII C** (University of Colorado Press, Boulder, 1965).

[2] W. Janke, D. A. Johnston and M. Stathakopoulos, Nucl. Phys. B **614** [FS], 494 (2001), Preprint cond-mat/0107013.

[3] W. Janke, D. A. Johnston and M. Stathakopoulos, Nucl. Phys. B (Proc. Suppl.) **106&107**, 983 (2002), Preprint hep-lat/0110100.

[4] G. Marchesini and R. Shrock, Nucl. Phys. B **318**, 541 (1989).
M. Biskup, C. Borgs, J. T. Chayes, L. J. Kleinwaks and R. Kotecky, Phys. Rev. Lett. **84**, 4794 (2000).

[5] V. A. Kazakov, Phys. Lett. A **119**, 140 (1986).
D. V. Boulatov and V. A. Kazakov, Phys. Lett. B **186**, 379 (1987).

[6] J. Ambjorn, K. Anagnostopoulos and U. Magnea, Mod. Phys. Lett. A **12**, 1605 (1997); Nucl. Phys. (Proc. Suppl.) **63**, 751 (1998).

[7] W. Janke, D. A. Johnston and M. Stathakopoulos, J. Phys. A **35**, 7575 (2002).

[8] B. P. Dolan, W. Janke, D. A. Johnston and M. Stathakopoulos, J. Phys. A **34**, 6211 (2001), Preprint cond-mat/0105317.

[9] L. C. de Albuquerque and D. Dalmazi, Preprint cond-mat/0206489.

14.4.6. The 6-Vertex Model on Quantum-Gravity Graphs

W. Janke, D. A. Johnston (Heriot-Watt University, Edinburgh) and M. Weigel

As an alternative to various other approaches towards a theory of quantum gravity, the *dynamical triangulations* method has proved to be a successful discrete formulation of Euclidean quantum gravity in two dimensions [1]. There, the necessary integration over all metric tensors as the dynamic variables of the theory occurring in the path-integral ansatz, is performed as a discrete summation over all possible gluings of equilateral triangles to form a closed surface of a given (usually planar) topology. The powerful methods of matrix integrals [2] and generating functions [3] allow for an exact solution of the pure gravity model in two dimensions. Furthermore, matrix models can be formulated for the coupling of classic spin models of statistical mechanics, such as the Ising, Potts or O(n) models, to the random graphs and some of them could be solved analytically [4]. More generally, the transformation or "dressing" of the weights of $c < 1$ conformal matter on coupling it to quantum gravity in two dimensions is predicted by the KPZ/DDK formula [5], in agreement with all known exact solutions.

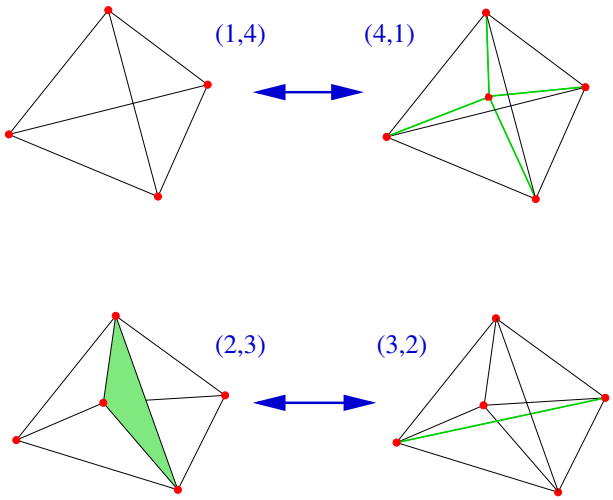

Figure 1. Illustration of the so-called Pachner moves employed for updating triangulated geometries.

One of the most general classes of models in statistical mechanics is given by Baxter's 8-vertex model [6], which includes as limiting cases most of the more well-known models such as the Ising and Potts models and exhibits an exceptionally rich phase diagram with lines of first- and second-order transitions as well as critical and multi-critical points. Thus its behaviour on coupling it to dynamical *quadrangulations*, i.e., surfaces built from simplicial squares, is of general interest. Although a solution of special slices of this model coupled to quantum gravity could recently be achieved [7], the general model could not yet be solved. Thus, one has to revert to numerical techniques, especially Monte Carlo simulations of the combined system.

Heading for the simulation of 6- and 8-vertex models, one first has to ensure the correct

functioning of a dynamics for the (quite unorthodox) geometry of four-valent graphs, corresponding to quadrangulations in the dual language. While simulations of three-valent graphs have already been extensively done, the code for ϕ^4-graphs had to be newly developed and tested against available exact solutions for the case of the Ising model. While for the 3-valent case the so-called Pachner moves, depicted in Figure 1 above, are known to be an ergodic set of updates [8], it is found that for the case of the ϕ^4-graphs one has to add a special "two-link flip" along self-energy insertions to ensure ergodicity there also [9]. Due to the fractal structure of the underlying graphs being described as a self-similar tree of "baby universes", this local dynamics suffers from critical slowing down. To alleviate the situation, we adapted a non-local set of update moves known as minBU surgery algorithm [10].

Combining the developed techniques, we study the F model, a symmetric case of the 6-vertex model, coupled to planar random ϕ^4 graphs by means of a set of Monte Carlo simulations. On regular as well as random lattices, this model is expected to exhibit a Kosterlitz-Thouless type phase transition to an anti-ferroelectrically ordered state [6,7]. We find the numerical analysis of this model to be exceptionally difficult due to the combined effect of the highly fractal structure of the lattices and the presence of strong logarithmic corrections. Thus, the analysis is hampered by rather extreme finite-size effects, the expected asymptotical behaviour not quite being reached with the accessible system sizes. Nevertheless, a scaling analysis of the staggered polarizability yields results in agreement with the predictions of Ref. [7] as far as the order of the transition and the location of the transition point are concerned.

This work was supported by the DAAD through the research grant 313-ARC-XII-98/41, the EC network HPRN-CT-1999-000161 "Discrete Random Geometries: From Solid State Physics to Quantum Gravity" and the ESF network "Geometry and Disorder: From Membranes to Quantum Gravity". MW was supported by the DFG through the Graduiertenkolleg "QFT".

References

[1] V. A. Kazakov, Phys. Lett. B **150**, 282 (1985).
F. David, Nucl. Phys. B **257**, 45 (1985).

[2] M. L. Mehta, Comm. Math. Phys. **79**, 327 (1981).
E. Brézin, C. Itzykson, G. Parisi and J.-B. Zuber, Comm. Math. Phys. **59**, 35 (1978).

[3] W. T. Tutte, Can. J. Math. **14**, 21 (1962).

[4] D. V. Boulatov and V. A. Kazakov, Phys. Lett. B **186**, 379 (1987).
J. M. Daul, Preprint hep-th/9502014.
B. Eynard and G. Bonnet, Phys. Lett. B **463**, 273 (1999).
I. K. Kostov, Mod. Phys. Lett. A **4**, 217 (1989).

[5] V. Knizhnik, A. Polyakov and A. Zamolodchikov, Mod. Phys. Lett. A **3**, 819 (1988).
F. David, Mod. Phys. Lett. A **3**, 1651 (1988).
J. Distler and H. Kawai, Nucl. Phys. B **321**, 509 (1989).

[6] R. Baxter, *Exactly Solved Models in Statistical Mechanics* (Academic Press, London, 1982).

[7] V. A. Kazakov and P. Zinn-Justin, Nucl. Phys. B **546**, 647 (1999).
I. Kostov, Nucl. Phys. B **575**, 513 (2000).
P. Zinn-Justin, Europhys. Lett. **50**, 15 (2000).

[8] M. Gross and S. Varsted, Nucl. Phys. B **378**, 367 (1992).

[9] M. Weigel and W. Janke, Nucl. Phys. B (Proc. Suppl.) **106–107**, 986 (2002).
M. Weigel, Ph.D. thesis, University of Leipzig, 2002.

[10] J. Ambjørn *et al.*, Phys. Lett. B **325**, 337 (1994).

14.4.7. Quantum Gravity with Matter Fields in Four Dimensions

E. Bittner, W. Janke and H. Markum (TU Wien)

A very efficient method for numerical studies of general relativity was suggested by Regge [1]. In this method a simplicial approximation is applied to a space-time manifold. The underlying lattice has fixed connectivities and the link lengths are taken as gravitational degrees of freedom. The Discrete Regge Model [2] employed in this work is structurally and computationally much simpler than the Standard Regge Calculus. Here the squared link lengths are restricted to only two possible values, both always compatible with the triangle inequalities.

Spin systems coupled to d-dimensional manifolds are studied as a simple example for matter fields coupled to gravity. To access the accuracy of the simplified formulation, we considered both versions of quantum Regge calculus and coupled these manifolds with Z_2 (Ising) spins [3]. We used the path-integral quantization of the theory and studied the partition function

$$Z = \sum_s \int \mathcal{D}\mu(q) \exp\left[-I(q) - KE(q,s)\right], \tag{1}$$

where the path-integral measure $\mathcal{D}\mu(q)$ was chosen as in our pure gravity simulations [4]. The Einstein-Hilbert action of gravitation

$$I(q) = -\beta_g \sum_t A_t \delta_t + \sum_i (\lambda V_i + a\frac{\delta_i^2}{A_i}) \tag{2}$$

consists of a curvature term with the gravitational coupling β_g, a volume term with the cosmological constant λ, and a squared curvature with coupling a. The deficit angle is denoted by δ_t, and A_t and A_i are triangular and barycentric areas, respectively. The energy of the matter field

$$E(q,s) = \frac{1}{2} \sum_{\langle ij \rangle} A_{ij} \frac{(s_i - s_j)^2}{q_{ij}} \tag{3}$$

results from the Ising spins $s_i = \pm 1$, which are located at the vertices i of the lattice. Here A_{ij} are barycentric areas associated with the edges $\langle ij \rangle$.

In our Monte Carlo simulations, the gravitational degrees of freedom of the partition function (1) were updated with the heat-bath algorithm. For the Ising spins we employed the single-cluster algorithm [5]. Between measurements we performed $n = 10$ Monte Carlo steps consisting of one lattice sweep to update the squared link lengths q_{ij}, followed by two single-cluster flips to update the spins s_i. The simulations were done for cosmological constant $\lambda = 0$, $a = 0$ and gravitational coupling $\beta_g = -4.665$. This β_g-value corresponds to a phase transition of the pure Discrete Regge Model [6]. The lattice topology is given by triangulated tori of size $N_0 = L^4$ with $L = 3$ up to 10. From short test runs we estimated the location of the phase transition of the spin model and set the spin coupling $K_0 = 0.024 \approx K_c$ in the long runs. After an initial equilibration time we took about 100 000 measurements for each lattice size. Analyzing the time series we found integrated autocorrelation times for the energy and the magnetization in the range of unity for all lattice sizes. To extract the critical exponent ratio γ/ν we used a finite-size scaling ansatz according to mean-field theory with logarithmic corrections

$$\chi \propto (L(\log L)^{\frac{1}{4}})^{\gamma/\nu} \tag{4}$$

of the susceptibility χ at its maximum as well as at K_c, yielding in the range $L = 4-10$ estimates of $\gamma/\nu = 2.039(9)$ and $\gamma/\nu = 2.036(7)$, respectively, being consistent with the mean-field value of $\gamma/\nu = 2$. In Fig. 1 this is demonstrated graphically by comparing the scaling of $\chi_{\max}$ with a constrained one-parameter fit of the form $\chi_{\max} = c(L(\log L)^{\frac{1}{4}})^2$ with $c = 4.006(10)$.

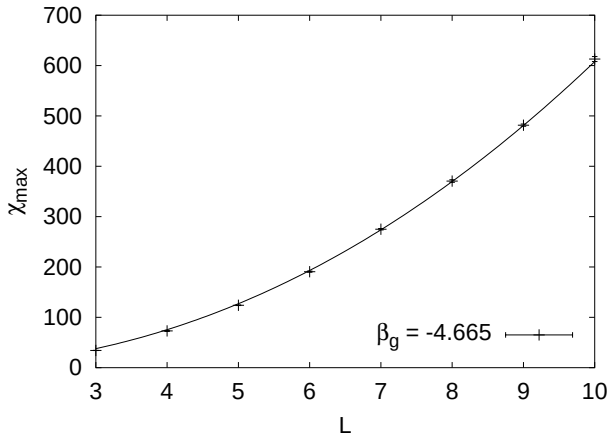

Figure 1. Finite-size scaling of the susceptibility maxima $\chi_{\max}$. The exponent entering the curve is set to the mean-field value $\gamma/\nu = 2$ for regular static lattices.

In two dimensions [7] we could measure the critical exponents α, β, γ, and ν whereas in four dimensions [8] only γ and ν could be determined. To get an estimate or bound for the remaining critical exponents we will need data for larger lattices and with higher statistical accuracy.

Work supported by the EU-Network HPRN-CT-1999-000161 "Discrete Random Geometries: From Solid State Physics to Quantum Gravity" and the ESF-Network "Geometry and Disorder: From Membranes to Quantum Gravity".

References

[1] T. Regge, Nuovo Cimento **19**, 558 (1961).

[2] T. Fleming, M. Gross and R. Renken, Phys. Rev. D **50**, 7363 (1994).
W. Beirl, H. Markum and J. Riedler, Int. J. Mod. Phys. C **5**, 359 (1994).
W. Beirl, P. Homolka, B. Krishnan, H. Markum and J. Riedler, Nucl. Phys. B (Proc. Suppl.) **42**, 710 (1995).

[3] C. Holm and W. Janke, Phys. Lett. B **335**, 143 (1994).

[4] E. Bittner, A. Hauke, H. Markum, J. Riedler, C. Holm and W. Janke, Phys. Rev. D **59**, 124018 (1999).

[5] U. Wolff, Phys. Rev. Lett. **62**, 361 (1989); Nucl. Phys. B **322**, 759 (1989).

[6] W. Beirl, A. Hauke, P. Homolka, B. Krishnan, H. Kröger, H. Markum and J. Riedler, Nucl. Phys. B (Proc. Suppl.) **47**, 625 (1996).
W. Beirl, A. Hauke, P. Homolka, H. Markum and J. Riedler, Nucl. Phys. B (Proc. Suppl.) **53**, 735 (1997).
J. Riedler, W. Beirl, E. Bittner, A. Hauke, P. Homolka and H. Markum, Class. Quant. Grav. **16**, 1163 (1999).

[7] E. Bittner, W. Janke, H. Markum and J. Riedler, Physica A **277**, 204 (2000).

[8] E. Bittner, W. Janke and H. Markum, Phys. Rev. D **66**, 024008 (2002).

14.4.8. Quantum Monte Carlo Simulations

W. Janke, J. Keller, T. Roscilde (University of Pavia), T. Sauer (California Institute of Technology), V. Tognetti (University of Florence), R. Vaia (IEQCNR Florence), P. Verrucchi (University of Florence)

The past few years have shown a rapidly growing interest in the properties of low-dimensional structures with pronounced quantum character. One of the main reasons for this interest is the availability of many novel materials, already having or promising for the future important technological applications, whose physical properties appear strictly connected to their layered structure and dominant two-dimensional (2D) character. From the scientific point of view, magnetic monolayers appear particularly attractive since, being truly 2D systems, they allow significant verifications of the proposed models.

With this project we wish to contribute to this line of research, especially for the quantum simulation part. In particular we shall study the XXZ model whose Hamiltonian is given by $H = -J \sum_{\langle ij \rangle} \left[\hat{S}_i^x \hat{S}_j^x + \hat{S}_i^y \hat{S}_j^y + \lambda \hat{S}_i^z \hat{S}_j^z \right]$, where $\hat{S}_i^\alpha$ denotes the α-component of the spin operator $\hat{\boldsymbol{S}}_i$ at site i of a square lattice with periodic boundary conditions. The spins are three-component quantum objects obeying the $\mathcal{SU}(2)$-group commutation relations $[\hat{S}_i^\alpha, \hat{S}_j^\beta] = i\,\delta_{ij}\,\epsilon^{\alpha\beta\gamma}\hat{S}_i^\gamma$ and belonging to the spin-S representation, $|\hat{\boldsymbol{S}}_i|^2 = S(S{+}1)$. The parameter $J > 0$ describes ferromagnets, and $J < 0$ yields anti-ferromagnets. The latter case is of particular interest and can be further classified into the cases of easy-*plane* ($|\lambda| < 1$) and easy-*axis* ($|\lambda| > 1$) magnets. Guided by their spin symmetries, one expects phase transitions of the Kosterlitz-Thouless respectively Ising type in these models.

We investigate above quantum systems with Monte Carlo (MC) simulations which are much more involved than in the classical case, and many new problems arise. One difficulty of quantum MC (QMC) simulations lies in the dramatic growth of the number of quantum states with the size of the simulated sample and with the value of the spin. In recent years this problem has partially been overcome by the discovery of efficient *non-local* QMC algorithms [1–5] based on clustering ideas (discrete and continuous loop algorithms). The theoretical formulation of these algorithms is highly non-trivial and, even with extensive experience in classical MC studies, their practical and efficient implementation is a major research project [6]. This is particularly pronounced for higher spin values and external magnetic fields, where the proposals made in the literature appear so complicated that innovative formulations are clearly called for.

The project is partially supported by a DAAD VIGONI research grant and, starting in 2002, by the EU through the Marie Curie Development Host Fellowship No. HPMT-CT-2001-00108.

References

[1] H. G. Evertz, Adv. Phys. **52**, 1 (2003), Preprint cond-mat/9707221.

[2] K. Harada, M. Troyer and N. Kawashima, J. Phys. Soc. Jpn. **67**, 1130 (1998).

[3] B. B. Beard and U.-J. Wiese, Nucl. Phys. B (Proc. Suppl.) **53**, 838 (1997).

[4] B. B. Beard, R. J. Birgeneau, M. Greven and U.-J. Wiese, Phys. Rev. Lett. **80**, 1742 (1998).

[5] B. Ammon, H. G. Evertz, N. Kawashima, M. Troyer and B. Frischmuth, Phys. Rev. B **58**, 4304 (1998).

[6] J. Keller, *Quantum Monte Carlo Studies of Magnetic Systems*, Diploma-Thesis, Universität Leipzig (2001).

14.4.9. Aspects of Protein Folding on the Lattice

M. Bachmann, W. Janke, R. Schiemann and T. Vogel

Proteins are essential constituents within a biological cell system, performing numerous functions, e.g. controlling transport processes of organells, stabilization of the cell structure, enzymatic catalyzation of chemical reactions, etc. Chemically, proteins are built up of sequences of amino acid residues linked by peptide bonds. Usually, proteins consist of 50–3000 of such residues. 20 different amino acids are known, most of them can be arranged in two groups, polar and hydrophobic. It is known that the sequence (also called primary structure), i.e. the consecutiveness of the amino acids within the chain, is responsible for the conformation (or the secondary, tertiary, and quartery structure), and this three-dimensional geometrical shape itself determines the biological function of a protein. Thus, the interplay between sequence and function can only be understood, if it is found out how the protein folds into its unique shape [1]. This is, however, an extremely difficult task, since the complex electrostatic and van der Waals interactions between atoms, molecules, and the aqueous environment inhibit an exact theoretical description of the folding process. For a qualitative understanding, computer simulations of quite simple effective models constrained upon a lattice are most promising.

The simplest model that allows a qualitative study of the folding of sequences of hydrophobic (H) and hydrophilic or polar (P) residues is known as the HP model [2], where the energy function is given by

$$E = \sum_{\langle i,j<i-1\rangle} \mathbf{s}_i^T C_{ij} \mathbf{s}_j. \tag{1}$$

Here $\langle i, j < i-1\rangle$ symbolizes that only contributions of monomers at i and at j are taken into account if they are next neighbours on the lattice but non-adjacent along the chain, i.e. they are not linked by a chemical bond. In this case, these monomers form a *contact* and the elements of the so-called contact matrix

$$C = \begin{pmatrix} c_{HH} & c_{HP} \\ c_{HP} & c_{PP} \end{pmatrix}$$

describe the strength of the interaction between the different types of residues. The components of the state vector of the ith monomer, $\mathbf{s}_i^T = (s_{iH}, s_{iP})$, contain the hydrophobic and the hydrophilic content of the corresponding residue, respectively. For pure HP sequences, only two states are used, $\mathbf{s}^T = (1, 0)$ for hydrophobic monomers and $\mathbf{s}^T = (0, 1)$ for hydrophilic ones.

It is anticipated that a qualitatively correct fold of the lattice protein is obtained, when the hydrophobic residues form an approximately compact core, i.e. a maximum of HH contacts is established. In that case the hydrophilic residues separate the hydrophobic core from the aqueous environment and the protein has folded into its native state with lowest possible energy. In order to primarily study this aspect of folding, the HP model (1) is often simplified by setting $c_{HH} = -1$ and $c_{HP} = c_{PP} = 0$. We analyze the properties of HP lattice proteins from different point of views. On the one hand we perform exact enumerations for chains with up to 18 monomers in the complete space of sequences and conformations, allowing for a statistical analysis of the interplay between sequences and conformations for the mostly interesting case of native, i.e. unique ground states. On the other hand, there is a great interest in the development of fast algorithms for finding low-energy states of HP sequences of lengths > 50 that render a more realistic image of natural proteins. Most-promising computational methods are based on chain growth algorithms like PERM and its extensions [3] which we apply to more generalized, e.g. triangular, lattices. Another important question we are dealing with is what we can learn

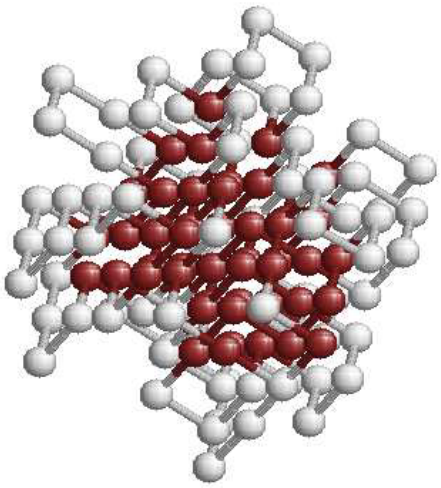

Figure 1. Low-energy conformation of a HP lattice protein with 124 monomers ($E = -70$ a.u.). The core of hydrophobic residues (dark spheres) is well-separated from the environment by the polar molecules (light spheres).

from the thermodynamics of lattice proteins. It is well known that maxima in the specific heat indicate collective conformational changes within the protein. In order to study these effects with reasonable accuracy it is necessary to apply an efficient conformational search algorithm that is applicable over a wide range of temperatures. Therefore "flat histogram" methods like the multicanonical Monte Carlo algorithm [4] and a related method by Wang and Landau [5] that directly simulates the density of states of the system, are preferable choices. In this regard, particular interest is devoted to the detection of conformational "barriers" that strongly influence the efficiency and applicability of Monte Carlo algorithms.

Work partially supported by the German-Israel-Foundation (GIF) under grant No. I-653-181.14/1999, the ESF-Network "Challenges in Molecular Simulations: Bridging the Length- and Time-Scale Gap (SIMU)", and the Studienstiftung des deutschen Volkes.

References

[1] K. A. Dill, Protein Science **8**, 1166 (1999).

[2] K. A. Dill, Biochemistry **24**, 1501 (1985).
K. F. Lau and K. A. Dill, Macromolecules **22**, 3986 (1989).

[3] P. Grassberger, Phys. Rev. E **56**, 3682 (1997).
H.-P. Hsu, V. Mehra, W. Nadler and P. Grassberger, J. Chem. Phys. **118**, 444 (2003).

[4] B. A. Berg and T. Neuhaus, Phys. Rev. Lett. **68**, 9 (1992).
W. Janke, Int. J. Mod. Phys. C **3**, 1137 (1992).

[5] F. Wang and D. P. Landau, Phys. Rev. Lett. **86**, 2050 (2001).

14.4.10. The 2D Ising Model with Brascamp-Kunz Boundary Conditions

E. Bittner, W. Janke, R. Kenna (Coventry University), A. Krinner and T. Vogel

The two-dimensional Ising model in zero external field is the simplest, exactly solvable statistical physics model displaying critical behaviour [1]. Exploiting the exactly known partition function for finite toroidal $L \times L$ lattices [2], the specific heat finite-size scaling (FSS) has been analytically determined to order L^{-1} a long time ago [3]. At the infinite volume critical point $\beta_c \equiv J/k_B T_c$ this was recently extended to order L^{-3} [4,5], demonstrating that only integer powers of L^{-1} occur.

In this project we studied lattices with Brascamp-Kunz boundary conditions [6,7] which can be depicted as a cylinder of length M with $2N$ boundary spins all pointing up at the one end and alternating between up and down at the other end. With these boundary conditions the partition function consists of only one product term (instead of a sum of four such terms in the toroidal case), and hence in particular the Fisher zeroes are almost trivial to obtain [7]. The product form also allowed for the detailed investigation of the FSS properties of the specific heat reported in Ref. [8] which was later confirmed and partially generalized in a more formalized way [9]. Recently we extended previous analyses of the singular part of the specific heat at T_c and at its maximum for aspect ratios $\rho = N/(M+1)$ to the full specific heat for aspect ratios $\sigma = 2N/M$, which now also includes the square lattice case.

In order to test the analytical results numerically, we adapted the single-cluster Monte Carlo algorithm to the special fixed boundary conditions at hand. To this end the boundary values are considered as part of the clusters and flipped as well ($\ldots + + + \ldots \to \ldots - - - \ldots$ and $\ldots + - + \ldots \to \ldots - + - \ldots$), thereby creating four different cases which are equivalent by symmetry. We furthermore extracted the exact density of states from the partition function which, due to its comparatively simple product form, can be driven to larger system sizes than for toroidal boundary conditions. The latter result was compared with multicanonical and Wang-Landau flat histogram Monte Carlo simulations.

Work partially supported by the German-Israel-Foundation (GIF) under grant No. I-653-181.14/1999.

References

[1] L. Onsager, Phys. Rev. **65**, 117 (1944).

[2] B. Kaufman, Phys. Rev. **76**, 1232 (1949).

[3] A. E. Ferdinand and M. E. Fisher, Phys. Rev. **185**, 832 (1969).

[4] J. Salas, J. Phys. A **34**, 1311 (2001).

[5] N. Sh. Izmailian and C.-K. Hu, Phys. Rev. E **65**, 036103 (2002).

[6] H. J. Brascamp and H. Kunz, J. Math. Phys. **15**, 65 (1974).

[7] W. T. Lu and F. Y. Wu, J. Stat. Phys. **102**, 953 (2001).

[8] W. Janke and R. Kenna, Phys. Rev. B **65**, 064110 (2002), Preprint cond-mat/0103332; Nucl. Phys. B (Proc. Suppl.) **106&107**, 929 (2002), Preprint hep-lat/0112037.

[9] N. Sh. Izmailian, K. B. Oganesyan and C.-K. Hu, Preprint cond-mat/0202282.

14.4.11. Information Geometry and Phase Transitions

W. Janke, D. A. Johnston (Heriot-Watt University, Edinburgh), R. Kenna (Coventry University) and Ranasinghe P. K. C. Malmini (University of Sri Jayewardenepura, Sri Lanka)

Various authors, motivated by ideas in parametric statistics [1], have discussed the advantages of taking a geometrical perspective on statistical mechanics [2,3]. The "distance" between two probability distributions in parametric statistics can be measured using a geodesic distance which is calculated from the Fisher information matrix for the system. To this end the manifold $\mathcal{M}$ of parameters is endowed with a natural Riemannian metric, the Fisher-Rao metric [1]. For a spin model in field, $\mathcal{M}$ is a two-dimensional manifold parametrised by $(\theta^1, \theta^2) = (\beta, h)$. The components of the Fisher-Rao metric take the simple form $G_{ij} = \partial_i \partial_j f$ in this case, where f is the reduced free energy per site and $\partial_i = \partial/\partial\theta^i$. A natural object to consider in any geometrical approach is the scalar or Gaussian curvature $\mathcal{R}$ which in various two parameter calculable models has been found to diverge at the phase transition point β_c according to the scaling relation $\mathcal{R} \sim |\beta - \beta_c|^{\alpha-2}$, where α is the usual specific heat critical exponent. For spin models the necessity of calculating in non-zero field has limited analytic consideration to 1D, mean-field and Bethe lattice Ising models [4].

In this project we used the solution in field of the Ising model on an ensemble of planar random graphs (where $\alpha = -1,\ \beta = 1/2, \gamma = 2$) [5] to evaluate the scaling behaviour of the scalar curvature explicitly, and find $\mathcal{R} \sim |\beta - \beta_c|^{-2}$ [6]. The apparent discrepancy with the general scaling postulate is traced back to the effect of a *negative* α [6].

As anticipated the same effect is found [7] in exact calculations for the three-dimensional spherical model, which was solved (in field) in the classic Berlin and Kac paper [8] and shares the same critical exponents as the Ising model on two-dimensional planar random graphs. We mainly concentrated on the 3D case, but also discussed other dimensions [7], in particular the mean-field like behaviour which sets in at $D = 4$.

Work partially supported by the EU-Network HPRN-CT-1999-000161 "Discrete Random Geometries: From Solid State Physics to Quantum Gravity" and the ESF-Network "Geometry and Disorder: From Membranes to Quantum Gravity".

References

[1] R. A. Fisher, Phil. Trans. R. Soc. Lond., Ser. A **222**, 309 (1922).
C. R. Rao, Bull. Calcutta Math. Soc. **37**, 81 (1945).

[2] G. Ruppeiner, Phys. Rev. A **20**, 1608 (1979); *ibid.* A **24**, 488 (1980); Rev. Mod. Phys. **67**, 605 (1995).

[3] H. Janyszek and R. Mrugała, Phys. Rev. A **39**, 6515 (1989).
D. Brody and N. Rivier, Phys. Rev. E **51**, 1006 (1995).
D. Brody and L. Hughston, Proc. Roy. Soc. London A **455**, 1683 (1999).

[4] B. P. Dolan, D. A. Johnston and R. Kenna, J. Phys. A **35**, 9025 (2002).

[5] V. A. Kazakov, Phys. Lett. A **119**, 140 (1986).
D. V. Boulatov and V.A. Kazakov, Phys. Lett. B **186**, 379 (1987).

[6] W. Janke, D. A. Johnston and Ranasinghe P. K. C. Malmini, Phys. Rev. E **66**, 056119 (2002), Preprint cond-mat/0207573.

[7] W. Janke, D. A. Johnston and R. Kenna, cond-mat/0210571, to appear in Phys. Rev. E.

[8] T. Berlin and M. Kac, Phys. Rev. **86**, 821 (1952).

14.4.12. Functional Closure of Schwinger-Dyson Equations in Quantum Electrodynamics

M. Bachmann, H. Kleinert (Freie Universität Berlin) and A. Pelster (Freie Universität Berlin)

In quantum field theory, the calculation of physical quantities usually relies on evaluating Feynman integrals which are pictured by diagrams. Each diagram is associated with a certain weight depending on its topology. In contrast to various convenient combinatorial computer programs (e.g. *FeynArts* or *QGRAF* [1]) and the star-graph generation [2], we use a more systematic and physical approach to construct all Feynman diagrams of a quantum field theory [3,4]. It is based on the observation that the complete knowledge of the vacuum energy implies the knowledge of the entire theory ("the vacuum is the world") [5]. In this spirit, all vacuum diagrams are initially generated by a recursive graphical procedure, which is derived from a functional differential equation involving functional derivatives with respect to free propagators and interactions. In a subsequent step, the n-point functions are found graphically by applying the functional derivatives to the vacuum energy [6]. In contrast to the conventional generating functional technique no external currents coupled to single fields are used, such that there is no need for introducing Grassmann sources for fermion fields. An additional advantage is that the number of derivatives necessary to generate a certain correlation function is half as big as with external sources.

The Feynman diagrams of n-point functions obey an infinite hierarchy of coupled Schwinger-Dyson equations which can be closed functionally by using functional derivatives with respect to the free propagators and the interaction. In this way we obtain a closed set of equations determining the connected electron and photon two-point function, the connected three-point function as well as the electron and photon self-energy and the one-particle irreducible three-point function [7]. A further advantage is that in these cases the closed set of Schwinger-Dyson equations can be converted into graphical recursion relations for the connected and one-particle irreducible Feynman diagrams. From these follow the corresponding vacuum diagrams by short-circuiting external legs.

References

[1] J. Külbeck, M. Böhm and A. Denner, Comp. Phys. Comm. **60**, 165 (1991).
T. Hahn, Preprint hep-ph/9905354.
P. Nogueira, J. Comp. Phys. **105**, 279 (1993).

[2] B. R. Heap, J. Math. Phys. **7**, 1582 (1966).
J. F. Nagle, J. Math. Phys. **7**, 1588 (1966).

[3] H. Kleinert, Fortschr. Phys. **30**, 187 and 351 (1982).

[4] A. N. Vasiliev, *Functional Methods in Quantum Field Theory and Statistical Physics* (Gordon and Breach Science Publishers, New York, 1998); translation from the Russian edition (St. Petersburg University Press, St. Petersburg, 1976).

[5] R. F. Streater and A. S. Wightman, *PCT, Spin and Statistics, and All That* (W. A. Benjamin, Reading, Massachusetts, 1964).
J. Schwinger, *Particles, Sources, and Fields*, Vols. I and II (Addison-Wesley, Reading, 1973).

[6] H. Kleinert, A. Pelster, B. Kastening and M. Bachmann, Phys. Rev. E **62**, 1537 (2000).
M. Bachmann, H. Kleinert and A. Pelster, Phys. Rev. D **61**, 085017 (2000).

[7] A. Pelster, H. Kleinert and M. Bachmann, Ann. Phys. (NY) **297**, 363 (2002).

14.4.13. Z_2-Spins on Dynamical 4D Z_2-Regge Lattices

E. Bittner, W. Janke and H. Markum (Technische Universität Wien)

This project is devoted to numerical studies of a non-perturbative formulation of (Euclidean) quantum gravity using Regge calculus [1]. In this path-integral approach the fluctuating space-time metric is modeled by varying edge lengths of the Regge skeleton. In contrast to the dynamical triangulation approach, here the connectivity of the skeleton is kept fixed. Spin models defined on such dynamical manifolds are often used to mimic the interaction of gravity with matter fields. In particular the Ising model may be viewed as the minimal representation of a scalar field, sharing the same Z_2 symmetry.

Numerical studies of the coupled system are extremely time demanding [2,3] and one therefore seeks for suitable approximations. One such candidate is the Discrete Regge Model [4] where the squared link lengths of the discretized manifold are constrained to take on only two different values. As a first step we qualitatively compared the two versions of pure quantum Regge calculus by means of Monte Carlo simulations, using in both models the same (local) functional integration measure, chosen such that the Z_2-Regge Model becomes particularly simple [5]. We also investigated an Ising spin system coupled to the two-dimensional Discrete Regge Model and compared it with the results of the Standard Regge Calculus [6]. Particular emphasis was placed on the phase transition of the spin system and the associated critical exponents, employing finite-size scaling analyses. Overall we can summarize that our numerical estimates agree with the Onsager exponents for regular static lattices and are thus fully consistent with the Standard Regge Calculus results [2,3].

In the current project we extended these studies to an Ising spin system coupled to a four-dimensional Z_2-Regge lattice [7,8] and compared with simulations of the Ising model on a regular four-dimensional hypercube where, being at the upper critical dimension, multiplicative logarithmic corrections play an important role and had to be considered with great care. As the main result of our finite-size scaling analyses, similar to two dimensions, the critical properties in the Regge case turn out to be compatible with those of the regular lattice model [7,8].

Work partially supported by the DFG Graduiertenkolleg "Quantenfeldtheorie" and the EU-Network HPRN-CT-1999-000161 "Discrete Random Geometries: From Solid State Physics to Quantum Gravity".

References

[1] T. Regge, Nuovo Cimento **19**, 558 (1961).

[2] M. Gross and H. Hamber, Nucl. Phys. B **364**, 703 (1991).

[3] C. Holm and W. Janke, Phys. Lett. B **335**, 143 (1994); *ibid.* B **375**, 69 (1996).

[4] T. Fleming, M. Gross and R. Renken, Phys. Rev. D **50**, 7363 (1994); W. Beirl, H. Markum and J. Riedler, Int. J. Mod. Phys. C **5**, 359 (1994).

[5] E. Bittner, A. Hauke, H. Markum, J. Riedler, C. Holm and W. Janke, Phys. Rev. D **59**, 124018 (1999).

[6] E. Bittner, W. Janke, H. Markum and J. Riedler, Physica A **277**, 204 (2000).

[7] E. Bittner, W. Janke and H. Markum, Nucl. Phys. B (Proc. Suppl.) **106&107**, 989 (2002), Preprint hep-lat/0110050.

[8] E. Bittner, W. Janke and H. Markum, Leipzig/Wien preprint (December 2001), submitted to Phys. Rev. D.

14.5. Molecule Dynamics/Computer Simulations(MDC)

Using methods of statistical physics and computer simulations we investigate classical many-particle systems interacting with interfaces. One aim of the research in our department is to build up a bridge between theoretical and experimental physics.

By means of analytical theories of statistical physics and computer simulations (Molecular dynamics, Monte Carlo procedures, percolation theories) using modern workstations and supercomputers we examine subjects for which high interest exists in basic research and industry as well. The examinations involve transport properties (diffusion of guest molecules) in zeolites and the structural and phase behaviour of fluids at biological active interfaces (membranes). Especially we are interested to understand

- the diffusion behaviour of guest molecules in zeolites in dependence on thermodynamic parameters, steric conditions, intermolecular potentials and the concentration of the guest molecules,
- structure and phase behaviour of dense fluids in pores, slits and model membranes in dependence on geometric and thermodynamic conditions
- and the migration of waste in deposits by use of percolation theories

in microscopic detail and to compare the results with experimental data. The use of a network of PC's and workstations (Unix, Linux, Windows), the preparation and application of programs (Fortran, C, C^{++}) and the interesting objects (zeolites, membranes) give excellent possibilities for future careers of undergraduates, graduate students and postdocs.

Our research in 2002 was a part of the long-term program of the Sonderforschungsbereich 294 'Molecules Interacting with Interfaces' granted by the Deutsche Forschungsgemeinschaft and is part of several other programs (e.g. a joint research project DFG/TRF-Thailand, other DFG projects and a NATO grant). We have a close collaboration with the Institute of Experimental Physics I (Physics of Interfaces and Biomembranes) of the University of Leipzig and many institutions in several countries (University of California, Irvine; University of Massachusetts, Amherst; Guelph, Canada; Athens/Patras; Prague; Sassari, Italy; Bangkok; Bordeaux; Warschau; Wien; Regensburg; MPI Mainz; Bundesanstalt für Geologie und Rohstoffe (BGR) Hannover).

14.5.1. Random Walk Treatment of Ethane in an LTA Zeolite

A. Schüring, S. M. Auerbach (University Amherst, Massachusetts, USA), S. Fritzsche and R. Haberlandt

Investigations of the dynamics and the diffusion of ethane in zeolite LTA showed a surprising temperature dependence of the self diffusion coefficient D. It could be shown that this dependence is caused by an entropic barrier [1].

To understand the mechanism and to reproduce the temperature dependence of D a random walk treatment has been derived in [2] in terms of jump probabilities. The jump probabilities can be taken from an MD run.

In analogy with the theory of vacancy diffusion,[3] a correlation factor $f(T)$ is used.

$$f(T) = \frac{1 + \langle \cos\theta \rangle_T}{1 - \langle \cos\theta \rangle_T}, \tag{1}$$

where θ is the angle between two successive cage-to-cage jumps on the simple-cubic lattice. Series of jump events are summed up. The agreement of the resulting D values from the model with those obtained from the mean square displacement (Einstein relation) can be seen in Fig. 1.

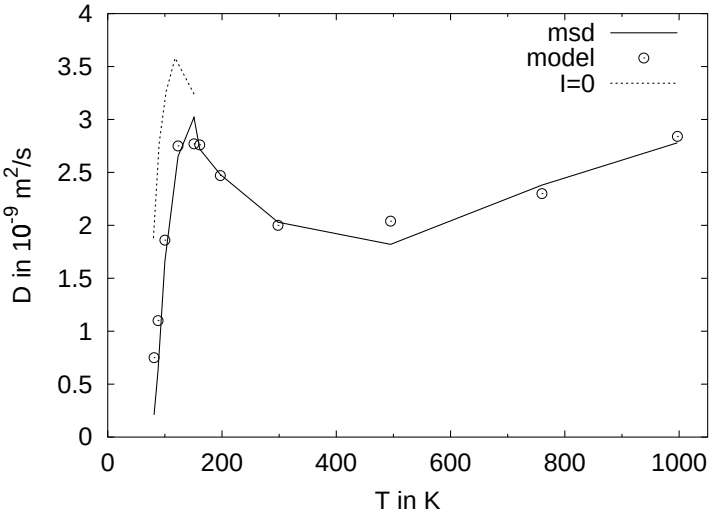

Figure 1. Comparison of self-diffusion coefficients calculated from mean square displacements (msd) via the Einstein equation and from the jump model. $I = 0$ shows the self-diffusion coefficients at infinite dilution.

References

[1] A. Schüring, S. M. Auerbach, S. Fritzsche and R. Haberlandt, J. Chem. Phys. **116**, 10890 (2002).

[2] A. Schüring, S. M. Auerbach, S. Fritzsche and R. Haberlandt, *Capturing geometric correlations for ethane diffusion in cation-free LTA zeolite through the vacancy correlation factor*, submitted to J. Phys. Chem. B.

[3] J. Kärger and D. M. Ruthven, *Diffusion in Zeolites and Other Microporous Solids* (Wiley, New York, 1992).

14.5.2. Analytical Theory and MD Simulations of Correlated Anisotropic Diffusion

S. Fritzsche and Jörg Kärger

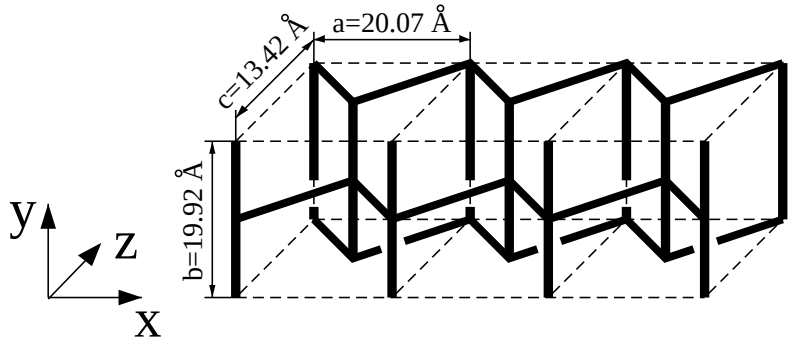

Figure 1. Channel structure of Silicalite–1

Summing up infinite series of transition probabilities between intersections in silalite–1 it has been shown that in the case of uncorrelated movements, which is a good approximation in many cases for small molecules, the elements of the diffusion tensor obey the relationship [1]

$$\frac{c^2}{D_z} = \frac{a^2}{D_x} + \frac{b^2}{D_y} \tag{1}$$

with a, b and c denoting the unit cell extensions in x–, y– and z–direction. Deviations from eq. (1) have been quantified by introducing a memory parameter β in ref. [2]

$$\beta = \frac{c^2/D_z}{a^2/D_x + b^2/D_y}. \tag{2}$$

Such processes are examined with inclusion of correlations [3–5]. In the case of silicalite–1 e.g. a surprisingly well working approximative formula

$$\beta \approx 1 + 2(p_y \Delta\pi_x + p_x \Delta\pi_y + \Delta\pi_{x,y}). \tag{3}$$

has been derived and confirmed by MD simulations. p_x means the probability that the next move is in x–direction, $p_{y,x}$ means the probability that the next move is in x–direction, if the preliminary one was in y–direction and so on.

$$\Delta\pi_x = p_{x,x} - p_{x,-x} \qquad \Delta\pi_y = p_{y,y} - p_{y,-y} \qquad \Delta\pi_{x,y} = p_{x,x} + p_{x,-x} - 2p_{y,x}. \tag{4}$$

References

[1] J. Kärger, J. Phys. Chem **95**, 5558 (1991).
[2] E. J. Maginn, A. T. Bell and D. N. Theodorou, J. Phys. Chem **100**, 7155 (1996).
[3] S. Fritzsche and J. Kärger, Studies in Surface Science and Catalysis **142**, 1955 (2002).
[4] S. Fritzsche and J. Kärger, submitted to Europhys. Lett.
[5] S. Fritzsche and J. Kärger, J. Phys. Chem., in print.

14.5.3. Cross Effects Between Molecular Vibrations and Diffusion

S. Fritzsche, R. Haberlandt and M. Wolfsberg (UCI, Irvine, USA)

In the literature a strong influence of the lattice vibrations on the diffusion of methane the cation free A zeolite was found in [1,2]. But our investigations showed by Molecular Dynamics Computer Simulations that the diffusion coefficient of the guest molecules was nearly the same for the rigid and the vibrating lattice [3] and we gave an explanation of the discrepancy. This earlier result could be confirmed and understood in more detail by investigating the equilibration of kinetic energy differences in small zeolite cavities [4] using e.g. the one particle kinetic energy autocorrelation function.

The influence of the molecule vibrations has now been included as well. It could be shown that for the diffusion of methane in silicalite–1 the lattice vibration have some influence on the value of D while the influence of the molecule vibrations is negligible [5].

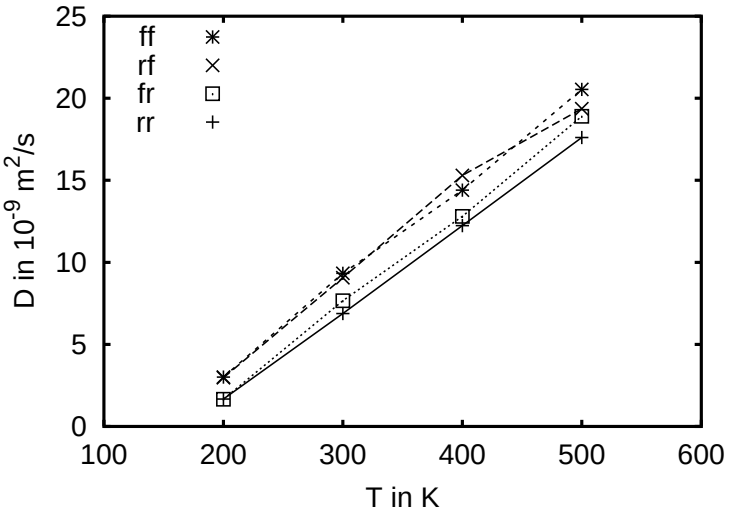

Figure 1. The average diffusion coefficient D in 10^{-9} m^2/s for $I = 1$. ff means lattice and molecule flexible, rf means molecule rigid and lattice flexible, fr means molecule flexible lattice rigid, rr means both lattice and molecule rigid.

References

[1] P. Demontis and G. B. Suffritti, Chem. Phys. Lett. **223**, 355 (1994).

[2] P. Demontis and G. B. Suffritti, in: *Proceedings of the the 10h International Zeolite Conference*, eds. J. Weitkamp, H. G. Karge, H. Pfeifer and W. Hoelderich (Elsevier, Amsterdam, 1994), p. 2107.

[3] S. Fritzsche, M. Wolfsberg, R. Haberlandt, P. Demontis, G. B. Suffritti and A. Tillocca, Chem. Phys. Lett. **296**, 253 (1998).

[4] S. Fritzsche, M. Wolfsberg and R. Haberlandt, Chem. Phys. **253**, 283 (2000).

[5] S. Fritzsche, M. Wolfsberg, and R. Haberlandt, *The Importance of Various Degrees of Freedom in the Theoretical Study of the Diffusion of Methane in silicalite–1*, submitted to Chem. Phys.

14.5.4. Molecular Dynamics Simulations of Water in Chabazite

S. Jost, S. Fritzsche, R. Haberlandt and Ph. A. Bopp (University of Bordeaux, France)

The simulation of this diffusional process [1] turned out to be at the limit of the computational capabilities, so we had to increase the temperature up to $T = 600$K, to get mean square displacements, which are large enough, to evaluate diffusion coefficients. At this temperature the system shows a quite uncommon dependence on the loading [**?**]: For the almost dehydrated zeolite with only one quarter of the full loading, there is a very slow diffusion. Then the diffusion coefficient increases with increasing loading, up to a maximum value for 75% of the full loading. Then it decreases with further increasing loading.

This abnormal behaviour can be explained by the knowledge about the adsorption places. At approximately half of the maximum loading, almost all preferred places in the hydration shells of the cations are filled up. Therefore, at higher loadings there are some water molecules which are only loosely bound and relatively free to move. With further increase in the loading, the fraction of mobile molecules increases, leading to more diffusional motion, but with more molecules, the number of potential collision partners increases as well, which limits the increase of D and dominates for the highest loadings.

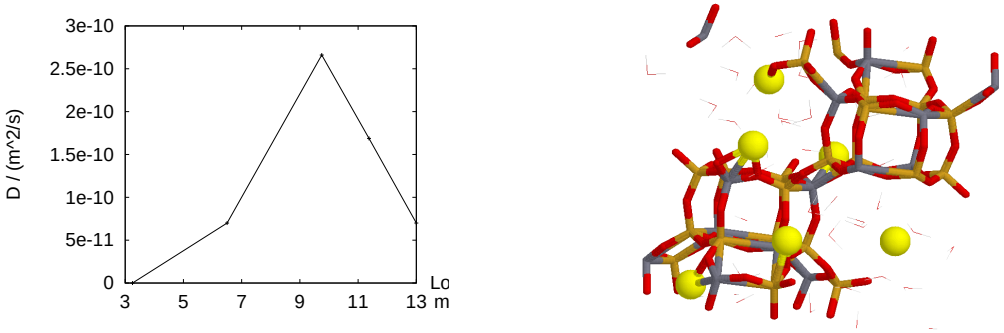

Figure 1. Left: Mean diffusion coefficient versus Loading at $T = 600$K. Right: Snapshot from MD-Simulation. Cations are bright, water molecules are represented by small ticks.

References

[1] S. Jost, S. Fritzsche and R. Haberlandt, Studies in Surface Science and Catalysis **142**, 1947 (2002).

14.5.5. Water in Silicalite

R. Haberlandt, S. Fritzsche, C. Bussai (Chulalongkorn University, Bangkok) and
S. Hannongbua (Chulalongkorn University, Bangkok)

Because of the hydrophobic nature of pure silica zeolites the diffusion of water in silicalite was not yet examined until the existence of water could be shown experimentally and investigated in comparison with MD simulations [1].

The research was based on a joint project of the DAAD (Germany) and the TRF (Thailand) including the Ph. D. study of Miss C. Bussai.

In ab initio calculations potential energies for several thousand configurations of an water molecule in silicalite have been calculated. Then, by fitting an analytical potential for the water/zeolite interaction has been developed [2–4]. This potential has then been used in Molecular Dynamics simulations [3,5,1]. For the water/water interaction a well established potential from the literature has been used [6].

The resulting D values from experiments (by PFG NMR measurements) and MD simulations are in satisfactory agreement with each other [1].

References

[1] C. Bussai, S. Vasenkov, H. Liu, W. Böhlmann, S. Hannongbua, S. Fritzsche, R. Haberlandt and J. Kärger, Applied Catalysis A **232**, 59 (2002).

[2] C. Bussai, S. Hannongbua and R. Haberlandt, J. Phys. Chem. B **105**, 3409 (2001).

[3] C. Bussai, R. Haberland, S. Hannongbua, S. Jost and S. Fritzsche, *Computer Simulations of Water in Zeolites*, in: *Studies in Surface Science and Catalysis*, eds. A. Galarneau, F. D. Renzo, F. Fajula and J. Vedrine (Elsevier, Amsterdam, 2001).

[4] C. Bussai, S. Hannongbua, S. Fritzsche and R. Haberlandt, Chem. Phys. Lett. **354**, 310 (2002).

[5] C. Bussai, S. Hannongbua, S. Fritzsche and R. Haberlandt, Studies in Surface Science and Catalysis **142**, 1979 (2002).

[6] P. Bopp, G. Jancso and K. Heinzinger, Chem. Phys. Lett. **98**, 129 (1983).

14.5.6. Chemical Potentials and Phase Equilibria in Aqueous Phases: Simulation and Gibbs-Duham integration

H. L. Vörtler, J. Galle (IZBI, Leipzig) and I. Nezbeda (Charles University, Prague)

This project is part of our long-term research on structure and thermodynamics of water-like fluid phases on the basis of Primitive Models of Association

We perform canonical computer simulations of primitive models of aqueous fluids. comprising the original Kolafa-Nezbeda model and more recent extended primitive water models [1] on both bulk conditions and geometrical restrictions.

In detail we compare bulk structural and thermodynamic properties of the extended five-site primitive water model (EPM-5) with the corresponding properties in two-dimensional films and narrow micropores. EPM-5 describes water by a hard core and short ranging off-center interactions modelling explicitly hydrogen bonds and repulsions between opposite charges. Structural quantities measured are site-site correlation functions, cluster size distributions saturation of hydrogen bonded molecular networks, and mean square distances.

Thermodynamic Quantities studied are internal energy, pressure and chemical potential. It turned out that Widom's test particle method for the estimation of the chemical potential is applicable for weak association only. For strong association (typical for liquid bulk water) the insertion probability becomes so small that sophisticated gradual insertion techniques have to be used [2] to get reproducible results.

In 2002 we focused our studies on simulating chemical potential versus packing fraction isotherms in a wide range of temperatures. With decreasing temperature a transition is observed from monotonous increasing isotherms to a van der Waals loop which indicates the existence of a two-phase region below a 'critical' temperature. This behaviour is found for both bulk and confined fluids. We estimate the densities of coexisting fluid phases [3] by means of Gibbs-Duham Integration (Maxwell construction in terms of the chemical potential) extending a method which we introduced recently [4].

Taking into account that the primitive models have to be considered as basic approximations describing the intermolecular interactions of aqueous fluids and solutions the obtained results provide basic information for an understanding of structure and phase behaviour of homogeneous and inhomogeneous aqueous phases on a molecular level. Examples of practical applications are bulk aqueous solutions, water confined to microporous media or thin water films in biological systems. The project is part of an tri-lateral international collaboration program, supported by NATO and granted by DFG (SFB 294)

References

[1] I. Nezbeda, J. Mol. Liquids, **73–74**, 317 (1997).

[2] I. Nezbeda and J. Kolafa, Molec. Simulation. **5**, 391 (1991).
M. Kettler, H. L. Vörtler, I. Nezbeda and M. Strnad, Fluid Phase Equilib. **181**, 83 (2001).

[3] H. L. Vörtler, M. Kettler and J. Galle, *Structure and Thermodynamics of Primitive Water Models on Bulk conditions and in 2-dimensional Layers: MC simulation studies*, 17th IUPAC Conference on Chemical Thermodynamics, Book of Abstracts, p. 3, Rostock, July 28, 2002.

[4] H. L. Vörtler, W. R. Smith, J. Chem. Phys. **112**, 5186 (2000).

14.5.7. Cavity Distribution Functions in Confined Fluids

H. L. Vörtler and W. R. Smith (University of Guelph, Ontario, Canada)

The project continues statistical-mechanical and simulation studies of the molecular structure of inhomogeneous fluids in terms of spatial distribution functions. Systems under consideration are basic models of confined fluids, such as hard-core fluids at single walls and in micropores of simple geometry.

We focus on cavity distribution functions, basic structural quantities for both bulk and confined fluid systems, which provide an efficient route to calculating excess chemical potentials and background correlation functions [1].

We develop novel MC simulation techniques to calculate efficiently cavity pair distribution functions of confined hard-sphere systems using virtual particle/cavity insertion moves in a canonical ensemble. Results were obtained for conditional distribution functions of pairs of hard-sphere cavities in fluids confined to slit-like micropores with hard walls [2].

To our best knowledge this is the first calculation of such functions, which are of interest as reference data for the improvement of statistical mechanical theories of confined fluids and additionally, represent quasi-experimental data for a modeling of the solubility of polyatomic molecules in simple molecularly confined solvents. Particularly, the simulated singlet and pair cavity functions provide basic information for developing analytical closures of the BGY integral equation hierarchy [3] connecting these distribution functions.

The results contribute to both the basic research in the field of statistical mechanics of confined fluids and to a deeper understanding of experimental solubility and sorption phenomena e.g.in microporous media and at biointerfaces on a molecular level.

We acknowledge financial support by DFG (SFB 294, TP H2) and by NATO (Collaborative Linkage Grant PST.CLG.978178/6343CRG).

References

[1] R. Speedy, J. Chem. Soc. Faraday II **76**, 693 (1980).

[2] W. R. Smith and H. L. Vörtler, *Computer Simulation of Cavity Pair Distribution Functions of Hard Spheres in a Hard Slit Pore*, Mol. Phys. (2003), in press.

[3] S. Labìk, W. R. Smith and R. Speedy, J. Chem. Phys. **88**, 1944 (1987).

14.6. Statistical Physics (STP)

We work on stochastic models, on the connections of statistical mechanics to quantum field theory, on the mathematical and physical aspects of renormalization group (RG) theory, and on its applications in condensed matter physics. Our methods range from mathematical proofs to the computational solution of large differential equations.

One of the central topics in our current research is an RG approach to many–fermion systems, which is used to investigate the properties of the Hubbard model in the parameter range relevant for high–temperature superconductivity. The RG method applied here is an exact functional transformation of the action of the system, which leads to an infinite hierarchy of equations for the Green functions. Truncations of this hierarchy are used in applications. In a number of nontrivial cases, this truncation can be justified rigorously, so that the method lends itself to mathematical studies. These mathematical aspects are also under investigation.

At present, we have collaborations with ETH Zurich, the Massachussetts Institute of Technology, the University of British Columbia, the University of Toronto, and the Courant Institute (New York).

14.6.1. RG Flows for Two-Dimensional Fermi Systems

C. Honerkamp (MIT), M. Salmhofer and T. M. Rice (ETH Zurich)

We study the (t, t')–Hubbard model in the parameter regime relevant for the description of high–temperature superconductors [3]. We use the functional renormalization group method developed in [1,2]. This technique provides a means to study the competition between different order parameters in an unbiased way. The renormalization group flow leads to strong coupling. Studying the response to external fields and varying the density, we find three regimes. The first corresponds to a d–wave superconductor, the third to an antiferromagnet. In the second, intermediate regime, the coupled flow of superconducting, antiferromagnetic and umklapp couplings leads to a suppression of the quasiparticle weights near the zone boundaries, hence a truncation of the Fermi surface. These findings agree qualitatively with the experiments.

To obtain information about the strength of Recently d–density wave and Pomeranchuk instabilities were proposed [4,5] as instabilities competing with antiferromagnetism and superconductivity. A direct comparison of these instabilities is difficult in the momentum–cutoff RG scheme because the momentum space cutoff removes all particle–hole excitations with a pair momentum near to zero. The temperature–flow RG of [6,7] allows us to do an unbiased comparison. Both d–density wave and Pomeranchuk susceptibilities are found to be growing, but more weakly than those of antiferromagnetism and superconductivity [8].

References

[1] M. Salmhofer, Commun. Math. Phys. **194**, 249 (1998).

[2] M. Salmhofer and C. Honerkamp, Prog. Theor. Phys. **105**, 1 (2001).

[3] C. Honerkamp, M. Salmhofer, N. Furukawa and T. M. Rice, Phys. Rev. B **63**, 035109 (2001).

[4] S. Chakravarty, R. B. Laughlin, D. K. Morr and C. Nayak, Phys. Rev. B **63**, 94503 (2001).

[5] C. Halboth and W. Metzner, Phys. Rev. Lett. **85**, 5162 (2000).

[6] C. Honerkamp and M. Salmhofer, Phys. Rev. B **64**, 184516 (2001).

[7] C. Honerkamp and M. Salmhofer, Phys. Rev. Lett. **87**, 187004 (2001).

[8] C. Honerkamp, M. Salmhofer and T. M. Rice, European Physical Journal B **27**, 127 (2002).

14.6.2. Wave Function Renormalization in Low-Dimensional Fermi Systems

C. Honerkamp (MIT) and M. Salmhofer

Selfenergy effects, in particular the wave function renormalization Z, become important near van Hove singularities. An important question is whether these effects significantly influence the classification of the instabilities of the Fermi gas near van Hove singularities. We analyze these effects for quasi–one–dimensional and two–dimensional systems using an RG including a flowing Z factor [1]. We obtain the standard Luttinger exponents [2] in one dimension and the crossover scales [3] in quasi-one–dimensional systems. In two dimensional systems near van Hove singularities, we find that Z gets small, but that the suppression of Z does not change the instabilities found in [4,5].

References

[1] C. Honerkamp and M. Salmhofer, *Flow of the quasiparticle weight in the N–patch renormalization group scheme*, Preprint cond–mat/0212066.

[2] W. Metzner, C. Castellani and C. Di Castro, Adv. Phys. **47**, 317 (1998).

[3] C. Bourbonnais, B. Guay, and R. Wortis, Preprint cond-mat/0204163.
C. Bourbonnais, Preprint cond-mat/0204345.

[4] C. Honerkamp, M. Salmhofer, N. Furukawa and T. M. Rice, Phys. Rev. B **63**, 035109 (2001).

[5] C. Honerkamp, M. Salmhofer and T. M. Rice, European Physical Journal B **27**, 127 (2002) .

14.6.3. Nonperturbative Studies of Two-Dimensional Fermi Systems

W. de Siqueira Pedra and M. Salmhofer

We use the sector method of [1] to do a mathematically rigorous study of many–fermion systems in two dimensions. Specifically, we work on a proof of the Fermi liquid criterion proposed in [2] for systems at positive temperature. This criterion has been verified for the model with dispersion relation $\varepsilon(p) = p^2/2m$ [3], where the Fermi curve is a circle. Our proof will cover the case of $\varepsilon(p)$ without rotational symmetry, where the Fermi curve is positively curved everywhere. In the absence of rotational symmetry, the regularity problem for the selfenergy and the Fermi curve becomes nontrivial (and difficult). It was treated to all orders in perturbation theory in [5]. We have implemented the overlapping loop method, which is one of the main ideas of the proofs in [5], in the tree expansions [4] used for nonperturbative proofs. Establishing that the curvature of the Fermi curve remains bounded requires analyzing double overlaps, as in [5].

Another important novel feature of our method is that we do not use counterterms, but instead adjust the fermionic covariance. This avoids the so–called "inversion problem" of constructions with counterterms.

References

[1] J. Feldman, J. Magnen, V. Rivasseau and E. Trubowitz, Helv. Physica Acta **65**, 679 (1992).

[2] M. Salmhofer, Commun. Math. Phys. **194**, 249 (1998).

[3] M. Disertori and V. Rivasseau, Commun. Math. Phys. **215**, 251 (2000).

[4] M. Salmhofer and C. Wieczerkowski, J. Stat. Phys. **99**, 557 (2000).

[5] J. Feldman, M. Salmhofer and E. Trubowitz, Journal of Statistical Physics **84**, 1209 (1996); Comm. Pure Appl. Math. **51**, 1133 (1998); Comm. Pure Appl. Math. **52**, 273 (1999); Comm. Pure Appl. Math. **53**, 1350 (2000).

14.6.4. Diffusion Constant of the Asymmetric Exclusion Process

C. Landim (IMPA, Brasil), J. Quastel (University of Toronto), M. Salmhofer and H.–T. Yau (Courant Institute, New York)

The asymmetric exclusion process is a Markov process describing the motion of a system of classical particles on a lattice. The hopping amplitude of the particles is asymmetric so that there is transport in the system. The other essential feature of the model is the hard–core constraint that no two particles can occupy the same site.

This stochastic process is one of the standard models of lattice gas dynamics. It is relevant e.g. for the study of hydrodynamic limits [3] and growth problems [1,2]. The main problem in its analysis is the hard–core constraint which cannot be treated perturbatively.

It is known that the diffusion constant is finite in three dimensions, and, as a result of an exact solution, the totally asymmetric exclusion process in one dimension is known to be superdiffusive, i.e. the diffusion coefficient $D(t)$ diverges as $t \to \infty$. For the general ASEP in one dimension and the two–dimensional case, the behaviour of $D(t)$ remained an open problem.

We prove that antisymmetric exclusion processes are superdiffusive in dimensions one and two. One of the main ideas in the proof is that the hard–core constraint can be removed at a suitable point in the equations by variational methods. The method is strong enough to give the precise asymptotics of the divergence of the diffusion coefficient $D(t)$ as $t \to \infty$.

References

[1] M. Prähofer and H. Spohn, Phys. Rev. Lett. **84**, 4882 (2000).

[2] K. Johansson, Commun. Math. Phys. **209**, 437 (2000).

[3] C. Landim and H. T. Yau, Probab. Theory Rel. Fields **108**, 321 (1997).

[4] C. Landim, J. Quastel, M. Salmhofer and H.-T. Yau, *Superdiffusivity of the Asymmetric Exclusion Process in Dimensions One and Two*, Commun. Math. Phys., to appear.

14.7. Graduate Studies Programme "Quantum Field Theory" (GSP)

Host institution: Center for Theoretical Sciences (NTZ) at Center of Advanced Studies (ZHS)
Cooperating institutions: Institute for Theoretical Physics, Mathematical Institute and Max-Planck-Institute "Mathematics in the Sciences".

Quantum field theory (QFT) is the basis of the overwhelming part of modern Theoretical Physics. Up to now it is by no means exhausted concerning its rich mathematical structures, its far-reaching physical consequences and also its conceptual meaning. Together with classical field theory, on which it rests, as well as with statistical and computational physics it is the most effective methodology of Theoretical Physics. QFT has essential applications reaching from the subnuclear through nuclear, atomic, molecular and mesoscopic systems up to the realm of cosmology. Much effort is required in order to fully understand all the topics in QFT which grow up in these areas. The history of QFT is closely connected with the development in many fields of modern mathematics. Obviously, no real success in QFT will be possible without evolving and intensively studying also its mathematical structures.

The closely related **Research Areas** of the Graduate Studies Programme, having a long-standing tradition at the University of Leipzig and being in accordance with the international state-of-the-art, are:

(1) The investigations of the *Mathematical Structures of Quantum Field Theory* and of its conceptual content are of principal as well as of methodological interest. They are motivated partly by actual physical problems, partly they grow up because of their pure mathematical relevance. The main methods to be applied are (non-commutative) differential geometry, theory of Lie (super)groups and their representations, theory of operator algebras and (nonlinear) functional analysis as well as functional integration.

(2) *Relativistic Quantum Field Theory* is the generally accepted frame for describing the primary interactions of elementary particles with each other, with external fields and under various boundary conditions. The actual investigations are directed especially to the perturbative as well as nonperturbative treatment of the Standard Model and its supersymmetric extensions, to the theory of strings, on lattice approximations and computer simulations, as well as to QFT under external conditions.

(3) The *Nonrelativistic Quantum Field Theory* is one of the outstanding methods to study basic properties of condensed matter and various many body systems; it is closely related to the methods of statistical and computational physics. The actual investigations are on (strong) correlations in spin and low-dimensional electron systems and on scaling behaviour, phase transitions and finite- size effects in ordered and disordered systems.

The Graduate Studies Programme contains also a well established **Academic Training Program** consisting of a thematically coordinated Course of Main Lectures and various Specialized Lectures covering the whole research area. This is supported by the weekly Colloquium and three Main Seminars on "Mathematical Physics", "Quantum Field Theory" and "Theory of Condensed Matter". The PhD students also profit from the running scientific activities (including periodic workshops, schools and conferences), from the guest programs and the scientific spirit of the cooperating institutions. Any of these research fields are investigated in cooperation with various national and international partners. The majority of the related projects – which are considered in detail in the description of the various research groups – belong to the *interdisciplinary area of Mathematical Physics*. Research and Education profits very much from

the scientific (and spatial) neighbourhood of mathematicians and theoreticians and from the longstanding, fruitful cooperation between the three cooperating institutions – being unique in Germany.

15. Publications

15.1. Quantum Field Theory (QFT)

[1] Alberti, P.M.; Matthes, R.
Connes' Trace Formula and Dirac Realization of Maxwell and Yang-Mills Action.
In: Scheck, F.; Upmeier, H.; Werner, W. (Eds.): *Noncommutative Geometry and the Standard Model of Elementary Particles (LNP 596).*
Berlin, Heidelberg, New York: Springer-Verlag, 2002; pp. 40–74.

[2] Blümlein, J.; Eilers, J.; Geyer, B.; Robaschik, D.
On the Structure of the Virtual Compton Amplitude with Additional Final State Meson in the Extended Bjorken Region.
Phys. Rev. **D65** (2002) 054029.

[3] Bordag, M.; Falomir, H.; Santangelo, E.M.; Vassilevich, D.V.
Boundary Dynamics and Multiple Reflection Expansion for Robin Boundary Conditions.
Phys. Rev. **D65** (2002) 064032.

[4] Bordag M.; Goldhaber, A.S.; van Nieuwenhuizen, P.; Vassilevich, D.
Heat Kernels and Zeta-Function Regularization for the Mass of the Susy Kink.
Phys. Rev. **D66** (2002) 125014.

[5] Bordag, M.; Kirsten, K.
Heat Kernel Coefficients and Divergencies of the Casimir Energy for the Dispersive Sphere.
Int. J. Mod. Phys. **A17** (2002) 813–819.

[6] Bordag, M.; Nesterenko, V.V.; Pirozhenko, I.G.
High Temperature Asymptotics in Terms of Heat Kernel Coefficients: Boundary Conditions with Spherical and Cylindrical Symmetries.
Nucl. Phys. Proc. Suppl. **104** (2002) 228–231.

[7] Bordag, M.; Skalozub, V.
Super Daisy Diagrams in the O(N)-model Near the Phase Transition Temperature.
Theor. Mat. Phys. **131** (2002) 450–458; translated from Teor. Mat. Fiz. **131** (2002) 4–14.

[8] Bordag, M.; Skalozub, V.
Temperature Phase Transition and an Effective Expansion Parameter in the O(N)-Model.
Phys. Rev. **D65** (2002) 085025.

[9] Bordag, M.; Skalozub, V.
Super Daisy Resummations and an Effective Expansion Parameter in the O(N)-Model near the Phase Transition.
Phys. Lett. **B533** (2002) 182–190.

[10] Calow, D.; Matthes, R.
Connections on Locally Trivial Quantum Principal Fibre Bundles.
J. Geom. Phys. **41** (2002) 114–165.

[11] Eilers, J.; Geyer, B.
Twist Cut-Off for Scalar Off-Cone Operators in q-Space.
Phys. Lett. **B546** (2002) 78–85.

[12] Geyer, B.; Lavrov, P.; Nersessian, A.
Integration Measure and Extended BRST-Covariant Quantization.
Int. J. Mod. Phys. **A17** (2002) 1183–1197.

[13] Geyer, B.; Lazar, M.; Robaschik, D.
Nonlocal Operators and Distribution Amplitudes of Definite Twist, WW-Relations, BC-Sum Rules and Power Corrections for Hard Hadronic Processes.
Nucl. Phys. **B108** (Proc. Suppl.) (2002) 318–320.

[14] Geyer, B.; Mülsch, D.
Topological Gauge Theories with Antisymmetric Tensor Matter Fields.
Phys. Lett. **B535** (2002) 349–357.

[15] Geyer, B.; Mülsch, D.
Hodge Type Cohomological Gauge Theories.
Int. J. Mod. Phys. **A17** (2002) 4425–4434.

[16] Gilkey, P.; Kirsten, K.; Park, J.H.; Vassilevich, D.
Asymptotics of the Heat Equation with 'Exotic' Boundary Conditions or with Time Dependent Coefficients.
Nucl. Phys. Proc. Suppl. **104** (2002) 63.

[17] Grumiller, D.; Kummer, W.; Vassilevich, D.V.
Dilaton Gravity in Two Dimensions.
Phys. Rep. **369** (2002) 327.

[18] Kijowski, J.; Rudolph, G.
On the Gauss Law and Global Charge for QCD.
J. Math. Phys. **43** (2002) 1796–1808.

[19] Kijowski, J.; Rudolph, G.
On the Notion of Global Charge in QCD.
Rep. Math. Phys. **49** (2002) 211–224.

[20] Kijowski, J.; Rudolph, G.
Global Gauss Law for Lattice QCD.
In: Kapuscik, E.; Horzela, A. (Eds.): *Proc. 2nd Symposium on Quantum Theory and Symmetries (Krakow 2001).*
Singapore: World Scientific, 2002; pp. 96–105.

[21] Klein, C.; Richter, O.
Physically Realistic Solutions to the Ernst Equation on Hyperelliptic Riemann Surfaces.
In: Gurzadyan, V.G; Jantzen, R.T.: Ruffini, R. (Eds.): *Proc. 9th Marcel Grossmann Meeting on General Relativity (Rome 2000).*
Singapore: World Scientific, 2002; pp. 789–790.

[22] Matthes, R.; Richter, O.; Rudolph, G.
Spectral Triples for the Kronecker Foliation.
In: Kapuscik, E.; Horzela, A. (Eds.): *Proc. 2nd Symposium on Quantum Theory and Symmetries (Krakow 2001).*
Singapore: World Scientific, 2002, pp. 481–486.

[23] Peltri, G.
Beiträge und Beispiele zur Bures-Geometrie.
PhD thesis, Fakultät für Mathematik und Informatik, Universität Leipzig, 2002.

[24] Rudolph, G.; Schmidt, M.; Volobuev, I.P.
On the Gauge Orbit Space Stratification.

In: Kapuscik, E.; Horzela, A. (Eds.): *Proc. 2nd Symposium on Quantum Theory and Symmetries (Krakow 2001).*
Singapore: World Scientific, 2002, pp. 553–558.

[25] Rudolph, G.; Schmidt, M.; Volobuev, I.P.
Classification of Gauge Orbit Types for SU(n)*-Gauge Theories.*
J. Math. Phys. Anal. Geom. **5** (2002) 201–241.

[26] Rudolph, G.; Schmidt, M.; Volobuev, I.P.
Partial Ordering of Gauge Orbit Types for SU(n)*-Gauge Theories.*
J. Geom. Phys. **42** (2002) 106–138.

[27] Rudolph, G.; Schmidt, M.; Volobuev, I.P.
On the Gauge Orbit Space Stratification: A Review.
J. Phys. A: Math. Gen. **35** (2002) R1–R50.

[28] Vassilevich, D. V.
Spectral Geometry for Strings and Branes.
Nucl. Phys. Proc. Suppl. **104** (2002) 208.

15.2. Theory of Elementary Particles (TET)

[1] Carimalo, C.; Schiller, A.; Serbo, V.G.
New Method for Calculating Helicity Amplitudes of Jet-Like QED Processes for High-Energy Colliders. I: Bremsstrahlung Processes.
Eur. Phys. J. **C23** (2002) 631–649.

[2] Chernodub, M.N.; Ilgenfritz, E.-M.; Schiller, A.
Monopoles, Confinement and Deconfinement in Lattice Compact QED in (2+1)D with External Fields.
Nucl. Phys. Proc. Suppl. **106** (2002) 703–705.

[3] Chernodub, M.N.; Ilgenfritz, E.-M.; Schiller, A.
Photon Propagator, Monopoles, and the Thermal Phase Transition in Three Dimensional Compact QED.
Phys. Rev. Lett. **88** (2002) 231601/1–4.

[4] Chernodub, M.N.; Ilgenfritz, E.-M.; Schiller, A.
String Breaking and Monopoles: A Case Study in the 3D Abelian Higgs Model.
Phys. Lett. **B547** (2002) 267–277.

[5] Göckeler, M.; Horsley, R.; Pleiter, D.; Rakow, P.E.L.; Schaefer, S.; Schäfer, A.; Schierholz, G.
A Lattice Study of the Spin Structure of the Λ Hyperon.
Phys. Lett. **B545** (2002) 112–118.

[6] Göckeler, M.; Horsley, R.; Pleiter, D.; Rakow, P.E.L.; Schaefer, S.; Schäfer, A.; Schierholz, G.
Hadron Spin Structure on the Lattice.
Nucl. Phys. **A711** (2002) 291–296.

[7] Göckeler, M.; Horsley, R.; Klaus, B.; Pleiter, D.; Rakow, P.E.L.; Schaefer, S.; Schäfer, A.; Schierholz, G.
Applied Lattice Gauge Calculations: Diquark Content of the Nucleon.
Nucl. Phys. **A711** (2002) 297–302.

[8] Hollik, W.; Kraus, E.; Roth, M.; Rupp, Ch.; Sibold, K.; Stöckinger, D.
Renormalization of the Supersymmetric Standard Model.
Nucl. Phys. **B639** (2002) 3–65.

[9] Karakhanian, D.; Kirschner, R.
Bjorken Asymptotics of QCD and Integrable Systems.
In: Gurzadian, V.G. *et al.* (Eds.): *From integrable models to gauge theories* (Proceedings of the Nor Hamberd Workshop in honour of S. Matinyan).
Singapore: World Scientific, 2002; pp. 203–216.

[10] Karakhanyan, D.; Kirschner, R.; Mirumyan, M.
Universal R Operator With Deformed Conformal Symmetry.
Nucl. Phys. **B636** (2002) 529–548.

[11] Karakhanian, D.; Kirschner, R.
Conserved Currents of the Three-Reggeon Interaction.
Phys. Atom. Nucl. **65** (2002) 1501–1512 [Yad. Fiz. **65** (2002) 1539–1550].

[12] Kraus. E.; Rupp, Ch.; Sibold, K.
Supercurrent and Local Coupling in the Wess-Zumino Model.

Eur. Phys. J. **C24** (2002) 631–637.

[13] Liao, Y.
One Loop Renormalization of Spontaneously Broken Gauge Theory with a Product of Gauge Groups on Noncommutative Spacetime: the $U(1) \times U(1)$ Case.
JHEP **0204** (2002) 042.

[14] Liao, Y.
Validity of Goldstone Theorem at Two Loops in Noncommutative $U(N)$ Linear Sigma Model.
Nucl. Phys. **B635** (2002) 505–524.

[15] Liao, Y.; Sibold, K.
Time-Ordered Perturbation Theory on Noncommutative Spacetime: Basic Rules.
Eur. Phys. J. **C25** (2002) 469–477.

[16] Liao, Y.; Sibold, K.
Time-Ordered Perturbation Theory on Noncommutative Spacetime: 2. Unitarity.
Eur. Phys. J. **C25** (2002) 479–486.

[17] Liao, Y.; Sibold, K.
Spectral Representation and Dispersion Relations in Field Theory on Noncommutative Space.
Phys. Lett. **B549** (2002) 352–361.

15.3. Theory of Condensed Matter (TKM)

[1] Behn, U.; John, T.; Stannarius, R.
On-Off Intermittency and Stochastically Driven Convection in Nematic Liquid Crystals.
In: Boccaletti, S.; Gluckman, B.J.; Kurths, J.; Pecora, L.M.; Spano, M.L. (Eds.): *Experimental Chaos* (Proc. 6th Experimental Chaos Conference, 22-26 July 2001, Potsdam, Germany), AIP Conference Proceedings **622**.
Melville, New York: American Institute of Physics, 2002; pp. 381–392.

[2] Birner, T.; Lippert, K.; Müller, R.; Kühnel, A.; Behn, U.
Critical Behaviour of Non-Equilibrium Phase Transitions to Magnetically Ordered States.
Phys. Rev. E **65** (2002) 046110/1–5.

[3] Wilmers, C.C.; Sinha, S.; Brede, M.
Examining the Effects of Species Richness on Community Stability: An Assembly Model Approach.
OIKOS **99** (2002) 363–367.

[4] John, T.; Behn, U.; Stannarius, R.
Quantitative Characterization of On-Off Intermittency in a Stochastically Driven Dissipative Pattern Forming System.
Phys. Rev. E **65** (2002) 046229/1–13.

[5] Nowotny, T.; Patzlaff, H.; Behn, U.
Phase Diagram of the Random Field Ising Model on the Bethe Lattice.
Phys. Rev. E **65** (2002) 016127/1–9.

[6] Richter, J.; Metzner, G.; Behn, U.
Venom Immunotherapy: A Mathematical model.
J. Theor. Med. **4** (2002) 119–132.

15.4. Computer-Oriented Quantum Field Theory (CQT)

[1] Berche, P.-E.; Chatelain, C.; Berche, B.; Janke, W.
Crossover Effects in the Bond-Diluted Ising Model in Three Dimensions.
Comp. Phys. Comm. **147** (2002) 427 – 430.

[2] Berg, B.A.; Billoire, A.; Janke, W.
Functional Form of the Parisi Overlap Distribution for the Three-Dimensional Edwards-Anderson Ising Spin Glass.
Phys. Rev. **E65** (2002) 045102(R)-1 – 4.

[3] Berg, B.A.; Billoire, A.; Janke, W.
Overlap Distribution of the Three-Dimensional Ising Model.
Phys. Rev. **E66** (2002) 046122-1 – 6.

[4] Bittner, E.; Janke, W.; Markum, H.
Spins Coupled to a Z_2-Regge Lattice in 4D.
Nucl. Phys. **B** (Proc. Suppl.) **106&107** (2002) 989 – 991.

[5] Bittner, E.; Janke, W.; Markum, H.
Ising Spins Coupled to a Four-Dimensional Discrete Regge Skeleton.
Phys. Rev. **D66** (2002) 024008-1 – 8.

[6] Bittner, E.; Markum, H.; Janke, W.
On the Continuum Limit of the Ising Model Coupled to Regge Gravity.
Acta Physica Slovaca **52** (2002) 241 – 246.

[7] Bittner, E.; Janke, W.
Phase Transition in Complex $|\psi|^4$ Theory,
Phys. Rev. Lett. **89** (2002) 130201-1 – 4.

[8] Chatelain, C.; Berche, P.-E.; Berche, B.; Janke, W.
3D Bond-Diluted 4-State Potts Model: A Monte Carlo Study.
Nucl. Phys. **B** (Proc. Suppl.) **106&107** (2002) 899 – 901.

[9] Chatelain, C.; Berche, P.-E.; Berche, B.; Janke, W.
Influence of Dilution on the Strong First-Order Phase Transition of the 3D 4-State Potts Model.
Comp. Phys. Comm. **147** (2002) 431 – 434.

[10] Hellmund, M.; Janke, W.
Random-Bond Potts Models on Hypercubic Lattices: High-Temperature Series Expansions.
Nucl. Phys. **B** (Proc. Suppl.) **106&107** (2002) 923 – 925.

[11] Hellmund,M.; Janke, W.
High-Temperature Series Expansions for Random-Bond Potts Models on Z^d.
Comp. Phys. Comm. **147** (2002) 435 – 438.

[12] Janke, W.; Kenna, R.
Exact Finite-Size Scaling and Corrections to Scaling in the Ising Model with Brascamp-Kunz Boundary Conditions.
Phys. Rev. **B65** (2002) 064110-1 – 6.

[13] Janke, W.
Statistical Analysis of Simulations: Data Correlations and Error Estimation.
In: Grotendorst, J.; Marx, D.; Muramatsu, A. (Eds.): *Quantum Simulations of Complex Many-Body Systems: From Theory to Algorithms*, Proceedings of the Euro Winter School,

Kerkrade, The Netherlands, 25 February – 1 March 2002.
Jülich: John von Neumann Institute for Computing NIC Series, Vol. **10**, 2002; pp. 423 – 445.

[14] Janke, W.
Pseudo Random Numbers: Generation and Quality Checks.
In: Grotendorst, J.; Marx, D.; Muramatsu, A. (Eds.): *Quantum Simulations of Complex Many-Body Systems: From Theory to Algorithms*, Proceedings of the Euro Winter School, Kerkrade, The Netherlands, 25 February – 1 March 2002.
Jülich: John von Neumann Institute for Computing NIC Series, Vol. **10**, 2002; pp. 447 – 458.

[15] Janke, W.; Kenna, R.
Phase Transition Strengths from the Density of Partition Function Zeroes.
Nucl. Phys. **B** (Proc. Suppl.) **106&107** (2002) 905 – 907.

[16] Janke, W.; Kenna, R.
Exact Finite-Size Scaling with Corrections in the Two-Dimensional Ising Model with Special Boundary Conditions.
Nucl. Phys. **B** (Proc. Suppl.) **106&107** (2002) 929 – 931.

[17] Janke, W.; Johnston, D.A.; Stathakopoulos, M.
Fat and Thin Fisher Zeroes.
Nucl. Phys. **B** (Proc. Suppl.) **106&107** (2002) 983 – 985.

[18] Janke, W.; Berg, B.A.; Billoire, A.
Multi-Overlap Simulations of Spin Glasses.
In: Rollnik, H.; Wolf, D. (Eds.): *NIC Symposium 2001*.
Jülich: John von Neumann Institute for Computing NIC Series, Vol. **9** (2002); S. 301 – 314.

[19] Janke, W.; Kenna, R.
Analysis of the Density of Partition Function Zeroes – A Measure for Phase Transition Strength.
In: Landau, D.P.; Lewis, S.P.; Schüttler, H.-B. (Eds.): *Computer Simulation Studies in Condensed-Matter Physics XIV*.
Berlin: Springer Proceedings in Physics, Vol. **89**, 2002; pp. 97 – 101.

[20] Janke, W.; Weigel, M.
Numerical Tests of CFT Conjectures for 3D Spin Systems.
Comp. Phys. Comm. **147** (2002) 382 – 387.

[21] Janke, W.; Kenna, R.
Density of Partition Function Zeroes and Phase Transition Strength.
Comp. Phys. Comm. **147** (2002) 443 – 446.

[22] Janke, W.; Johnston, D.A.; Stathakopoulos, M.
A Kertész Line on Planar Random Graphs?
J. Phys. **A35** (2002) 7575 – 7584.

[23] Janke, W.
66. Physikertagung in Leipzig.
Physik Journal **1** Nr. **7/8** (2002) 29 – 30.

[24] Janke, W.; Villanova, R.
The Ising Model on Three-Dimensional Random Lattices: A Monte Carlo Study.
Phys. Rev. **B66** (2002) 134208-1 – 13.

[25] Janke, W.; Johnston, D.A.; Malmini, R.P.K.C.

The Information Geometry of the Ising Model on Planar Random Graphs.
Phys. Rev. **E66** (2002) 056119-1 – 5.

[26] Pelster, A.; Kleinert, H.; Bachmann, M.
Functional Closure of Schwinger-Dyson Equations in Quantum Electrodynamics. Part 1: Generation of Connected and One-Particle Irreducible Feynman Diagrams.
Ann. Phys. (NY) **297** (2002) 363 – 395.

[27] Weigel, M.,
Vertex Models on Random Graphs.
Ph.D. thesis, Universität Leipzig, unpublished (May 2002).

[28] Weigel, M.; Janke, W.; Hu, C.-K.
Random-Cluster Multihistogram Sampling for the q-State Potts Model.
Phys. Rev. **E65** (2002) 036109-1 – 11.

[29] Weigel, M.; Janke, W.
Algorithmic Tools for Simulations of Vertex Models on Random Graphs.
Nucl. Phys. **B** (Proc. Suppl.) **106&107** (2002) 986 – 988.

[30] Wernecke, A.
Q-Zustand Potts-Modelle auf einem quenched Ensemble von zufälligen ϕ^3-Graphen.
Diploma thesis, Universität Leipzig, unpublished (November 2002).

15.5. Molecule Dynamics/Computer Simulations(MDC)

[1] Schüring, A.; Auerbach, S.M.; Fritzsche, S; Haberlandt, R.
J. Chem. Phys. **116** (2002) 10890.

[2] Fritzsche, S.; Kärger, J.
Studies in Surface Science and Catalysis **142** (2002) 1955.

[3] Jost, S.; Fritzsche, S.; Haberlandt, R.
Studies in Surface Science and Catalysis **142** (2002) 1947.

[4] Cukrowski, A.S.; Fort, J.; Fritzsche, S.
Acta Physica Polonica **B33** (2002) 1085.

[5] Bussai, C;. Hannongbua, S.; Fritzsche, S.; Haberlandt, R.
Studies in Surface Science and Catalysis **142** (2002) 1979.

[6] Bussai, C.; Hannongbua, S.; Fritzsche, S.; Haberlandt, R.
Chem. Phys. Lett. **354** (2002) 310.

[7] Bussai, C.; Vasenkov, S.; Liu, H.; Böhlmann, W.; Fritzsche, S.; Hannongbua, S.; Haberlandt, R.; Kärger, J.
Applied Catalysis **A232** (2002) 59.

15.6. Statistical Physics (STP)

[1] Honerkamp, C.; Salmhofer, M.; Rice, T.M.
Flow to Strong Coupling in the Two–Dimensional Hubbard Model.
European Physical Journal **B27** (2002) 127.

16. Talks

16.1. Quantum Field Theory (QFT)

Michael Bordag

1. *Effective Expansion Parameter in the O(N) Model Near Phase Transition*,
   Theoretical High Energy Seminar, Nordita, Kopenhagen, Denmark, September 19.

2. *Vacuum Energy of a Color Magnetic String*,
   Casimir workshop, Harvard-Smithonian Center for Astrophysics, Boston, USA, November 15.

Christian Fleischhack

1. *Der verallgemeinerte Eichorbitraum im Ashtekarprogramm*,
   Theoretisch-Physikalisches Seminar, Universität Göttingen, April 25.

Bodo Geyer

1. *2-Dimensional $N_T = 4$ Super Yang-Mills is a Hodge Type Cohomological Gauge Theory*,
   (with Mülsch, D.), 66th DPG-Tagung, Leipzig, March 18–22.

2. *Cohomological Gauge Theories of Hodge Type*,
   (with Mülsch, D.), 5th Alexander Friedman Seminar, João Pessoa, Brazil, April 23–30.

3. *$N_T = 8, D = 2$ Hodge Type Cohomological Gauge Theory with Global Symmetry Group $SU(4)$*,
   (with Mülsch, D.), 3rd Andrej Sacharov Conference, Moscow, Russia, July 24–29.

4. *Extended BRST Quantization in General Coordinates*,
   (with Lavrov, P.; Nersessian, A.), 3rd Andrej Sacharov-Conference, Moscow, Russia, July 24–29.

5. *Hodge Type Cohomological Gauge Theories (Review)*,
   Jayme Tiomno-Colloquium, U São Paulo, Brazil, October 9.

6. *Hodge Type Cohomological Gauge Theories (Status Report)*,
   (with Mülsch, D.), XXIIIrd Encontro Nacional de Fisica de Particulas e Campos, Aguas de Lindoa, Brazil, October 15–19.

7. *Power Corrections of Off-Forward Quark Distributions (Status Report)*
   (with Eilers, J.; Lazar, M.; Robaschik, D.), XXIIIrd Encontro Nacional de Fisica de Particulas e Campos, Aguas de Lindoa, Brazil, October 15–19.

Olaf Richter

1. *Algebro-Geometric Solutions to the Ernst Equation and Twistor Theory*,
   66th DPG-Tagung, Leipzig, March 18–22.

2. *Spectral Triples Related to the Kronecker Foliation*,
66th DPG-Tagung, Leipzig, March 18–22.

3. *Spectral Triples for Foliated Manifolds*,
Bayrischzell Workshop, Bayrischzell, April 2002.

Gerd Rudolph

1. *Observablenalgebren und Superauswahlstrukturen für Gitter-Eichtheorien*,
Institut für Theoretische Physik, Universität Freiburg, February 2002.

2. *On the Structure of the Gauge Orbit Space*,
Dept. of Mathematical Methods in Physics, University of Warsaw, Poland, March 2002.

3. *Classification of Gauge Orbits for Gauge Group* SU(n),
Dept. of Mathematical Methods in Physics, University of Warsaw, Poland, March 2002.

4. *On the Problem of Charged States in Gauge Theories*,
Center for Theoretical Physics, PAN Warsaw, Poland, March 2002.

5. *Evening Lecture on Geometry and Physics*,
School of Mathematics and Physics, University of Tasmania, Hobart, Australia, May 2002.

6. *The Observable Algebra and Its Representations for Scalar QED on the Lattice*,
School of Mathematics and Physics, University of Tasmania, Hobart, Australia, May 2002.

7. *The Functional Integral in Terms of Gauge Invariants*, School of Mathematics and Physics, University of Tasmania, Hobart, Australia, May 2002.

8. *Observable Algebras and Their Representations for Lattice Gauge Theories*,
Faculty of Physics, University of Adelaide, Australia, June 2002.

9. *On the Structure of the Gauge Orbit Space Stratification*,
Faculty of Physics, University of Adelaide, Australia, June 2002.

10. *Observable Algebras for Lattice Gauge Theories, with Special Emphasis on Algebraic Aspects*,
Institute of Mathematics, University of Queensland, Brisbane, Australia, July 2002.

11. *Observable Algebras and Their Representations for Lattice Gauge Theories*,
11th Workshop on Foundations and Constructive Aspects of QFT, Institut für Theoretische Physik, Universität Göttingen, December 2002.

Matthias Schmidt

1. *How to Study the Physical Relevance of Gauge Orbit Space Singularities?*,
34th Symposium on Mathematical Physics, Toruń, Poland, June 14–18.

2. *On the Stratification of the Yang-Mills Configuration Space for the Gauge Group* SU(n),
Séminaire de Physique Mathématique et Géométrie, Université de Lille, France, December 10.

Armin Uhlmann

1. *Transition Probability and Bures Metric*,
   Dresden, MPI KS, June 5.

2. *The Bures Distance and its Riemann Metric*,
   Invited talk, Conf. on Information Geometry and Its Applcations, Pescara, Italy, July 4.

3. *Concurrence and Foliations Induced by Some 1-Qubit Channels*,
   Invited talk, Conf. on Quantum Composite Systems, Ustron, Poland, September 6.

4. *Quantum Information Transfer from One System to Another One*,
   Opening of the Conf. General Theory of Information Transfer and Combinatorics, Universität Bielefeld, ZiF, November 9.

Wolfgang Weller

1. *Composite Fermions – Electrons in Two Dimensions in a Strong Magnetic Field*,
   (with Apel, W.; Dietel, J.; Koschny, T.), Theoretisches Kolloquium, Universität Bayreuth, Bayreuth, May 7.

2. *Three-Particle Interaction for Composite Fermions*,
   (with Koschny, T.), 7th International Conference "Path Integrals from Quarks to Galaxies", Antwerpen, Belgium, May 27–31.

16.2. Theory of Elementary Particles (TET)

Meinulf Göckeler

1. *Applied Lattice Gauge Calculations*,
   European Workshop on the QCD Structure of the Nucleon, Ferrara, Italy, April 3–6.

2. *Nucleon Form Factors from Lattice QCD*,
   EU IHP Network on Hadron Phenomenology from Lattice QCD: Workshop on Light Quark Phenomenology and Kaon Physics, Zeuthen, April 21–24.

3. *Lattice QCD: Proton Properties from First Principles*,
   Seminar, CNRS Luminy, Marseille, France, June 21.

4. *Lattice Gauge Theory and Chiral Symmetry (Breaking)*,
   Seminar CPT, CNRS Luminy, Marseille, France, July 8.

5. g_A *on the Lattice*,
   Workshop "Quark Mixing – CKM Unitarity", Heidelberg, September 19–20.

6. *Non-Perturbative Renormalisation of Composite Operators in the RI-MOM Scheme*,
   EU IHP Network on Hadron Phenomenology from Lattice QCD: Workshop on Fermion Actions and Chiral Symmetry, Bern, Switzerland, October 16–19.

7. *What do Lattice Simulations Tell us about Hadronic Structure Functions?*,
   Seminar, TU München, December 2.

8. *Nucleon Form Factors from Lattice QCD*,
   4th meeting of DFG Research group, Regensburg, December 20–21.

Roland Kirschner

1. *Parton Interactions in the Bjorken Asymptotics*,
   36th Winter School of St. Petersburg Nucl. Phys. Institute, St. Petersburg, Russia, February 2002.

2. *Factorization in Diffractive Electroproduction*,
   Theory Seminar, Ecole Polytechnique, Paris, France, September 2002.

3. *Diffractive Vector Meson Production at HERA*,
   Intern. workshop on low x physics, Antwerpen, Netherlands, September 2002.

Yi Liao

1. *Unitarity of Time-ordered Perturbation Theory on Noncommutative Spacetime*,
   (with Sibold, K.), "Noncommutative geometry and quantum field theory, Feynman diagrams in mathematics and physics", ESI, Wien, Austria, October 20–26.

2. *Spectral Representations and Dispersion Relations in Field Theory on Noncommutative Spacetime*,
   (with Sibold, K.), 11. Workshop "Grundlagen und konstruktive Aspekte der QFT", ITP, Göttingen, December 6–7.

Arwed Schiller

1. *Photon Propagator, Monopoles and the Thermal Phase Transition in 3D Compact QED* , 12th Workshop on Lattice Field Theory, Debrecen, Hungary, May 9-11.

2. *Gauge Boson Propagator and Monopoles in 3D Compact QED* , 1st meeting of DFG Research group, Regensburg, June 8–9.

3. *Monopoles, Confinement and the Photon Propagator in QED_3* , XX International Symposium on Lattice Field Theory, Cambridge, USA, June 24–29 (poster).

4. *Confinement and the Photon Propagator in 3D cQED on the Lattice* , 5th International Conference "Quark Confinement and Hadron Spectrum", Gargnano, Italy, September 10–14.

5. *Confinement and the Photon Propagator in 3D cQED on the Lattice* , 3rd NTZ-Workshop on Computational Physics, Institut für Theoretische Physik, Universität Leipzig, Leipzig, December 10.

6. *Overview on Lattice and DSE Computations of Gluon and Ghost Propagators in QCD* , 4rd meeting of DFG Research group, Regensburg, December 20–21.

Klaus Sibold

1. *Ward Identities: The Realization of Symmetries in Perturbative Quantum Field Theory* Hesselberg Workshop on "Theory of Renormalization and Regularization". Hesselberg February 24 – March 1.

2. *Perturbative Treatment of Field Theories on Non-Commutative Space-Time* Particle Physics Seminar, Kyoto University, Japan, December 25.

16.3. Theory of Condensed Matter (TKM)

Ulrich Behn

1. *Kritisches Verhalten bei rauschgetriebenen Nichtgleichgewichts-Phasenübergängen*,
   Theorie-Kolloquium, Physik-Department, TU München, July 17.

Markus Brede

1. *Patterns in Randomly Evolving Networks: Idiotypic Networks*,
   (with Behn, U.), Seminar "Complex Nonlinear Processes" HU Berlin, Berlin, July 16.

2. *Patterns in Randomly Evolving Networks: Idiotypic Networks*,
   Seminar "Mathematical modeling of biological systems", MPI MIS, Leipzig, October 16.

3. *Patterns in Randomly Evolving Networks*,
   CompPhys02, Leipzig, December 16.

Thomas John

1. *Measurement of Scaling Laws in a Stochastic, Multiplicatively Driven, Spatially Extended System*,
   (with Behn, U., Stannarius, R.), Dynamics Days Europe 2002, Heidelberg, July 15–19.

2. *Statistische Auswertung von Zeitreihen bei multiplikativ antreibendem Rauschen*,
   (with Behn, U., Stannarius, R.), DPG-Tagung Regensburg, March 11–15.

3. *Laserbeugung zur quantitativen Charakterisierung raum-zeitlicher Muster in anisotropen Flüssigkeiten*,
   (with Stannarius, R.), DPG-Tagung Regensburg, March 11–15 (poster).

4. *Measurement of Scaling Laws in a Stochastic, Multiplicatively Driven Spatially Extended System*,
   Gruppenseminar Nichtlineare Dynamik und Zeitreihenanalyse, MPI PKS, Dresden, November 27

5. *Measurement of Scaling laws in a Spatially Extended Pattern Forming System Driven by Multiplicative Noise*,
   (with Behn, U., Stannarius, R.), 3. Dresdener Herbstseminar Nichtlineare Physik, MPI PKS, Dresden, December 1–4 (poster).

Adolf Kühnel

1. *Kritisches Verhalten von Nichtgleichgewichts-Phasenübergängen in magnetische Zustände*,
   Seminar, Institut für Theoretische Physik, TU Berlin, May 22.

Jan Richter

1. *Modelling Th1-Th2 Regulation, Allergy and Immunotherapy*,
   (with Metzner, G. and Behn, U.), 21st Congress of the European Academy of Allergology and Clinical Immunology (EAACI), Naples, Italy, June 1–5 (poster).

16.4. Computer-Oriented Quantum Field Theory (CQT)

Michael Bachmann

1. *Native Ground-States of Lattice Proteins*,
(with Schiemann, R.; Janke, W.), 1. Research Festival of Biosciences and Medicine in Leipzig, October 18 (poster).

Elmar Bittner

1. *Critical Exponents of the Discrete Regge Model in 4D*,
Deblat02 – 12. Workshop on Lattice Field Theory, Debrecen, Hungary, May 9–11.

2. *On the Continuum Limit of the Discrete Regge Model in 4D*,
(with Janke, W.; Markum, H.), Lattice 2002, MIT, Cambridge, USA, June 24–29 (poster).

Meik Hellmund

1. *High-Temperature Series Expansions for Disordered Systems*,
Seminar on Condensed Matter Theory, Universität Mainz, February 19.

Wolfhard Janke

1. *Pseudo Random Numbers: Generation and Quality Checks*,
invited lecture, Euro Winter School *Quantum Simulations of Complex Many-Body Systems: From Theory to Algorithms*, Kerkrade, The Netherlands, February 25 – March 1.

2. *Statistical Analysis of Simulations: Data Correlations and Error Estimation*,
invited lecture, Euro Winter School *Quantum Simulations of Complex Many-Body Systems: From Theory to Algorithms*, Kerkrade, The Netherlands, February 25 – March 1.

3. *Statistics of Rare Events in Spin Glasses*,
MECO-27 conference, Sopron, Hungary, March 7–9.

4. *Fat and Thin Fisher Zeroes*,
66. Physikertagung, Universität Leipzig, March 18–22.

5. *Exact Finite-Size Scaling with Corrections in the Two-Dimensional Ising Model with Brascamp-Kunz Boundary Conditions*,
66. Physikertagung, Universität Leipzig, March 18–22.

6. *Statistics of Extremes in the EA Ising Spin Glass*,
Deblat02 – 12. Workshop on Lattice Field Theory, Debrecen, Hungary, May 9–11.

7. *Fat and Thin Fluctuating Graphs*,
PI2002 – 7th International Conference on *Path Integrals from Quarks to Galaxies*, Universiteit Antwerpen, Belgien, May 27–31.

8. *Tests of Extreme Value Statistics*,
Statistical Physics Workshop, Nancy, France, May 29–31.

9. *Extreme Order Statistics*,
   Lattice 2002, MIT, Cambridge, USA, June 24–29.

10. *New Methods to Measure Phase Transition Strength*,
    (with Kenna, R.; Johnston, D.A.), Lattice 2002, MIT, Cambridge, USA, June 24–29 (poster).

11. *EUROGRID: Leipzig Team*,
    EUROGRID Network Meeting, Edinburgh, Scotland, July 5–6.

12. *First-Order Phase Transitions*,
    invited lecture, NATO Advanced Study Institute *Computer Simulations of Surfaces and Interfaces*, Albena, Bulgaria, September 9–20.

13. *Histograms and All That*,
    invited lecture, NATO Advanced Study Institute *Computer Simulations of Surfaces and Interfaces*, Albena, Bulgaria, September 9–20.

14. *Monte Carlo Studies of Three-Dimensional Bond-Diluted Ferromagnets*,
    HLRB and KONWIHR Workshop, TU München, Campus Area Garching, October 10–11.

Andreas Nußbaumer

1. *Parallel Tempering at Second-Order Phase Transitions*,
   (with Janke, W.), 7. Granada Seminar on Computational Physics, Granada, Spain, September 2–7 (poster).

Reinhard Schiemann

1. *Exact Statistical Analysis of Native Ground-States of 2D Lattice Proteins*,
   (with Bachmann, M.; Janke, W.), 7. Granada Seminar on Computational Physics, Granada, Spain, September 2–7 (poster).

Martin Weigel

1. *Vertex Models on Random Graphs*,
   EUROGRID Network Meeting, Edinburgh, Scotland, July 5–6.

2. *The F Model on Random Planar ϕ^4 Graphs*,
   CompPhys02, 3rd NTZ Workshop on Computational Physics, Leipzig, December 10.

Andreas Wernecke

1. *The 3-State Potts Model on Quenched Random Planar Graphs*,
   CompPhys02, 3rd NTZ Workshop on Computational Physics, Leipzig, December 10.

16.5. Molecule Dynamics/Computer Simulations(MDC)

Siegfried Fritzsche

1. *Negative Arrhenius Behaviour in Diffusion of Ethane in Zeolite LTA*,
(with Schüring, A.), Mahidol University, Bangkok, Thailand, February 22.

2. *An Entropic Barrier Explaining an Diffusion Coefficient that Decreases with Increasing Temperature*,
(with Schüring, A.), Chemistry Departement of the Chulalongkorn University, Bangkok, Thailand, February 25.

3. *Application of Transition State Theory to Diffusion of Guest Molecules in Zeolites*,
(with Schüring, A.), Physics Department, University of Khon Kaen, Thailand, March 8.

4. *Correlations in Anisotropic Diffusion of Methane in Silicalite*,
(with Kärger, J.), second FEZA conference, Giardini Naxos, Greece, August 2002 (poster).

Horst Ludger Vörtler

1. *MC Simulations of Extended Primitive Models of Water in Bulk and Confined Systems: Structure and chemical Potential*,
(with Kettler, M.), 6th Liblice Conference on the Statistical Mechanics of Liquids, Spindleruv Mlyn, Czech Republic, June 9–14 (poster).

2. *Structure and Thermodynamics of Primitive Water Models on Bulk Conditions and in 2-Dimensional Layers: MC Simulation Studies*,
(with Kettler, M.; Galle, J.), 17th IUPAC Conference on Chemical Thermodynamics, Rostock, July 28.

3. *Chemical Potential and Phase Coexistence in Primitive Water Models: Simulation Studies of Bulk Fluids and Thin Films*,
(with Galle, J.; Kettler, M.), Symposium *Molecules in Interaction with Interfaces* (SFB 294), Leipzig, October 9–11 (poster).

4. *Computer Simulation of Cavity Distribution Functions in Confined fluids*,
(with Smith, W.R.), 3rd Workshop on Computational Physics CompPhys02, Leipzig, December 10.

Steffen Jost

1. *Diffusion of Water in Chabazite: an MD-Study in Comparison with PFG NMR Experiments*,
(with Bopp, Ph.A.; Fritzsche, S.; Haberlandt, R.; Spohr, E.), talk on the Symposium of the Collaborative Research Centre *Molecules in Interaction with Interfaces* (SFB 294), Leipzig, October 11.

2. *Molecular Dynamics Simulations of Static and Dynamic Properties of Water adsorbed in Chabazite*,
(with Fritzsche, S.; Haberlandt, R.), second FEZA conference, Giardini Naxos, Greece, August 2002 (poster).

3. *Diffusion of Water in the Zeolite Chabazite*,
(with Fritzsche, S.; Haberlandt, R.), 14th Deutsche Zeolith-Tagung, Frankfurt am Main, 2002 (poster).

Andreas Schüring

1. *Entropic Barriers for Diffusion in Zeolites*,
(with Auerbach, S.M.; Fritzsche, S.; Haberlandt, R.), 14th Deutsche Zeolith-Tagung, Frankfurt am Main, 2002 (poster).

2. *MD Analysis of Rate Processes in Zeolites*,
(with Auerbach, S.M.; Fritzsche, S.; Haberlandt, R.), Symposium of the Collaborative Research Centre *Molecules in Interaction with Interfaces* (SFB 294), Leipzig, October 11 (poster).

Jörg Galle

1. *Molecular Modelling of Aqueous Phases at Complex Interfaces and in Thin Planar Films*,
(with Vörtler, H.L.; Kettler, M.), Symposium *Molecules in Interaction with Interfaces* (SFB 294), Leipzig, October 9–11.

Chuenchit Bussai

1. *Diffusion of Water in Silicalite by Molecular Dynamics Simulations: Ab Initio based interactions*,
(with Fritzsche, S.; Hannongbua, S.; Haberlandt, R.), second FEZA conference, Giardini Naxos, Greece, August 2002 (poster).

2. *The Energy Barrier and the movement of Water Molecule through the Silicalite-1 Lattice: Ab Initio and Molecular Dynamics Studies*,
(with Fritzsche, S.; Haberlandt, R.; Hannongbua S.), The 10th Conference on Science and Technology of Chulalongkorn University, Bangkok, Thailand, March 20–22.

3. *Diffusion and Structure of Water Molecule in the Pore of Silicalite-1 as Studied by MD Simulations: Temperature and Concentration Dependence*,
(with Fritzsche, S.; Haberlandt, R.; Hannongbua S.), The 6th Annual National Symposium on Computational Science and Engineering, Nakornsrithammarat, Thailand, April 3–5.

4. *Binding, Energy Barrier and Diffusion of Water in Silicalite-1: Ab initio, Molecular Dynamics and PFG NMR Studies*,
(with Fritzsche, S.; Haberlandt, R.; Hannongbua S.), The 3rd Royal Golden Jubilee Ph. D. Congress, Pataya, Thailand, April 25–27.

5. *Diffusion of Methane in Silicalite by Molecular Dynamics Simulations: Møller- Plesset Second Order Perturbation Based Interaction*,
(with Fritzsche, S.; Haberlandt, R.; Hannongbua S.), PACCON 2002, International Conference and Exhibition on Pure and Applied Chemistry 2002, Bangkok, Thailand, May 29–31.

6. *Methane Diffusivity in Silicalite-1 Based on an Ab Initio Fitted Potential*,
(with Fritzsche, S.; Haberlandt, R.; Hannongbua S.), The 28th Congress on Science and Technology of Thailand, Bangkok, Thailand, October 24–26.

Arthorn Loisruangsin

1. *Reliability of the Force-Field Potential Energy Surface: Ab Initio Studies of Methane and n-Pentane in Silicalite-1 Interaction*,
(with Bussai, C.; Fritzsche, S.; Hannongbua, S.) PACCON 2002, International Conference and Exhibition on Pure and Applied Chemistry 2002, Bangkok, Thailand, May 29–31.

16.6. Statistical Physics (STP)

Manfred Salmhofer

1. *Renormalization of Φ^3_6 by Flow Equations*,
   Hesselberg Meeting, February 24 – March 1.

2. *Fermi Systems*,
   Hesselberg Meeting, February 24 – March 1.

3. *Continuous Renormalization and Tree Expansions I*,
   Mitteldeutsche Physik–Combo, Leipzig, April 19 and 20.

4. *Continuous Renormalization and Tree Expansions II*,
   Mitteldeutsche Physik–Combo, Jena, May 31 and June 1.

5. *Continuous Renormalization and Tree Expansions III*,
   Mitteldeutsche Physik–Combo, Halle, June 28 and 29.

6. *Algebra, Analysis and Applications of the RG*,
   Program on *Realistic Theories of Correlated Electron Materials (CEM02)*, Institute for Theoretical Physics, University of California at Santa Barbara, USA, September–October.

7. *RG Flows for 2d Fermions. Progress and Problems*,
   Université de Sherbrooke, Canada, November 4.

8. *Regularität der Fermifläche in wechselwirkenden Systemen*,
   Theoretisch–Physikalisches Seminar, Universität Göttingen, November 19.

17. Organizational Activities

17.1. Quantum Field Theory (QFT)

Bodo Geyer

- Spokesman of the Graduiertenkolleg "Quantenfeldtheorie: Mathematische Struktur und Anwendungen in der Elementarteilchen- und Festkörperphysik".
- Member of the scientific advisory board of the Andrejewski Foundatio
- "Vertrauensdozent" of the "Gesellschaft Dt. Naturforscher und Ärzte" (GDNÄ).
- Referee for the DFG, the DAAD und the Humboldt Foundation.

Armin Uhlmann

- Board member of *Rep. Math. Phys.* and *Open Systems and Information Dynamics.*

Wolfgang Weller

- Board member of *Physikalische Blätter.*

17.2. Theory of Elementary Particles (TET)

Klaus Sibold

- Co-organizer of the "Mitteldeutsche Physik-Combo": Lectures at graduate level on subjects of theoretical physics.
  January 18 – 20, Jena. Subjects: Supergravity; Selected Chapters of Gravity; Quantum Field Theory in Curved Space-Time.
  April 19 – 20, Leipzig; May 31st – June 1st, Jena; June 28 – 29, Halle. Subjects: Renormalization Group Equations and Tree Expansions; Perturbative Unitarity from the Cutting Rules; The Background Field Method; Kinks, Monopoles and Other Solitons.
  October 18 – 20, Leipzig; November 8 – 10, Halle. Subjects: Applications of the Heat Equation Methods to Problems in Physics and Geometry; Cosmological Microwave Background; Gauge Theories on the Computer.
- Activities as member in the "Graduiertenkolleg: Quantenfeldtheorie".
- Activities as associated member in the "Graduiertenkolleg: Analysis, Geometrie und ihre Verbindung zu den Naturwissenschaften"

17.3. Theory of Condensed Matter (TKM)

Adolf Kühnel

- Member of the International Advisory Board of the *Middle European Cooperation (MECO) on Statistical Physics.*
- Member of the Executive Commitee of the *International Center for Scientific Cooperation* with residence in Tübingen.
- Member of the Beirat of the Fachverband "*Dynamik und Statistische Physik*" of the Arbeitskreis Festkörperphysik of the DPG.

17.4. Computational Quantum Field Theory (CQT)

Michael Bachmann

- Scientific Secretary of the *66. Physikertagung* of the German Physical Society (DPG) in Leipzig, March 18 – 22, 2002.

Wolfhard Janke

- Organizer of the *66. Physikertagung* of the German Physical Society (DPG) in Leipzig, March 18 – 22, 2002.
- Organizer of the Workshop *CompPhys02 – 3. NTZ-Workshop on Computational Physics*, ITP, University of Leipzig, December 10, 2002.
- Member of Advisory Committee, *DEBLAT01 – 12. Workshop on Lattice Field Theory*, Universität Debrecen, Ungarn, May 9 – 11, 2002.
- Member of International Advisory Committee, *V International Congress on Mathematical Modeling*, Joint Institute for Nuclear Research, Dubna, Russia, September 30 – October 6, 2002.
- Member of the Faculty Committee ("Fakultätsrat") of the Faculty of Physics and Geosciences, University of Leipzig.
- Vice-Dean of the Faculty of Physics and Geosciences, University of Leipzig.
- Director of the Institut for Theoretical Physics, University of Leipzig.
- Director of the Naturwissenschaftlich-Theoretisches Zentrum (NTZ) at the Zentrum für Höhere Studien (ZHS), University of Leipzig.

17.5. Molecule Dynamics/Computer Simulations(MDC)

Siegfried Fritzsche

- Project leader in the SFB 294.

Horst Ludger Vörtler

- Project leader in the SFB 294.

17.6. Statistical Physics (STP)

Manfred Salmhofer

- Organization (together with H. Knörrer (ETH) and D.C. Brydges (UBC)) of the Conference *Renormalization Group*, Mathematisches Forschungszentrum Oberwolfach, Oberwolfach, June 9–15.

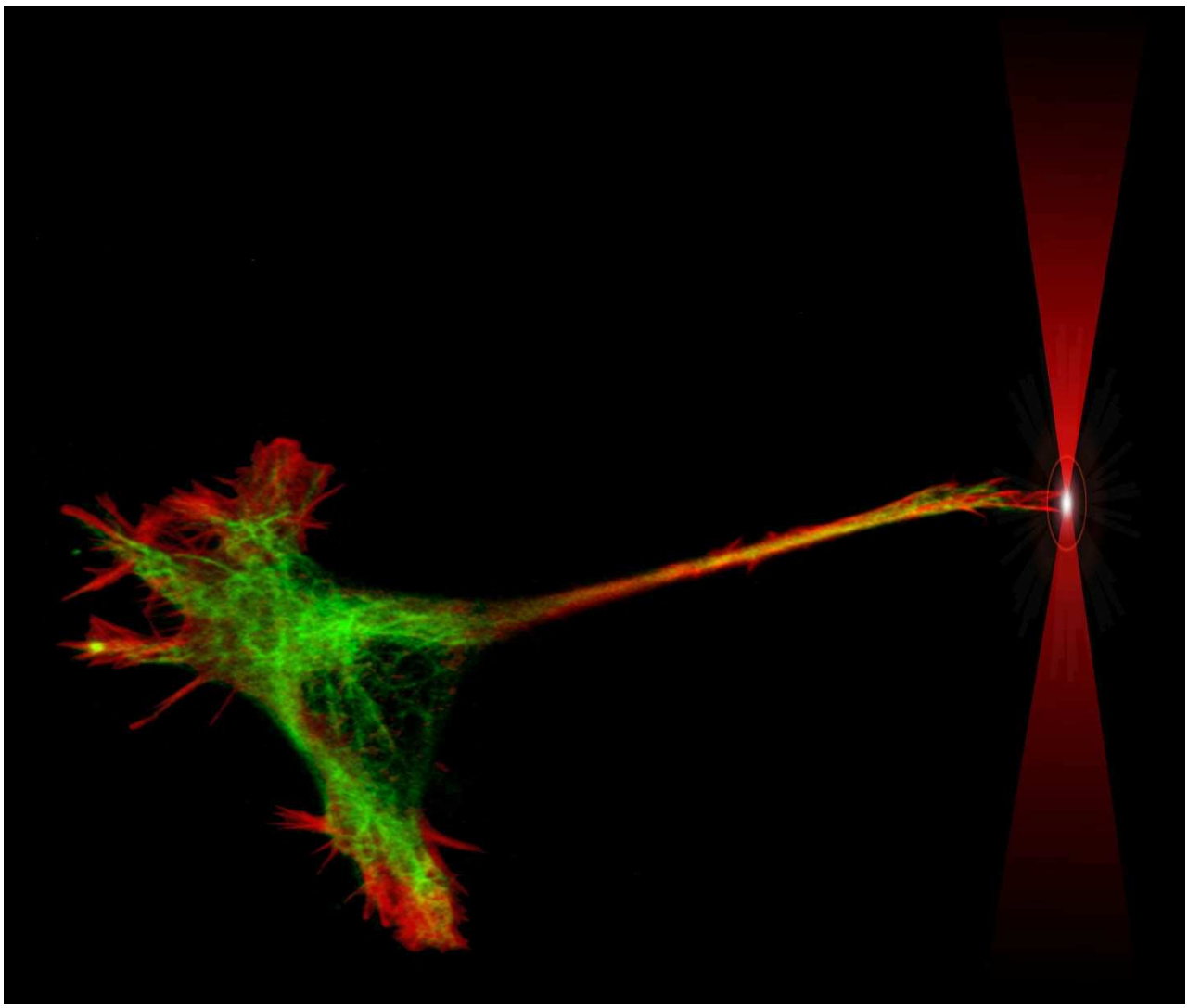

ISBN 3-934178-25-1